Topics:
Solar-thermal conversion
Solar power generation
Performance testing
Solar energy
Solar concentrators
Solar power plants

EPRI AP-4608
Project 2003-5
Final Report
July 1986

Performance of the Vanguard Solar Dish–Stirling Engine Module

Prepared by
Energy Technology Engineering Center
Canoga Park, California

(H) 415-743-9196

T 6+1 DAC

(W) 415-291 6472

Dublin CA

Byron Washom

213 273 9690

St Wash

March 8?

15? last day

Have data in another room?

Want tapes?

Energy Technology Engineering Center
Rocketdyne Division
Rockwell International Corporation
P.O. Box 1449
Canoga Park, California 91304

(818) 700-8200

Operated for U.S. Department
of Energy

Rockwell
International

May 15, 1986

In reply refer to 86ETEC-DRF-0915

Mr. Tom Mancini
Solar Distributed Receiver Div (6227)
Sandia National Laboratory
P.O. Box 5800
Albuquerque, N.M. 87185

Subject: Tapes from Solar Dish - Stirling Engine Test

Dear Mr. Mancini:

The subject tapes (72 total) were transferred to Mr. Byron Washom of Advanco Corp. We understand ~~that~~ Byron and you have made the arrangement to make these tapes available to you.

Enclosed is the information on the tape format and sample printout of the tape data.

Sincerely,

Oscar Hillig
Program Manager
Solar Heating and Cooling
Energy Technology Engineering Center

Enclosure: as noted

cc w/o encl.: Byron Washom, Advanco Corp.
Dr. John C. Schaefer, EPRI

OH24

Byron's # (Apr 90)
W: (415) 291-6472
h: (415) 743-9196

April 26, 1990

Byron -
I counted 72 tapes in the enclosed boxes, so I think we're returning everything you sent us in 1986.
It was good talking to you the other day.

Hugh

Hugh E. Reilly
Solar Thermal Technology
Division 6217

Sandia National Laboratories
Albuquerque, New Mexico 87185-5800
Phone (505) 846-5845 Res. 298-6517

UPS: Byron Washom

2358 Alameda Diablo

Diablo, CA 94528

loaded on backup tape

our tape: 1 min intervals

backup: 4 min

cover letter if can't find last day

Feb 21 ?

Energy Technology Engineering Center
Rocketdyne Division
Rockwell International Corporation
P.O. Box 1449
Canoga Park, California 91304

(818) 700-8200

Operated for U.S. Department
of Energy

Rockwell
International

May 15, 1986

In reply refer to 86ETEC-DRF-0915

Mr. Tom Mancini
Solar Distributed Receiver Div (6227)
Sandia National Laboratory
P.O. Box 5800
Albuquerque, N.M. 87185

Subject: Tapes from Solar Dish - Stirling Engine Test

Dear Mr. Mancini:

The subject tapes (72 total) were transferred to Mr. Byron Washom of Advanco Corp. We understand that Byron and you have made the arrangement to make these tapes available to you.

Enclosed is the information on the tape format and sample printout of the tape data.

Sincerely,

Oscar R. Hillig

Oscar Hillig
Program Manager
Solar Heating and Cooling
Energy Technology Engineering Center

Enclosure: as noted

cc w/o encl.: Byron Washom, Advanco Corp.
Dr. John C. Schaefer, EPRI

OH24

FORMAT OF ADVANCO DATA TAPES

The tapes are 9 track, 800 BPI. The data are recorded in ASCII. The physical record length is 256 words (16 bit words). One data slice (one logical record) is equal to

$$((N + 1) * 18) + 2$$

bytes long, where N is the number of channels recorded. The extra "1" in the (N + 1) term is for the time. The record ends with a carraige return (CR) and a line feed (LF). These account for the additional +2 at the end of the logical record.

The time at which the data slice was recorded is 18 bytes long; the data for each channel is also 18 bytes long. The time occurs at the beginning of each logical record, and is formatted as

JJJ HH:MM:SS

where

JJJ is the Julian day,
HH is the hour,
MM is the minute,
SS is the second.

Each data channel is formatted as

CCCXXVVVVVVVVVUUU

where

CCC is the channel number,
XX is blank or some characters of unknown purpose,
VVVVVVVVV is the data value for channel CCC,
UUU is the units for channel CCC.

Several problems were encountered during the data reduction of the tapes. A few of the more significant ones are listed below.

1) Some tapes have data written past the "end of tape" mark.
2) The carraige return (CR) & line feed (LF) is not always on a word boundary.
3) During daylight savings time, the hour is sometimes Pacific Daylight Time (PDT) and sometimes Pacific Standard Time (PST).

EXAMPLE DUMP OF FIRST SIX RECORDS
OF TYPICAL ADVANCO TAPE

HH MM SS XX UUU

REC# 1 LEN 256
082 06:25:30 150 +05.754 V, 151 +00.691 V, 152 +00.790 V, 153 +06.110 V, 156 +000.
01 MV, 157 +00.001 V, 158 -017.00 MV, 159 +00.068 V, 164 +00016. C, 165 +00016. C, 16
6 +00016. C, 167 +00016. C, 168 +00017. C, 169 +00017. C, 170 +00017. C, 171 +00016.
C, 172 +00017. C, 173 +00016. C, 174 +00016. C, 175 +00016. C, 176 +00016. C, 177
+00016. C, 178 +00017. C, 179 +00016. C, 180 +00016. C, 181 +00016. C, 182 +00016.
C, 183 +00

REC# 2 LEN 256
016. C, 184 +00016. C, 185 +00016. C, 186 +00016. C, 187 +00016. C, 188 +00015. C,
189 +00015 C, 190 +00015 C, 191 +00015 C, 192 +00017 C, 193 +00017 C, 194 +0001
7. C, 195 +00017. C, 196 +00017. C, 197 +00016. C, 198 +00017. C, 199 +00017. C, 20
0 +01.965 V, 201 +00.997 V, 202 +02.571 V, 203 +00.898 V, 204 +00.097 V, 205 -00.008
V, 206 +00.050 V, 207 -00.010 V, 208 -00.023 V, 209 +00.027 V, 210 +04.090 V, 211
+04.209 V

REC# 3 LEN 256
, 212 +04.212 V, 213 +07.964 V, 214 +02.998 V, 215 +00.000 V, 216 -00.264 V, 217 -00
.001 V, 218 +00.000 V, 219 +00.000 V, 220 -00.226 V, 221 -00.339 V, 222 -00.949 V,
223 -00.013 V, 224 -00.001 V, 225 +000.00 MV, 227 -00.031 V, 228 -00.250 V, 229 -00.0
59 V, 230 +00.000 V, 231 +00.035 V, 232 +00.061 V, 233 +002.735 MV, 234 -00.002 V, 23
5 -00.001 V, 236 -00.194 V, 237 +00.004 V, 238 +099.99 MV (CR LF) 082 06:26:29 , 150 +06.0
02 V, 151

carriage return
line feed

REC# 4 LEN 256
+00.634 V, 152 +00.298 V, 153 +05.489 V, 156 +000.00 MV, 157 +00.000 V, 158 +000.00
MV, 159 +00.001 V, 164 +00016. C, 165 +00016. C, 166 +00016. C, 167 +00016. C, 168 +
00017. C, 169 +00017. C, 170 +00017. C, 171 +00016. C, 172 +00016. C, 173 +00016. C
, 174 +00016 C, 175 +00016. C, 176 +00016. C, 177 +00016. C, 178 +00016. C, 179 +00
016. C, 180 +00016. C, 181 +00016. C, 182 +00016. C, 183 +00016. C, 184 +00016. C,
185 +00016.

REC# 5 LEN 256
C, 186 +00016. C, 187 +00016. C, 188 +00015. C, 189 +00015. C, 190 +00016. C, 191
+00015. C, 192 +00017. C, 193 +00017. C, 194 +00017. C, 195 +00017. C, 196 +00016.
C, 197 +00016. C, 198 +00017. C, 199 +00017. C, 200 +01.964 V, 201 +00.997 V, 202 +
02.583 V, 203 +00.932 V, 204 +00.097 V, 205 -00.007 V, 206 +00.052 V, 207 -00.009 V
, 208 -00.025 V, 209 +00.028 V, 210 +04.089 V, 211 +04.211 V, 212 +04.213 V, 213 +07
.975 V, 21

REC# 6 LEN 256
4 +02.998 V, 215 +00.000 V, 216 -00.265 V, 217 -00.001 V, 218 +00.000 V, 219 +00.000
V, 220 -00.108 V, 221 -00.306 V, 222 -00.279 V, 223 -00.014 V, 224 +00.000 V, 225
+00.02 MV, 227 +00.081 V, 228 +00.227 V, 229 -00.345 V, 230 -00.001 V, 231 +00.147

NOTES FROM CONVERSATION WITH CALVIN MIYAZONO OF JPL ON DECEMBER 12, 1985

Subject:

Data from solar thermal program testing at JPL was acquired with a PDP11/34 computer operating under an RSX11M system. Calvin described the form in which the test data is stored on the discpaks and mag tapes which were shipped to SANDIA together with the PDP11 system in 1984.

All the test data files for the last 2/3rds of solar testing at jpl is indexed in two directory files called MASTER.FIL and MASTER1.FIL. These files can be found on each diskpack, but the most recent diskpack will have the up to date index.

The information given about each data file includes: the test filename;type of test identified by filename (eg. OG-Omnium G tests, BR=Brayton tests); tests are numbered in sequence starting at 100.; the number of minutes of data collected; the tape number; and short description of test.

The two files are ascii files so should be able to print easily.

(The last disc pack which was at Edwards Air Force Base was also backed up by Miyazono with a mag tape.)

All tapes with names containing the root "ARC" were written using DEC's PIP utility, so will not be retrievable except with DEC system.

Tapes marked BRU are back up and recovery tapes produced by dec's BRU utility. Those can only be read after transfering them back to the disk using BRU.

Weather tape were produced in block of ASCII data in 512 bytes per block.

There are a number of files associated with each test for which data was recorded and archived:

For any one test, say ST0222, (sterling test) you will find a .NOT file produced at end of test describing weather, test conditions, mirror condicitons, etc. Not all tests have such. Was added toward end; a refinement.

.CMT (comment file), were comments which could be placed into the file during the test. not often used. May be printed directly with PIP (?).

.EUS (engineering units) file. This file contained the test data in engineering units.

A .SET file was created at the outset of testing with input from the

cognizant engineer. The file
indicated what devices and instruments would be read during the test, what the range was over which voltage were to be made, and a short description as to device location.
Information in this file was accessed in the program which was run to program the datalogger.

The .ACQ file was for acquisition of the actual raw data such as voltages from flow meters and pressure gages, and thermocouple output (in degrees).

The .CLC file told which calculations were used, ie the lines of fortran code for processing the instrument outputs.

The .EUS file has the reduced or processed raw data in engineering unites based on SET,CLC and ACQ files. I.e. the .EUS file was the output of a program which used .SET,.CLC, and .ACQ files as input.

The .EUS file is input for plotting program to produce graphs, plots , etc. The printouts are created by a program which also accesses the EUS file. IE the EUS file is a binary file, not readable without translation.
To recover an EUS file you will need to use a different block size from the default. Under normal circumstances, to recover a file you would type

PIP =mt0:filename.ext (REturn)

then computer would copy from mag tape to disk. But for EUS file you need to add the following to end of command line:

... /bs:840. (Return)

This would transfer the EUS file in readable form onto the disk.

At test conclusion the raw data is held on disk in temporary file; the first thing done is to run program called CNVRT (for convert) which takes data from that raw data file, compresses it and puts it into the .ACQ file. After that NEWVRT processes .acq file data into engineering units and outputs to .EUS file.

A program called NWPRNT takes .eus file to produce a .LST file which is finally an ASCII FILE which is readable or printable. To do this you need to have present a copy of the .SET file renamed as TBLx.SET (x BEING 1, 2, or 3). You also must run DBGEN, prior to NWPRNT. tHE Latter will use the output from dbgen to determine filename, number of lines to print out, date, etc. The output of NEPRNT is TRANSx.LST, x being 1,2, or 3, corresponding to the concentrator (tbc-1, tbc-2, or the low cost concentrator). The .LST file can be printed or viewed; it's an ascii file. These were not saved (they also took up a lot of space.) Typically if you wanted to printout the asccii file you'd then type:

PIP TRANSx.LST/SP (rETURN)

to spool it out.

After that, to generate plots you had to run two more programs:

1. PLTSET (plot set) would go into the SET file and determine which plots were appropriate for that given test and the ranges over which to plot. Software was set up to generate twenty plots with four lines per plot. The selection of parameters to plot versus time was indicated and placed in SET file at outset. On some tests all 20 plots were done, on others not plots were produced.

This program goes back to SEt to determine which channels to plot; it then goes and opens up the EUS file and retrieves the data, placing it into a file named "testname".PLT.

2. PLOT is then run using .PLT file as input. All the versatek commands are in the plot program. Two .BIN (VECTOR1 and PARM) files are the output.

A versatec supplied program called "RASM" generates the actual plots. That program runs in the rsx11m environment. This program is on one of the disks.

For computer to access information in SET file, three programs have to first be run; they are DBGEN, DECODE, and NWDBGEN. Those progms put the SET file into machine readable form. This would be done if you wanted to re-work the data in some way. (Recall that you can simply print out the data on EUS file by runnin the NWPRNT program.

The last discpack at Pasadena has a batch file that does all the steps needed to process a file on tape and produce a set of plots. It's a .CMD file. You could use it as a tutorial on how to process data; Calvin M. couldn't recall its name, but knowing the general sequence of commands from the above description of the process, the batch file can be hunted down amoung the .CMU files on that discpak.

MISCELANEOUS NOTES:

The VAX has a rsx11m mode, (verify this), which would allow you to do these things on in (giving us alternative of getting rid of our pdp11 system here at solar tower.

Check and see is we've gotten rancho mirage sterling test tapes from Advanco.

There are several green notebooks which were sent from JPL in the last shipment, in which test realated information was written down at the test site during the testing. Should help to provide background info surrounding given tests.

REPORT SUMMARY

SUBJECTS: Solar-thermal electric systems / Power system planning

TOPICS:
- Solar-thermal conversion
- Solar power generation
- Performance testing
- Solar energy
- Solar concentrators
- Solar power plants

AUDIENCE: R&D engineers and scientists

Performance of the Vanguard Solar Dish–Stirling Engine Module

A new solar technology that combines a parabolic dish concentrator with a 24-kW Stirling engine power conversion unit has achieved the highest known efficiencies in converting sunlight to electricity. An 18-month test of the prototype demonstrated that, with the design improvements indicated, dish-Stirling modules could become a cost-effective generation option for utilities.

BACKGROUND: Under an agreement with DOE, the Advanco Corporation designed, manufactured, and installed in California a promising new solar-electric technology—a 25-kW parabolic dish–Stirling engine generator module. Because the concept has potential for commercial electricity production, EPRI and the Southern California Edison Company initiated this project to obtain and evaluate performance data from the test program.

OBJECTIVES: To evaluate operating and performance data on the dish-Stirling technology over an 18-month test period; to study engineering and design changes made to the system during that time; and to identify issues important to the technology's possible future use by utilities.

APPROACH: The prototype test module, known as Vanguard 1, consisted of a mirrored parabolic dish concentrator, 10.7 m in diameter; a solar receiver; a four-cylinder Stirling engine that used hydrogen as a working gas; an induction generator; and an air-cooled radiator. Using two independent data acquisition systems, researchers collected data on the module from the start of operation in February 1984 through July 1985. They monitored key parameters such as gross and net electrical output, insolation, weather, engine temperatures and pressures, and auxiliary power requirements. They also kept a log of operating incidents and component failures, repairs, and modifications. At the end of the test period, they summarized and documented the results and identified future actions needed to develop the dish-Stirling concept for electric utility use.

RESULTS: The Vanguard prototype demonstrated a maximum conversion efficiency from sunlight to electricity of 31.6% on a gross instantaneous basis—higher than any other known solar technology. The average net conversion efficiency

during sunny periods over the 18 months was lower (22.8%) because of power consumption by auxiliary equipment and because lower insolation levels reduce efficiency. The study found that efficiency depended on insolation, temperature, wind speed, and dish reflectivity.

During the test period, Vanguard equipment availability averaged 72%. Repairs to the Stirling engine, overheating of the receiver, difficulties with aperture plates, modifications to the emergency detrack system, replacement of mirror facets, and failure of control systems reduced availability. Such problems also pinpointed the areas needing design modifications.

Other major barriers to be overcome before the technology is cost-effective for utilities are high capital cost and potentially high operating and maintenance costs.

EPRI PERSPECTIVE

This report describing the Vanguard test program will help utility personnel to better understand this new solar technology. The high conversion efficiencies, if combined with the advantages of low-cost mass production, modularity, factory assembly, and rapid construction, would make the system a potentially attractive option for utilities with adequate solar resources. Related EPRI reports AP-3792, AP-4464, and AP-4466 document the results of field tests of photovoltaic installations—another major solar technology.

PROJECT

RP2003-5
EPRI Project Managers: R. W. Taylor; John Schaefer
Advanced Power Systems Division
Contractor: Energy Technology Engineering Center

For further information on EPRI research programs, call EPRI Technical Information Specialists (415) 855-2411.

Performance of the Vanguard Solar Dish–Stirling Engine Module

AP-4608
Research Project 2003-5

Final Report, July 1986

Prepared by

ENERGY TECHNOLOGY ENGINEERING CENTER
Post Office Box 1449
Canoga Park, California 91304

Principal Investigators
J. J. Droher
S. E. Squier

Contributor
S. Shinnamon

Prepared for

Electric Power Research Institute
3412 Hillview Avenue
Palo Alto, California 94304

EPRI Project Managers
R. W. Taylor
D. Augenstein
J. Schaefer

Solar Power Systems Program
Advanced Power Systems Division

ORDERING INFORMATION

Requests for copies of this report should be directed to Research Reports Center (RRC), Box 50490, Palo Alto, CA 94303, (415) 965-4081. There is no charge for reports requested by EPRI member utilities and affiliates, U.S. utility associations, U.S. government agencies (federal, state, and local), media, and foreign organizations with which EPRI has an information exchange agreement. On request, RRC will send a catalog of EPRI reports.

NOTICE

Prepared by
Energy Technology Engineering Center
Canoga Park, California

ABSTRACT

This report summarizes information on the performance of the Vanguard Parabolic Dish/Stirling Engine Module during an 18-month period of operational testing (February 1984 through July 1985) at Rancho Mirage, California. The test module consisted of a 10.7-m-diameter parabolic dish to collect and concentrate solar beam radiation, a solar receiver, a four-cylinder Stirling engine using hydrogen as the working gas, an induction generator, and an air-cooled radiator. Historical beam insolation data are summarized for the Palm Springs area. Gross and net output of electricity, auxiliary power requirements, system availability, and capacity factors are summarized on a monthly and annual basis. Models are presented for predicting electrical output. Operating and maintenance experience is delineated chronologically and by subsystem. The performance of each major subsystem is discussed. An assessment is made of the present and future status of the dish/Stirling system. Recommendations are made for future developmental work involving dish/Stirling applications for the utility industry.

In Memory of J. J. (Joe) Droher

On May 30, 1986, shortly after completion of the project documented in this report, Joe Droher passed away from complications resulting from a heart attack. He was 64 years old.

Joe began working with the EPRI Solar Power Systems Program staff on solar-thermal field experiments in 1978. He served as EPRI's on-site representative during the testing of the Institute's 1-MW_t Gas-Cooled Central Receiver at the newly opened Department of Energy's Central Receiver Test Facility. This was the first major test of a solar central receiver at a brand-new facility demonstrating a new technology. Very early, Joe demonstrated a quiet competence which came to be highly valued by personnel from both EPRI's contractor, Boeing Engineering and Construction and the test facility's operator, Sandia National Laboratories. Although personnel involved in that inaugural effort were experienced engineers and scientists, Joe's experience and capability served as an example to all of a true professional test engineer.

Joe gained a thorough knowledge of both the solar receiver and the facility's capabilities, and his questions prevented many problems from either cropping up or growing. He usually knew the answers, but we didn't; and in this way, he taught us about thoroughness and attention to the smallest details.

Subsequently, Joe supported EPRI efforts associated with the Department of Energy's Total Energy Project, the Shenandoah Project, and then with the Vanguard Solar Project, documented in this report. In all of these projects, Joe brought his quiet excellence to the effort to help ensure a successful project.

Joe will be missed by the EPRI staff. Those of us who were fortunate to work directly with him have all learned from his experience and excellence.

J. E. Bigger
Project Manager
Renewable Resource Systems Department

ACKNOWLEDGMENTS

Work by ETEC in support of the Vanguard project was performed under EPRI auspices. EPRI technical assistance was provided by John Cummings, Ed DeMeo, Roger Taylor, Don Augenstein, and John Schaefer.

Advanco Corporation, headed by Byron Washom, was the prime contractor for fabricating and testing the Vanguard module. Permission of Advanco to use a number of pertinent figures from their report, DOE-AL-16333-2 (84-ADV-6), is gratefully acknowledged. All Advanco employees were most cooperative. Particular thanks are due Larry Hall and Terry Hagen for providing information relating to Vanguard performance.

As the on-site representative of United Stirling, Inc., during the period from December 1983 to October 1984, David Wells performed an outstanding job, working assidously for long hours. He contributed a great deal to solving problems during the intial phase of operations, and along with Larry Hall of Advanco, helped develop much of the on-site data analysis software.

Raymond Cedillo and Bob Yinger of the Southern California Edison Company helped by providing tapes and data on direct insolation measurements made at the SCE service center. Southern California Edison provided the two photographs of the overall test site used in this report.

Floyd Livingston and Jack Stearns of the Jet Propulsion Laboratory provided pertinent information on JPL work on dish/Stirling systems. Cal Miyazono provided computer printouts made by JPL during initial stages of the project.

Dana Sears of Onan, Inc., supplied test data on the induction generator and valuable background on the electrical system. Bill Wilcox of Rockwell International provided background information on fabrication and installation of the Vanguard module.

Utility members attending project review meetings and providing inputs on utility needs included Bob Potthoff of San Diego Gas and Electric; Willard King of Georgia Power Company; and Joe Reeves, John Stolpe, Ray Cedillo, John Zeller of Southern California Edison Company; and Robert Davis of Pacific Gas & Electric Company. Other meeting attendees who provided valuable inputs were Joe Wiesiger of DOE-Albuquerque, Dick Cummings of Cummings Solar Company; Oscar Hillig of ETEC; and Jim Leonard, Kevin Linker of Sandia National Laboratory - Albuquerque.

John East and Shelie Evans performed an outstanding job in expediting this report through the editing phase.

CONTENTS

CONTENTS (continued)

CONTENTS (continued)

ILLUSTRATIONS

ILLUSTRATIONS (continued)

ILLUSTRATIONS (continued)

ILLUSTRATIONS (continued)

TABLES

TABLES (continued)

SUMMARY AND CONCLUSIONS

An effective method for converting solar energy to electrical energy combines two technologies, namely that for a parabolic dish concentrator and for a Stirling engine. As solar radiation strikes curved, mirrored surfaces on the dish, the solar rays are concentrated and redirected to a solar receiver. The receiver converts the radiant energy to thermal energy which is transferred by high-pressure, high-temperature hydrogen gas to operate the Stirling engine. Mechanical shaft power from the engine is then used to drive an electric generator.

In May 1982, Advanco Corporation entered into a cooperative agreement with the U.S. Department of Energy (DOE) for the design, manufacture, and test of a 25-kWe solar parabolic dish module utilizing a Stirling engine power conversion unit. Market assessment and conceptual design were completed in November 1982, detailed design was completed in June 1983, system fabrication and assembly were completed in November 1983, and module installation at the test site was completed in February 1984. The Vanguard module was dedicated on 24 February 1984, and significant electrical power production was achieved in March 1984. The operational test program spanned an 18-month period and ended on 28 July 1985.

Southern California Edison (SCE), in October 1982, and the Electric Power Research Institute (EPRI), in July 1984, entered into separate cooperative agreements with Advanco in order to further their understanding of the technology. SCE provided design review and data analysis, land for the test site, and monetary support. In December 1983, EPRI retained the Energy Technology Engineering Center (ETEC) to follow the Vanguard test program and to provide an independent assessment of its performance.

In cooperation with Advanco, ETEC developed a detailed test and evaluation plan intended to provide information of interest to utilities, investors, and other potential users. ETEC also independently reduced and evaluated all Vanguard performance data recorded on 70 magnetic tapes and 24 diskettes. ETEC results verified those reported by Advanco within an error band of 1 or 2%. The differences

were due to a small variation in the zero point of the gross power sensor. ETEC integrated power output only over the time span when power was being generated. Advanco integrated power over the 18-hour period that data were recorded on diskettes; this procedure occasionally led to a slight difference in kilowatt-hours generated (see Appendix D for results) due to the greater cumulative effect of off-set error.

Joe Weisinger 10/23/86 graph boom - to be soon released (Linda have copy?) call Byron Washom (213) 278-6418

In the view of the authors, management of the project by Advanco has been excellent in meeting test objectives, presenting high visibility, and providing excellent public relations. Reports issued by Advanco have been exemplary in comprehensive, accurate, and timely reporting of operational results. Advanco has been candid in reporting problem areas as well as successes. Monthly progress reports have been issued by Advanco during the operational test program. In addition, a topical report, DOE-AL-16333-2 (64-ADV-5), entitled "Vanguard 1, Solar Parabolic Dish - Stirling Engine Module, Final Report" was issued which summarized results of the program from its inception in May 1982 through the end of September 1984.

OVERALL SYSTEM PERFORMANCE

Data on performance of the Vanguard dish/Stirling module were acquired during operational testing which spanned a period of 18 months.

1st final report was after system characterize (1983) - Joe reading this one.

Various definitions of performance factors (efficiency, availability, capacity factor) can be proposed, depending on assumptions made about the system being studied and on the basis for comparison between conventional and solar-based technologies. In this report, it was assumed that this system will be compared with conventional as well as other solar/alternative energy-based systems and as such, the performance factors were defined in conventional terms. This provides the most consistent basis for comparison and eliminates the need for and potential confusion involved in presenting several definitions and calculational methods for the same performance indicator.

Agreement between predicted (based on the previous SCE 7-year average) and observed direct insolation at the Rancho Mirage test site was reasonably good considering the actual variation from year to year in monthly averages. This provides a good basis for reporting the performance of the system, since the site was experiencing "typical" direct insolation during the test program. In using data obtained during previous years to predict performance, the analyst should realize that monthly variations of plus or minus 10% are likely, and that occasionally variations of plus or minus 20% will occur.

The module generated approximately 32,600 kWh of electricity during the 18-month test period; net on-sun electrical energy produced was about 30,200 kWh, and the net energy output accounting for overnight auxiliary power losses as well (to maintain the tracking system on standby) was roughly 27,000 kWh. Therefore, approximately 17% of the gross generated electrical energy was consumed by module parasitic draws.

The three main auxiliary energy demands are the concentrator tracker, the engine radiator fan, and the engine/receiver coolant pump. The hydrogen and air compressor systems require minimal energy throughout the day compared to the above three systems. Auxiliary energy required in winter is roughly 40% lower than that in summer. Though in summer the fan and tracker require equal amounts of energy, in winter the tracker's needs exceed those of the fan by 3 times. Overall, on a "good" day, approximately 10 to 15% of the gross generated power supplies the total auxiliary power demands.

Performance data were obtained during a number of days surrounding the summer and winter solstice periods in June and December as well as the spring and fall equinox periods in March and September. These periods are of interest because the highest and lowest output (in kWe-h) might be expected on the longest and shortest days (summer and winter solstice), while equinox days are more representative of an average day during the year. The Vanguard module output varied as expected during these periods, producing approximately 230 kWh on an average day close to the summer solstice, 190 kWh during either the spring or fall equinox, and about 130 kWh on an average winter solstice day.

Though intended as a demonstration program for parabolic dish/Stirling engine technology, in some areas the test program tended to take a developmental approach. Therefore, the amount of actual power produced by the module is not indicative of that which could be generated by a large-scale, continuously operating plant. Extrapolation for this purpose must be done with care, keeping in mind the varied objectives of the test program.

Data on cloudy day as well as clear day performance were obtained. On totally overcast days, the module could not generate power because the direct insolation level did not exceed the minimum threshold required for operation. On partly cloudy days, the module could produce power whenever sufficient beam radiation was available. On bright days with scattered discrete clouds, there was no reduction in electrical output as long as a cloud did not shade the parabolic dish mirrors.

Once the beam insolation exceeded the start-up threshold of about 300 W/m^2, the dish/Stirling module came on line and generated power in just a few minutes, due to its low thermal inertia. On one occasion with the rapid passage of small clouds shading the dish, the module exhibited the ability to stay on-line, track the sun's projected position in the sky, and then continue to generate power after sufficient insolation was again available. As with any concentrating device without thermal storage, however, the module could not stay on line during any sustained period of low-beam insolation.

The power conversion unit was subjected to thermal transients during startup and shutdown of the module, power outages, other detrack alarms, and cloud passages. No detrimental effects due to these thermal transients manifested themselves during the period of operational testing.

Gross and net efficiencies were obtained for the Vanguard module: (1) on an instantaneous basis, (2) during the time the dish was on-sun and generating power, and (3) during a 24-hour, midnight-to-midnight period encompassing both on-sun and off-sun spans.

The overall performance of the parabolic dish/Stirling engine module can be described concisely by a graph of gross generated electrical power versus incident thermal power. This plot turns out to be linear throughout most of the range and provides a substantial amount of information on the performance characteristics of the module. The slope of the line is proportional to dish reflectivity; the intercept with the X-axis is an approximate value of the threshold value of incident power required in order to produce positive electrical power, and the intercept with the Y-axis is the electrical power lost as heat from the solar receiver and Stirling engine by friction and windage.

Though instantaneous module gross conversion efficiencies can be high (in excess of 31%), when the data are integrated over a 24-hour period, the gross efficiency amounts to roughly 25% on a "perfect" day, and only about 18% on an average operating day. Several performance records set by the Vanguard module in June 1984 are given below.

Highest instantaneous gross conversion efficiency	31.6%
Highest instantaneous net conversion efficiency	29.4%
Highest daily average gross conversion efficiency	27.4%
Highest daily average net conversion efficiency	25.2%
Highest daily gross electrical output per collector area	2.74 kWh/m^2-day
Highest daily average net electrical output per collector area	2.52 kWh/m^2-day

The overall conversion efficiency of the module is likely to be slightly higher in the winter than in the summer due to lower engine coolant temperatures and shorter periods of radiator fan operation. However, the net generated electrical energy is greater in the summer than in the winter due to the capability to operate for longer periods during the day.

Overall module equipment availability for the 18-month test period averaged 72%; this value does not penalize the system for periods of planned outage required for test preparation and for days when no site personnel were present. Days unavailable (ranked in decreasing order of importance) were caused by problems with the Stirling engine, instrumentation and control, the parabolic dish concentrator, and the solar receiver. To minimize costs, a minimum spare parts inventory was on hand at the test site, which sometimes resulted in prolonged downtime. The system was actually operated without any interruption on 40% of the total days in the test period (213 out of 540). Unplanned outage days numbered 190 (35%) and planned outage days accounted for the remaining 137 days (25%).

Although system availability was reasonably high and although insolation and weather conditions were generally good, the Vanguard module was not operated during every opportunity hour. This is because the primary emphasis during the first year was not on maximizing power output, but instead on debugging the system and measuring performance characteristics. As a result, the module usually was not operated on weekends and holidays, accounting for the large number of scheduled outage days. (Advanco personnel worked on at least 40 weekend days or holidays when the test schedule required it.) Also, on many potential test days during the week, the operating staff was occupied in preparing for tests, writing up test results, or conducting tours for visitors.

Capacity factors were calculated using the conventional method, which severely penalizes a solar plant which can operate only during daylight hours and which attains peak outputs only at solar noon. The system capacity factor for the test period was 8%, based on the actual performance of the module for all 540 days. The capacity factor was calculated using a 20-kW net rating for the system. When sustained operation was performed during March 1985, a monthly capacity factor of 20% was attained. Overall, the module generated power on roughly 17% of all hours in the 18-month period. In March 1985, power was produced on 33% of all hours in that month. These values do not include any correction for nighttime periods, scheduled outages, or equipment downtime.

A predictive equation for determining instantaneous electrical power output from the module was derived by Advanco based on the demonstrated correlation between electrical power output and solar thermal power input. This equation includes corrections for reflectivity and ambient temperature variations around nominal values. These two parameters have been shown to have a significant effect on the performance curve of the system. ETEC verified this predictive equation by showing that it provides agreement with actual data to within 7% on both clear and primarily cloudy days. Other integrated-types of predictive methods developed by ETEC (utilizing bin data and all-day totals of electrical energy produced and solar energy input) provide similar accuracies. With some caution, these predictive tools may be used to estimate the energy output from a similar module at other prospective sites.

OPERATION AND MAINTENANCE

Throughout the 18-month test period, one person was required on site to monitor module operation and to acknowledge and clear alarms that occurred frequently. The system was designed and capable of hands-off operation, but was not tested in this regard due to recurring minor tracking problems that required operator assistance. In addition to the operator who also performed most of the data acquisition and reduction functions, a full-time field engineer was necessary to take care of system maintenance and repair and general shop duties.

A mobile two-man platform was especially useful in providing access to all mirror facets on the parabolic dish, to the Stirling engine, and to the radiator mounted adjacent to the engine. The 42-ft lift enabled personnel to reach and replace or adjust any mirror facet in the 10.7-m- (35-ft-) diameter dish.

The major material requirements for the dish/Stirling module were replacement mirror facets and make-up hydrogen gas. Approximately 20 mirrors were replaced over the test period due to breakage and delamination, and about 50 mirrors were replaced in May 1985, after these facets showed signs of desilvering. Total hydrogen consumption for the test period was 5300 cubic feet (23 cylinders) at a cost of about $530. The high hydrogen consumption reflects many plumbing system leaks which were either unlocatable or were not repaired. This figure can be reduced by improved leak detection and by developing ways to utilize more of the hydrogen in a cylinder--currently only half is used due to the design of the hydrogen delivery system.

Several problems occurred with the parabolic dish concentrator. Significant problems were encountered with the gravity slew system, which required substantial hardware modification. Limitations on space within the pedestal caused a number of initial tracking component problems. Electrical-related incidents included several control logic problems within the subconcentrator control unit, motor controller board failures, and the failure of the uninterruptible power supply to the tracker drive system. Problems with the mirror facets were varied, dealing with facet alignment, mirror delamination and occasional breakage, mirror desilvering, and the demonstrated potential danger from off-axis rays.

Operating events related to the receiver were the incidents that occurred during the development of an acceptable aperture cone, two independent material degradation problems, persistent problems with the water-cooled aperture plates, and occasional overheating of the receiver tubes during transient periods. A newly designed receiver utilizing a different material of construction was badly damaged from overheating.

Significant operation incidents related to the Stirling engine were two engine overhauls (for unrelated reasons), substantial power conversion unit noise and vibration, engine rpm sensor and shaft problems, on-going hydrogen leakage, and repetitive failure of the United Stirling monitor circuit boards. Check-valve failure was the reason for the initial engine disassembly, while the breakage of an oil pump shaft in the engine (with the concurrent replacement of unhardened gears) necessitated the second overhaul.

Routine and preventive maintenance activities are presented for each subsystem and an estimated frequency is given for each task. These data are derived from project experience, manufacturer's recommendations, and site observation. One item of specific interest is the method and frequency of mirror facet cleaning to maintain high dish reflectivity. Based on site reflectivity degradation data, it appears that the optimum process for the Rancho Mirage site is a simple 15-minute dish rinse accomplished every 4 days without rain. The reflectivity recovery is almost as great as that from washing/scrubbing the mirrors, and it takes only a tenth as much time.

SUBSYSTEM PERFORMANCE

The parabolic dish concentrator exhibited no structural problems during the test period. However, problems were encountered with other components of the concentrator. Some mirror-delamination problems were encountered early in the test program, but apparently were overcome by improvements in quality control during the bonding process. Slight desilvering of some mirrors were observed near the end of the test period. Numerous problems were encountered in electronic components used in tracking control. The emergency gravity slew system was occasionally unreliable and site personnel recommended several design changes to the system. Lack of space inside the pedestal caused some problems in the routing of wires and cables.

Although several minor problems with the solar receiver were observed, it nevertheless remained operational throughout the test period with the exception of one severe incident. The aperture material, though damaged occasionally from improper tracking, performed adequately for the test period. The receiver shutter plates provided a recurring source of problems due to their mechanical configuration. The plates would frequently not open when desired, causing several dish detracks and requiring operator action. Uneven working gas temperatures were observed in the four receiver quadrants, apparently due to an orientation-dependent convection heating of the upper tubes of the receiver throughout the day. A newly designed Inconel receiver was damaged from high gas pressure due to incorrect quadrant temperature measurements. Two separate material degradation problems were observed with the ceramic insulation and the multimet receiver tubes.

The Stirling engine required two overhauls during the test period, the first associated with a check-valve failure and the second with failure of a lubricating oil pump. Unhardened gears connecting the crankshaft to the generator caused excessive noise and may have indirectly caused the two aforementioned failures. Replacement with hardened gears in late 1984 solved these problems for the remainder of the test program. The USI display monitor and Stirling engine control circuit boards presented sporadic problems.

Engine performance was evaluated from fast-scan data taken with the IBM data acquisition system. Engine control appeared good, and a thermal lag during cloud transients of approximately 1 minute (solar input to energy output) was observed. The Stirling engine was cooled by a glycol-water mixture in a closed system so that essentially there was no significant water loss. This is an advantage for desert sites, where water is usually in short supply.

The Vanguard induction generator itself exhibited no problems during the 18-month test period, although there was a problem with an associated rpm sensor.

The interface between the utility grid and the Vanguard module was made through a Group Electric Power System (which could have accommodated up to 32 modules) and a Module Electric Power System. The interface worked well in normal connect and disconnect of power to and from the grid. However, following one of several loss of grid incidents, an engine check-valve problem was observed, which was attributed to extreme high gas surge transients caused by short-circuiting the engine.

In general, the instrumentation installed at the site performed satisfactorily with only minor exceptions. Outputs from various sensors were mostly analog signals. Calibration checks on key sensors in the middle and end of the test program revealed good accuracy and no change in calibration.

Two data acquisition systems were utilized. The first system acquired data on magnetic tape at 1-minute intervals from 82 sensors. These tapes were sent to JPL early in the test program and to ETEC later in the program for reduction to engineering values and for providing plots. The second system utilized an IBM-XT and a Keithley DAS to acquire data on diskettes by sampling 27 sensors at 4-minute intervals. An IBM-PC and a Hewlett-Packard 6-pen color plotter provided by EPRI permitted quick onsite analysis of key operating data and preparation of plots for progress reports.

RECOMMENDATIONS

GENERAL

The recommendations in this section of the report are based primarily on experience acquired and observations made during testing of the Vanguard module. However, the recommendations generally are applicable to all future developmental work involving dish/Stirling applications for the utility industry.

- Additional operating experience should be obtained with the parabolic dish concentrators, receivers, and Stirling engines to determine their useful lifetimes. The ability of mirror facets to operate for 10 to 20 years without delaminating should be evaluated. The extent of mirror reflectivity degradation with time at a specific site and the percent of initial reflectivity recovered with periodic cleaning at that particular site should be determined. Likewise for the Stirling engine, the number of operating hours between engine overhauls and of total lifetime should be determined. Deposits on the receiver have raised questions as to lifetime of the receiver tubes. As soon as possible, receivers with tubing made of the commercial alloy selected for production should be fabricated and tested over significant time periods.

- During the next phase of dish/Stirling development, greater emphasis should be on demonstrating the ability of a module to generate significant quantities of electricity day after day (insolation conditions permitting) over a very long period of time.

- Better status indication is necessary for the various tracking and standby modes of dish operation. It is sometimes difficult to determine from the recorded data when the dish was in each mode; this information is important to determine when the dish is tracking.

- Detailed guidelines should be established on how to record operating and maintenance data in the log book. Frequently, the recording of some data (e.g.,

meter readings, maintenance tasks) was inconsistent; on some occasions, specific information was recorded and on other occasions, the same type of information was not. Data that is necessary to determine module performance should be explicitly described and should be routinely recorded in the log book to aid subsequent performance analysis.

- Since the performance and acceptability of this module depends in part on the amount of net power produced, each auxiliary power parameter should have a separate sensor. The Vanguard module followed this practice with one exception. Tracking power, hydrogen compressor power, and a field receptacle were connected to a single sensor making it difficult to isolate individual contributions.

- The water-cooled receiver aperture plates had consistent problems throughout operational testing, due basically to the original design. A more reliable system of operation should be devised and the plates modified accordingly. A passively cooled plate design may function adequately in this service as well and this approach should be investigated further.

- It was found that black or grey colored polyethylene sheathed cable was susceptible to burning by off-axis rays of the sun. Since the possibility of off-axis rays always exists, future units should use Teflon or other white, high-temperature cable sheathing. If this is unavailable, cables may be sprayed with a commercially available high-temperature white paint.

- Currently, the module is automatically taken off line when a single problem is encountered by the system. This frequently is the result of spurious electronic interference with the controls, a connector, or a sensor, and is not an actual operational problem. Many large generating plants require two or more such incidents before the generating system is taken off line. This double-check feature should be evaluated for use in subsequent control software to prevent unnecessary detracks while operating.

- The failure of a check valve in the power control block of the engine necessitated the removal and overhaul of the engine. It is important to minimize the number of times the engine must be removed from the module. Therefore, the power control block check valve should be studied in greater detail to determine if this would be a recurring problem and, if so, to determine ways of improving it in future modules. Similarly, the failure of the rpm sensor/shaft

should also be fully investigated, since this event precipitated an engine overhaul and required significant downtime.

- It is recommended that further work on the effect of environmental parameters (temperature, humidity, wind speed, etc.) on the performance of the module be attempted. This may involve a multiple regression analysis with several variables. In order to provide good correlation, substantial performance data must be collected over as wide a range of environmental factors as possible.

- Stowage of a parabolic dish in a position facing the zenith is not recommended during summer daylight hours because of the unexpected impingement of off-axis rays on various parts of the module when the sun is at a high elevation. The zenith position is the most stable, however, during periods of high winds. The potential for wind damage should be balanced against the potential for off-axis ray damage to determine whether an alternate position would be more beneficial, or whether the various parts of the module susceptible to off-axis ray damage could be better protected.

- Based on the number of parts that failed and required either repair or replacement, effort should be made to retain on-site spares of those parts requiring substantial replacement time. This will reduce the downtime of the test module if similar problems occur in the future. As more operating experience is acquired, this list should be updated.

- At times, operating data was lost when the magnetic tape on the data acquisition system ran out and went unnoticed by the operators. To ensure good data collection, a hardware or software modification should be made to the data acquisition system to prevent this from occurring by giving a commensurate alarm that must be acknowledged by the operator. Alternately, the magnetic tapes could be changed every two data-acquisition days, regardless of the amount of tape remaining, in order to prevent partial days' data from being recorded on two separate tapes, with a gap in the middle. This will greatly simplify data reduction and analysis.

- It has been observed that offset values for some parameters drift slowly throughout the course of operation. Offset values should be checked periodically and the software used to reduce the data on site should be updated following any significant change.

- Calibration of crucial parameters (power, insolation) should be done every 6 months to ensure accurate reporting of test data.

- During testing of the Vanguard module, small hydrogen leaks were ignored if they did not seriously affect module operation. Since hydrogen leakage presents a significant economic drain on the revenue from module operation, all leaks should be found and repaired. It is important to determine how much unavoidable leakage of hydrogen exists in subsequent modules, so that the system may be redesigned if necessary.

- Data on failure rate of system components should be recorded to permit the comparison of anticipated failure rates of system components with actual data.

- Certain repetitive tasks that are performed on site should be governed by procedures to ensure that these tasks are properly performed and also to document the steps involved in the more complicated tasks. For example, reflectivity measurement involves the averaging of reflectivities from several facets across the face of the dish. The exact facets included in this measurement should be specified, and the procedure involved should be written down so that all operators perform the same sequence of steps. This will increase the reliability of data throughout extended periods of time when several people may perform the same duties. Other examples of tasks which may be included in this category are mirror facet replacement and facet alignment.

- The Master Concentrator Control (MCC) unit often locked up when entering commands. Ideally, one should be able to clear this problem by pressing the reset button on the MCC. Following a reset, however, the display did not always completely return. A complicated sequence of commands was required to get the MCC operating again. Software or hardware changes should be made so that the reset button is the only required action in this and similar situations.

- A printer option for the MCC would be very useful in accumulating test data. This option would allow screen dumps of the MCC onto a printer as well as programmed printer operation throughout the day for recording various MCC/SCC information and alarms.

- Several minor software and hardware modifications are recommended for the Sub-concentrator Control (SCC) unit. These are discussed more fully in the Subsystem Performance section under Instrumentation and Control.

- In conjunction with the previous recommendation, the feasibility of mounting a small hydrogen-gas cylinder and a hydrogen compressor adjacent to the Stirling engine should be explored. This should obviate the need for long runs of tubing, flexible joints to allow for dish rotation, and any valves between a centralized hydrogen supply system and individual modules; this in turn should eliminate the principal potential sources for hydrogen leakage. With a compact and relatively leak-tight hydrogen supply source, other Stirling engine test experience indicates relatively low hydrogen consumption. After the rate of hydrogen consumption is established, the optimum bottle size should be determined (five cylinder sizes are commercially available ranging from 2 to 260 cubic feet of gas at standard temperature and pressure).

- The ability of the dish/Stirling module to come on and off lines automatically and to operate unattended should be one of the performance goals of future versions of the dish/Stirling system.

- In a multi-module system following the Vanguard approach, a Master Control System will control a number of individual modules in a master/slave fashion. Because there was only one module at the Santa Rosa test site, the ability of the Vanguard Master Control System to control its complement of 16 modules was not evaluated. The ability of a Master Control System to function properly in all control modes should be evaluated in future tests. This could include both real and simulated inputs from individual modules. For example, if a Master Control System capable of controlling 16 modules could only be evaluated initially for multi-module control using only 4 modules, then simulated inputs could be used for the other 12 modules.

- An operating strategy should be derived which determines the most cost-effective approach for periodic washing of mirrors. The calculations should take into account revenues gains from increases in daily output of kilowatt-hours balanced against the costs of washing the mirrors. In addition, increase in receiver and engine life from a more uniform flux (reflectivity does not decrease uniformly on every mirror in the dish) must be considered, as well as effects of washing on mirror life and on ability to recover reflectivity values comparable to a new mirror.

Section 1

INTRODUCTION

Solar thermal technologies use solar radiant energy to produce heat that can be converted to mechanical or electrical power. An effective method for converting solar energy to electrical energy combines two relatively well known energy conversion technologies: (1) the parabolic dish-shaped reflective collector based on microwave and satellite communications antenna design and (2) the Stirling engine. The Stirling engine, which was invented in 1816, is presently the focus of major development to update its technology.

In this energy conversion process, as solar radiation strikes curved, mirrored surfaces on the parabolic dish, the solar rays are concentrated and redirected to a solar receiver. The receiver converts the radiant energy to thermal energy, which is transferred by high-pressure, high-temperature hydrogen gas to operate the Stirling engine. Mechanical power created from the engine is then used to drive an electric generator.

The Stirling engine is similar in some ways to a conventional internal combustion engine. The difference is that in the Stirling engine energy is supplied externally and continuously to heat a working gas (hydrogen or helium) within a completely closed system. The working gas flows through closely spaced tubing in the solar receiver, where it is heated by the concentrated radiant energy. Thermal energy is converted to mechanical energy in the Stirling engine, and rejected heat is dissipated through an air-cooled radiator. Stirling engine operating principles and Stirling cycle thermodynamics are discussed in Appendices A and B, respectively.

The combination of a parabolic dish collector and a Stirling engine has demonstrated overall efficiency (incident solar power to gross electrical power) of 25 to 30% or more with current technology. No other solar process is comparable in power conversion efficiency.

Point-focus, parabolic dish technology for solar applications was developed for the Department of Energy, Albuquerque Operations Office (DOE/ALO) by the Jet Propulsion

Laboratory (JPL) under an interagency agreement with National Aeronautics and Space Administration (NASA) and by Sandia National Laboratories at Albuquerque. In 1982, Advanco Corporation and DOE/ALO signed a cooperative agreement for the development of a new parabolic dish that would utilize a Stirling heat engine to drive an induction generator. Based on the agreement, a project was organized to design, construct, and test a solar-energy-powered, 25-kW electric generating module known as Vanguard I. For this project, Advanco assembled the following technology development team.

Team Member	Area of Responsibility
Advanco Corporation	Team leader/concentrator subsystem
United Stirling, Inc.	Power conversion system
Rockwell, Rocketdyne Division	System integrator
Electrospace Systems, Inc.	Solar tracking hardware and software
Onan Corporation	Generator and electrical equipment
Winsmith (Division of UMC Industries) and Sumitomo	Dish gear drive
Southern California Edison Co.	Utility design interface
Georgia Institute of Technology	Solar optics
Modern Alloys, Inc.	Concentrator foundation

As a result of efforts by the Vanguard team, a parabolic dish/Stirling engine module was designed and fabricated. By late 1983, the concentrator had been erected at a test site adjacent to the Santa Rosa Substation of the Southern California Edison Company (SCE) near Palm Springs. Early in 1984, the Stirling engine was mounted on the concentrator, and testing of the completed module was initiated.

The Electric Power Research Institute (EPRI) was invited to participate in the Vanguard program to provide a utility perspective to the overall plant performance evaluation. EPRI's broad-based interests in alternative energy sources would also benefit from the acquisition of operational test data.

EPRI retained the Energy Technology Engineering Center (ETEC), operated for DOE by Rockwell International, to (1) develop a Test and Evaluation Plan in cooperation with Advanco; (2) ensure that sufficient calibration has been performed to yield accurate test data; (3) serve as on-site monitor and representative of EPRI during periodic visits to the test site; (4) conduct an overview of data acquisition, reduction, and analysis; (5) perform independent data reduction and analysis to verify test results presented by the Advanco team; and (6) prepare a final project report.

Under EPRI auspices, ETEC, in cooperation with Advanco, developed a detailed test and evaluation plan intended to provide information on several topics of interest to utilities, investors, and potential users. The test program had the following objectives:

- Determine the ability of the Vanguard solar parabolic dish/Stirling engine module to produce electric power over a sustained period
- Determine the performance characteristics of system components and of the module by obtaining operating data under a variety of test conditions
- Collect and analyze data on installation, operation, maintenance, auxiliary load requirements, and reliability of the module and auxiliary components
- Develop performance correlations among module output, solar insolation, and other weather conditions to facilitate future assessment of similar modules at other geographic locations
- Provide an independent assessment of the performance of the Vanguard module

Key tests in the detailed test plan are summarized briefly in Appendix C.

The Vanguard module began operating in February 1984 with a small number of shakedown tests. This report describes the performance characteristics of the Vanguard module that were measured or observed during the 18 months of operational testing from February 1984 through July 1985.

Section 2

VANGUARD I CONFIGURATION

TEST SITE

The test site for the Vanguard solar parabolic dish/Stirling engine module is at 40701 Monterey Avenue in Rancho Mirage, California, about 10 miles southeast of Palm Springs, California, at a latitude of 33°45'. The test site is on Southern California Edison Company (SCE) property adjacent to their Santa Rosa Substation (Figure 2-1).

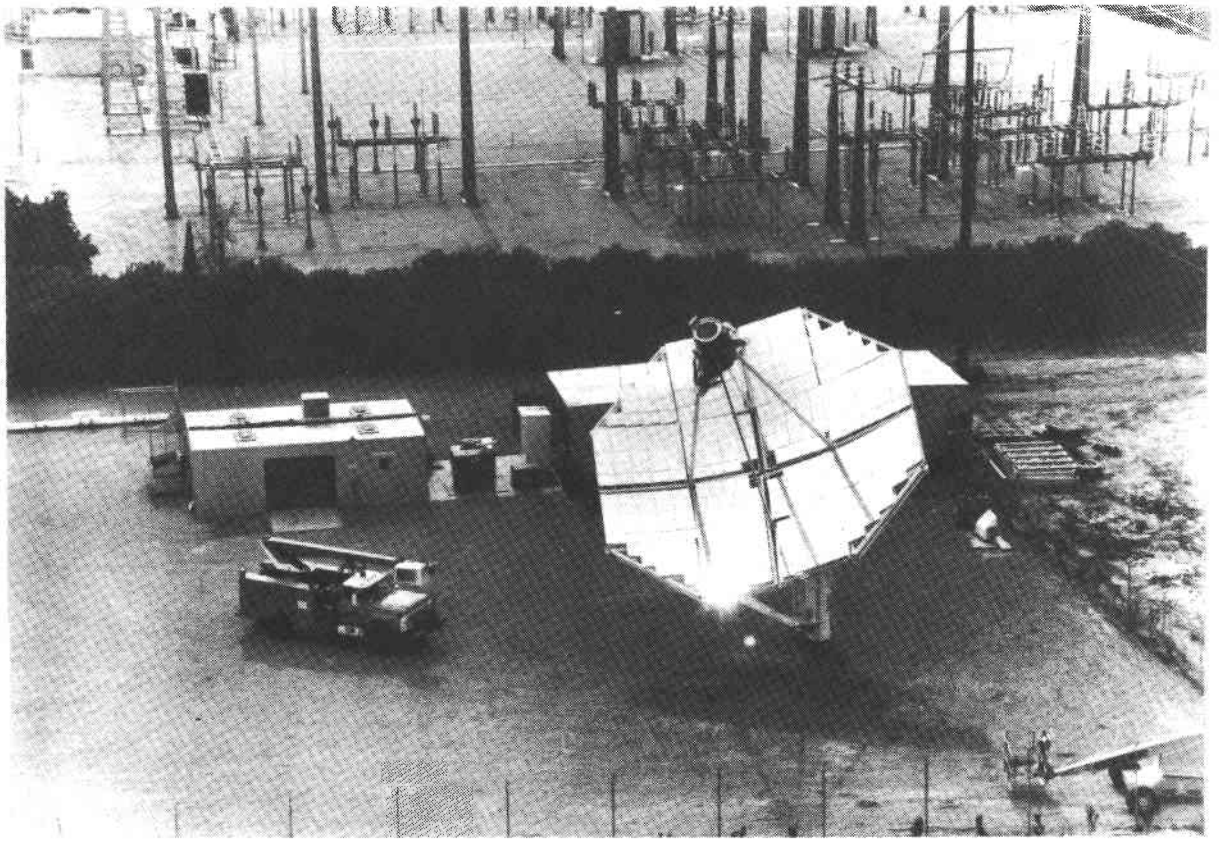

Figure 2-1. Test Site Adjacent to Santa Rosa Substation

The surrounding area is generally flat, with limited structures (Figure 2-2). To the west is a row of tall palm trees that blocks the sun in the late afternoon. There is no obstruction to the east and south. A nearby riding stable and a construction site cause significant dust to be thrown in the air from time to time. The expected daily average value for direct solar insolation is about 7 $kW \cdot h/m^2$.

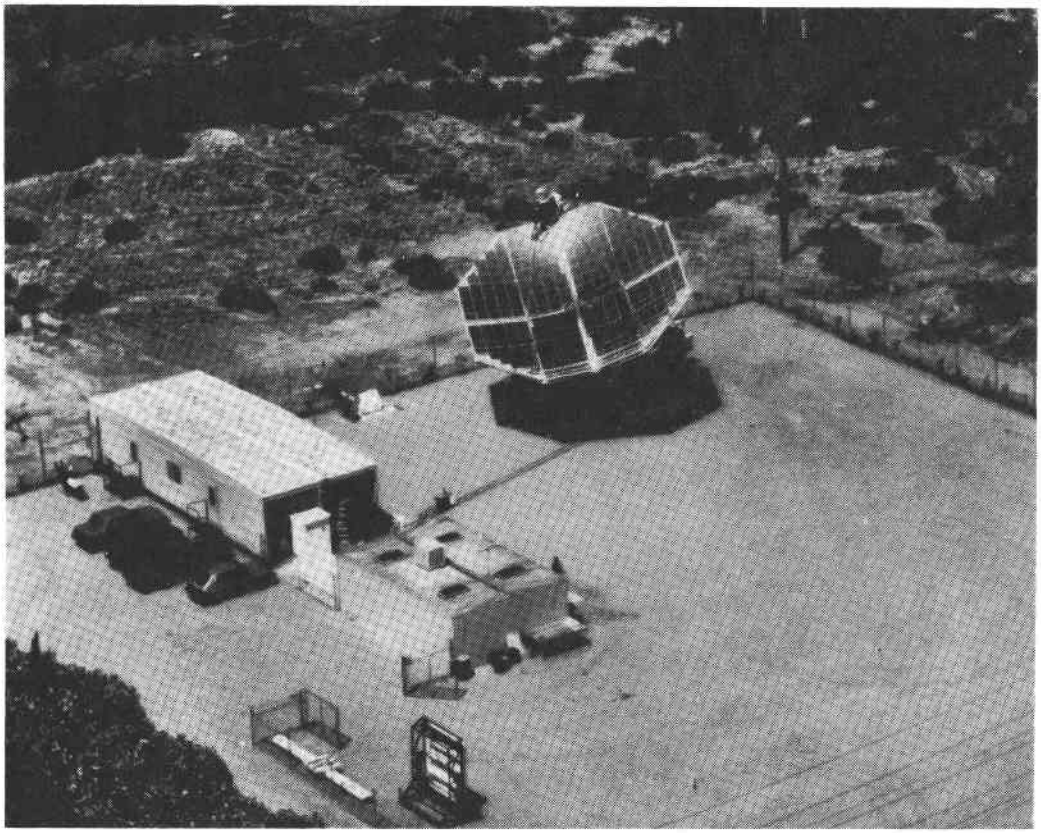

Figure 2-2. Aerial View of Vanguard I Solar Electric Generator

TEST MODULE

The test module is an integrated parabolic dish/Stirling engine system, consisting of the (1) parabolic dish collector; (2) solar receiver; (3) Stirling engine; (4) heat rejection equipment for the solar engine; (5) induction generator; and (6) associated electrical, instrumental, and control devices needed to initiate, control, and terminate operation. A schematic and a photograph of the test module are given in Figures 2-3 and 2-4, respectively.

Table 2-5

ALARM CLASSIFICATION FOR VANGUARD MODULE

TYPE X	TYPE Y	OTHERS
Gimbal synchro error (single)	Subconcentrator control unit (SCCU) watchdog	Ephemeral data error - inhibit coming out of stow in morning.
Gimbal counterclockwise limit (single)	Subconcentrator control unit (SCCU) error	High wind - slew to high wind stow position B (zenith).
Gimbal clockwise limit (dual)	Skew synchro error (single)	Master concentrator control unit (MCCU) watchdog - subconcentrator control unit (SCCU) will continue in mode last commanded by the MCCU and will monitor for possible contact closure from control room indicating a high wind condition. If this contact closure occurs, the SCCU will stow itself in the high wind stow position B. If the high wind condition ceases, the SCCU will stow itself in the north-facing position A.
Gimbal motor controller fault (single)	Skew motor thermostat (single)	
Stirling detract request (dual)	Skew motor controller fault (single)	
Gimbal motor thermostat (single)	Skew UP limit (dual)	
	Skew DOWN limit (single)	
	Excessive tracking error	
	Failure to react to type X alarm	
	Loss of grid	

Electrical Grid Interface

The electrical grid interface of the test site includes those items required to supply power when needed and to transmit power generated by the parabolic dish/Stirling engine module to the Southern California Edison grid. Necessary items include circuit breakers, transformers, a backup generator, and a ground-fault detection system.

Data Acquisition System

Two separate data acquisition systems existed onsite for testing the Vanguard module. These consisted of a DAS Series 520 front end (manufactured by Keithly Data Acquisition Systems, Inc., of Boston, Massachusetts) coupled to an IBM-XT computer and an Autodata Nine DAS (manufactured by Acurex Corporation) coupled to a Kennedy Model 1629 serial communications interface and a Kennedy Model 9800 reel-to-reel tape system.

Table 2-4

POINTS MONITORED BY SUBCONCENTRATOR CONTROL UNIT

Point	Message
Check sum on nonvolatile memory	CHECK PARMS
Timer not functioning	TIMER FAIL
Excessivse interrupt activity	INTERRUPT FAIL
Analog failure	ANALOG FAIL
Gimbal synchro error[a]	GIMBAL SYNC
Skew synchro error[a]	SKEW SYNC
Proximity alert	PROX ALERT
Gimbal counterclockwise limit (P2)	GIMBAL CCW
Gimbal clockwise limit (P2)	GIMBAL CW
Gimbal motor controller fault[a]	GIMBAL M/C
Skew UP limit (P2)	SKEW UP
Skew DOWN limit (P2)	SKEW DOWN
Skew motor controller fault[a]	SKEW M/C
Gravity slew mechanism tripped	SLEW TRIP
Gimbal stow error	GIMBAL STOW
Skew stow error	SKEW STOW
Gimbal movement failure	GIMBAL FAIL
Skew movement failure	SKEW FAIL
Excessive tracking error	TRACK ERROR
Ephemeral data error	EPHM ERROR
Gimbal motor thermostat[a]	GIMBAL THRM
Skew motor thermostat[a]	SKEW THRM

[a]This alarm is latching and requires acknowledgment at the console before the messagae will stop, even if the alarm has passed.

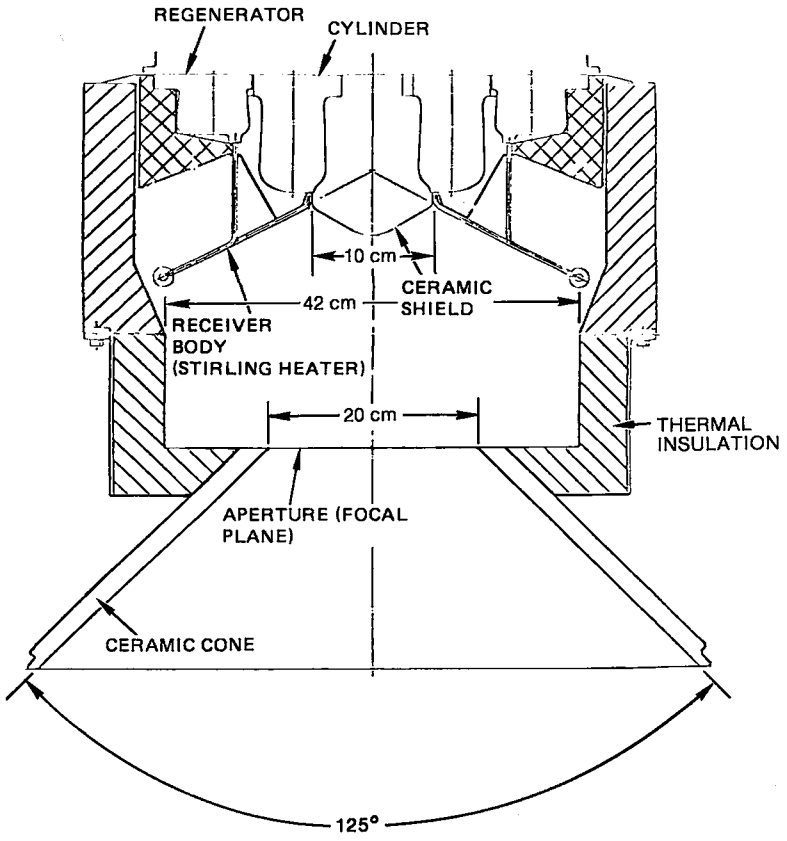

Figure 2-7. Relationship of Receiver to Aperture and to Stirling Engine

All alarms are classified into three categories: type X, type Y, and those that are neither X nor Y. A type X alarm is one where the concentrator is capable of slewing off-sun itself via the motors. A type Y alarm is one where the concentrator needs to use the emergency system to slew off-sun. Table 2-5 lists all the alarms that the control system is capable of acting on.

Certain type X alarms allow dual-axis movement to stow position A (north-facing), while others only allow single-axis (skew) movement. A dual-axis movement sequence involves 15° skew movement above the sun followed by dual-axis movement to position A. A single-axis movement sequence only uses the 15° movement in skew. Certain Y alarms allow gimbal movement, one allows dual movement, and some do not allow any movement except the weight's action. These are also noted in Table 2-5. If an alarm allows dual movement, and the weight has dropped for 15 seconds, both axes move to position A. Single-axis alarms result in only the gimbal axis moving to position A.

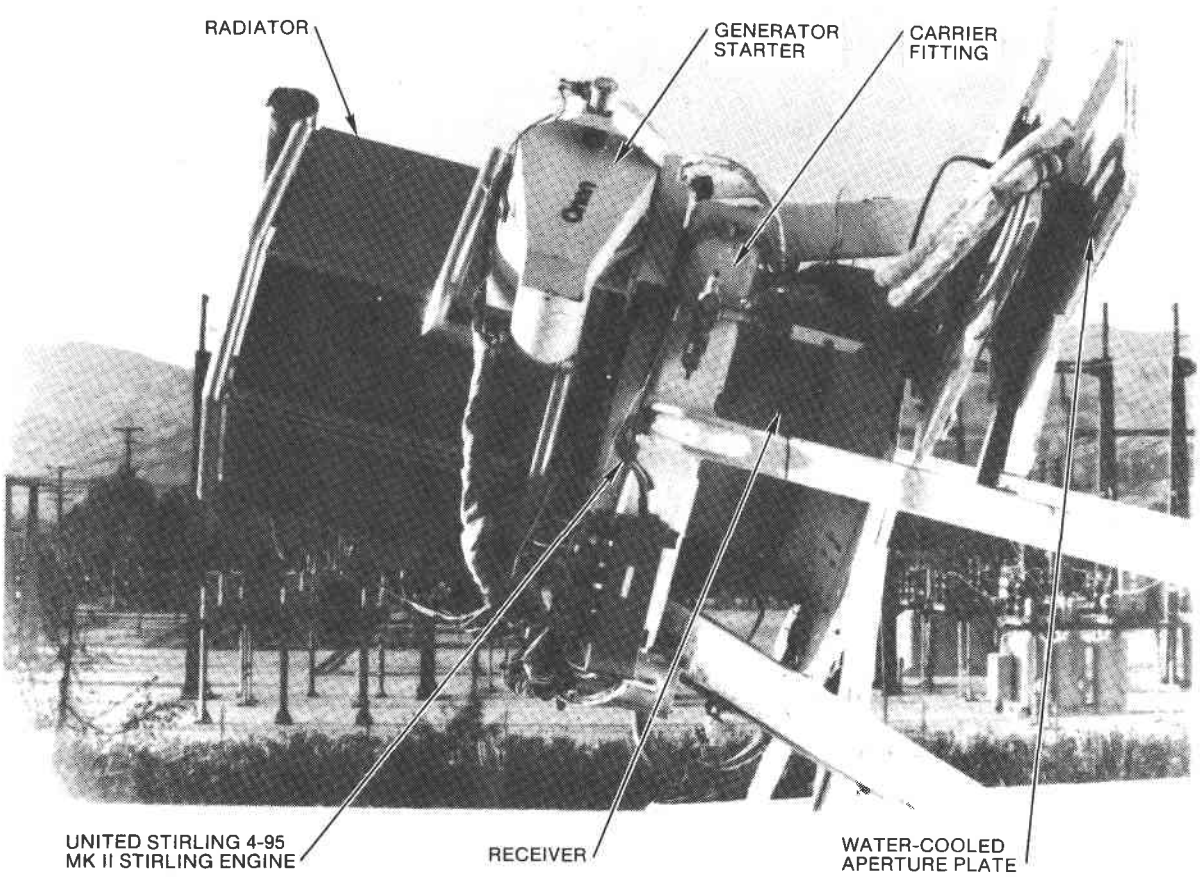

Figure 2-6. Main Components of the Power Conversion Unit

have its own control unit, designated a subconcentrator control unit (SCCU); and the group formed by these 32 modules would be controlled by a single master concentrator control unit (MCCU).

Detailed status is provided at the control console whenever a fault occurs. Each point monitored has an associated status message of up to nine characters in length. Table 2-4 lists the points monitored and the corresponding message. If more than one fault is reported at the same time, the display shows the various fault messages on an alternating basis.

Some of the alarms are put on a priority basis, meaning that the occurrence of a higher priority alarm will mask the possible occurrence of a lower priority alarm until the higher priority alarm has been cleared. The priority of affected alarms is also shown in Table 2-5 with a "P" followed by a number to indicate priority (1 being the highest priority).

electrical, instrumental, and control components. The PCU is mounted on the parabolic dish collector near the focal plane (see Figure 2-4). Additional design and performance characteristics of the PCU and its principal components are shown in Table 2-3 and in Figures 2-6 and 2-7.

Table 2-3

DESIGN CHARACTERISTICS OF THE POWER CONVERSION UNIT

Parameter	Value
Solar receiver	
Aperture diameter	20 cm
Heater head, ID	10 cm
OD	42 cm
Apex angle	125.2°
Flux average	60 W/cm^2
Maximum tube temperature	750°C
Stirling engine	
Working gas	Hydrogen
Efficiency, peak	41%
Number of cylinders	4
Swept volume	4 x 95 cm^3
Maximum gas pressure	12 MPa (1740 psi)
Induction generator	
Efficiency	93%
Speed	1800 to 1837 rpm (0 to 28 kWe)
Voltage	480 Vac
Phase	3
Power factor	0.85 nominal at full rated output
Power conversion unit	
Weight	690 kg (1521 lb)
Output rating, maximum	30 kWe

Instrumentation and Control

The parabolic dish/Stirling engine module is controlled through a supervisory control system. Although there is only one module at the test site, the instrumentation and control system is designed to handle up to 32 modules. Each module would

The Stirling engine output is controlled by varying its mean working fluid pressure to keep the receiver body temperature constant at different levels of solar insolation. This control and the power conversion unit (PCU) are located near the focal plane.

High- and low-pressure hydrogen gas lines, which traverse the dish outside the exocentric gimbal, are used to connect the focal-plane-mounted engine and the hydrogen gas-pressurization system, which includes a hydrogen compressor unit.

The key sensors, which are pressure, temperature, and engine rpm transducers, are tied to the PCU-mounted engine control box. This control box, which is linked with a control room monitor, provides the logic and control required for start, operate, stop, shutdown, transient, and emergency modes.

Induction Generator

A highly efficient induction generator, with its squirrel-cage rotor, is contained within a drip-proof enclosure. The induction generator, which is driven by the Stirling engine, delivers electrical power to the electric utility system.

The physics of induction machine operation governs the engine and generator rpm during generator operation and matches the generator load with the Stirling engine output power. During normal operation, excitation for the induction generator is derived from the connected electric utility.

The primary generator control utilizes an rpm input signal to either close ($\geq$1800 rpm) or open (<1800 rpm) the utility connection contactor. In addition to this primary control, the generator control also protects the generator against torque and current transients caused by loss of utility power, short-term transients, or Stirling engine overspeed after loss of utility. Protective equipment is also provided for protection against line-to-line faults and lightning-induced or utility voltage transients.

Power Conversion Unit

The Power Conversion Unit (PCU) combines several of the components described above, including (1) the solar receiver; (2) the Stirling engine; (3) heat rejection equipment for the Stirling engine; (4) the induction generator; and (5) associated

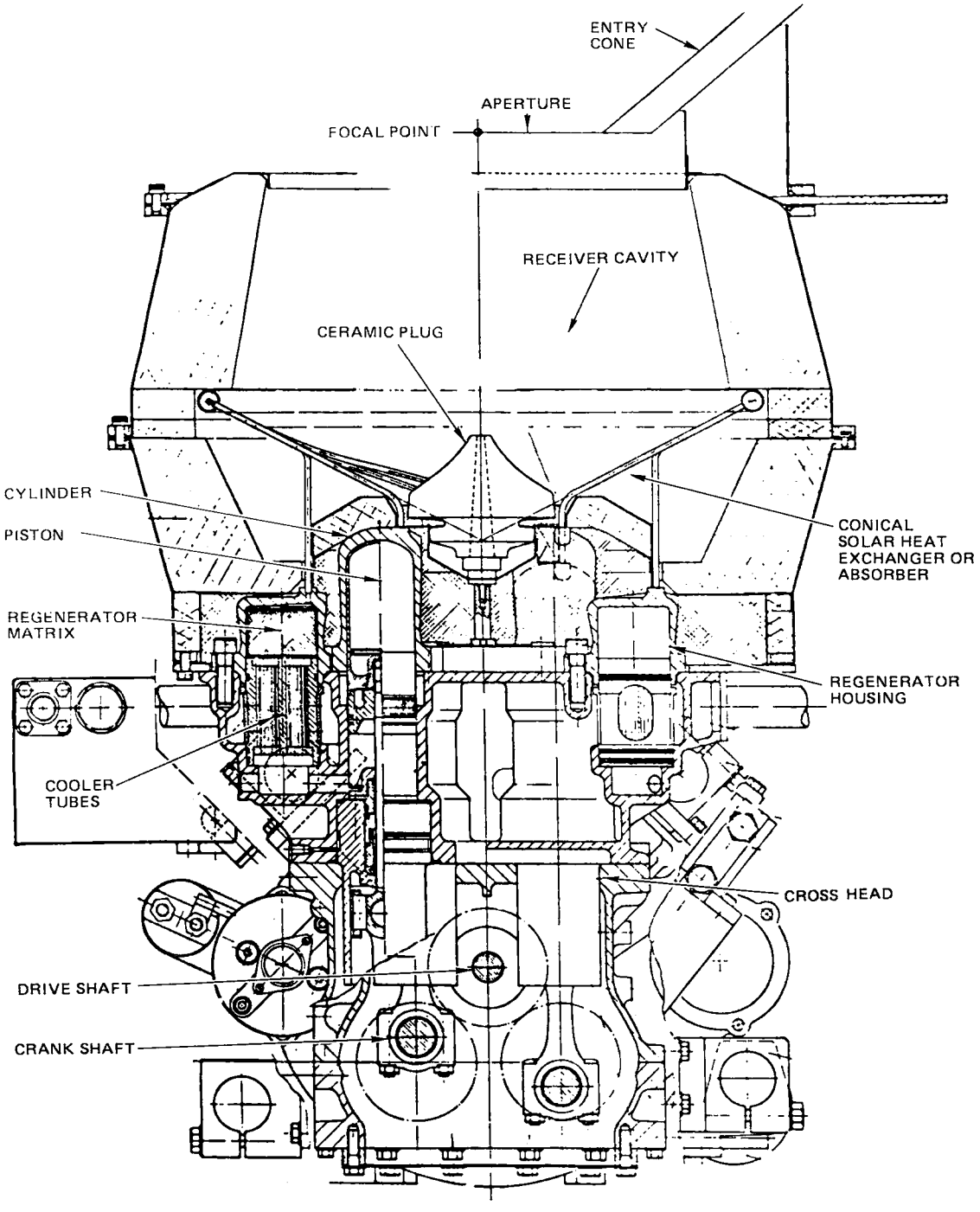

Figure 2-5. Cross Section of Stirling Engine with Solar Receiver

Table 2-2

DESIGN CHARACTERISTICS OF DRIVE MOTORS AND SPEED REDUCERS

	Skew Gimbal Motor Assembly	Azimuth Gimbal Motor Assembly
Input at 1750 rpm	0.75 hp	0.75 hp
Slew rate	60°/min	30°/min
Output	930 ft·lb	1450 ft·lb
Speed reducer ratio	841	1711
Overall ratio	10,176	20,703

Solar Receiver

The solar receiver comprises (1) the receiver body (a heat exchanger for transferring the solar insolation energy to the engine working fluid), (2) the aperture ring, (3) thermal insulation, and (4) the exterior housing. The receiver body consists of many small-diameter, high-temperature alloy tubes through which hydrogen gas flows at varying pressures. The pressure is varied as the insolation level changes to keep the working fluid and receiver body at constant temperature.

Stirling Engine

The 4-95 Solar MKII Stirling engine is a 4-cylinder, double-acting design with a 95-cm^3 displacement per cylinder (see Figure 2-5). It consists of parallel cylinders arranged in a square pattern and interconnected by a heat exchanger (a cooler, regenerator, and receiver body).

The engine is built up from three assemblies: a drive unit with crankcase, a cylinder block, and a receiver body. The drive unit uses twin crankshafts geared to drive a central output shaft, which also serves as a balancing unit. The receiver body is divided into four identical quadrants, each composed of a cylinder, two parallel-coupled regenerator housings, and 18 receiver body tubes. The crankcase and lubrication system is designed to function with the Stirling engine in an inverted position.

Waste heat is removed from the engine by circulating a water-glycol mixture to an aluminum radiator, where the heat is rejected to the atmosphere by fan-blown, forced-air cooling.

The support truss provides support for the facet racks and is fabricated from plate and tubular steel sections. The truss provides the structural depth necessary to assure optical alignment of the facets both under deadweight and active load. The support truss is also a transition between the exocentric gimbal and pedestal, and the carrier fitting and struts. The carrier fitting and struts provide a means for supporting and locating the receiver/Stirling engine and provide a means of locating the power conversion unit assembly at the focal plane. The fitting is the attachment point of the focal plane components; the struts support and index the fitting.

The exocentric gimbal connects the support truss to the module pedestal assembly. The gimbal is comprised of two joints, at 45° to each other, to form an upper elbow joint with its axis through the modular rotatable center of gravity and a lower shoulder joint with its axis perpendicular to ground. This configuration eliminates the need for vertical motion of the rotatable center of gravity and provides advantages of reduced gimbal drive loads.

The module pedestal assembly transmits the wind and deadweight loads from the exocentric gimbal into the pedestal footing. The pedestal is fabricated from 76.2-cm (30-in.) diameter, 0.95-cm (3/8-in.) wall, 6.7-m (22-ft) long steel pipe. The pipe is placed 3.7 m (12 ft) into the ground and encased with 15 to 30 cm (6 to 12 in.) of concrete. The annular concrete structure surrounding the pedestal assembly is designed to transmit all applied loads of the module into the site soil.

Gimbal Drives. Two drive motors are required: one for 45° skew gimbal rotation, the other for the azimuth gimbal rotation. These drive motors, along with the speed reducers, ring/pinion gearing, and cabling, are mounted within the exocentric gimbal housing to eliminate dust and sand buildup on the mechanisms. The design characteristics of the drive motors are presented in Table 2-2.

To hold the parabolic dish collector at either of two stow positions (zenith and north-facing), locking pawl assemblies are installed on both gimbals. Also installed on the 45° gimbal motor assembly is a gravitational emergency slew system to drive the dish off-sun in the event of a power outage or an alarm condition that prevents operation of the 45° gimbal motor.

Appropriate sensors and devices are provided for (1) tracking control, (2) power to the drive motors, (3) component fault data, (4) performance test diagnostic data, and (5) module supervisory control.

surface; (2) support structures; (3) gimbal drives; and (4) electrical, instrumentation, and control components. The design and performance characteristics of the parabolic dish concentrator are shown in Table 2-1.

Table 2-1
DESIGN AND PERFORMANCE CHARACTERISTICS OF THE PARABOLIC DISH CONCENTRATOR (PDC)

Parameter	Value
Optical:	
Dish diameter	10.7 m
Effective reflective surface area (projected)	86.7 m^2 (85.6 m^2 prior to 7 June 1984)
Reflectivity	93.0% (new and clean)
Blocking and shadowing factor	0.92
Focal length/diameter	0.58
Optical rim angle	45°
Energy at focal plane	63.1 kWt at 850 W/m^2 (62.3 kWt prior to 7 June 1984)
Tracking:	
Tracking error correctable by sun sensor	5°
Slewing speed	60°/min (skew gimbal) 30°/min (azimuth gimbal)
Concentrator weight, excluding power conversion unit and foundation	10,400 kg (23,000 lb)

Facet Reflector Surfaces. The concentrator reflector surfaces consist of curved, mirrored, optical-quality glass facets, 45.1 by 60.3 cm (17-3/4 by 23-3/4 in.) in size that form a physically discontinuous parabolic surface with a common focal point. Each facet is constructed by bonding a thin layer of back-silvered solar glass to a thick, lightweight structural layer of cellular glass. These facets are attached to facet racks that provide structural support and allow optical alignment. The original Advanco concentrator had 328 mirror facets with a projected area of 85.6 m^2. On 7 June 1984, eight more mirror facets were added to the dish perimeter, which boosted the projected mirror area to 86.7 m^2.

Support Structure. A total of 16 facet racks grouped at 4 per quadrant are fabricated from sheet metal tubes. These racks provide support for the facet mirror sections.

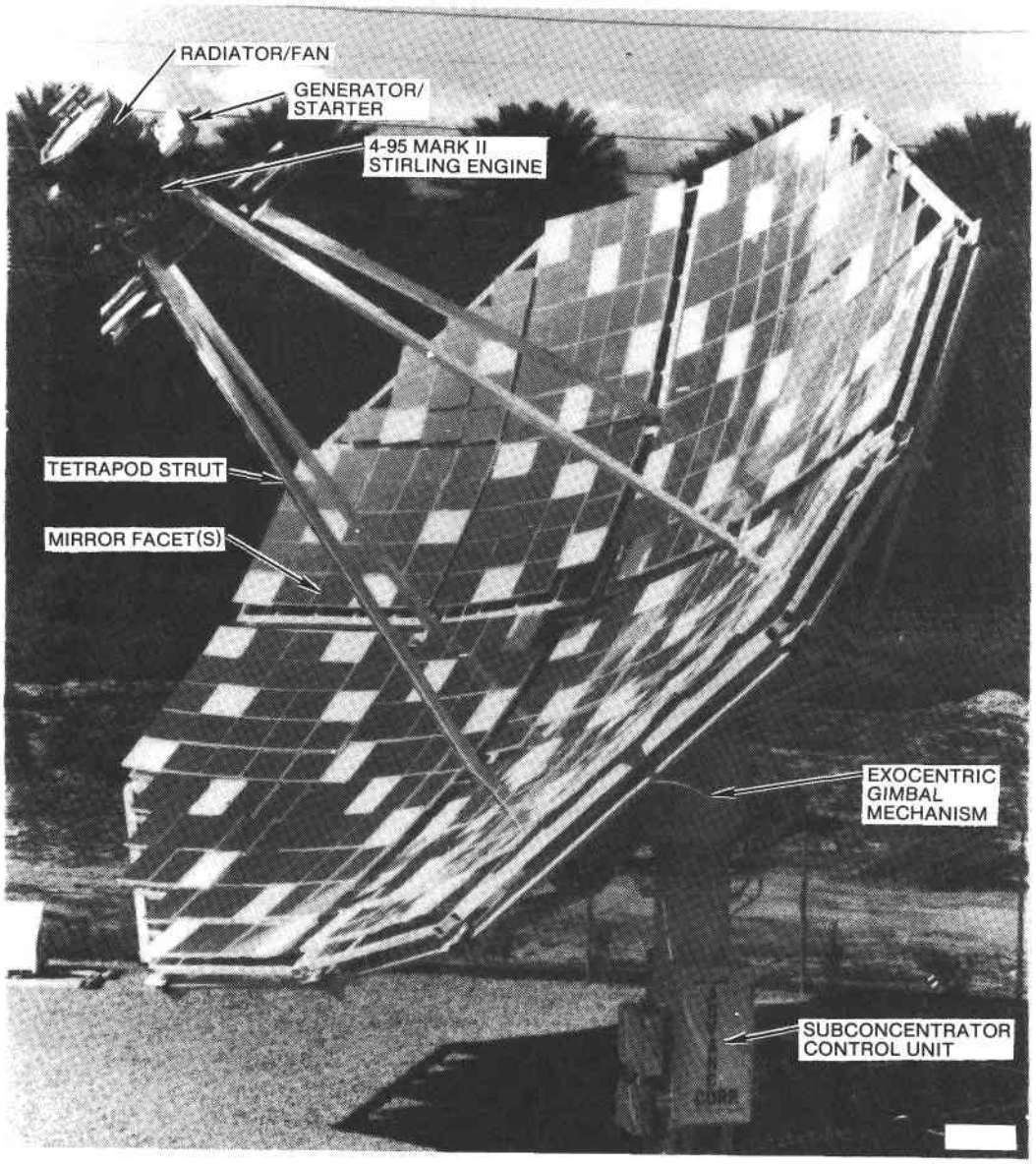

Figure 2-4. Main Components of Advanco Vanguard Module

stored face upward in the horizontal plane. One of the test objectives was to verify these design targets.

Parabolic Dish Concentrator

The parabolic dish concentrator collects and focuses the sun's radiant energy onto the receiver. The parabolic dish collector comprises: (1) the facet reflector

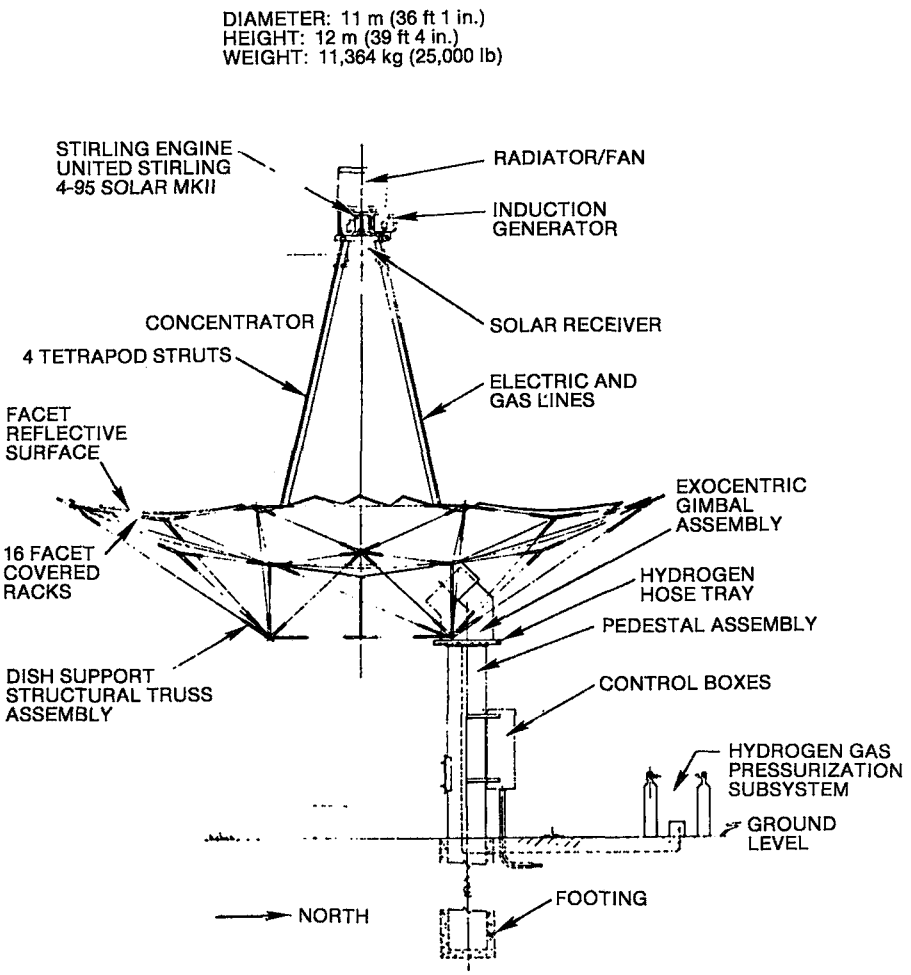

Figure 2-3. Vanguard Dish/Stirling Module

The parabolic dish collector tracks the sun in two axes and concentrates and redirects the radiant energy onto a receiver at or near the focal point of the paraboloidal concentrator. Heat energy from gaseous hydrogen circulating through the receiver is converted into mechanical energy by the Stirling engine. Reject heat from the Stirling engine is dissipated by pumping a mixture of glycol and water to an air-cooled radiator. The Stirling engine drives an induction generator to produce electricity, which is fed into the Southern California Edison utility grid.

The test module was designed to produce a net output of 20 kWe at 480 Vac, 60 Hz, at a direct normal insolation level of 850 W/m^2. The module also was designed to operate at insolation levels as low as 200 W/m^2 and as high as 1100 W/m^2 in ambient temperatures ranging from -25 to 50°C (-13 to 122°F). The module was designed to operate at wind speeds up to 30 mph and to survive wind speeds up to 90 mph if

The Autodata Nine system was the primary data-taking mechanism in the initial months of the project. In June 1984, the IBM-XT system was installed and is the preferred method of data acquisition and analysis because the data stored on magnetic tape with the Autodata Nine system cannot be reduced onsite. Differences between the two DASs are displayed in Table 2-6.

Table 2-6

DAS SYSTEMS FOR VANGUARD TESTING

	Keithley DAS/IBM-XT	Autodata Nine/HP-100
Sensors	27	82
Sampling interval	4 min	1 min
Operates	18 hours/day	During testing only
Storage	Floppydisk	Magnetic tape
Data reduction	Onsite	ETEC
Days of data	~10/disk	~3/tape

MODULARITY CONSIDERATIONS

Each Vanguard module will have a net electrical power generation capability of about 25 kWe at 1000 W/m^2. For larger power plant applications, preliminary studies by Southern California Edison Company have indicated that the optimum cluster size is a group of 32 modules, which corresponds to about 800 kWe. Thus, a larger power plant could be constructed using basic building blocks of 800-kWe capacity additions. The test assembly at Rancho Mirage included some of the features of the 32-module cluster, including (1) the master concentrator control unit, which can accommodate 32 subconcentrator control units; (2) the group electrical power system, which can accommodate 32-module electric power systems; and (3) a hydrogen compressor, which can accommodate 16 modules.

SCE study showed 32 modules optimum.

Section 3

OVERALL SYSTEM PERFORMANCE

This section discusses overall system performance. The performance of the Vanguard module is evaluated in terms of how efficiently it utilizes the available solar energy resource. Information is presented on electrical power production during the 18 months of operation. System availability and capacity factor are determined, and several means of predicting electrical output based on available solar energy are presented.

Because of manpower limitations, the dish/Stirling module usually was not operated on weekends, and there were only intermittent efforts to maximize power production over a substantial number of days. This leads to two alternative approaches in summarizing certain performance factors. One approach is to base the performance factors strictly on the historical record and take into account all the downtime that actually occurred. However, it could be argued that such an approach unduly penalizes the performance record and that a more accurate approach would be to eliminate from the performance calculations all downtime that probably could be avoided in a large, multimodule plant aimed at maximizing electrical power generation. Such a plant would attempt to operate every day of the year (weather and equipment availability permitting) and it would maintain enough replacement components to repair any failed equipment and restore the module to service by the following day. Because this approach is more useful in evaluating the potential of the dish/Stirling module, it has also been considered.

SOLAR RESOURCE

The solar resource for the parabolic dish concentrator represents the available beam radiation from the sun that is incident on the effective area of the dish. The solar energy received is often referred to in terms of insolation, expressed as a rate of energy per unit area (e.g., kW/m^2). In this section, the amount of solar energy available at the test site during each month of the year is estimated,

and the estimated and measured values are compared. A reasonably accurate estimate of the solar resource is needed to predict the potential of a given site for a particular solar application and to evaluate the monthly efficiency of a solar device in converting solar energy to electricity.

The rate at which solar energy arrives at the top of the earth's atmosphere is called the solar constant and is equal to 1.353 kW/m^2. As the solar radiation penetrates the earth's atmosphere, several different mechanisms come into play. Part of the radiation is reflected back into space (especially by clouds); part is absorbed by molecules in the air; and part is scattered by water droplets in clouds, by atmospheric molecules, and by dust particles.

Solar radiation that has not been absorbed or scattered and reaches the ground directly from the sun is called "beam" or "direct" radiation. It is the radiation of interest in concentrating collectors, because only the parallel rays can be focused accurately. The radiation received after scattering is generally referred to as "diffuse" radiation. The total solar radiation received at any point on the earth's surface is the sum of the direct and diffuse radiation.

The direct beam solar radiation is usually measured by an instrument called a pyrheliometer. The pyrheliometer is a small collimating device mounted on a drive mechanism that allows it to follow the path of the sun throughout the day. Total solar radiation is measured by an instrument called a pyranometer. The pyranometer is usually mounted horizontally in a fixed position, so that it can intercept scattered radiation from an entire hemisphere, as well as direct radiation.

The direct or beam radiation is the energy available for focusing by the parabolic dish collector-concentrator. The lower the sun's altitude, the greater the thickness of atmosphere through which the solar radiation must pass to reach the ground. On a clear day, the direct insolation increases from zero at just before sunrise to a maximum at solar noon, and then decreases to zero at sunset, as seen in Figure 3-1. At the Rancho Mirage test site, the direct beam radiation at solar noon occasionally exceeded 1000 W/m^2 on clear, cloudless days. On a cloudy day, if a cloud passes directly between the sun and the concentrating device, the moisture in the cloud can block or scatter some or all of the direct radiation impinging on the concentrator and thus greatly reduce solar energy input.

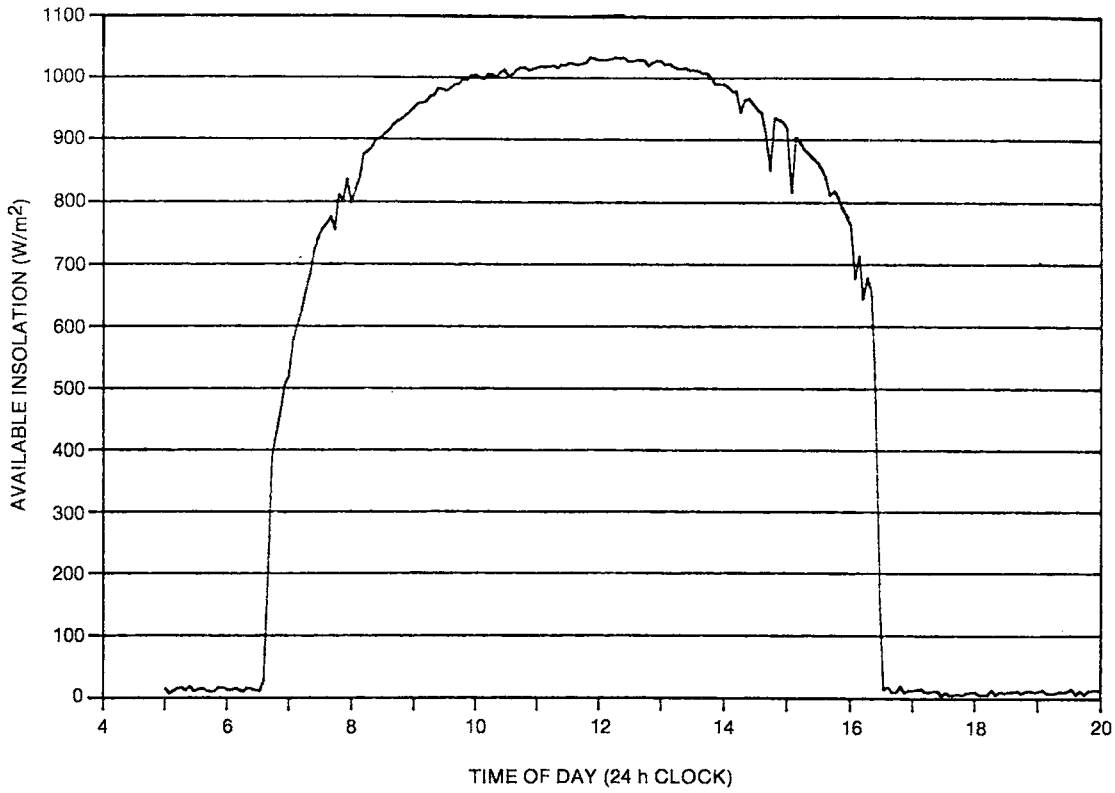

Figure 3-1. Typical Insolation Curve with Peak Insolation Greater Than 1000 W/M^2

To evaluate the effectiveness of a concentrating device such as a parabolic dish/Stirling engine module at a particular site requires knowing the average daily direct insolation received on a monthly and annual basis. This average value is usually given in terms of $kW \cdot h/m^2 \cdot day$. Since 1977, the Southern California Edison Company (SCE) has been gathering data on direct and total insolation at several potential solar sites including Palm Springs and Yucca Valley in the low-desert region and various cities in the high desert. The Palm Springs data are obtained at the SCE Service Center, about 7 miles from the Vanguard site. The Yucca Valley monitoring station is about 25 miles away from the Palm Springs test site. Figure 3-2 shows the relationship between direct solar insolation at these desert sites and their respective elevations above sea level. As expected, influence of the atmosphere on the amount of solar energy transmitted is less at higher elevations, and hence these sites show higher average daily levels of insolation. The variation in insolation levels between two sites only 30 miles apart (i.e., Palm Springs and Yucca Valley) points out that local climatic and physical factors must

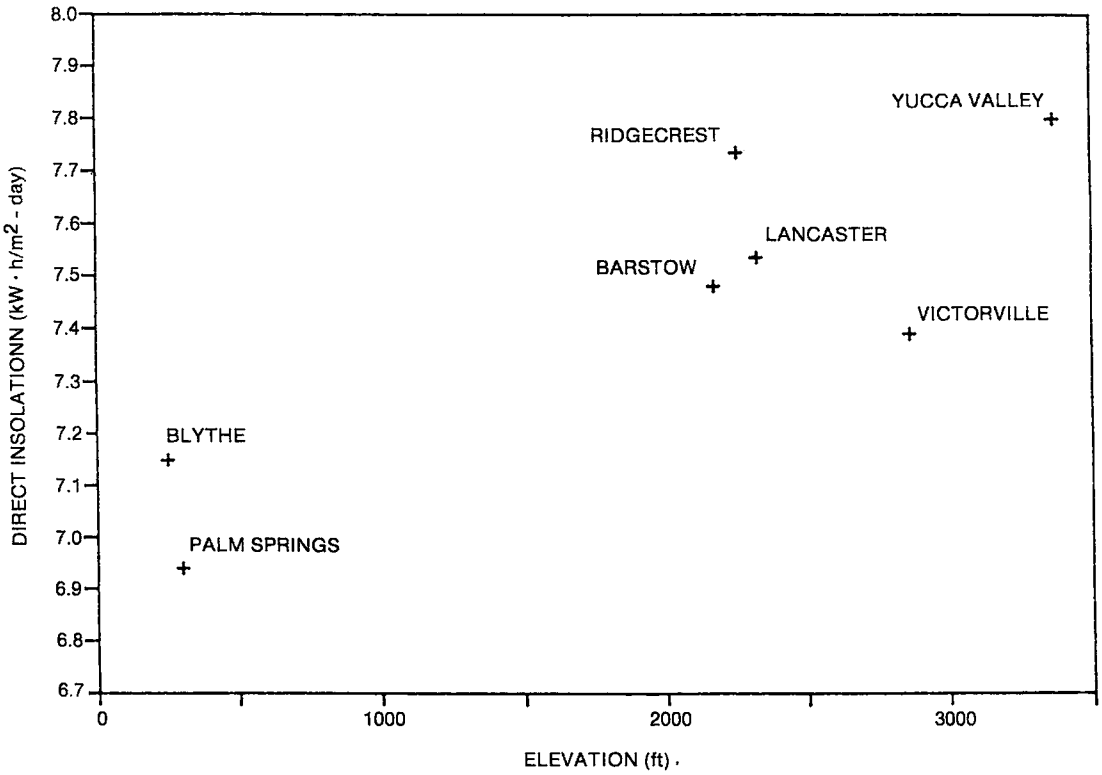

Figure 3-2. Annual Average Direct Insolation for Several Desert Sites

be considered in the search for a suitable site for a solar system. To predict the performance of a solar system at specific site requires reliable local data to ensure meaningful comparisons between potential sites.

Table 3-1 shows the average daily direct insolation measured by SCE during each month of the year from 1977 to 1983 at Palm Springs. This body of data will form the basis for comparing the direct insolation measured at the test site on an average day during any given month of the year with the previous 7-year average. In the February to mid-June period of 1984, direct insolation measurements were made at the Vanguard test site, but only during those periods when the Vanguard module was generating electricity. Starting in mid-June 1984, direct insolation measurements were made at the test site on a test day during the entire daylight period. Only direct insolation data recorded at the Vanguard test site were used in evaluating Vanguard performance.

Table 3-1

MONTHLY AVERAGE DAILY DIRECT INSOLATION AT PALM SPRINGS
FOR PERIOD 1977 THROUGH 1983

Year	Jan	Feb	Mar	Apr	May	Jun	Jul	Aug	Sep	Oct	Nov	Dec	Annual Average
1977	3.69	4.64	7.92	8.31	7.22	8.79	8.56	8.07	7.39	6.19	6.29	3.98	6.75
1978	3.52	5.75	5.85	6.94	8.79	9.63	9.14	8.62	7.79	6.23	5.72	5.12	6.93
1979	3.35	6.33	6.17	8.21	7.90	9.13	9.06	7.44	7.39	6.62	6.57	5.86	7.00
1980	4.00	5.14[a]	6.92	6.70	8.30	9.27	8.21	8.22	7.86	7.22	6.70	5.92	7.04[a]
1981	5.67	6.01	5.57a	7.49	7.24	9.11	8.08	6.48	6.59	6.91	5.72	5.18	6.59[a]
1982	5.23	5.04[a]	5.18	7.26	7.55	8.30	7.88[a]	5.59	5.77	5.45[a]	3.83	3.65	5.89[a]
1983	4.97	3.66	5.38	7.13	8.38	8.34	9.06	5.30	4.46	4.77	4.65	4.67	5.88
Monthly Average	4.17	5.22	6.13	7.42	7.91	8.94	8.57	7.10	6.75	6.20	5.64	4.92	6.52

[a]Interpolated value due to insufficient data.

In Figure 3-3, the daily direct insolation measured at the test site and averaged on a monthly basis for the June 1984 through July 1985 period is compared with the average predicted value based on SCE measurements obtained for the previous 7 years. In general, the average daily direct insolation over the 14-month period for which all-day measurements were made at the test site is close to the average predicted value and is usually within the maximum-minimum range. The 2 months with the widest differences between measured and predicted direct insolation values are July 1984 and July 1985. This discrepancy is probably due to the limited number of days in each of these 2 months in which available solar energy data were taken (14 and 7 days, respectively).

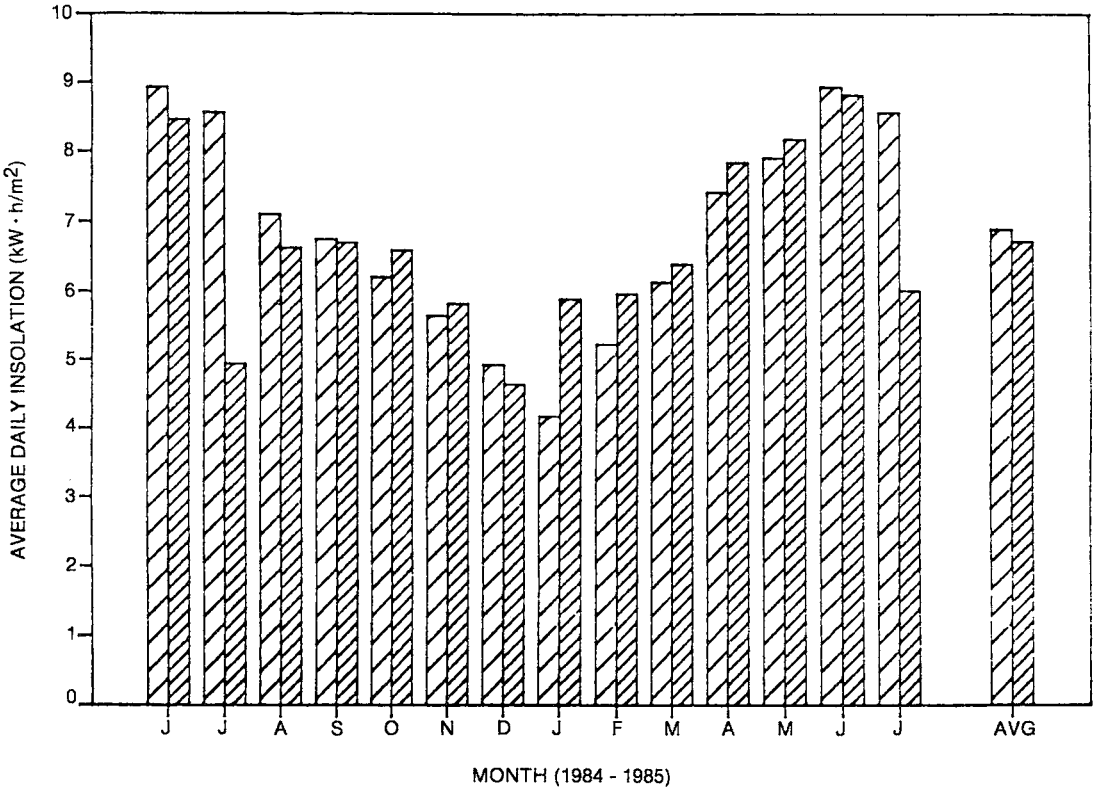

Figure 3-3. Monthly Average Daily Available Direct Insolation - Predicted versus Actual

ELECTRICAL POWER PRODUCTION

In evaluating the electrical power generating performance of an alternative and renewable energy resource, a utility is interested in several factors, including

(1) the amount of power that can be produced; (2) the specific time period during the day in which the power can be produced; (3) the variation, if any, of power production during a day, month, and year; (4) efficiency; (5) availability; and (6) capacity factor. Information derived on these performance factors during the 18-month period of operation testing is discussed below.

Summary of Gross and Net Output

The gross power production is the output of the generator in kilowatts before deducting any of the auxiliary power requirements of the generating system. The gross power output is of interest because it represents the power output that could be achieved if all auxiliary power requirements could be reduced to zero. Figure 3-4 shows the relationship between insolation and gross generated power throughout a typical day.

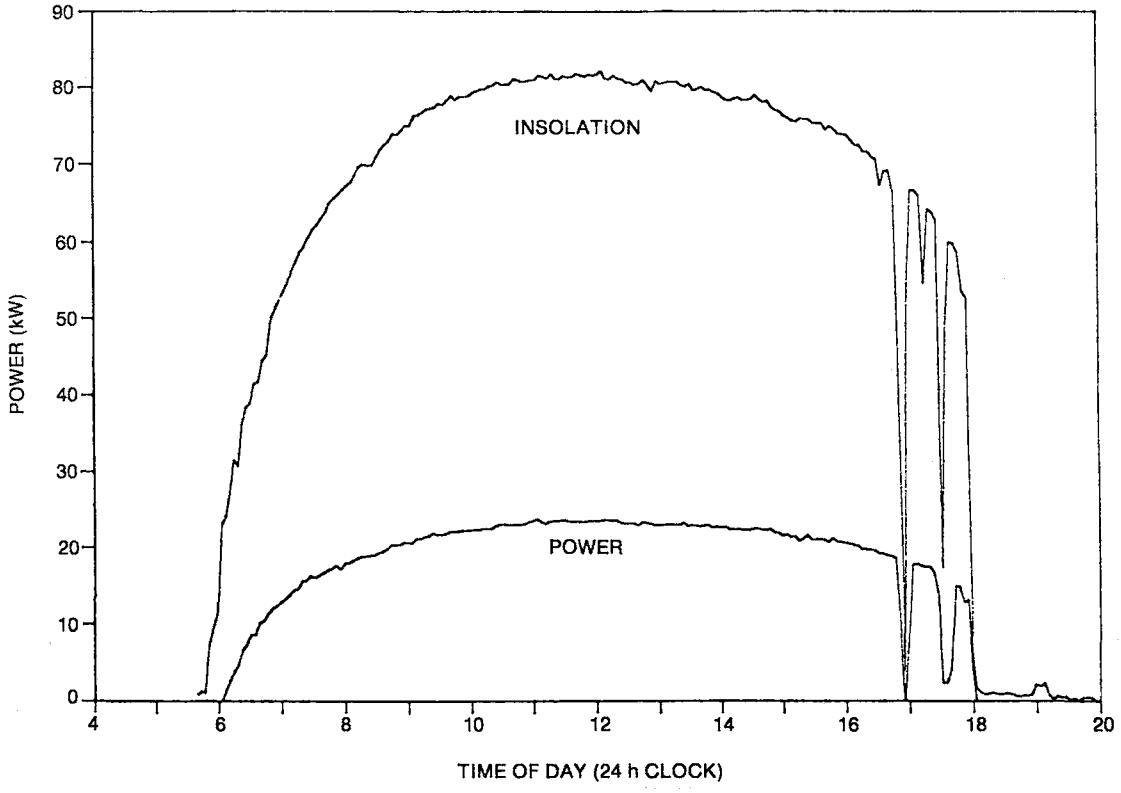

Figure 3-4. Typical Daily Curve of Thermal Incident Power and Gross Electrical Power

Net power output is the power delivered to the utility grid after deducting all auxiliary power requirements from the gross power output. In an electrical generating unit that does not operate around the clock, such as a solar unit, it is important to recognize that there can be some auxiliary power requirements that continue even when the unit is not operating. For example, the tracker for the Vanguard module consumes power even when the module is not operating during the day and also when it is in the standby mode of operation during the overnight period from sunset to sunrise. Hence, one must also consider the net electrical power production on a 24-hour basis throughout the year in evaluating performance. The gross and net outputs of the Vanguard module are summarized on a monthly basis for the 18-month test period in Table 3-2, and this information is presented graphically in Figure 3-5.

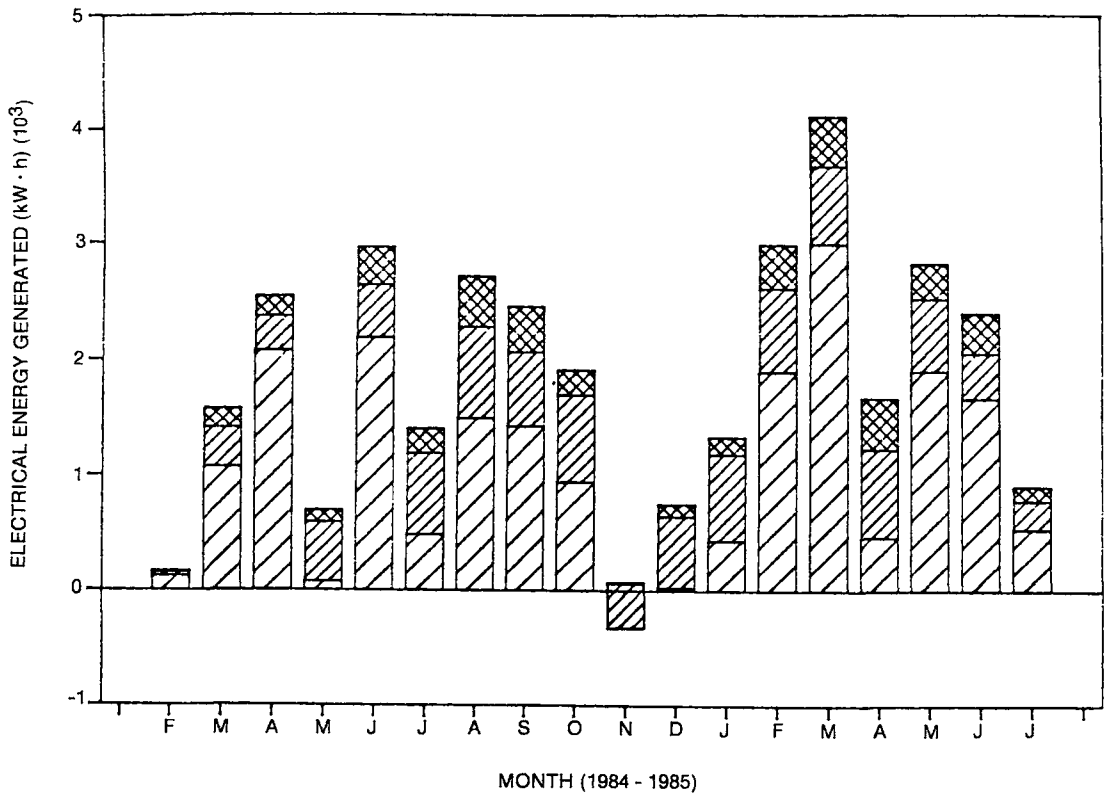

Figure 3-5. Summary of Electrical Energy Production on a Monthly Basis - Gross, On-Sun Net, and 24-Hour Net

Table 3-2

ELECTRICAL ENERGY PRODUCTION FOR TEST PERIOD

Month	Gross On-Sun (kW·h)	Auxiliary On-Sun (kW·h)	Net On-Sun (kW·h)	Auxiliary Off-Sun (kW·h)	Net 24-Hour (kW·h)
1984					
February	212	17	195	57	138
March	1,056	76	980	94	885
April	2,549	177	2,372	164	2,208
May	679	64	615	111	504
June	2,934	247	2,687	149	2,538
July	1,343	128	1,215	124	1,091
August	2,557	218	2,339	296	2,043
September	2,406	216	2,190	212	1,978
October	1,880	136	1,744	264	1,480
November	73	5	68	296	(228)
December	738	43	695	286	409
1985					
January	1,321	72	1,249	176	1,073
February	2,962	187	2,775	195	2,580
March	4,043	227	3,816	154	3,662
April	1,702	131	1,571	221	1,350
May	3,025	240	2,785	175	2,610
June	2,300	162	2,138	58	2,080
July	783	49	734	59	675
Total	32,563	2,395	30,168	3,091	27,027

During the 18-month test program (through July 1985), the Vanguard module had a gross electrical output of approximately 32,600 kW·h. The net electrical output delivered to the grid during operating hours was roughly 30,200 kW·h, and the net electrical output delivered to the grid, after taking into account auxiliary power requirements, on a 24-hour basis was roughly 27,000 kW·h, 90% of that of the on-sun period. The difference between the two net electrical outputs illustrates the importance of operating whenever possible and of minimizing auxiliary power requirements during times when the system cannot be operated. Although the preceding figures may be representative of results during initial phases of a developmental test program, higher net outputs for a similar time span might be expected in later

phases after initial operating problems have been solved, and when greater emphasis can be placed on maximizing the production of electricity.

Auxiliary power requirements for the dish/Stirling system are those associated with the cooling system for the Stirling engine, the tracking system for the parabolic dish, and the air compressor to open and close the receiver shutter plates. The engine cooling system requires about 0.9 kW to power the radiator fan and about 0.15 kW to pump the water-glycol coolant through the engine and radiator. The tracker requires about 0.7 kW when tracking during the daylight hours and slightly more than 0.5 kW when in the standby position overnight. The air compressor requires about 1 kW, but should only run about 10 seconds each hour. Thus, the auxiliary power requirements total about 1.75 kW when operating during the day, and about 0.5 kW when the module is in standby (at night and during some weekends and holidays). These power requirements for the tracker include about 0.3 kW for the gravity slew coil, regardless of whether the dish is tracking or is in the standby mode. Figure 3-6 shows a plot of gross power and total auxiliary power as a function of time during a typical operating day. The saw tooth pattern between 8 and 9 a.m. for auxiliary draw of power is due to the effect of the radiator fan turning on and off as required to maintain engine coolant temperaure. As the coolant warms up and as the generated power level increases, the fan remains on continuously to maintain coolant temperature. The sharp spikes that occur around 1 p.m. and 3 p.m. are due to the activation of the air compressor. Since data points are only taken every 4 minutes on the IBM system, the short, almost instantaneous power draw of the air compressor occasionally goes unrecorded. However, integrated auxiliary power over the day measured by a watt-hour meter is based on continuous measurement and includes all periods of air compressor operation. Figure 3-7 shows a similar plot of the parasitic loads described above with an expanded power scale to permit a more detailed examination of the individual auxiliary power requirements.

The tracking system was energized continuously during the test period for three reasons. First, if high wind conditions occurred during the night, the dish should automatically move to a different stow position than is normally required to minimize damage to the concentrator. Maintaining the tracking system in the standby mode allowed it to move the dish to a safer position if the need arose. Second, the voltage spikes that occur when the tracking system is turned on and off might have shortened the life of the electrical components. It was felt that leaving the system on and using energy was more cost effective in the long run. Third, any

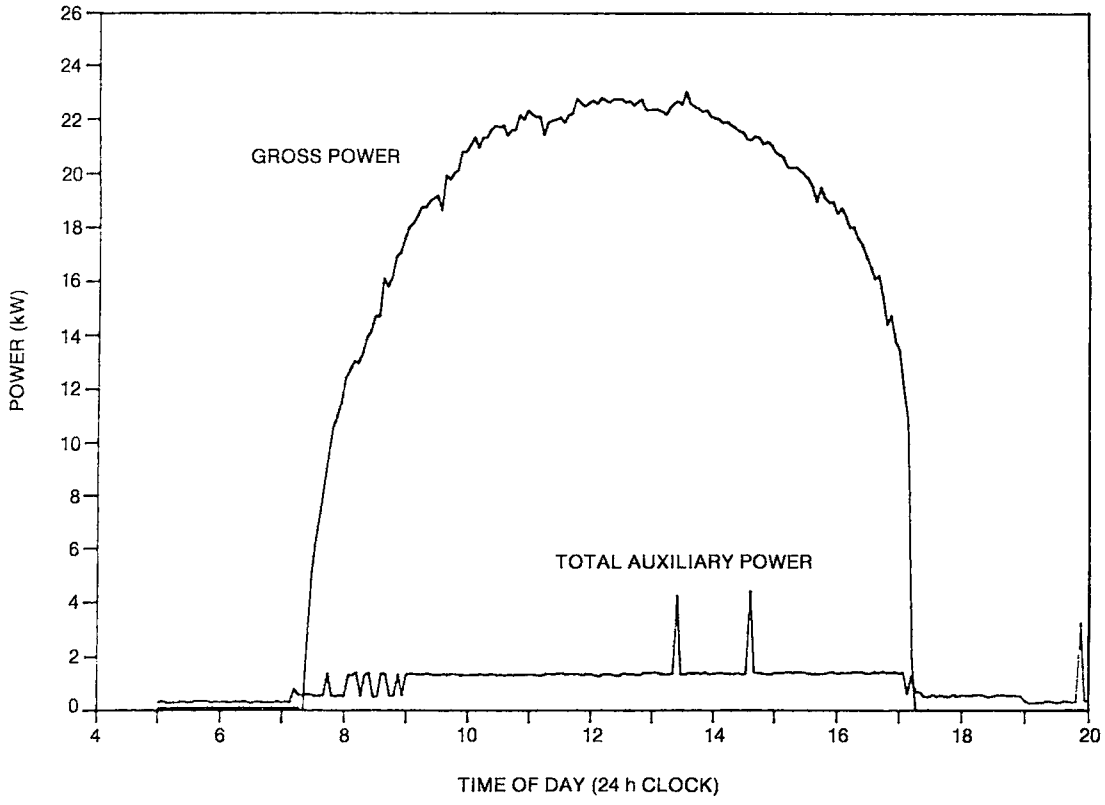

Figure 3-6. Typical Daily Curve of Gross Power Generated ant Total Auxiliary Power Required

moisture that might build up inside the control and drive system could have damaged sensitive electronic components. Therefore, the heat generated by leaving the tracking system on continuously helped to prevent moisture buildup.

Auxiliary power was usually fairly consistent, although some variability was noted, particularly in tracker power. The tracker power included 10-second draws of power for the air compressor used to provide compressed air to open and close the water-cooled aperture plate. Tracker power also included occasional power demands imposed by the use of a field receptacle supplying power for hand tools. Figure 3-8 shows the predicted auxiliary power load for a typical operating day.

Auxiliary power requirements for each month of the 18-month test period are also shown in Table 3-2. On-sun auxiliary energy requirements were about 7% of the gross power output. During the 18-month test period, off-sun auxiliary energy requirements were 10% of gross output. Therefore, total on-sun and off-sun auxiliary

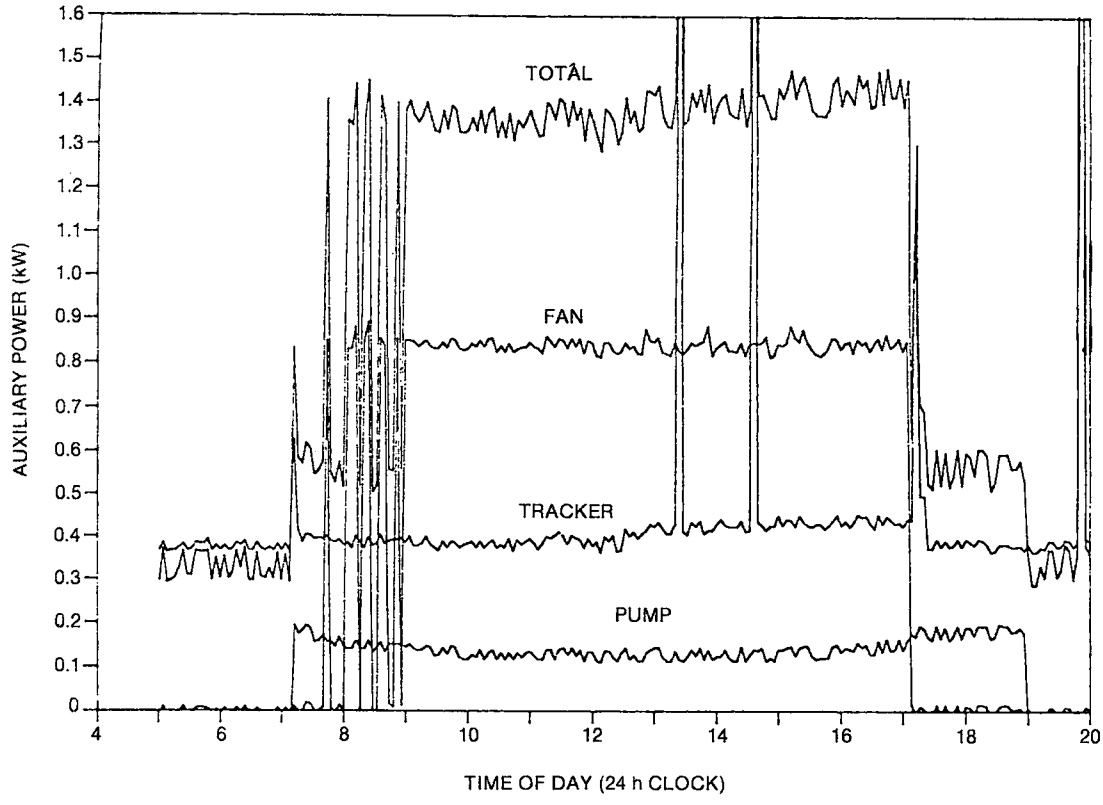

Figure 3-7. Individual Auxiliary Power Requirements (12 October 1984)

energy requirements represented about 17% of the gross electrical output during the test period. Although it is unlikely that on-sun auxiliary energy requirements can be reduced significantly, the same is not true for the off-sun auxiliary load, which is a larger percentage of gross output. Off-sun auxiliary energy requirements as a percentage of gross output can be greatly reduced by operating more frequently (e.g., the Vanguard module usually was not operated on weekends or holidays or during preparation for a test). If the module had operated during all periods when it was available (72% of total sunlight hours), the off-sun auxiliary energy requirements would have been approximately 6% of the gross output. Assuming no unplanned outages during the test period (100% availability), the off-sun auxiliary energy requirements would only have been about 4% of the gross electrical output. On-sun auxiliary energy as a percentage of gross output for the above cases would remain essentially constant at 7%. Besides increasing the operating frequency, attention also should be directed toward the possibility of reducing the off-sun auxiliary energy requirements (e.g., the tracking draw).

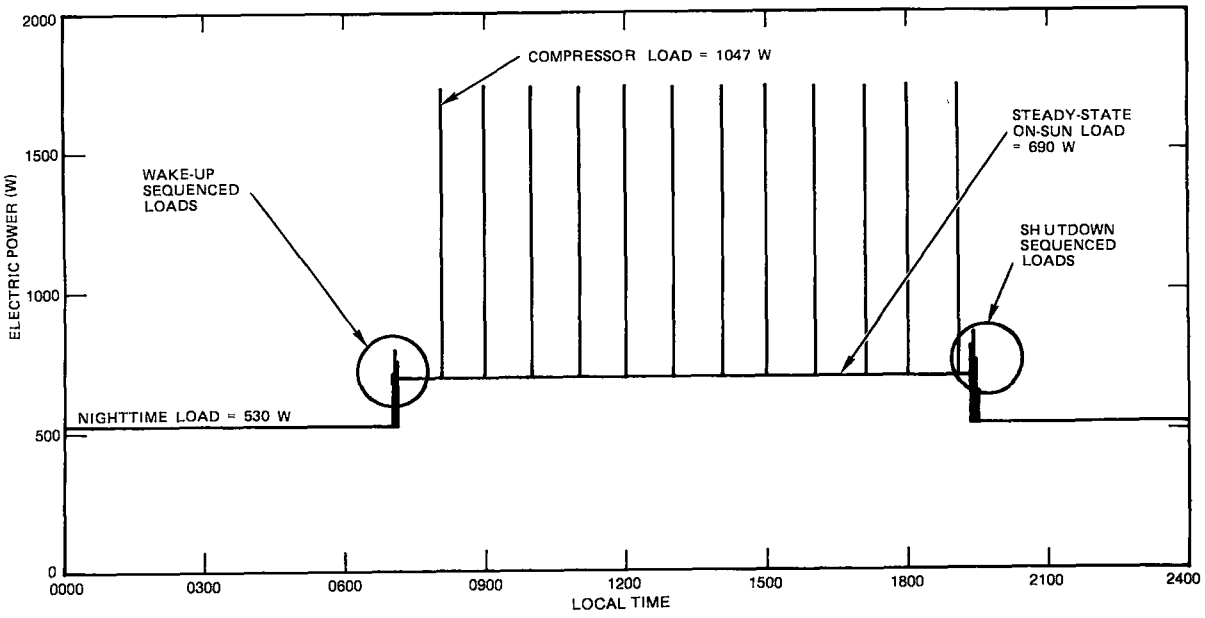

Figure 3-8. Idealized Histogram of the Auxiliary Power Load for a Typical Operating Day

Solstice and Equinox Performance

A solstice occurs twice a year when the sun is at its greatest distance from the celestial equator: about 21 June, when the sun reaches its northernmost point on the celestial sphere, and about 22 December, when it reaches it southernmost point. An equinox occurs when the sun crosses the plane of the earth's equator, making night and day of equal length all over the earth; this also happens twice a year: about 21 March (vernal or spring equinox) and 22 September (autumnal or fall equinox).

These periods are of interest in characterizing the output of a solar unit. All other things being equal, one could expect the highest and lowest output in kilowatt-hours to occur on the longest and shortest day (summer and winter solstice), respectively. This may not always occur because a winter day could be clearer with higher peak values of direct insolation than a longer hazy summer day. Moreover, as will be discussed below, a decrease in the ambient temperature is reflected in a decrease in the engine coolant temperature, which causes an increase in the power output of the Stirling engine. The equinox days are more representative of an average day during the year.

During the summer solstice in June 1984, the Vanguard module participated in a summer "olympics" for the various solar projects Southern California Edison (SCE) has under evaluation. The Vanguard module was operated from dawn to dusk during a 15-day period (for 1 week preceding and following the summer solstice). It set several performance records for solar thermal applications during this period, as shown in Table 3-3.

Table 3-3

PERFORMANCE RECORDS SET BY VANGUARD MODULE DURING JUNE 1984

Highest instantaneous gross conversion efficiency	31.6%
Highest instantaneous net conversion efficiency	29.4%
Highest daily average gross conversion efficiency	27.4%
Highest daily average net conversion efficiency	25.2%
Highest daily gross electrical output per collector area	2.74 $kW \cdot h/m^2$-day
Highest daily net electrical output per collector area	2.52 $kW \cdot h/m^2$-day

The performance of the Vanguard module during the periods closest to the solstice and equinox periods is summarized in Figure 3-9 in terms of average daily gross electrical output. Only days in which the module was operated during all daylight hours are included in the solstice and equinox data summarized in Figure 3-9. Good agreement is obtained between the three equinox periods. The average electrical output for the summer and winter solstice periods is higher and lower, respectively, than for the equinox periods, as might be expected. Problems with the receiver prevented the module from operating during the summer solstice in June 1985.

Clear and Cloudy Day Performance

Because a high percentage of the total radiation from the sun can be blocked or scattered by clouds passing between the sun and the parabolic dish concentrator, there can be a pronounced degradation in the performance of the solar unit on a cloudy day. This is particularly true of solar units involving concentrating devices, as they utilize only direct (unscattered) insolation. On totally overcast days, the gross output of the module is zero. On partly cloudy days, however, the module can produce power whenever sufficient beam radiation is available.

During the 18-month test period, it was observed that slightly overcast days caused a small reduction in incident energy impinging on the parabolic dish and a consequent small reduction in electrical output. On bright days with scattered discrete

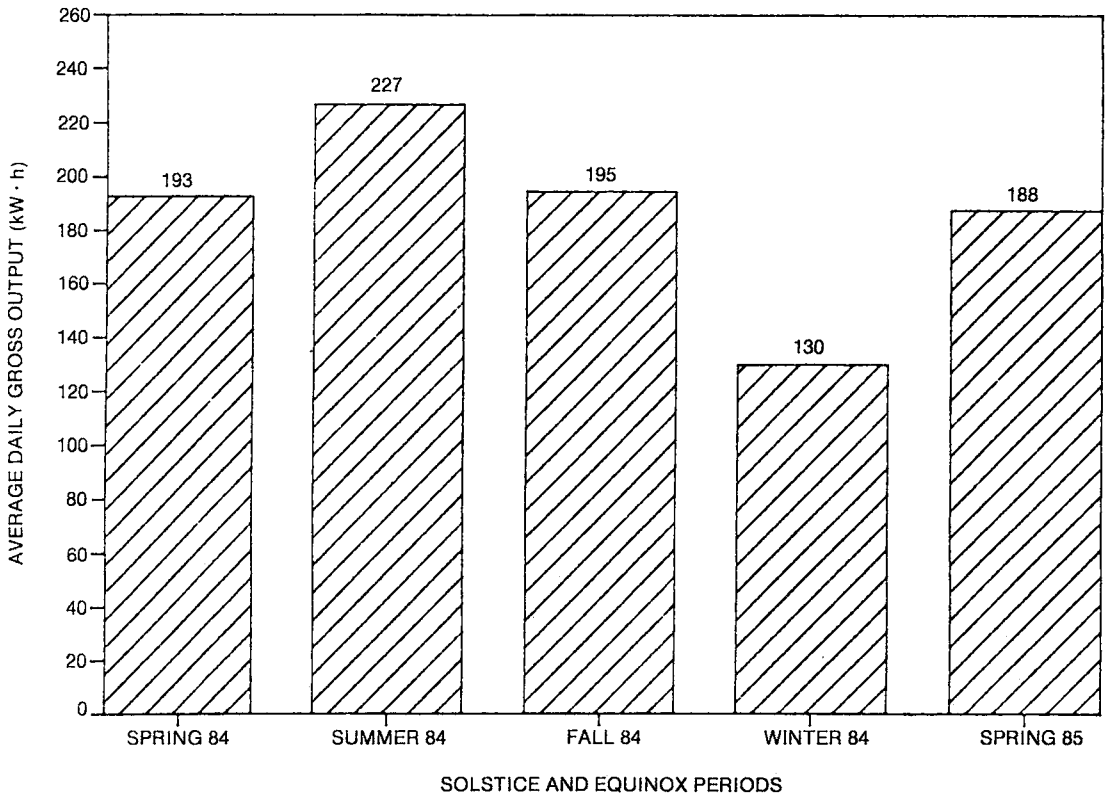

Figure 3-9. Average Daily Gross Electrical Output for Solstice and Equinox Periods

clouds, there was no reduction in output as long as a cloud did not directly shade the parabolic dish (i.e., did not intercept the direct insolation incident on the dish).

Figure 3-10 shows the behavior of the Vanguard module on a day when three different types of cloud conditions were encountered. The morning hours were essentially clear except for the passage of two small clouds. Around mid-day, there were extreme variations in thermal energy input caused by the rapid passage of a number small clouds, and the afternoon was essentially overcast with little or no direct insolation. This figure shows that the response of the module to insolation fluctuation is almost instantaneous. Throughout the day, the curve of gross power generated follows that of direct insolation quite closely. Based on the scattered cloud conditions present in the afternoon, it appears obvious that a level of isolation above 250 W/m^2 (corresponding to approximately 22 kWt) is necessary to produce electrical power.

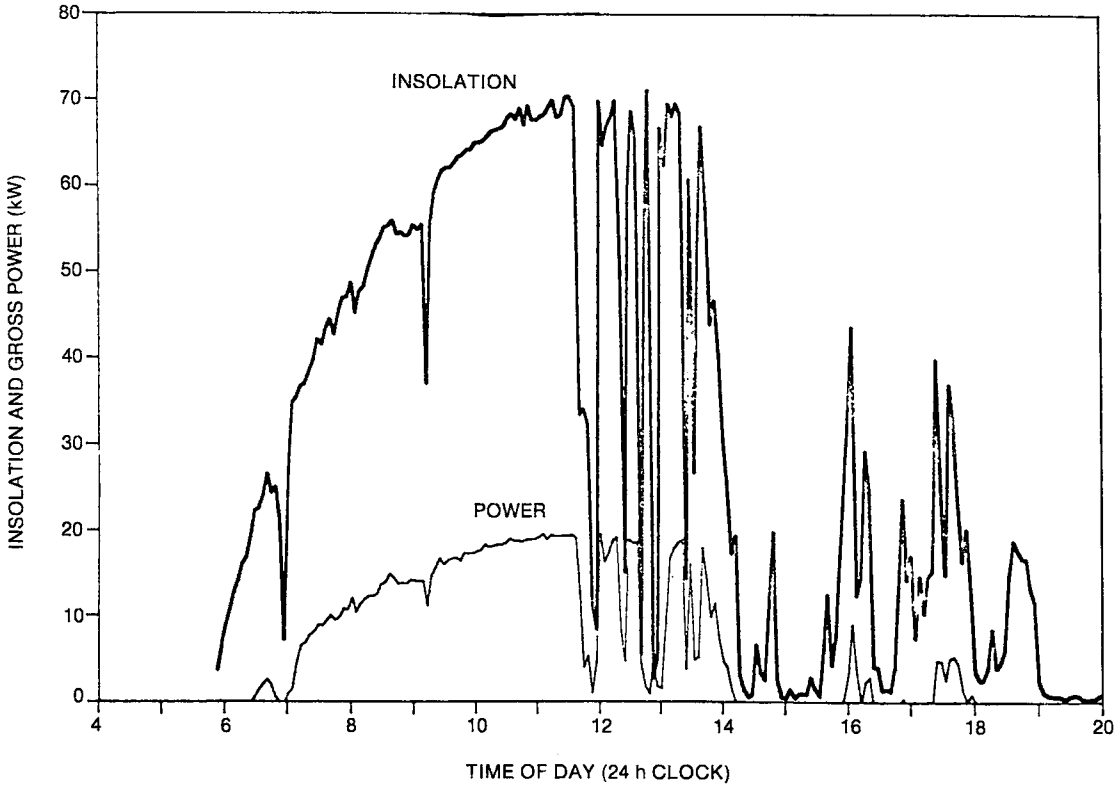

Figure 3-10. Incident Thermal Power and Gross Generated Power for a Cloudy Day - 28 June 1984

Transient Performance

During the 18-month period of operation, the power conversion unit (solar receiver, Stirling engine, and induction generator) of the Vanguard module was subjected to numerous thermal transients of varying severity. Transients were due to startup and shutdown of the module, power outages, alarm conditions, and cloud passage.

Thermal transients can be imposed on components of the module whenever sudden increases in receiver temperature or power output occur. This routinely happens during startup of the module as the dish is brought on sun. For a short period during startup, the concentrated beam of energy reflected from the parabolic dish is focused on two water-cooled plates covering the receiver. These water-cooled plates are not withdrawn simultaneously; instead, they are withdrawn sequentially over a period of a few seconds. Thus, the receiver is initially exposed to the "fireball" asymmetrically. Although this short-term asymmetric flux does not cause any severe problem with the receiver components, a method of more uniform distribution while

coming on-sun would be preferred. The heat energy incident on the receiver during startup or shutdown depends on the direct insolation at that time. Early morning startups and late afternoon shutdowns usually involved insolation levels of about 300 W/m^2, while noontime startup or shutdown could involve levels exceeding 1000 W/m^2.

Module shutdown involves closing the water-cooled plates of the receiver and leads to a down transient of temperature and power. Down transients occur during routine or emergency shutdown of the module and during the passage of clouds while the dish is on sun.

Figures 3-11 and 3-12 give the number of Stirling engine cycles on and off, respectively, within each hour of the day for the entire test program. The data for engine cycles occuring before 5 a.m. or after 9 p.m. are spurious because of the inaccurate setting of the Autodata Nine clock for several weeks. The engine was started up primarly early in the morning or in early afternoon (sometimes after preparing the module for a specific test), although a significant number of on cycles occurred at almost any daylight hour. Engine off cycles occurred on an increasing basis throughout the day, with the highest number in late afternoon, as would be expected. Even though over the 18-month test period a significant number of startups and shutdowns occurred at high insolation levels, no damage to components due primarily to thermal transients was evident.

SYSTEM PERFORMANCE CURVES

Figure 3-13 is a plot of gross generated electrical power versus incident solar thermal power measured with a ground-mounted pyrheliometer for a typical October day. The fact that the individual instantaneous values lie along a straight line is important in that system performance can be expressed in terms of the slope of the line and of the intercepts with the x and y axes.

The slope of the line in Figure 3-13 is representative of the overall electrical conversion efficiency of the parabolic dish/Stirling engine module. This slope is directly proportional to the overall reflectivity of the mirrors in the parabolic dish concentrator. For example, if the reflectivity is reduced to 90% of the original clean condition, then the slope also will be reduced to 90% of its original value for the clean condition.

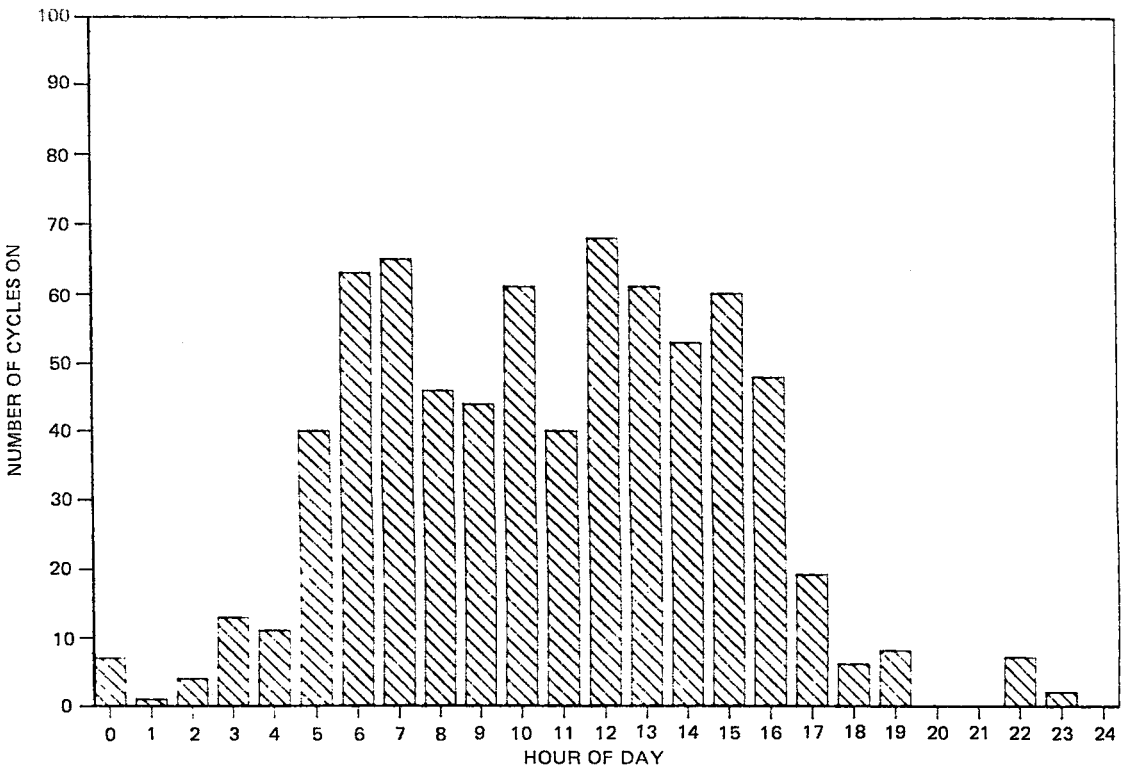

Figure 3-11. Number of Hourly Cycles On

The x-intercept represents the "break-even" point. This is the insolation level, or in this case the thermal input level, at which the electrical power produced by the Stirling engine balances the electrical power lost because of heat losses and friction and windage losses. For this particular module, a threshold value of 20 kWt (230 W/m^2) is observed. In actuality, however, the system efficiency is significantly lower at lower levels of insolation, and a more realistic threshold value of 25 kWt (300 W/m^2) is usually assumed. This is demonstrated by the downward curvature of the line as it approaches lower insolation values.

The y-intercept of the linear performance curve represents the electrical power lost as a result of heat losses from the receiver and as a result of friction and windage losses in the Stirling engine and the induction generator. In this particular example, the heat and frictional losses amount to approxiamtely 7 kW of electrical power.

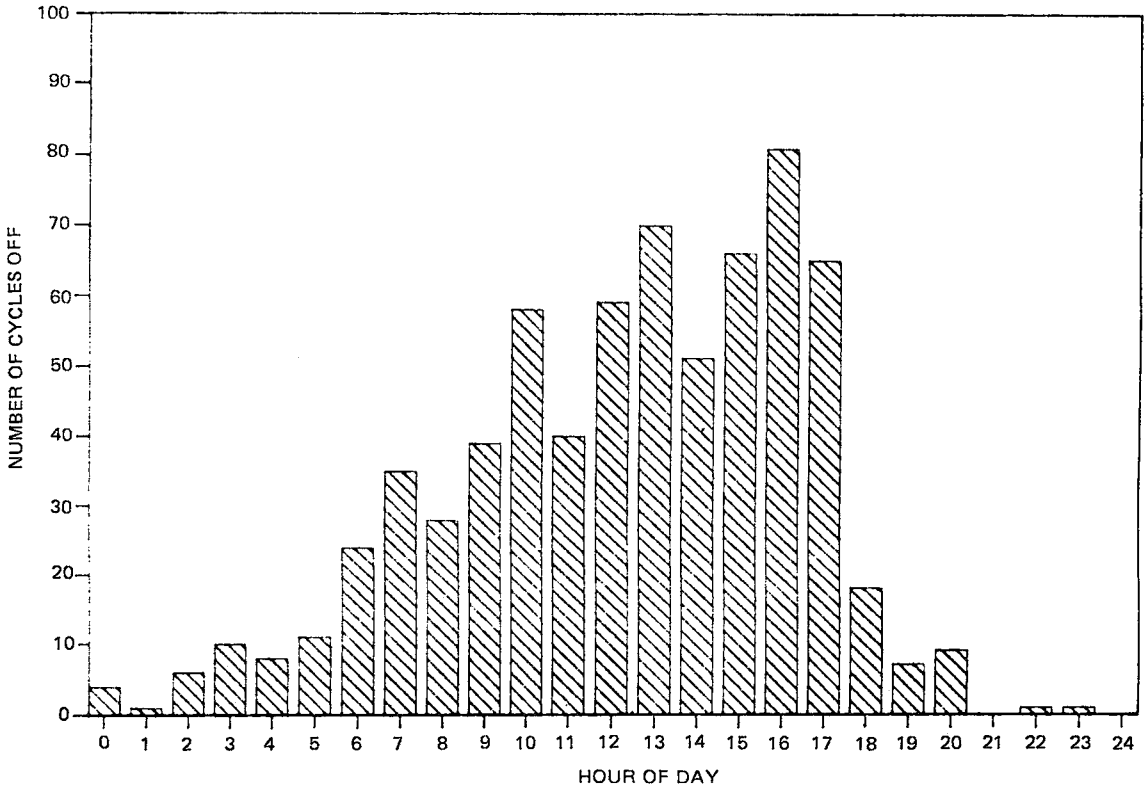

Figure 3-12. Number of Hourly Cycles Off

The information that can be derived from the plot of gross electrical power output versus incident beam insolation input makes such a plot a very powerful tool for characterizing module performance. Moreover, variation of the slope with time gives one of the best and easiest ways of monitoring changes in overall reflectivity of the mirrors in the dish. Mirror reflectivity values have been found to vary with elevation and position on the dish so that it is difficult to obtain an accurate measure of overall mirror reflectivity. The slope method avoids this problem, and the information derived from the slope and the x and y axis intercepts makes this type of plot one of the best ways to characterize the overall performance of the parabolic dish/Stirling engine module. Figure 3-14 shows the effect of a change in mirror reflectivity on the slope of the performance curve. As would be expected, the widest variation exists at high values of incident insolation.

SYSTEM EFFICIENCY

The efficiency of conversion of solar energy into electrical energy (the percentage ratio of output over input) is one measure of the performance of a solar-electric

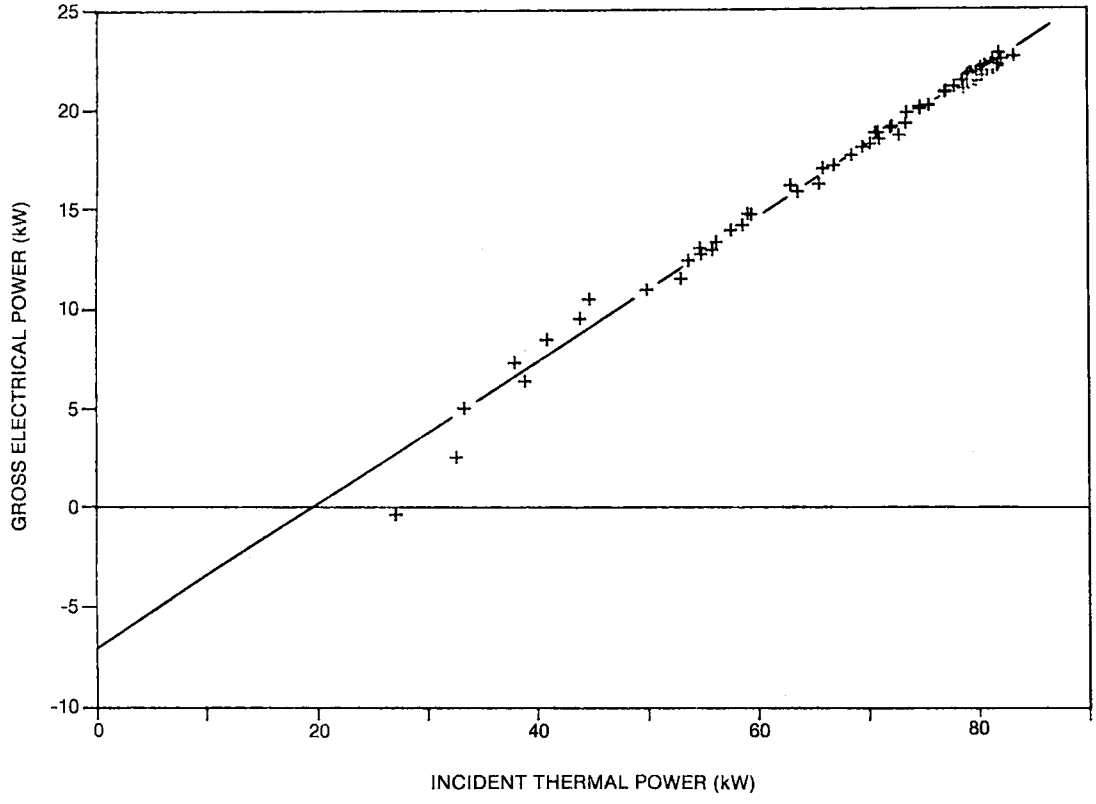

Figure 3-13. Gross Generated Power as a Function of Incident Thermal Power for 12 October 1984

system. Efficiency can be defined in several ways, as shown in Table 3-4. As the table shows, efficiency can be defined by either the ratio of instantaneous power output to thermal power input or by the ratio of electrical energy output to thermal energy input integrated over some designated time period. This period of operation may be, daily, weekly, monthly, annually, or even the overall life span of the system. Moreover, for a solar unit, a further distinction must be made between periods of operation covering on-sun hours only and periods of operation covering an entire 24-hour day. The distinction is important because net efficiency is affected by periods of low or no solar input, during which auxiliary electrical demand can exceed electrical output. All other things being equal, a high electrical conversion efficiency is desirable for a solar unit in that it reduces land requirements for the solar collectors, reduces mirror and dish size, and reduces capital costs for the power conversion unit.

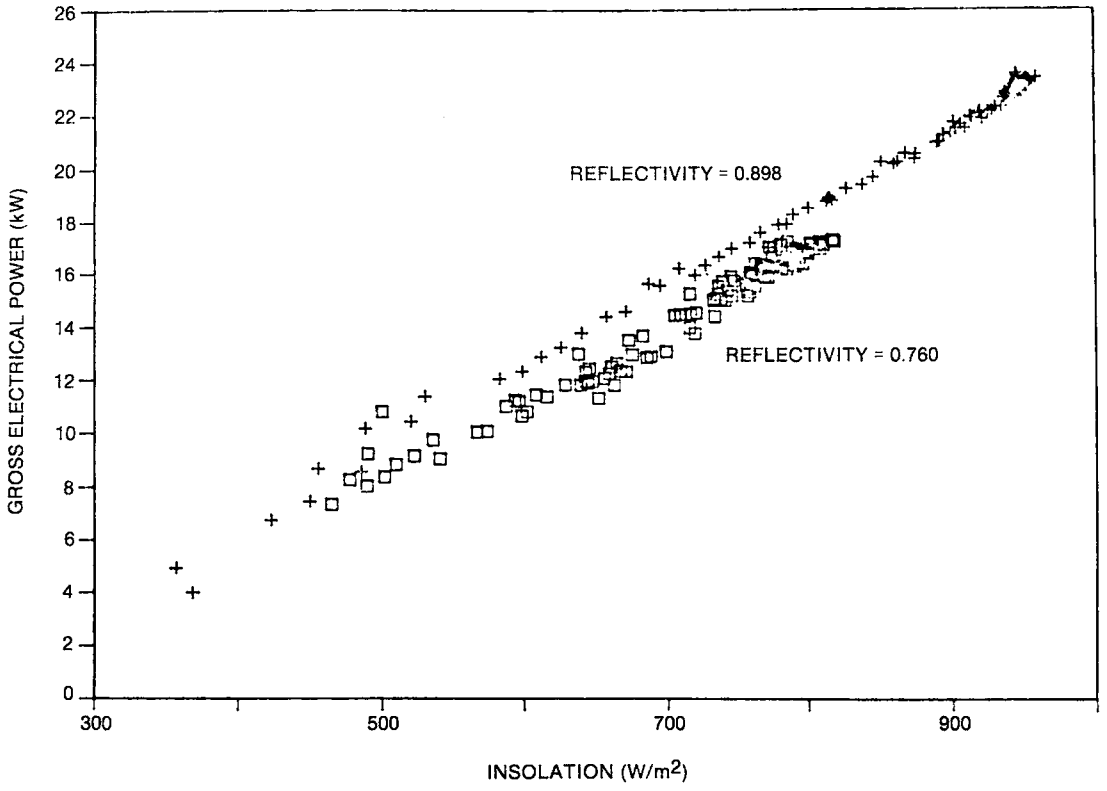

Figure 3-14. Effect of Dish Reflectivity on Electrical Power versus Direct Insolation Curve

Instantaneous Efficiency

The Vanguard module had very high instantaneous efficiencies for the conversion of solar energy into electrical energy, the highest conversion of any known solar-electric device to date. During the 18-month test program, gross and net conversion efficiencies as high as 31.6 and 29.4%, respectively, were attained.

The instantaneous efficiency of the Vanguard module increases as the level of electrical power output increases. This is because there is a rather constant auxiliary power drain that is independent of electrical power output. As electrical power output increases, this constant power draw becomes a smaller proportion of the output, and hence the ratio of electrical power output to thermal power input (i.e., the instantaneous efficiency) increases. On a clear day, the peak instantaneous efficiency for that day should therefore occur at solar noon when thermal power input and hence electrical power output should peak.

Table 3-4

VARIOUS METHODS OF CALCULATING EFFICIENCY

Type of Efficiency	Calculation Method
Instantaneous Gross Efficiency	$\frac{\text{Gross power output (kWe) at a given instant in time}}{\text{Thermal power (kWt) incident on the dish at the same instant in time}}$
Instantaneous Net Efficiency	$\frac{\text{Net power output (kWe) at a given instant in time}}{\text{Thermal power (kWt) incident on the dish at the same instant in time}}$
On-Sun Gross Efficiency	$\frac{\text{Gross electrical energy output (kWe·h) while on-sun during a given time span}^a}{\text{Thermal energy (kWt·h) incident on the dish while on-sun during a given time span}^a}$
On-Sun Net Efficiency	$\frac{\text{Net electrical energy output (kWe·h) while on-sun during a given time span}^a}{\text{Thermal energy (kWt·h) incident on the dish while on-sun during a given time span}^a}$
24-Hour Gross Efficiency	$\frac{\text{24-Hour Gross electrical energy output (kWe·h) during a given time span}^a}{\text{Thermal energy (kWt·h) incident on the dish from sunrise to sunset during a given time span}^a}$
24-Hour Net Efficiency	$\frac{\text{24-Hour Net electrical energy output (kWe·h) during a given time span}^a}{\text{Thermal energy (kWe·h) incident on the dish from sunrise to sunset during a given time span}^a}$

[a] The timespan selected may be daily, weekly, monthly, annually, etc. Also, the timespan selected must be designated. For example, daily on-sun net efficiency or monthly on-sun net efficiency.

When observed over a span of several hours, the instantaneous efficiencies are slightly lower than that of the peak instantaneous value. This is due to lower individual efficiencies of the module components at lower levels of solar thermal input power and higher relative values of auxiliary power, since auxiliary power requirements remain fairly constant regardless of solar insolation. The effect of solar thermal input on module net conversion efficiency can be seen in Figure 3-15. The efficiency curves for 28 February 1985 and 14 June 1985 show that the net instantaneous conversion efficiency during the winter is slightly higher than that during the summer, presumably due to lower ambient and coolant temperatures and consequently higher Stirling engine efficiency. The difference between the seasonal efficiency curves is not as great at lower insolation levels, where the margin gained by the lower ambient temperature is overshadowed by the relatively high auxiliary power requirement.

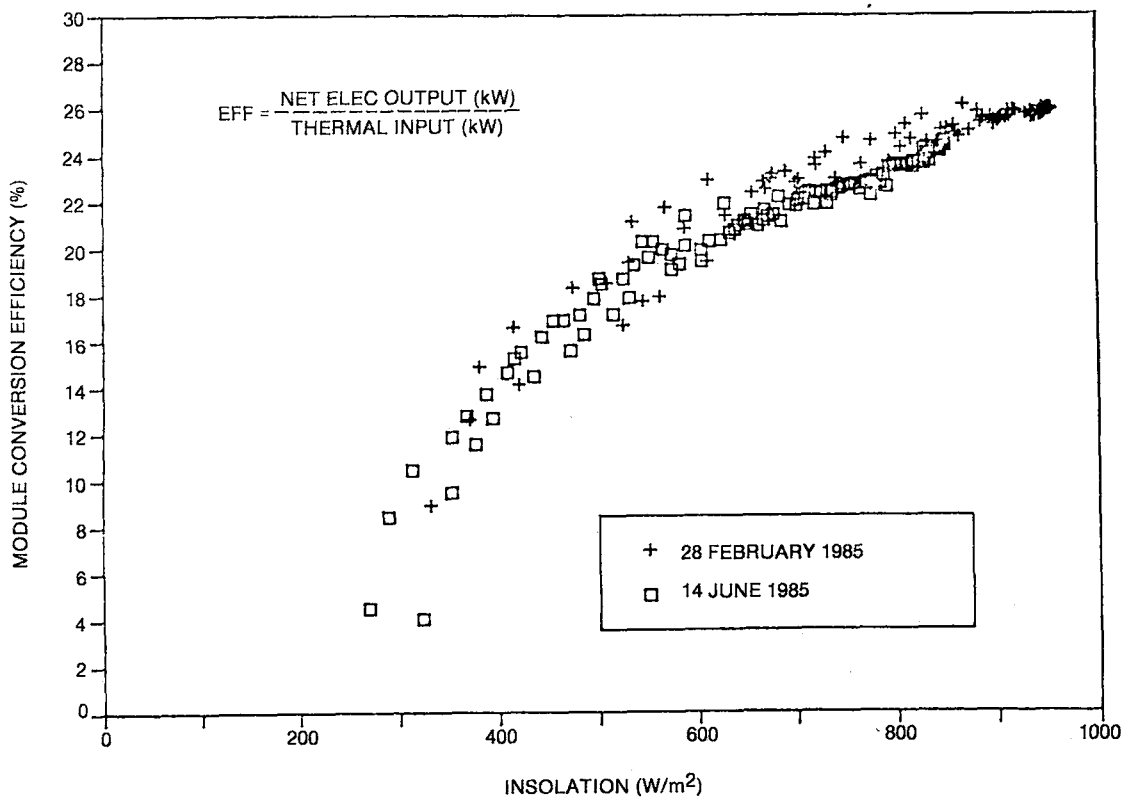

Figure 3-15. Module Conversion Efficiency as a Function of Direct Insolation for a Winter and Summer Day

On-Sun Efficiency

During a typical operating day, the dish might track the sun from early in the morning until late in the afternoon. During the time the dish is "on-sun" the power generated would gradually increase to a maximum value at solar noon and then slowly decrease in magnitude during the afternoon hours. As was shown in Figure 3-15, the efficiency at any one point in time varies with the insolation level (i.e., the thermal power input level). The on-sun efficiency is the energy output (in kWe·h) divided by the input (in kWt·h) during the timespan that the dish is generating electrical power. In effect, the on-sun efficiency is an integrated value of all the instantaneous efficiencies.

Although the net on-sun efficiency of an average day during the winter months may be slightly higher than that during the summer months, the kilowatt-hours of electrical output from an average summer day will usually be higher because of a longer period of insolation. For example, during June at the Rancho Mirage site power can be generated for about 13-1/2 hours on a clear day versus only about 10-1/2 hours on a clear winter day in December. Figure 3-16 shows the distribution of gross and net on-sun daily efficiencies for a 2-week period in March 1985. This figure shows that, in general, efficiencies for days in which at least moderate electrical power is produced (>50 kW·h) range from 20 to 28% gross and 18 to 26% net. As a reference, the overall gross and net on-sun efficiencies for the period shown in the figure are 24.9% and 23.5%, respectively.

On-sun efficiencies on a monthly basis for the 18-month test period are shown in Table 3-5. The average gross and net on-sun efficiencies for the entire test program were 24.6 and 22.8%, respectively.

24-Hour Efficiency

In calculating the 24-hour net efficiency for an entire month, one must not only take into account the off-sun auxiliary power requirements, but also the available solar resource for the entire month. These two factors impose an extremely high penalty if every opportunity to operate is not utilized. Net 24-hour efficiencies for each month during the Vanguard test program are shown in Tables 3-6 and 3-7. The net 24-hour operating efficiencies shown in Table 3-6 take into account the total auxiliary power requirements and available direct insolation during only

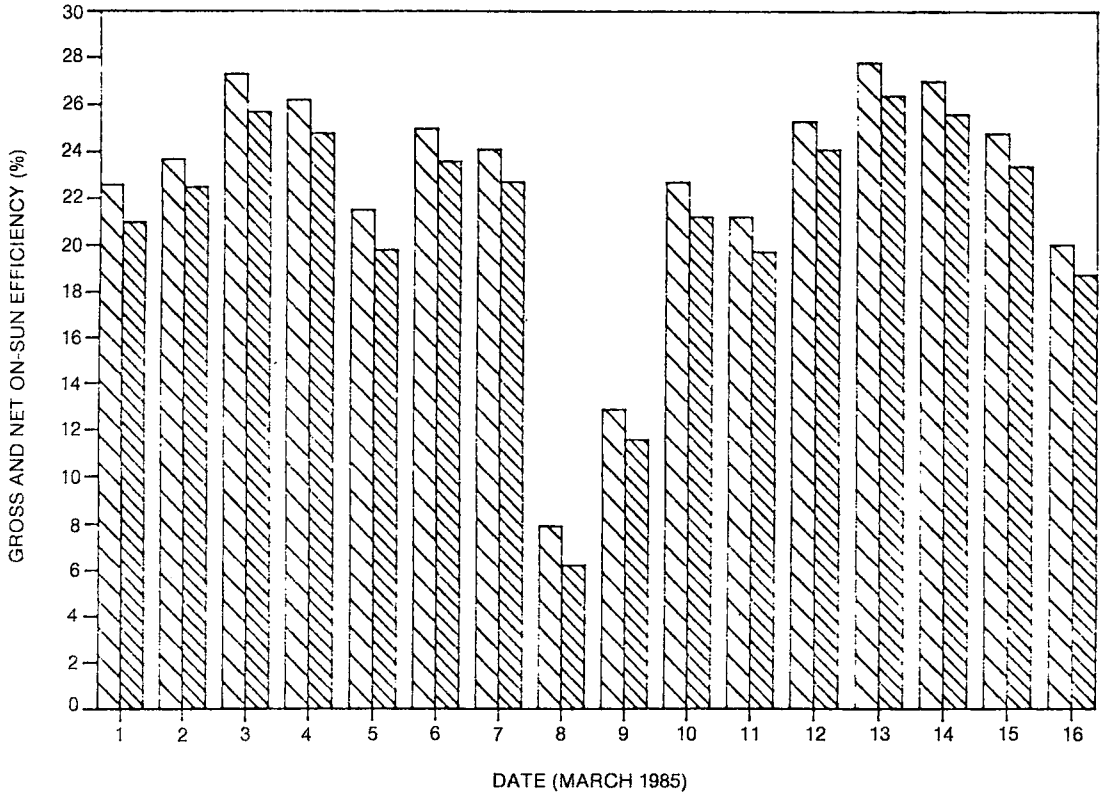

Figure 3-16. Gross and Net On-Sun Efficiencies for 16 Consecutive Days in March 1985

those days in the month when the module was operating. The average 24-hour efficiency for the entire 18-month test period gives a good indication of the efficiency that would have been achieved if the system had operated each day during the test period (i.e., was not unavailable due to either weather or planned/unplanned outages). The average 24-hour operating efficiency was approximately 18.5%. The net 24-hour efficiencies in Table 3-7 are based on the total calculated available insolation during the month, estimated from the daily average calculated earlier. This method of calculating efficiency penalizes the module for all daylight periods that the system is down for whatever reason. The average 24-hour efficiency for the test period was 9.7%, but the monthly values varied widely, primarily because the operating hours each month varied. Much higher efficiencies can be attained when the module is not involved in a varied test program and can be devoted solely to maximizing power production. This was not the case during the Vanguard test program, except for several intermittent timespans surrounding the solstice and equinox periods.

Table 3-5

ON-SUN EFFICIENCIES FOR VANGUARD MODULE

Month	On-Sun Direct Insolation (kW·h)	On-Sun Electrical Output		On-Sun Efficiency	
		Gross (kW·h)	Net (kW·h)	Gross (%)	Net (%)
1984					
February	845	212	195	25.1	23.1
March	4,130	1,056	980	25.6	23.7
April	9,302	2,549	2,372	27.4	25.5
May	3,467	679	615	19.6	17.7
June	11,407	2,934	2,687	25.7	23.6
July	5,654	1,343	1,215	23.8	21.5
August	10,635	2,557	2,339	24.0	22.0
September	9,599	2,406	2,190	25.1	22.8
October	8,071	1,880	1,744	23.3	21.6
November	287	73	68	25.4	23.7
December	2,996	738	695	24.6	23.2
1985					
January	5,210	1,321	1,249	25.4	24.0
February	11,163	2,962	2,775	26.5	24.9
March	16,175	4,043	3,816	25.0	23.6
April	7,013	1,702	1,571	24.3	22.4
May	12,541	3,025	2,785	24.1	22.2
June	10,353	2,300	2,138	22.2	20.7
July	3,189	783	734	23.8	22.3
Total	132,127	32,563	30,168	24.6	22.8

Table 3-6

NET 24-HOUR OPERATING EFFICIENCIES FOR VANGUARD MODULE

Month	Operating Available Direct Insolation[a] (kW•h)	Net 24-Hour Electrical Output[b] (kW•h)	Net 24-Hour Operating Efficiency (%)
1984			
June	11,748	2,550	21.7
July	5,358	934	17.4
August	13,006	1,886	14.5
September	10,570	2,059	19.5
October	8,956	1,623	18.1
November	572	58	10.1
December	3,416	574	16.8
1985			
January	6,158	1,155	18.8
February	11,432	2,615	22.9
March	17,039	3,669	21.5
April	8,590	1,470	17.1
May	15,514	2,612	16.8
June	13,211	2,091	15.8
July	3,644	545	15.0
Total	129,214	23,841	18.5

[a]Not available prior to June 1984.
[b]Totals for operating days only.

Table 3-7

NET 24-HOUR OVERALL EFFICIENCIES FOR VANGUARD MODULE

Month	Days In Month	Average Daily Direct Insolation[a] ($kW \cdot h/m^2$)	Total Monthly Direct Insolation ($kW \cdot h$)	Net 24-Hour Electrical Output[b] ($kW \cdot h$)	Net 24-Hour Overall Efficiency (%)
June	30	8.47	22,000	2,538	11.5
July	31	4.94	13,300	1,091	8.2
August	31	6.63	17,800	2,043	11.5
September	30	6.70	17,400	1,978	11.4
October	31	6.59	17,700	1,480	8.4
November	30	5.81	15,100	(228)	-
December	31	4.63	12,400	409	3.3
1985					
January	31	5.89	15,800	1,073	6.8
February	28	5.96	14,500	2,580	17.8
March	31	6.39	17,200	3,662	21.3
April	30	7.85	20,400	1,350	6.6
May	31	8.18	22,000	2,610	11.9
June	30	8.18	22,900	2,080	9.1
July	24	6.00	12,500	675	5.4
Total	518		241,000	23,341	9.7

[a] Based on days in month for which actual insolation data were available.
[b] Totals for all days in month.

Surge

20' length

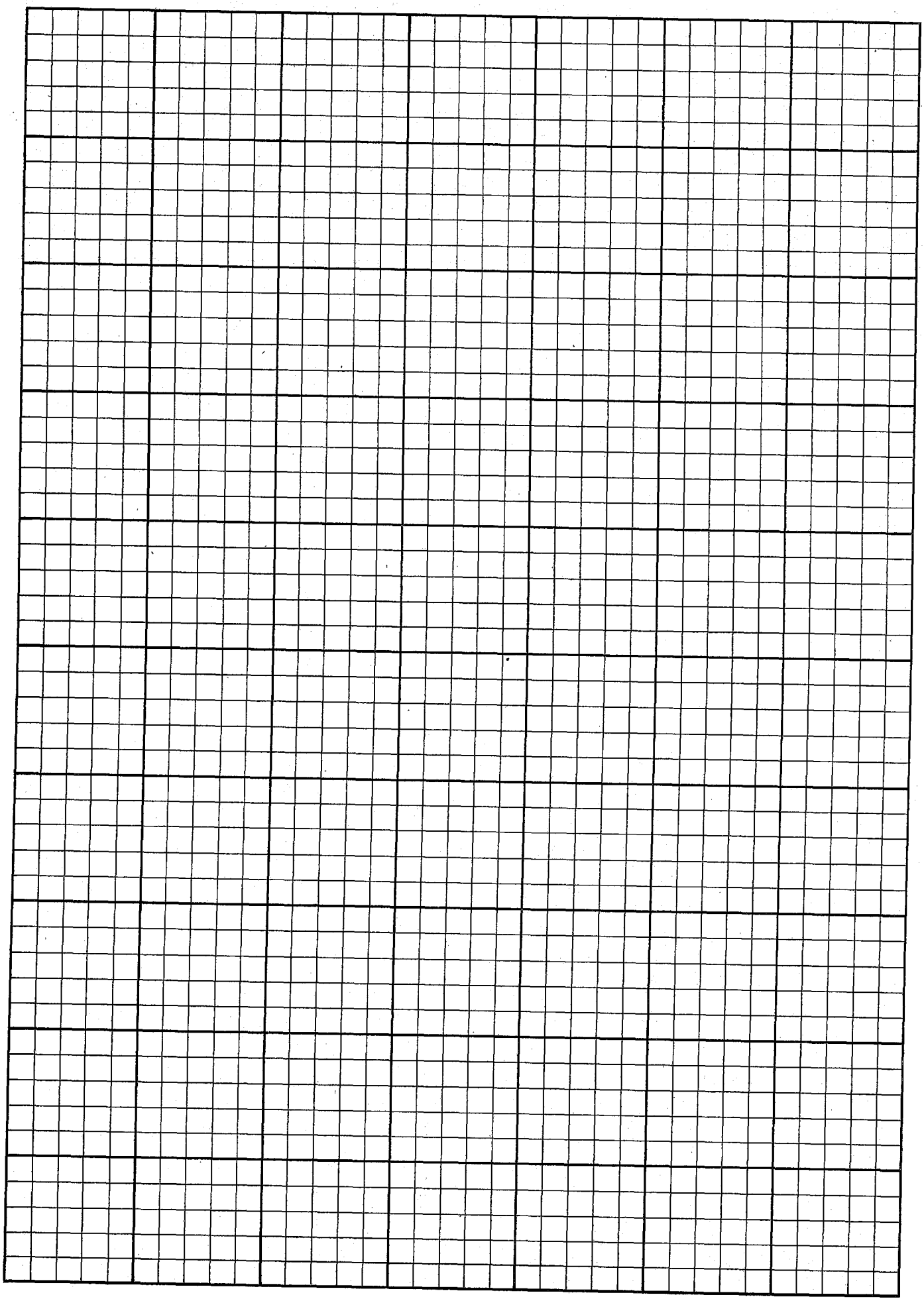

Comparison of Methods for Calculating Efficiency

March 85

The relative magnitude of the efficiencies calculated by the various methods are shown in Figure 3-17 for the month of March 1985. This month was the best month in terms of electrical energy produced since Advanco was testing the module in a sustained-power-generation mode. Therefore, the performance during this month would be most similar to that of a multimodule plant, the primary purpose of which would be to maximize the output of electricity.

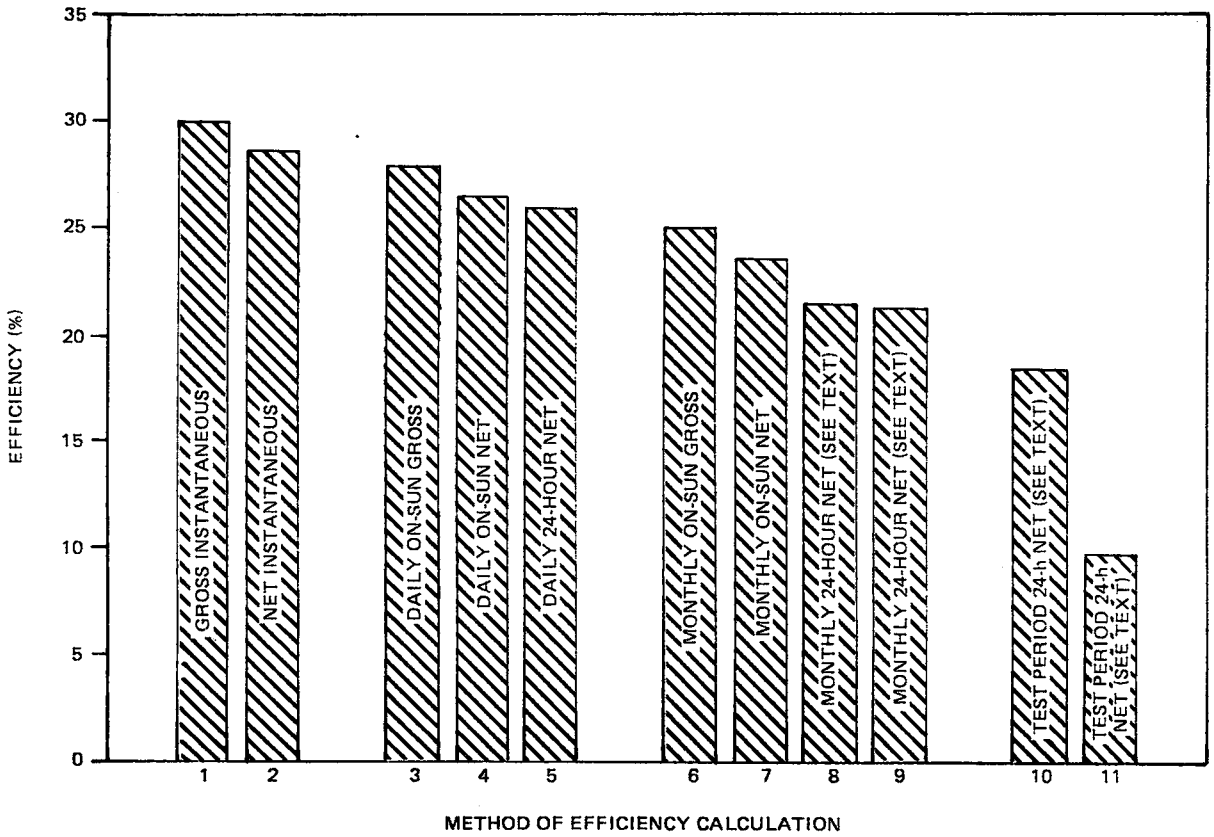

Figure 3-17. Comparison of Efficiencies Calculated on Several Bases

Bars 1 and 2 indicate the magnitude of the peak gross and net instantaneous efficiencies during 13 March, the best day of the month. These peak instantaneous efficiencies occurred near solar noon on the day in March with the highest direct insolation. Bars 3 and 4 represent the gross and net on-sun efficiencies while the dish was generating power on that same day. Bar 5 is the net efficiency for that

same day calculated over a 24-hour period; the 24-hour net efficiency is slightly lower than the on-sun net efficiency because the 24-hour period takes into account an additional off-sun auxiliary power demand (the trackers required some power even when not tracking). Bars 6 and 7 show the gross and net efficiencies based upon all the on-sun timespans during the month. Bars 8 and 9 show the net 24-hour operating and overall efficiencies, respectively, for the entire month of March and are lower than that of Bar 7 because the off-sun auxiliary power is taken into account. Bar 8 is calculated using only those days during which the dish generated power (29 days out of 30). Bar 9 is based on all days of the month and hence is slightly lower than Bar 8. Although the 24-hour overall efficiency includes days during which no power was generated, in this instance, it appears that there is no detectable difference between Bars 8 and 9. This is because the dish operated almost every day during that timespan. However, if the timespan includes a large number of days during which little or no power was generated, there can be a large effect on efficiency. This may be seen from Bars 10 and 11 in Figure 3-17. Bar 10 shows the net 24-hour operating efficiency calculated for the entire 18-month test period based only upon these days during which electrical power was generated. Bar 11 shows the net 24-hour overall efficiency based upon all the days in the test period, including days during which no power was generated. The importance of maximizing the number of days during which power is generated may be seen by comparing the sizes of Bars 10 and 11. Bar 11 indicates an efficiency only about half as great as Bar 10.

In summary, the instantaneous efficiency varies during a given day and on a clear day reaches a peak at solar noon. The daily on-sun efficiency may be thought of as an average efficiency during a given day. The 24-hour efficiency takes into account auxiliary energy consumption during off-sun hours and hence always will be less than the on-sun efficiency. The overall monthly, annual or test-period efficiency can give the bleakest picture, since it is affected by any downtime during the daylight hours. However, it is the most realistic efficiency to use in economic calculations.

Waterfall Diagrams of Module Performance

The previous discussion on efficiencies has been based on the ability of the overall module as a system to convert solar energy into electrical energy. It is instructive to examine the individual subsystem efficiencies, which taken together comprise the overall efficiency. This is often done through the use of a waterfall diagram, which shows the progression of energy through the system.

Figures 3-18 and 3-19 are waterfall diagrams for a typical summer and winter day, respectively. The first bar in both figures is the thermal energy incident on the dish; this is the maximum amount of energy available for conversion into electrical energy for that day. The second bar accounts for the efficiency of the mirrors in reflecting the incident energy toward the solar receiver. The reflectivity varies daily and therefore is different in both cases. The third bar accounts for the shading of the incident direct insolation and the blocking of the reflected beam by the dish structural supports. This shading and blocking factor depends on the physical construction of the dish and hence remained constant for the entire test program. The next four bars take into consideration the efficiencies of the receiver optical, receiver thermal, Stirling engine, and induction generator subsystems. The individual values could not be determined separately from the data collected, and are based on reliable estimates from information supplied by their respective manufacturers. The eighth bar accounts for the auxiliary power utilized during on-sun operation of the module. This efficiency is lower during the summer months, because the fan power required to remove heat from the engine is higher during the warm summer days. The final bar accounts for the auxiliary energy consumed during daylight off-sun periods and overnight while the system is on standby. The efficiency here is significantly lower in winter than in summer because the off-sun periods during a 24-hour day are longer. Overall, the 24-hour system efficiency is approximately 24% for the summer day, and about 23% for the winter day.

SYSTEM AVAILABILITY

"Operating availability" for a solar-thermal power generating system is the percentage of time that a unit is available to produce power during daylight hours regardless of whether the unit is or is not operated. Thus, availability is a measure of the state of readiness of the module to produce power regardless of whether insolation is satisfactory. Availability is equal to 100% less the percentage of time on forced outage. Scheduled outages for periods of routine maintenance and for days where site personnel were not present were not counted against availability, since the module could have operated and produced power if desired. Availability should not be confused with "capacity factor," which is a measure of energy actually produced compared with the energy that could have been produced if the unit were operated at its maximum rated output continuously. The availability of

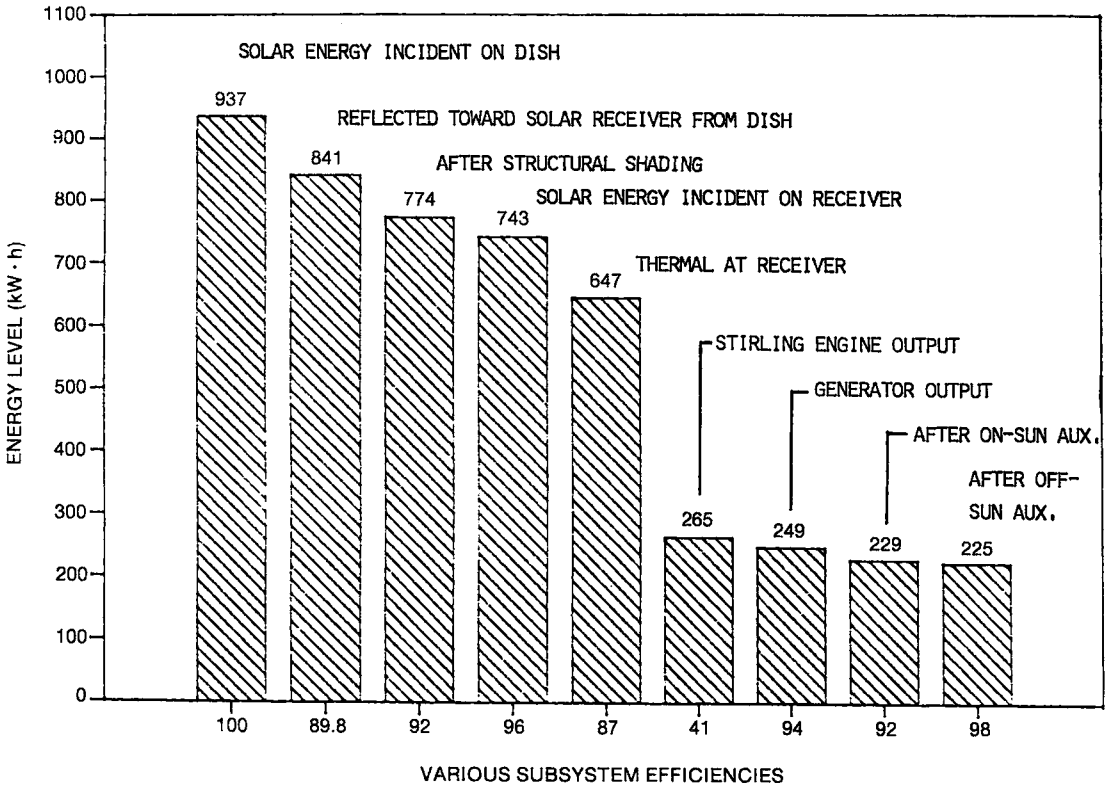

Figure 3-18. Waterfall Diagram for 22 June 1984

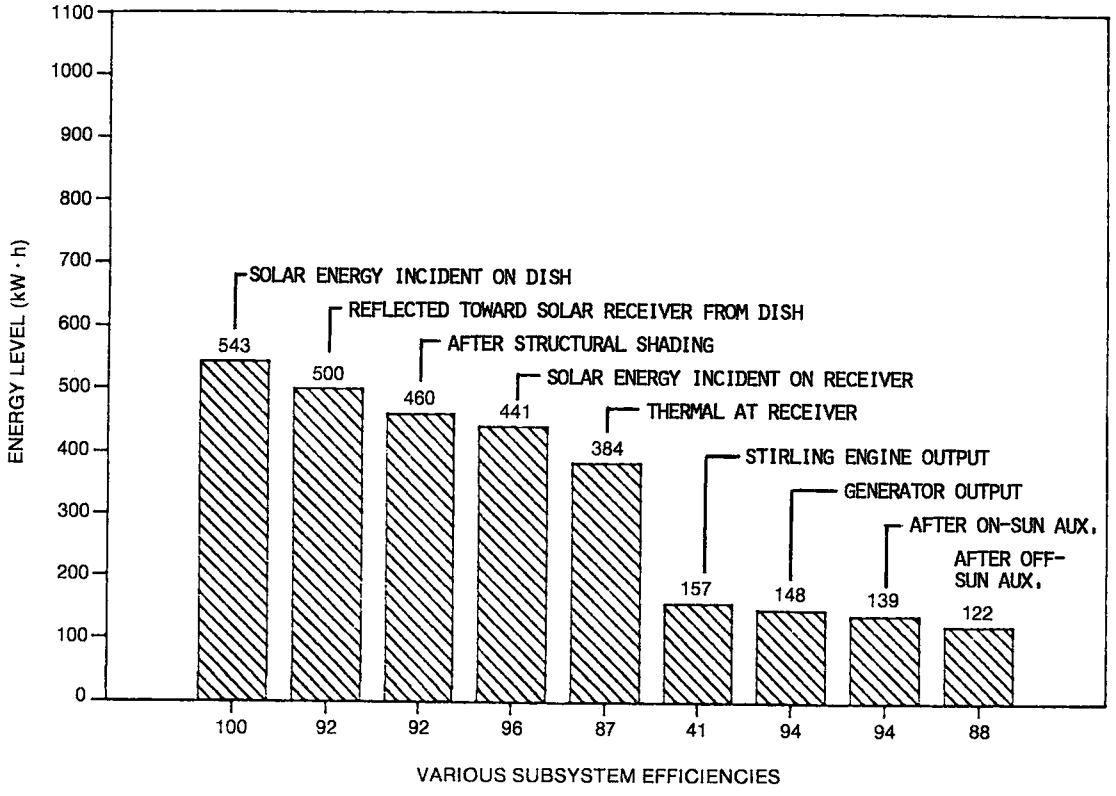

Figure 3-19. Waterfall Diagram for 21 December 1984

the Vanguard module during the operational test period is summarized in Table 3-8. An overall availability of 72% was achieved for the 18-month test period. The data in Table 3-8 are shown graphically in Figure 3-20.

Figure 3-21 categorizes all daylight hours of the test program by availability classification. The module operated and produced power essentially 50% of the time during which sufficient solar energy was available. Planned outages (including routine maintenance performed during daylight hours and days when site personnel were not present) accounted for roughly 22% of the entire daylight period and were not counted against system availability since the module would have been able to produce power if desired. During the remaining 28% of the daylight hours, the module was inoperable due to mechanical or electrical problems. These unplanned outages are categorized in more detail by subsystem in Figure 3-22. The Stirling engine accounted for the largest fraction of downtime hours, primarily because of the long time required to obtain any needed replacement parts. Had there been an on-site inventory of spare parts, as would be the case in a multimodule power plant, the Stirling engine downtime could have been drastically reduced. The downtime hours of the other major subsystems listed were relatively equal in magnitude. The category listed as "other" contains items such as hydrogen system plumbing problems, loss of control parameters due to power failure, and failure of the uninterruptible power supply.

Of the 540 days in the Vanguard test program, 213 days (40%) were free from either planned or unplanned outages (not including early morning or late evening detracks). These were days in which the module operated from dawn to dusk. Days in which at least one significant planned outage occurred numbered 137 (25%). The number of days in this category could be easily reduced by performing maintenance during off-sun hours and operating 7 days per week. Days in which at least one unplanned outage occurred account for the remaining 190 days (35%). The significance of this number is that a knowledgeable maintenance and repair person was required at the site on over one-third of the total days in the test program. Successful commercialization of this technology requires substantial cost reduction, and frequent repair calls reduce the overall cost effectiveness of the system. A summary of this information by month is presented in Table 3-9.

Table 3-8

VANGUARD EQUIPMENT AVAILABILITY

Month	Days Unavailable						Availability (%)
	Concentrator	Receiver	Engine	Instrumentation	Other	Total	
1984							
Feb	0.5	0	1.4	1.5	1.7	5.1	82
Mar	10.8	0.3	0	0.4	0.1	11.6	63
Apr	0	0.2	0	0.1	0	0.3	99
May	4.0	0	0.7	0	0	4.7	85
Jun	2.0	0.1	0.1	0	3.5	5.7	81
Jul	7.2	0.2	0	0	0	7.4	76
Aug	0	0.2	0	0.5	0	0.7	98
Sep	2.2	0	9.0	0	0	11.2	63
Oct	1.5	0	7.4	0.1	0.7	9.7	69
Nov	0	0	6.7	22.5	0	29.2	3
Dec	0.8	0.3	5.8	9.0	0	15.9	49
1985							
Jan	0.5	0	10.0	0	0	10.5	66
Feb	0.7	0.3	0	0	0	1.0	96
Mar	0.3	0	0.2	0	0	0.5	98
Apr	0	2.1	14.9	0	0	17.0	43
May	0.2	0.5	0.5	0	0	1.2	96
Jun	1.0	11.5	0	0.1	0	12.6	58
Jul	0	9.0	0.5	0.1	0	9.6	60
Total	31.7	24.7	57.2	34.3	6.0	153.9	72

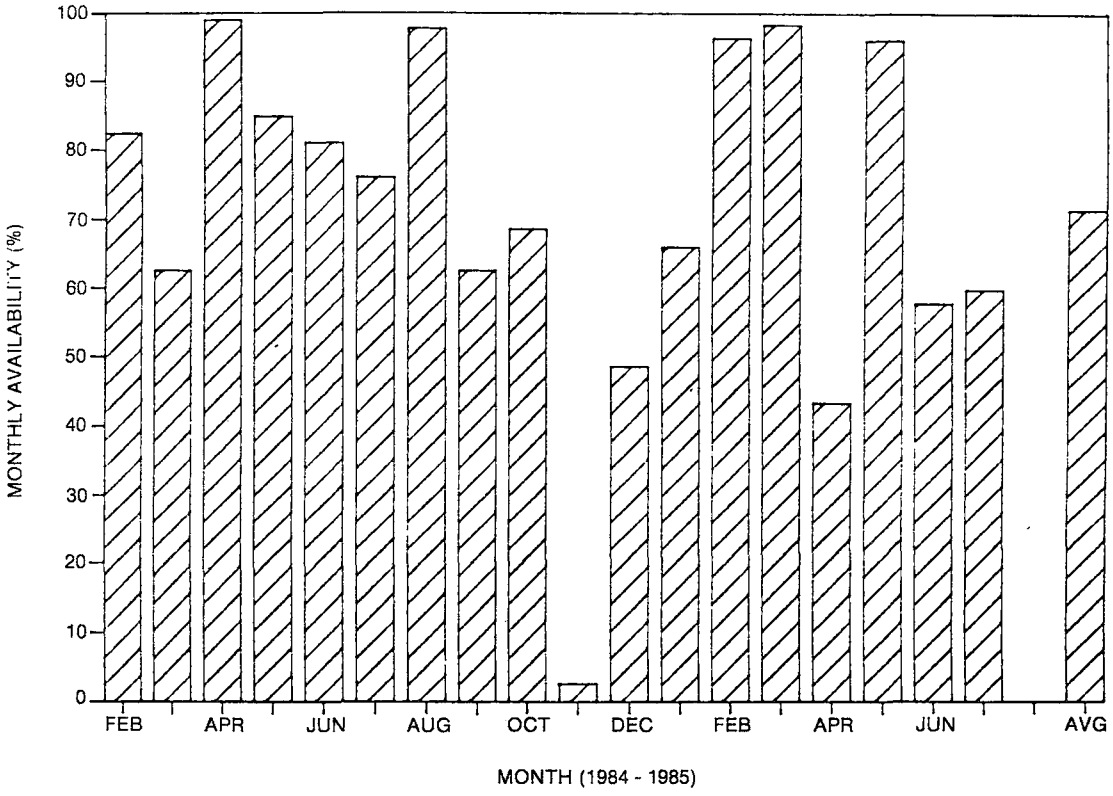

Figure 3-20. Monthly Vanguard Availability for the 18-Month Test Period

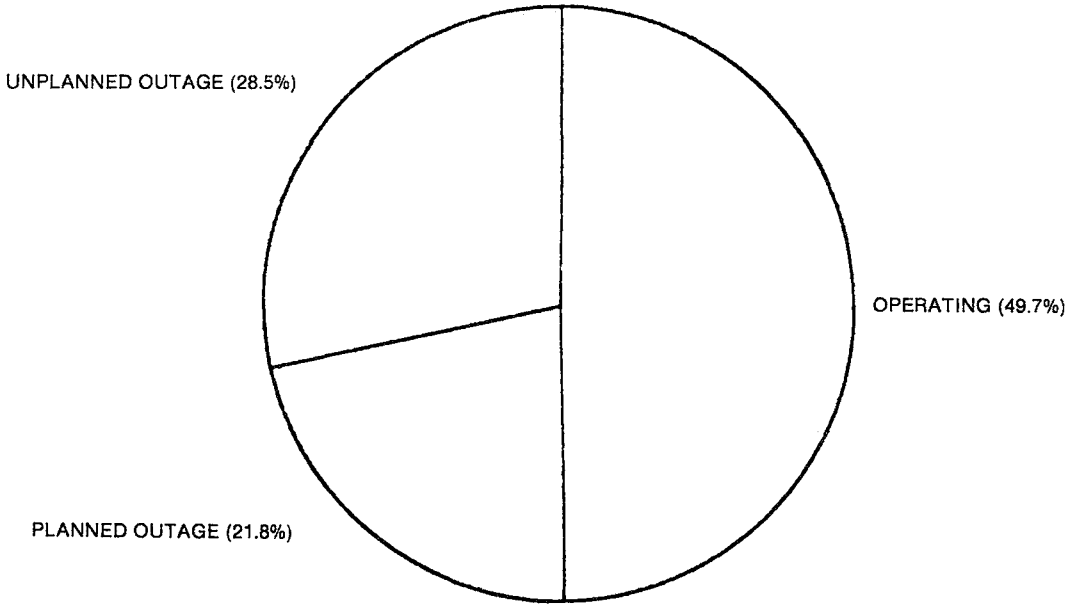

Figure 3-21. Categorization of Daylight Hours by Availability

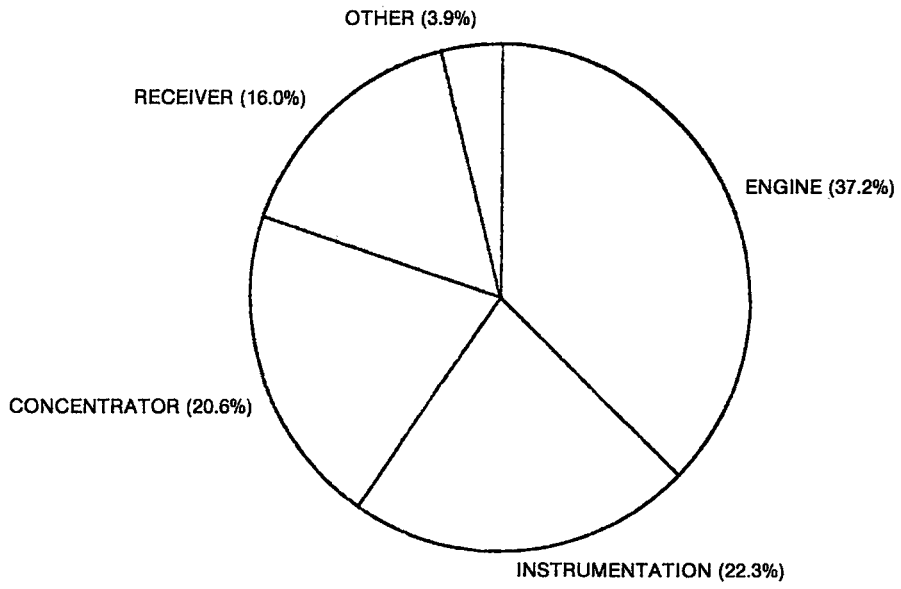

Figure 3-22. Categorization of Unplanned Outages by Subsystem

SYSTEM CAPACITY FACTOR

Capacity factor is the ratio of the total actual electrical energy generated to the electrical energy that would have been generated if the unit had operated continuously at its maximum rating:

$$\text{Annual capacity factor} = \frac{\text{actual annual energy generated (kWh)}}{\text{[maximum rating (kWe)] [8760 (hours)]}}$$

The above definition illuminates a definite need to establish a realistic maximum rating for a solar-electric unit. Capacity factors for such systems calculated on the basis of maximum output are low compared with those of conventional units because solar-electric units operate at maximum rating only on clear days at solar noon. Nevertheless, it is of interest to calculate the capacity factor for two reasons: (1) conventional power plant practice is to estimate annual output by multiplying rated output by the capacity factor and (2) it provides a measure of actual performance compared with rated output. In this case, the rated output of the Vanguard module was assumed to be 20 kW net.

Another way of evaluating the operational characteristics of a solar-electric unit is to compare the power-generation hours to the total available hours during a

Table 3-9

BREAKDOWN OF MODULE AVAILABILITY BY FULL DAYS

Month	Total Days	Full Operating Days	Planned Outage Days	Unplanned Outage Days
1984				
Feb	29	6	15	8
Mar	31	8	8	15
Apr	30	15	13	2
May	31	6	20	5
Jun	30	13	9	8
Jul	31	12	10	9
Aug	31	17	11	3
Sep	30	16	2	12
Oct	31	10	8	13
Nov	30	0	0	30
Dec	31	5	6	20
1985				
Jan	31	17	3	11
Feb	28	24	2	2
Mar	31	27	2	2
Apr	30	8	2	20
May	31	16	11	4
Jun	30	8	7	15
Jul	24	5	8	11
Total	540	213	137	190

given time period. Such a method shows the advantage of a combined solar and fossil-fired unit, which would permit operation at night and during days of poor solar insolation.

Table 3-10 shows the capacity factor and also the percent of total hours generating power. During the Vanguard test program, the module had a capacity factor of 0.104 and was operated 15.4% of the total hours in the test period (about 33% of the daylight hours). As might be expected, the maximum values of both capacity factor and percent of total hours generating power occurred during March 1985, when the module was being endurance tested. These performance factors are presented graphically in Figures 3-23 and 3-24.

PERFORMANCE PREDICTION

The ability to predict the power output accurately from the dish/Stirling module given specific input conditions is important for several reasons. First, it would be useful to estimate the power output of the module in its present configuration at the site under differing environmental conditions. Second, if the predictive model is fairly reliable, the effect of certain parameters on the overall performance of the module can be evaluated (for example, to determine acceptable ranges of conditions or to determine those parameters that are most important in selecting a potential site). Third, and perhaps most important, the ability to predict the power-generating capacity of the module at other sites is needed to permit potential users to evaluate the cost effectiveness. To be useful, such a predictive tool must be simple to use, utilize available input data, and provide reasonable accuracy for a preliminary analysis, especially if several different sites are being considered.

The dish/Stirling module is more adaptable to modeling than many other solar systems because of a nearly linear correlation between incident solar power and generated electrical power. In addition, the low thermal inertia of the dish/Stirling module permits a very quick response to fluctuations in incident insolation.

Two types of simplified models can be developed for this system: (1) a dynamic model that predicts the instantaneous kilowatt power output at any particular set of conditions and (2) an integrated model that predicts the total daily or yearly energy output in kilowatt-hours given overall values for input parameters. Both simplified models were developed from data collected during the first operating year of the module and are discussed below.

Table 3-10

CAPACITY FACTOR AND PERCENT OF TIME GENERATING POWER
FOR EACH MONTH DURING TEST PERIOD

Month	Total Hours	Conventional Monthly Output (20 kWe Net)	Actual Monthly Output (Net 24-hour)	Capacity Factor	Power Generating Hours	Percent of Total Hours Generating Power
1984						
Feb	696	13,920	138	0.010	12.5	1.8
Mar	744	14,880	886	0.060	63.0	8.5
Apr	720	14,400	2,208	0.153	146.0	20.3
May	744	14,880	504	0.034	53.4	7.2
Jun	720	14,400	2,538	0.176	174.4	24.2
Jul	744	14,880	1,091	0.073	88.5	11.9
Aug	744	14,880	2,043	0.137	169.9	22.8
Sep	720	14,400	1,978	0.137	150.0	20.8
Oct	744	14,880	1,480	0.099	112.8	15.2
Nov	720	14,400	(288)	-	4.3	0.6
Dec	744	14,880	409	0.027	41.7	5.6
1985						
Jan	744	14,880	1,073	0.072	78.4	10.5
Feb	672	13,440	2,580	0.192	164.9	24.5
Mar	744	14,880	3,662	0.246	245.0	32.9
Apr	720	14,400	1,350	0.094	104.9	14.6
May	744	14,880	2,610	0.175	183.3	24.6
Jun	720	14,400	2,080	0.144	141.7	19.7
Jul	576	11,520	675	0.059	56.9	9.9
Total	12,960	259,200	27,077	0.104	1,991.6	15.4

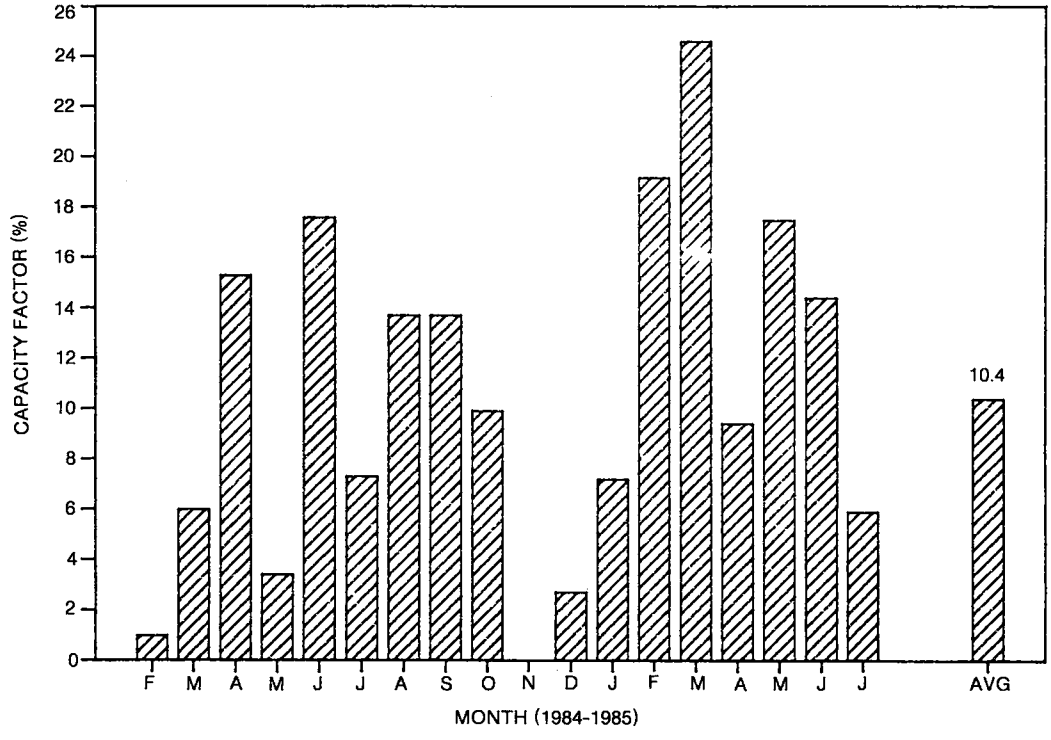

Figure 3-23. Monthly Vanguard Capacity Factor for the 18-Month Test Period Based on a Module Net Rating of 20 kW

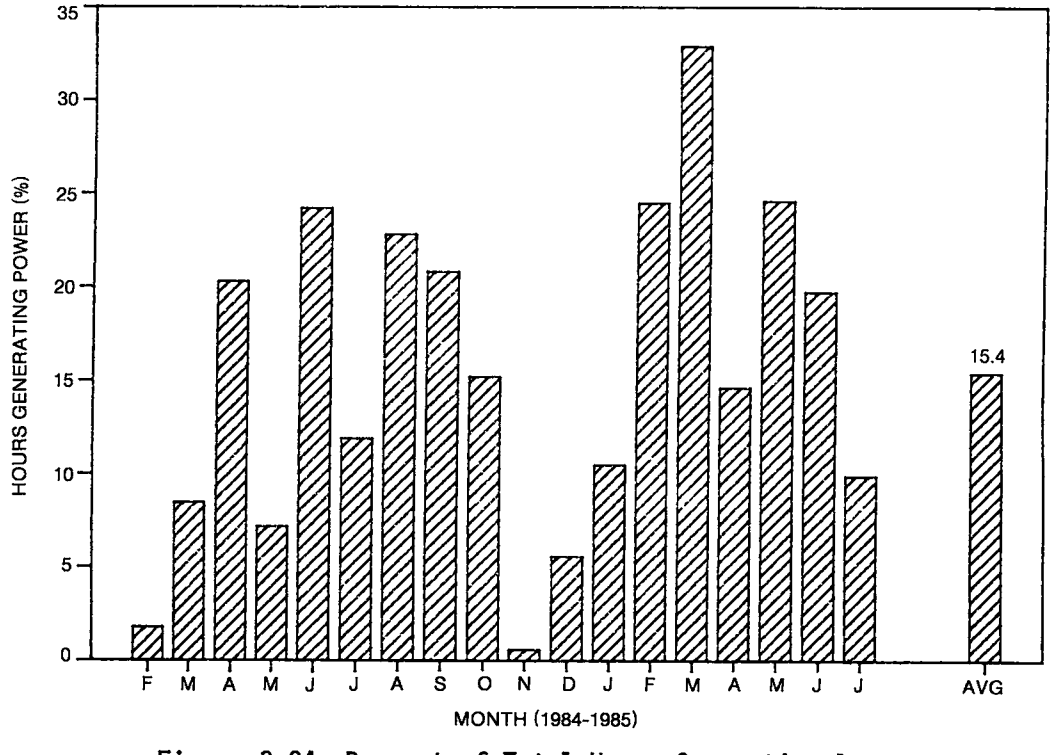

Figure 3-24. Percent of Total Hours Generating Power by Month for 18-Month Test Period

Instantaneous Method

The simplified dynamic model is primarily based on instantaneous (usually minute-by-minute) values of insolation and generated power, as well as other secondary variables. This model can be used to predict total generated energy output by integrating the instantaneous results calculated for each minute. However, this requires input data that are seldom available for the majority of potential site locations. This method would be expected to give more accurate results than an integrated-type model since generated power is calculated from the actual instantaneous level of insolation from each 1-minute period.

The general shape of the model equation is shown previously in Figure 3-13, where the x-axis is an insolation parameter, and the y-axis is a power parameter. The straight-line relationships between power and insolation are defined by two independent variables. The slope of the line is a function of the various parameters affecting both the amount of insolation input to the receiver and the internal efficiency of the Stirling engine in converting the input solar energy to electrical power. These parameters would include mirror facet reflectivity, shading and blocking factors, total dish area, tracking accuracy, evenness of distribution of solar energy across the receiver, and ambient temperature. The y-intercept of the line represents the electrical power lost as a result of processes that occur at any power level, provide a constant drain on the power output from the engine, and are not a function of insolation. Energy lost to overcome friction in maintaining generator speed at 1800 rpm and thermal losses from the cavity at a constant engine working gas temperature are typical examples. Because the engine temperature is so high, the effect of ambient temperature on the cavity heat loss is negligible.

The x-intercept represents the insolation level at which the power produced by the Stirling engine balances the power lost as a result of the operation of the engine (friction and cavity losses). Usable insolation would then be defined as that insolation occurring at or above this level. For this particular module, a threshold value of 300 W/m^2 appears reasonable.

The model equation developed by Advanco to estimate instantaneous power output was based on summer solstice data collected in June 1984 and has the following form:

$$P = \left[1 + 0.004\ (40.67 - T_a)\right]\left[\frac{R}{0.93}\ I(30.63) - 5.066\right],$$

P = gross generated power (KW)
T_a = ambient temp (°C)
R = dish reflectivity
I = incident direct insolation (KW/m^2)

where P is gross generated power in kW, T_a is ambient temperature in °C, R is average dish reflectivity, and I is incident direct insolation in kW/m^2. This equation compensates for ambient temperature and dish reflectivity deviations from the nominal values of 40.67°C and 0.93, respectively. The effects of other parameters such as wind speed and humidity are yet to be determined.

The effect of increasing ambient temperature is to cause the cooling water in the Stirling engine to circulate at a higher average temperature for a constant input power to the fan. The effect of cooling water temperature on the performance of the engine was measured for the second Mark II solar heat engine. For a peak pressure set point of 18 MPa, a 30°C difference in water temperature gave a 12% difference in power output, or about 0.4%/°C. At lower peak pressure set points, the difference was similar.

The effect of reflectivity variation on power output can be considered an insolation variation. The original equation was normalized using data from "clean" (93% reflectivity) mirrors; a drop in the reflectance of the mirrors reduces the amount of insolation hitting the receiver by the same ratio.

Figure 3-25 shows the predicted and actual power generation over a typical clear day in August. The thick line represents the actual gross power, and the thin line represents the predicted gross power. Actual gross electrical energy generated on this day was 167.5 kW•h, compared with the predicted value of 173.4 kW•h. The model equation estimates daily gross generated energy in this case to within 3.5%. If periods where the insolation is below a threshold value of 200 W/m^2 are eliminated, the actual energy produced is 163.9 kW•h, compared with the predicted value of 163.7 kW•h, which shows agreement to within 0.1%.

Bin Data Method

The dynamic model can also be applied to a site where only bin insolation data are available. The bin method is an alternative way of presenting insolation data, which gives the number of minutes that the level of insolation is within a particular band (between 300 and 400 W/m^2, for example). In the present case, the total electrical energy generated within a particular bin is estimated by calculating the power level for a representative insolation level for the bin (usually the midpoint) from the predictive equation and multiplying the representative level by the time period the insolation level stays within the range of that particular bin.

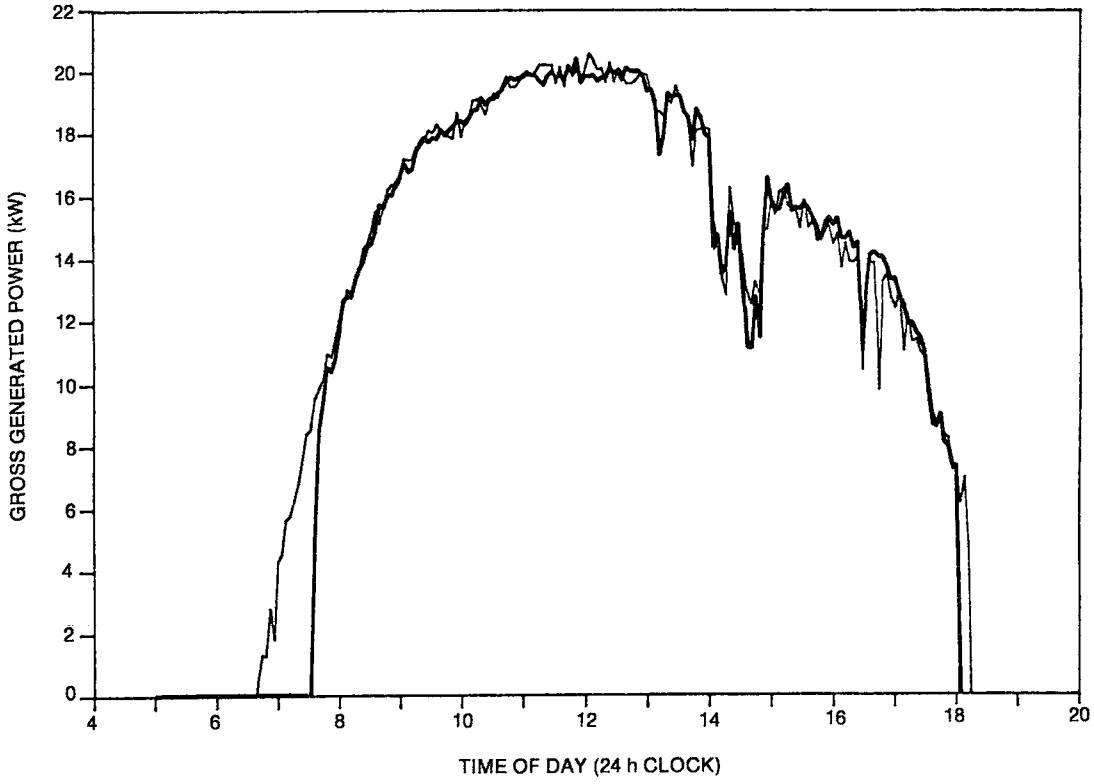

Figure 3-25. Actual versus Predicted Gross Generated Power for a Clear Day - 23 August 1984

Summing the results of this computation for each bin gives the total gross generated electrical energy.

Table 3-11 shows this computation for the same typical August day, where each bin represents a direct insolation span of 100 W/m^2. Total gross generated electrical energy is predicted to be 174.3 kW•h over the day, compared with the actual energy generation of 167.5 kW•h. The accuracy of the estimation for this particular case is within 4%. As expected, the accuracy of this method is slightly less than that using minute-by-minute data, but it is still adequate for most purposes. Smaller bands on the insolation level within each bin would increase the precision of the results.

The example day used in the above comparison was essentially clear. The accuracy of either method given above (instantaneous or bin data) would be expected to suffer primarily on partly cloudy days. Figure 3-26 shows the predicted and actual

Table 3-11

BIN METHOD FOR PREDICTING TOTAL GENERATED ELECTRICAL ENERGY - CLEAR DAY EXAMPLE

Insolation Level (W/m^2)	Number of Minutes Within Bin	Predicted Power Output[a] (kW)	Electrical Energy (kW•h)
0 to 200	388	0	0
200 to 300	16	2.2	0.5
300 to 400	32	5.1	2.7
400 to 500	48	8.0	6.4
500 to 600	60	10.9	10.9
600 to 700	144	13.8	33.1
700 to 800	148	16.7	41.1
800 to 900	244	19.6	79.6
900 to 1000	0	22.5	0
Total predicted electrical output			174.3

[a]Based on a reflectivity of 0.88 and no ambient temperature correction.

gross power generated on 17 August 1984, a partly cloudy day. Again, the thick line corresponds to the actual power generated and the thin line to the predicted power generated. Actual gross electrical energy generated was 78.1 kW•h over the day. The instantaneous model equation predicts a gross output of 83.6 kW•h on a minute-by-minute basis and 82.8 kW•h using bin data for the day (see Table 3-12). These estimates deviate by 7 and 6%, respectively, which indicates a slight drop in the precision of both estimating methods. If only insolation levels greater than a threshold value of 200 W/m^2 are considered, the actual electrical energy produced is 77.3 kW•h, and the predicted electrical energy from minute-by-minute calculations is 83.4 kW•h, a deviation of 8%.

The predicted values of gross energy produced are in all cases greater than the actual values, which indicates that these predictive methods tend to overestimate the generating power of the module. This must be kept in mind when these methods are applied to other site data to evaluate the absolute power generating capacity of the module at those locations.

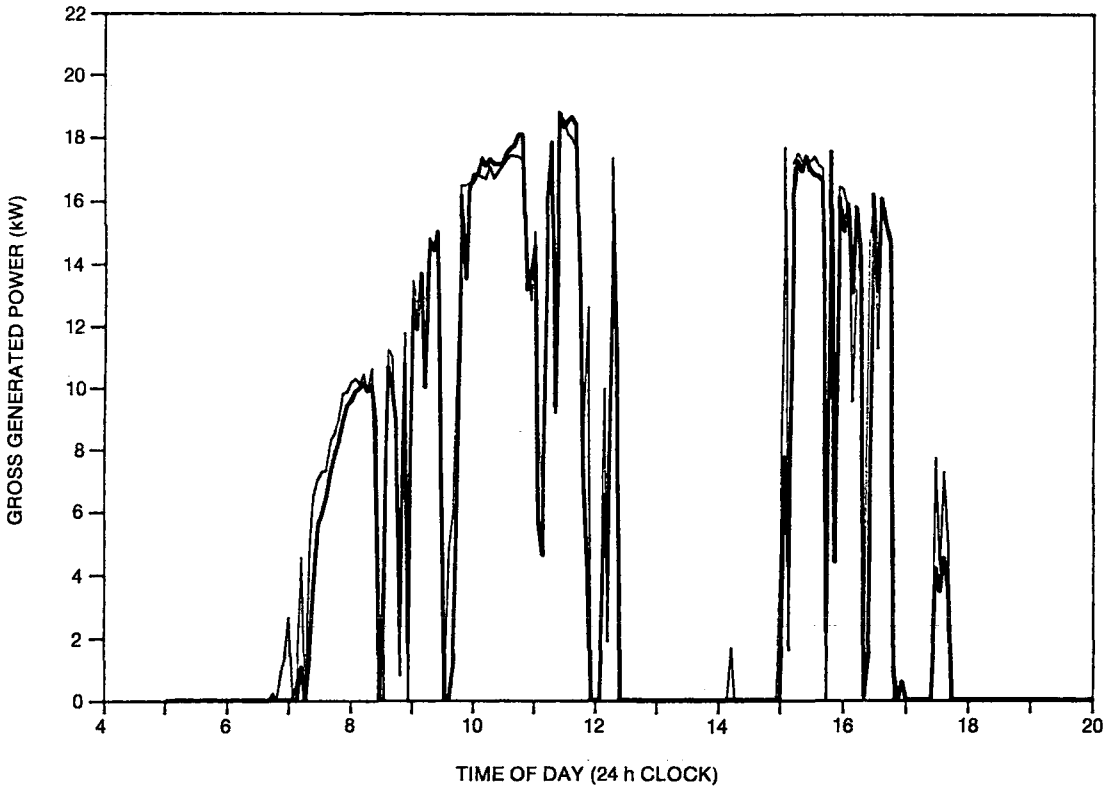

Figure 3-26. Actual versus Predicted Gross Generated Power for a Cloudy Day - 17 August 1984

Integrated Method

A third method that can be used to predict total output is the integrated model, which is simply a linear correlation relating total daily gross electrical energy generated with total daily direct insolation available. Several days are therefore required to provide enough data for a good correlation. Since data from individual days throughout the year were used, wider variations in parameters such as reflectivity and ambient temperature were expected, and these variations could affect the "fit" of the linear curve. No attempt was made to normalize each individual day's result to standard reflectivity or temperature, since these data were collected infrequently; however, this could be done provided that reflectivity data and average on-sun ambient temperature were available for each day. Only days in which the module operated continuously from sunrise to sunset were used in the development of the equation, because partial operation on full sun days would increase the data scatter dramatically, while significantly reducing the usefulness of the correlation.

Table 3-12

BIN METHOD FOR PREDICTING TOTAL GENERATED ELECTRICAL ENERGY - CLOUDY DAY EXAMPLE

Insolation Level (W/m^2)	Number of Minutes Within Bin	Predicted Power Output[a] (kW)	Electrical Energy (kW·h)
0 to 200	676	0	0
200 to 300	20	2.3	0.6
300 to 400	44	5.3	3.9
400 to 500	68	8.3	9.4
500 to 600	64	11.2	12.0
600 to 700	52	14.2	12.3
700 to 800	156	17.2	44.6
800 to 900	0	20.1	0
900 to 1000	0	23.1	0
Total predicted electrical output			82.8

[a] Based on a reflectivity of 0.9 and no ambient temperature correction.

Selected months of the year were chosen to provide data for the regression analysis. Data from typical days in June, September, and December 1984 and March 1985 were chosen to establish a correlation applicable to an entire year-long period. These data are plotted in Figure 3-27, along with the line of best fit. The equation based on these data is

$$E = 26.0\ I^* - 36.2$$

where E is the predicted gross electrical energy generated for the day (kW·h), and I* is the integrated direct insolation for the day ($kW \cdot h/m^2$). For the 57 sample days selected, the correlation coefficient, r, was 0.984. This is a very good correlation, given the number of environmental and system parameters that vary over a year's time. When monthly data were plotted separately, there was essentially no significant difference between the monthly and annual curves, further implying that the above equation can be used for any day of the year with relatively good accuracy.

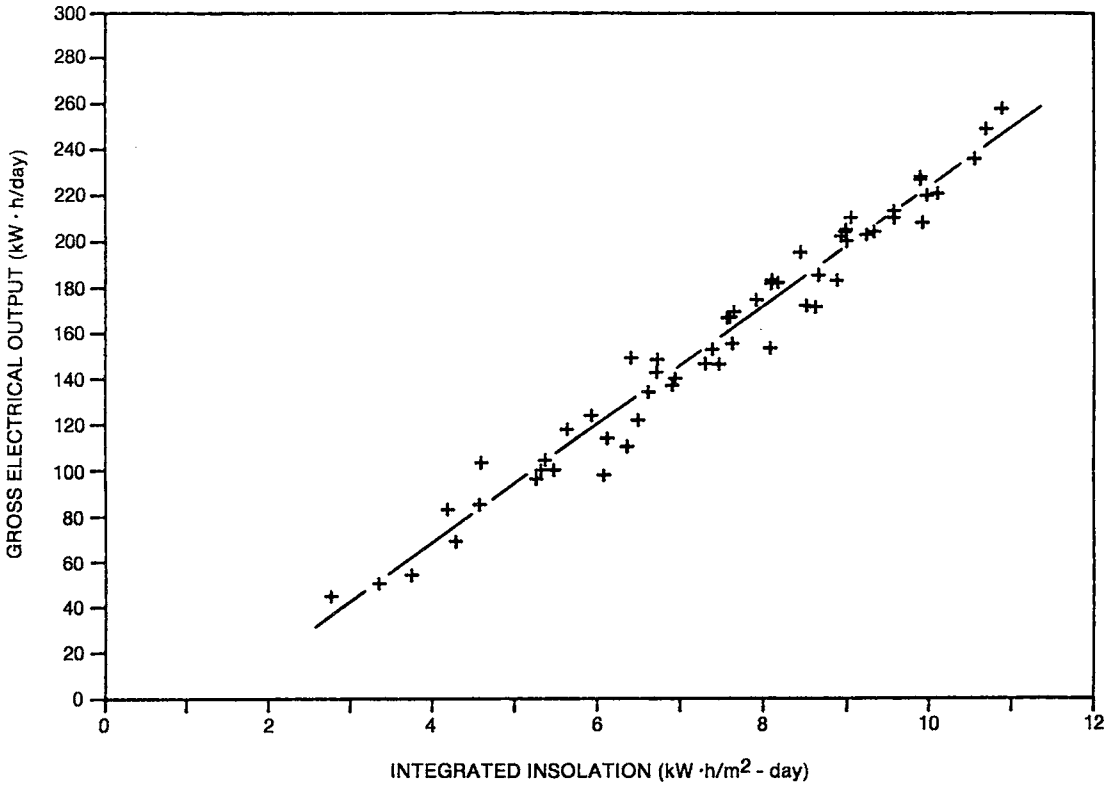

Figure 3-27. Daily Gross Electrical Output as a Function of Daily Integrated Insolation

For the example clear day used in the previous discussion, the total direct insolation available on site was 8.15 kW•h/m^2. The daily gross output predicted by the above equation is 175.7 kW•h. When compared to the actual energy generated of 167.5 kW•h, an accuracy of within 5% is calculated. For the predominently cloudy example day, the direct insolation totaled 4.23 kW•h/m^2, and the predicted energy output is 73.8 kW•h. An error of 5.5% is calculated when compared to the actual energy generation of 78.1 kW•h.

Table 3-13 summarizes the results and inaccuracies of the predictive methods discussed above. The numbers listed in the table and discussed in the text should not be taken as absolutes; these values are calculated only to show order of magnitude and relative differences between the various predicting methods. There can be no significance attached to the presumed trend in percent error within a particular example. The data above tend to show that any predictive method suffers more when applied to variable insolation periods (partly cloudy days) than to periods of consistent insolation. The errors observed above are due primarily to the assumption

Table 3-13

ORDER OF MAGNITUDE AND RELATIVE DIFFERENCES BETWEEN PREDICTING METHODS

Predicting Method	Clear Example Day			Cloudy Example Day		
	Actual Output (kW·h)	Predicted Output (kW·h)	Percent Error (%)	Actual Output (kW·h)	Predicted Output (kW·h)	Percent Error (%)
Instantaneous	167.5	173.4	3.5	78.1	83.6	7
Bin data	167.5	174.3	4	78.1	82.8	6
Integrated	167.5	175.7	5	78.1	73.8	-5.5

that insolation is a continuous function between given points in time. The accuracy of the above methods (in particular, the instantaneous method) may be increased if smaller time spans between data points are used to provide a more precise picture of the actual insolation function throughout the day.

Section 4

OPERATION AND MAINTENANCE

This section deals with the operation and maintenance (O&M) requirements of the Vanguard parabolic dish/Stirling engine module during the Vanguard test program. O&M information was obtained from a variety of sources including the site logbook, Advanco monthly and topical reports, discussions with site personnel, and personal observations by the authors.

The O&M section is divided into four parts. Operating personnel utilized at the test site are described in the first part. The second section examines major material and equipment requirements. Significant operating incidents occurring during installation of the module and during the 18-month test period are described next. Finally, routine and preventive maintenance practiced at the site during the test program is discussed.

OPERATING PERSONNEL REQUIREMENTS

The operating staff at the Vanguard test site during the January through October 1984 period consisted of three Advanco employees (chief engineer and site manager, chief technician, and field technician) and one United Stirling employee. The United Stirling on-site representative was an engineer who not only contributed his expertise to the Stirling engine test aspects, but also aided in resolving other technical problems as they arose.

As operating experience accumulated, the system became more and more independent of human interaction, and personnel requirements decreased. In October 1984, the United Stirling on-site participation was eliminated except on an ad hoc basis for any Stirling engine problems that could not be resolved by Advanco personnel.

The Vanguard system could operate in the fully automatic mode as of October 1984; however, for safety reasons a minimum of one Advanco person was stationed on-site during routine operation of the module for the remainder of the test period

(October 1984 through July 1985). In the fully automatic mode, an operator does not have to be present in the control room but must be within range of the alarm system should a problem arise that requires human interaction.

Duties for on-site personnel were quite varied due to the need to acquire performance data under different test conditions. Data acquisition system operation and maintenance was a large fraction of this work. Specific duties related to the data acquisition system included: monitoring morning startup and evening shutdown; reducing data; debugging hardware and software; connecting and installing data sensors and sensor leads; calibrating sensors; replacing/changing data tapes and diskettes; formatting data disks; maintaining data files; developing computer software; generating performance charts, tables, and graphs; evaluating and interpreting performance data; and transmitting data to other locations (e.g., Southern California Edison headquarters).

Other specific tasks related to testing the module included: proposing and developing procedures for special tests, monitoring the operation of all subsystems, acknowledging alarms and taking corrective action, troubleshooting and repairing system components, setting and optimizing control parameters, reading data sensors and meters not on the data acquisition system, and performing general maintenance.

Miscellaneous duties included maintaining a logbook, reordering miscellaneous supplies as necessary, interfacing with visitors and other off-site personnel, contacting organizations involved in the repair and maintenance of subsystem components, preparing monthly status reports and topical reports, and proposing potential modifications to the module.

Tasks dealing with routine maintenance at the site included manufacturing mirror facets, performing general maintenance of the dish, replacing mirror facets, performing site groundskeeping, maintaining the test and shop areas in a clean and safe condition, and fabricating and machining parts.

MATERIALS AND EQUIPMENT REQUIREMENTS

The major materials requirements at the test site were (1) replacement mirrors for the parabolic dish concentrator and (2) hydrogen gas, which was used as the working fluid in the Stirling engine.

During the test period, it was necessary to replace 19 mirrors due to breakage and mirror delamination. This subject is discussed more fully in Section 5. It is recommended that a supply of replacement mirrors be located on-site.

Hydrogen gas can be lost from the Stirling engine subsystem due to leakage from connections in the plumbing system and from the solar receiver by diffusion of the gas through the walls of the receiver tubing. Several major and minor leakage points were discovered during operation of the module over the 18-month period. In addition, the receiver tubes operate at temperatures about 700°C, and hydrogen gas can slowly diffuse through metal at these elevated temperatures. Hydrogen makeup requirements for the test period are shown in Table 4-1. In general, these losses were due almost exclusively to leaks in the plumbing system that were not repaired rather than by diffusion through the receiver tubes or by leakage through seals in the Stirling engine. Additional information on system hydrogen losses is presented later in this section.

Table 4-1
HYDROGEN MAKEUP REQUIREMENTS FOR VANGUARD

Purchase Date (month/year)	Number of Cylinders	Gas Volume[a] (ft^3)	Initial Delivery Pressure (psig)	Approximate Cost ($)
08/83	3	966	3500	207
05/84	2	432	2200	32
06/84	2	432	2200	32
08/84	2	432	2200	32
09/84	2	432	2200	32
10/84	4	864	2200	64
12/84	1	216	2200	16
01/85	1	216	2200	16
03/85	2	432	2200	32
05/85	2	432	2200	32
06/85	2	432	2200	32
Total		5286		527

[a]At standard temperature and pressure (60°F, 14.7 psig)

Major equipment at the site included a well-stocked work shop (which had welding, machining, and facet manufacturing equipment, as well as general shop tools),

safety gear, video equipment (which was very useful in testing), and equipment for data acquisition and reduction (see also Section 5). A Condor 42-40 mobile two-man platform was especially useful in providing access to all mirror facets on the parabolic dish, to the Stirling engine, and to the radiator mounted adjacent to the engine. The 42-ft lift enabled personnel to reach and replace or adjust any mirror facet in the 10.7-m- (36-ft-) diameter dish.

SIGNIFICANT OPERATING INCIDENTS

This section briefly describes operating incidents that occurred during assembly, checkout, and operation of the Vanguard module from January 1984 through July 1985.

Table 4-2 lists in chronological order all operating incidents, major or minor, that occurred during the 18-month operating period. The table classifies the incident by subsystem and gives the relative impact the incident had on module availability and the reference page of the logbook at the test site on which the problem was first noted. Incidents are ranked on a scale of 1 to 3, where "1" denotes that the incident prevented further operation of the module, "2" denotes significant impact but operation could continue, and a "3" indicates a relatively insignificant effect on continued operation.

In examining this chronological listing, two facts should be noted. First, many of these incidents are of the type normally encountered during the startup of a new and innovative piece of equipment. Second, a significant number of the incidents are relatively minor (having a ranking of 3). All incidents have been included in order to provide a comprehensive history and overview of the problems encountered during the 18-month period of operation.

Several problems occurred with the parabolic dish concentrator. Significant problems were encountered with the gravity slew system, which required substantial hardware modification. Limitations on space within the pedestal caused several initial tracking component problems. Electrical-related incidents included several control logic problems within the subconcentrator control unit, motor controller board failures, and the failure of the uninterruptible power supply to the tracker drive system. Problems with the mirror facets were varied, dealing with facet alignment, mirror delamination and occasional breakage, and the demonstrated potential danger from off-axis rays.

Table 4-2

CHRONOLOGICAL LIST OF OPERATING INCIDENTS
(Sheet 1 of 3)

INCIDENT DESCRIPTION	DATE	CLASSIFICATION	IMPACT ON AVAILABILITY	LOGBOOK REFERENCE PAGE
BURNT CABLES AT FOCAL POINT	12-Jan-84	CC	1	6
OSCILLATION OF DISH- MEMTRACK/SUNTRACK	18-Jan-84	CC	3	8
HYDROGEN DUMPING- BAD PLUMBING JOB	03-Feb-84	E	2	8
PROBLEM WITH H2 COMPRESSOR AND RELIEF VALVE	07-Feb-84	E	2	11
SLIDE PLATE OPENS TOO SOON	08-Feb-84	R	3	13
WATER IN SUN SENSOR	09-Feb-84	CC	2	11
DISH VIBRATION	09-Feb-84	CC	3	11
LOOSE CLAMP ON SYNCHRO AND ATTACHMENT SHAFT	10-Feb-84	CM	2	11
OPEN WIRE ON SUN SENSOR CABLE	11-Feb-84	CC	1	12
BURNT RPM CABLES	17-Feb-84	E	1	13
WEIGHT FELL OFF SLEW CABLE	27-Feb-84	CM	1	16
SOLENOID OF SLEW SYSTEM MODIFIED- STIFF SHAFT	28-Feb-84	CM	2	17
GORE BOX BROKEN FROM HOLDING TABS	02-Mar-84	CM	1	19
CORROSION OF SUN SENSOR CIRCUIT BOARDS	02-Mar-84	CC	1	19
MOTOR CONTROLLER FOR SKEW AXIS NOT ENGAGING	10-Mar-84	CM	1	20
OPEN RELAY- DIRTY CONTACTS ON JACK SCREW MOTOR	11-Mar-84	CC	1	21
STIFFNESS AND SLIDING OF CABLE/WIRING IN POWER TRACK	12-Mar-84	CM	2	22
BENT PIN ON SOLAR SENSOR/ TRACKING OSCILLATION	13-Mar-84	CC	2	22
APERTURE PLATE FELL OFF OF RECEIVER	20-Mar-84	R	1	26
LARGE GEAR CAME LOOSE	20-Mar-84	CM	1	25
INTERNAL GEAR SLIPPED ON GRAVITY SLEW	22-Mar-84	CM	1	27
BROKEN RETAINER BRUSH SPRING IN VACUUM PUMP MOTOR	26-Mar-84	E	1	28
SHATTERED MIRROR FACET WHEN WRAPPED IN BLACK PLASTIC	26-Mar-84	CD	2	30
STICKING PLATES DUE TO DIRTY TRACKS	02-Apr-84	R	2	31
TOOLS DROPPED FROM RECEIVER BROKE TWO MIRRORS	04-Apr-84	CD	2	32
GRAVITY SLEW DIDNT WORK DURING POWER FAILURE	26-Apr-84	CM	2	40
GRAVITY SLEW TRIP	27-Apr-84	CM	2	41
CHARRED AIR HOSE TO PLATES	02-May-84	R	1	43
DELAMINATION OF 10 FACETS	02-May-84	CD	2	43
THREE INCH PIPE FROM ENGINE BROKE MIRROR	02-May-84	CD	2	43
REPLACED AIR COMPRESSOR IN PCU	04-May-84	E	1	43
REPLACED PISTON ROD & RINGS IN ENGINE	04-May-84	E	1	43
RADIATOR LEAK	04-May-84	E	2	43
GIMBAL AXIS REACHED FULL TRAVEL	09-May-84	CM	2	45
BOLTS ON COOLING PLATES LOOSE FROM VIBRATION	11-May-84	R	2	45
POSSIBLE LEAKS IN AIR COMPRESSOR	11-May-84	E	3	50
REPLACE SHOCK ABSORBERS ON AIR COMPRESSOR/ VIBRATION	11-May-84	E	3	46
INSTALL AIR COMPRESSOR MOTOR MOUNT	17-May-84	E	3	52
BANGING SOUND IN GIMBAL EVERY 10 SECONDS	21-May-84	CM	2	54
SIX DELAMINATED MIRRORS	26-May-84	CD	2	56
PCU APERTURE CONE SLIGHTLY DAMAGED	26-May-84	R	3	56
SEVERE BLACKENING OF QUADROPOD/BURNT CABLES	28-May-84	CC	1	58
H2 COMPRESSOR ON FOR 48 HOURS	28-May-84	E	3	58
FOUR DELAMINATED MIRRORS	29-May-84	CD	2	58
SHAFT COUPLING DISINTEGRATED IN H2 COMPRESSOR	05-Jun-84	E	1	62
TWO DELAMINATED MIRRORS	07-Jun-84	CD	2	63
LIGHT SOURCE BURNED OUT DURING MIRROR ALIGNMENT	07-Jun-84	CD	3	63
MOTOR CONTROLLER BOARD GOING BAD	12-Jun-84	CC	2	65
OIL COOLER SYSTEM WONT SHUT DOWN AUTOMATICALLY	14-Jun-84	E	2	67
WATER COOLED PLATES WOULD NOT STAY OPEN	17-Jun-84	R	1	71
ENGINE MONITOR CIRCUIT BOARD DAMAGED/BURNED,CRACKED	18-Jun-84	CC	1	72
WATER PUMP WOULDNT SHUT DOWN	19-Jun-84	E	2	73
THREE DELAMINATED MIRRORS	19-Jun-84	CD	2	73

Table 4-2

CHRONOLOGICAL LIST OF OPERATING INCIDENTS
(Sheet 2 of 3)

INCIDENT DESCRIPTION	DATE	CLASSIFICATION	IMPACT ON AVAILABILITY	LOGBOOK REFERENCE PAGE
FIVE DELAMINATED FACETS	21-Jun-84	CD	2	77
DAMAGED MIRROR DUE TO VANDALISM	23-Jun-84	CD	2	81
MASTER CONTROLLER BOARD BAD- BLOWN FUSES	02-Jul-84	CC	1	95
OBSTRUCTION IN PATH OF GRAVITY SLEW WEIGHT	02-Jul-84	CM	2	94
TWO DELAMINATED MIRRORS	05-Jul-84	CD	2	96
RELIEF VALVE PROBLEM IN H2 COMPRESSOR	10-Jul-84	E	2	98
BOLT CAME LOOSE AT SHUTTER PLATE	11-Jul-84	R	2	98
DAMAGE TO PCU ANALOG OUTPUT	23-Jul-84	E	1	113
REPAIR OIL SENSOR UNIT	26-Jul-84	E	1	118
BURN MARK ON PINS 11,12 OF A/D CONVERTER	31-Jul-84	E	1	124
SCREWS LOOSE ON PLATE TRACK SYSTEM	31-Jul-84	R	2	124
TWISTED MICRO SWITCH ON SKEW	08-Aug-84	CM	1	130
MAGNETIC DEPOSIT ON RECEIVER TUBES	08-Aug-84	R	3	130
CENTER PLUG FELL FROM RECEIVER, HIT FACET	11-Aug-84	R	1	133
REPAIRED WATER COOLED APERTURE PLATES	12-Aug-84	R	2	134
CAMERA MELTED FROM OFF-AXIS RAYS	03-Sep-84	CC	3	148
MORE MATERIAL ON RECEIVER	05-Sep-84	R	3	150
CLUTCH FOR PAWL CLICKED	16-Sep-84	CM	2	157
BEARING GOING OUT ON MOTOR SYSTEM	17-Sep-84	CM	2	158
SOLONOIDS HAVE OVERHEATED DUE TO FIRE	19-Sep-84	CC	1	159
GRAVITY SLEW GEAR LOOSE, FELL OFF SHAFT	19-Sep-84	CM	1	159
EMERGENCY GENERATOR SYSTEM FAILED	19-Sep-84	CM	2	160
USI ENGINE MONITOR NOT WORKING	20-Sep-84	E	2	160
GRAVITY SLEW PROBLEMS-SET SCREW,WEIGHT CATCHING	24-Sep-84	CM	2	161
BURNED OUT LAMPS- U.S. CONTROL BOX	24-Sep-84	E	3	161
EXCESSIVE ENGINE NOISE	05-Oct-84	E	3	165
LARGE HYDROGEN LEAK- VENT VALVE HAD LEAK	08-Oct-84	E	2	166
ENGINE OIL LEAK	16-Oct-84	E	3	170
UPS UNIT FAILURE	19-Oct-84	CM	1	176
BLACK POWDER IN RECEIVER AREA	19-Oct-84	R	3	172
RPM SENSOR SHAFT BROKEN TWICE	29-Oct-84	E	1	177
ALLEN SET SCREW LOOSE FROM PLAY IN ENGINE	29-Oct-84	E	2	178
NOISE LEVEL IN ENGINE INCREASING	07-Nov-84	E	3	182
BROKEN RPM SENSORS	08-Nov-84	E	1	183
INSOLATION TRACKER MOTOR FAILURE	29-Nov-84	CM	1	186
RAIN ON PCU CAUSES USI MONITOR FAILURE	10-Dec-84	E	1	187
WATER PUMP STUCK AND/OR RUSTED	12-Dec-84	E	1	187
RPM SHAFT BROKE AGAIN	13-Dec-84	E	1	187
TILE BROKE LOOSE FROM APERTURE	14-Dec-84	R	1	188
FROST ON COMPRESSOR/FROZEN PLATES WOULDNT MOVE	15-Dec-84	R	1	189
OIL PUMP SHAFT WORN OUT	16-Dec-84	E	1	190
FAILURE OF LOCKING PAWL DEVICE- NO DISENGAGEMENT	22-Dec-84	CM	1	193
NEW ELECTROSPACE TRACKING PROMS DONT WORK	22-Dec-84	CC	2	193
PLATE PROBLEMS	23-Dec-84	R	1	194
APERTURE PLATE IS MELTED ON LOWER LEFT	23-Dec-84	R	3	194
INTERCONNECTING PUMP SHAFT WORN AWAY AGAIN	09-Jan-85	E	1	202
PROBLEM REMOVING RADIATOR FROM ENGINE MODULE	14-Jan-85	E	3	205
RELAY CONTACT FAILURE DUE TO OVERHEATING	15-Jan-85	CC	1	206
CONTINUED PLATE PROBLEMS	25-Jan-85	R	2	209
WEATHER STATION WENT DOWN	25-Jan-85	I	3	209
HOUR METER NOT RUNNING CORRECTLY	12-Feb-85	I	3	225
NEW GIMBAL STOW LOCK- OPEN LEAD TO PAWL	18-Feb-85	CM	2	231
GRAVITY SLEW NOT OPERATIONAL	19-Feb-85	CM	2	232

Table 4-2

CHRONOLOGICAL LIST OF OPERATING INCIDENTS
(Sheet 3 of 3)

INCIDENT DESCRIPTION	DATE	CLASSIFICATION	IMPACT ON AVAILABILITY	LOGBOOK REFERENCE PAGE
FAILURE OF LIMIT SWITCH FOR PLATES	25-Feb-85	R	1	236
FALLING INSULATION AROUND RECEIVER TUBES	25-Feb-85	R	2	236
AIR COMPRESSOR LEAK	25-Feb-85	E	3	236
OSCILLATION BETWEEN SUN AND MEM TRACK	05-Mar-85	CC	3	240
REPAIR LEAKY AIR REGULATOR	08-Mar-85	R	1	242
REPAIR PLATE HARDWARE	08-Mar-85	R	1	242
CONTROL BOX PROBLEMS	12-Mar-85	CC	2	244
ENGINE RPM OSCILLATION	18-Mar-85	E	2	247
H2 COMPRESSOR OIL LEAK	19-Mar-85	E	1	248
ELECTROSPACE PROMS DONT WORK	27-Mar-85	CC	2	251
HYDROGEN HOSE TRACK BENT	27-Mar-85	CM	2	251
CONTROL BOARD BLOWN FUSE	28-Mar-85	CC	1	252
OIL PUMP FAILURE - WORN SHAFT AGAIN	01-Apr-85	E	1	253
MOTOR CONTROLLER BOARD FAILURE	04-Apr-85	CC	1	254
BROKEN UPPER LOCK PAWL MOTOR	15-Apr-85	CM	2	255
GRAVITY SLEW CABLE BROKEN	15-Apr-85	CM	2	255
SKEW AXIS BOARD REPLACED	19-Apr-85	CC	1	256
DISH WILL NOT GO TO POSITION A	24-Apr-85	CC	1	257
MIRROR DAMAGED BY FALLEN OBJECTS	24-Apr-85	CD	2	257
BURNT FIBERGLASS DUE TO POWER LOSS	24-Apr-85	R	2	257
CONDUCTED REPAIRS ON RECEIVER	26-Apr-85	R	2	258
REPLACE FAULTY CONTROL CIRCUIT BOARD	27-Apr-85	CC	1	258
HYDROGEN HOSES STIFF - REPLACED	29-Apr-85	E	2	258
UPPER PAWL TIE CABLE BROKEN	03-May-85	CM	1	260
FIBERFAX MATERIAL COMING LOOSE	06-May-85	R	2	261
MOTOR CONTROL CIRCUIT BOARD FAILURE	11-May-85	CC	1	263
ENGINE CONTROL BOX / US DISPLAY MONITOR	14-May-85	E	2	264
MOTOR BURNOUT ON LOCKING PAWL	01-Jun-85	CM	1	267
THERMOCOUPLE FAILURES	11-Jun-85	R	2	271
TEMPERATURE DIFFERENTIAL DISCREPANCIES	18-Jun-85	R	3	273
NEW RECEIVER TUBES EXPLODED	20-Jun-85	R	1	275
ONE BROKEN CHECK VALVE IN ENGINE	22-Jul-85	E	1	281

KEY:

CC = CONCENTRATOR ELECTRICAL COMPONENTS
CD = CONCENTRATOR MIRROR FACETS
CM = CONCENTRATOR MECHANICAL COMPONENTS
E = STIRLING ENGINE & RELATED SUBSYSTEMS
I = DATA ACQUISITION & INSTRUMENTATION
R = SOLAR RECEIVER

1 = PREVENTED FURTHER OPERATION OF THE MODULE
2 = SIGNIFICANT IMPACT BUT OPERATION COULD CONTINUE
3 = INSIGNIFICANT EFFECT ON CONTINUED OPERATION

Operating events related to the receiver were the incidents that occurred during the development of an acceptable aperture cone, two independent material degradation problems, persistent problems with the water-cooled aperture plates, and occasional overheating of the receiver tubes during transient periods.

Significant operating incidents related to the Stirling engine were two engine overhauls (for unrelated reasons), substantial power conversion unit noise and vibration, engine rpm sensor and shaft problems, on-going hydrogen leakage, and repetitive failure of the United Stirling monitor circuit boards. Check-valve failure was the reason for the initial engine disassembly, while the breakage of an oil pump shaft in the engine (with the concurrent replacement of unhardened gears) necessitated the second overhaul.

The above incidents, as well as others deemed significant, are discussed in much greater detail in Section 5.

ROUTINE AND PREVENTIVE MAINTENANCE

The routine and preventive maintenance tasks discussed in this section include those actually observed at the site and those recommended by ETEC for a small single-module operation based on conversations with site personnel and with operating experience. No projection of operation and maintenance tasks for large-scale multimodule plants was attempted.

Current Maintenance Activities

Current practice indicates that several maintenance tasks are necessary to provide consistent operation of the dish/Stirling module and support equipment. Specific tasks pertaining to subsystem failures are not included; these are not considered either routine or preventive, since they are basically a corrective action to a particular problem. The routine and preventive maintenance activities are sorted by subsystem and are presented in Tables 4-3 through 4-7 along with an estimated frequency based on average reported project experience to date. These preventive maintenance tasks are also designated with either a "C" or an "R," separating those tasks that are current practice from those that are recommended by ETEC based on operating experience. Current tasks are those in which a regular frequency of performance was established by the on-site personnel or in which an average frequency could be projected based on repetitive entries in the log book.

Table 4-3

ROUTINE AND PREVENTIVE MAINTENANCE ACTIVITIES - CONCENTRATOR

Task	Current (C) or Recommended (R) Practice	Estimated Frequency
Measure reflectivity	C	1 day
Rinse dish	C	4 days
Clean/align sun sensor	C	1 week
Check sun sensor condensation	R	2 weeks
Wash dish	C	3 weeks
Measure dish vibration	R	1 month
Check carbon deposits on M/C boards	R	1 month
Check power track, cable system	R	1 month
Lubricate gravity slew	C	2 months
Check looseness of tracking gears	R	2 months
Check facet alignment	C	6 months
Inspect locking pawl	R	6 months
Check and adjust synchro	R	6 months
Grease gimbal mechanism	C	1 year
Manufacture facets	C	As necessary
Replace facets	C	As necessary
Touch up paint, rust spots	C	As necessary
Check SCCU parameter settings	C	After power outage

Recommended tasks are those that may or may not have been performed on site and for which no entry was ever recorded in the maintenance log. The noted frequency in these tables varies to some extent, depending on the environmental and other operating conditions surrounding the site. Therefore, these numbers should be considered reasonable estimates, rather than absolutes. Some of the tasks listed in the tables are described more fully below.

Site personnel recommend that at sites with limited rainfall (such as the Rancho Mirage site), the dish mirror facets should be rinsed with water approximately every 4 days to maintain high reflectivity. This frequency will also depend on the quality of the air surrounding the site in terms of proximity to roads and construction sites and the prevalence of high winds and duststorms. Rinsing the dish will not produce fully clean reflectivity but will restore a large fraction. Measurements on site indicate a sharp increase in reflectivity on the days immediately

Table 4-4

ROUTINE AND PREVENTIVE MAINTENANCE ACTIVITIES - SOLAR RECEIVER

Task	Current (C) or Recommended (R) Practice	Estimated Frequency
Clean receiver with air	C	1 month
Lubricate plate tracks	C	1 month
Gather material from receiver	R	1 month
Check looseness of bolts, screws	R	1 month
Inspect aperture for loose tiles	R	1 month
Service plates	C	2 months
Inspect air compressor system	R	3 months
Clean receiver with brush	C	4 months

Table 4-5

ROUTINE AND PREVENTIVE MAINTENANCE ACTIVITIES - STIRLING ENGINE

Task	Current (C) or Recommended (R) Practice	Estimated Frequency
Refill hydrogen	C	1 day[a]
Check radiator coolant level	C	2 weeks
Check engine oil level	C	2 weeks
Inspect water hoses, radiator for leaks	C	1 month
Measure engine noise level	R	1 month
Inspect engine exterior for damage	C	1 month
Check for hydrogen leaks	R	2 months
Inspect water pump for rust buildup	R	6 months
Replace monitor display lights	C	As necessary
Service engine	C	As necessary

[a]Interval between hydrogen refills would be greatly increased with a leak-tight system delivering hydrogen to the module.

Table 4-6

ROUTINE AND PREVENTIVE MAINTENANCE ACTIVITIES - EMERGENCY GENERATOR

Task	Current (C) or Recommended (R) Practice	Estimated Frequency
Check oil, coolant, and fuel levels	C	2 weeks
Check battery water level and charge	R	2 weeks
Inspect fan belt	R	1 month
Check oil filter, fuel filter, air cleaner	R	3 months
Check valve clearance	R	6 months

Table 4-7

ROUTINE AND PREVENTIVE MAINTENANCE ACTIVITIES - DAS

Task	Current (C) or Recommended (R) Practice	Estimated Frequency
Check operation of DAS equipment	C	1 day
Check function of engine kW•h meter	R	1 week
Check sensor accuracy/calibration	R	6 months
Replace DAS magnetic tapes	C	As necessary
Check function of MCCU	C	After power outage

following a wash or rinse. The time required for a simple dish rinse is typically 15 minutes.

Washing the dish is a more thorough way of promoting the highest attainable reflectivity but requires the hand-scrubbing of each individual facet (there are currently 336 facets) with a cleaning solution. Washing will eliminate the non-water-soluble film that cannot be removed by simple rinsing. Reflectivity can be increased to a maximum of 93% by washing. Total time required is approximately 2 to 3 hours.

Reflectivity measurements over a 60-day period (when reported) are shown in Figure 4-1. Also noted on the figure are the days of significant rainfall and the days in which the dish was either rinsed or washed. These data indicate that washing the dish (positions 3, 5, and 8) only provides a slight reflectivity increase over a simple rinse (positions 1 and 7) or a moderate rainfall (positions 2 and 6). Since the time required to wash the dish (2 to 3 hours) is significantly

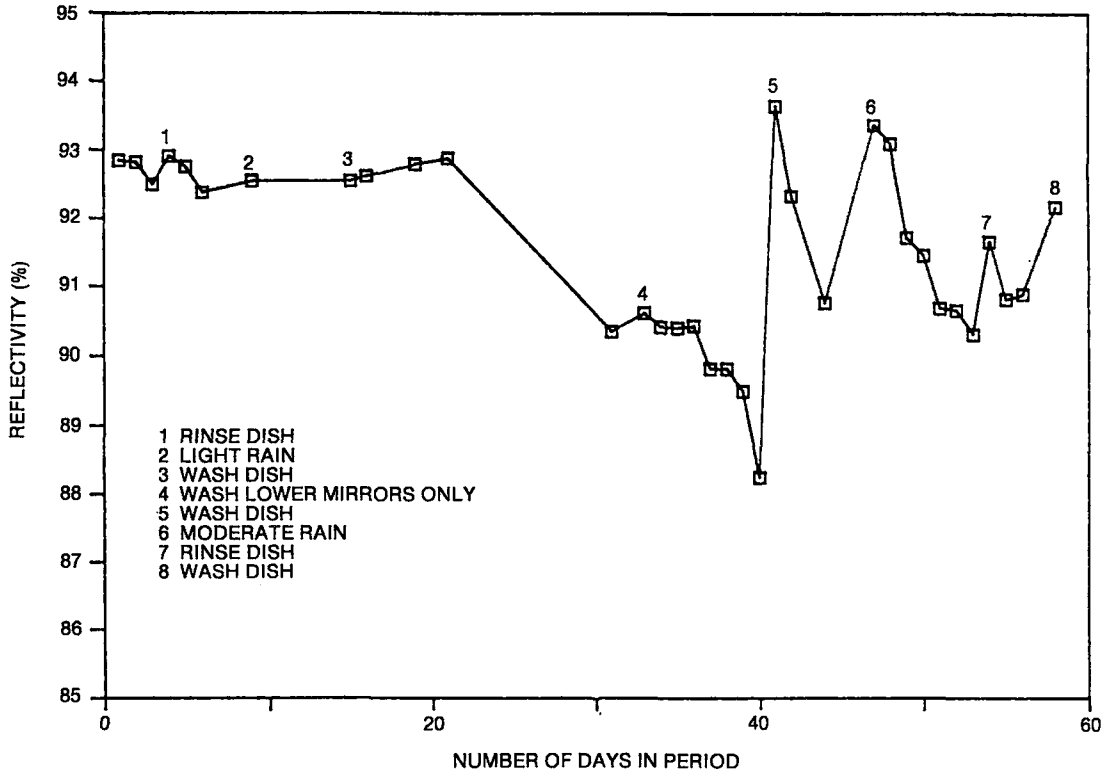

Figure 4-1. Reflectivity Measurements During a 60-Day Period

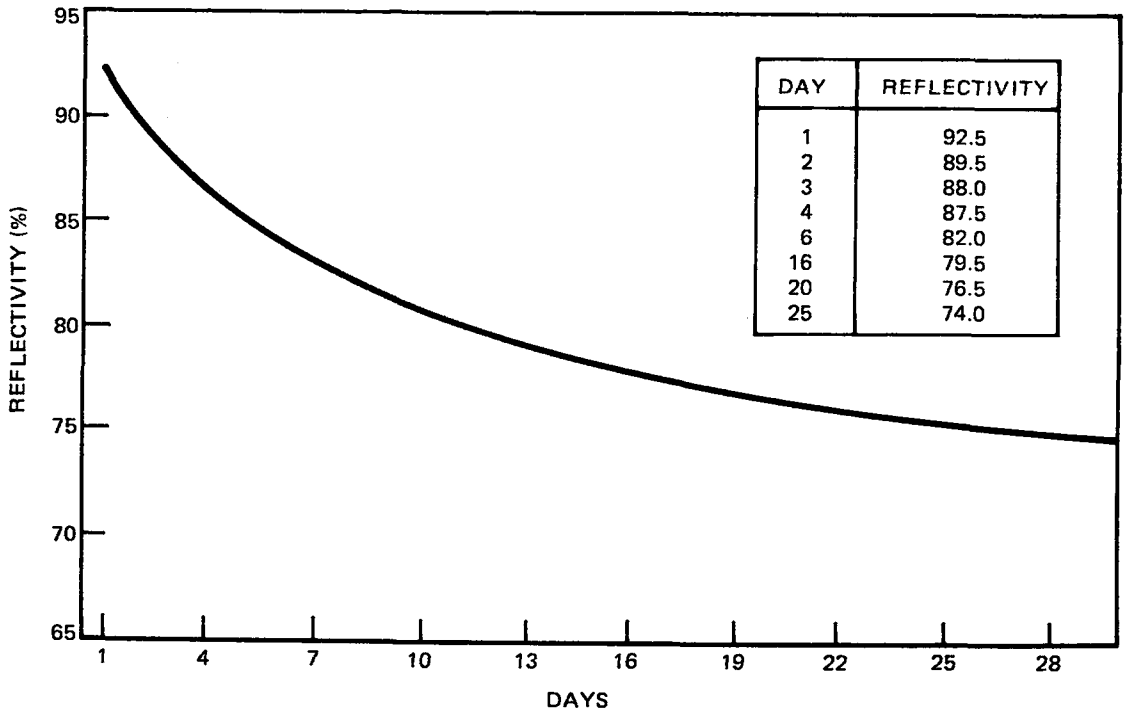

Figure 4-2. Typical Mirror Reflectivity Degradation During Summer

longer than that required to rinse the dish (15 minutes), the washing operation appears not to be cost effective if performed frequently.

Typical summer mirror reflectivity degradation without rinsing or washing reported by Advanco is shown in Figure 4-2. The 25-day period presented here included no days of rain. If washing the dish is the desired practice, the decrease in revenue due to lowered reflectivity will equal the manpower cost to wash the dish after approximately 3 weeks (assuming 7¢/kW•h and $12/hour labor). This would be the break-even point (the economic wash point) for the dish at this particlar site. As shown previously, rinsing the dish will provide a reflectivity recovery almost as high as washing, and at a substantial savings in manpower. Based on the same reflectivity degradation curve, the economic rinse point occurs after only 4 days. Over the same 3-week period, then, the dish will produce more energy (since the average reflectivity will be higher), and the manpower requirements will be lower (by approximately one-half hour) if rinsing is the preferred practice. At sites where precipitation is more frequent, washing or rinsing may not be required for several weeks. The individual site characteristics must be considered when determining a dish maintenance schedule.

The exterior glass element of the sun sensor will also collect a film that will hinder the passage of solar radiation and may affect the accuracy of dish tracking. This element should be cleaned periodically. The alignment of the sun sensor is also important in providing a uniform flux pattern on the receiver. The alignment should be spot checked weekly to avoid high-temperature gradients on the receiver.

Lubrication of the cables, pulleys, and tracks in the emergency gravity slew system should be done every 2 months, since it is this system that will detrack the dish off-sun during certain system failures to prevent damage to the receiver and other sensitive components.

Once the mirror facets on the dish are properly aligned and locked into position, no additional alignment should theoretically be required. However, if facets are replaced frequently or dish vibration is excessive, some mirror facets may become misaligned over months of operation. This would be noticed as a decrease in the performance of the engine, specifically in a nonuniform working gas temperature between quadrants. Mirror facet alignment should be checked twice yearly to ensure that the system is operating at the highest possible efficiency.

The deposit of powdery material on the receiver tubes indicates possible receiver tube material degradation (black powder) and condensation of volatile components from surrounding insulation outgassing (white powder). Although the effect of this on receiver tube life is presently unknown, the powdery material must be removed to provide an even flux of radiation across the entire receiver. Since the material deposition rate does not appear high, cleaning the receiver monthly with compressed air should be adequate to remove most of the loosely bound powder.

Cleaning the receiver with a wire brush or steel wool three times per year will remove deposits that would ordinarily not come off with compressed air and will help restore the original heat transfer capability of the tubes.

Because of the design of the aperture shutter system, this component demands periodic attention to maintain the quick response of the plates when commanded to open or close. Experience dictates that the plate track system be lubricated regularly to provide consistent service. Similarly, the aperture plates themselves must be serviced bimonthly to ensure proper operation.

The hydrogen system design required that additional gas be transferred from the supply bottle into the low-pressure reservoir daily. The gas was then pumped up to a higher pressure for use by the engine. Several small hydrogen leaks were present in the system, which necessitated the daily refilling operation; in a large-scale plant, these plumbing leaks would have to be repaired, cutting the hydrogen consumption down substantially. Very little gas was apparently lost through the receiver tubes by diffusion or from the Stirling engine by leakage past seals. Hydrogen consumption in terms of the number of supply bottles used appears high (see previous discussion), partly because the gas was not pumped out of the bottles to the reservoir and gas could be transferred only as long as the bottle pressure remained above that of the low-pressure reservoir. The bottles were routinely returned one-half full.

Both the Stirling engine and the induction generator should be overhauled and serviced when the performance of these components indicates a problem. Over the test period, engine overhaul was done yearly, which may or may not be representative for continually operating plants. The components of particular interest in terms of lifetime are the engine piston rods and seals and receiver tubes. Further operation of the module in excess of the 18-month test period would have given additional O&M data on the lifetime of system components. It is premature to estimate the lives of these major components.

Several other tasks appeared frequently throughout the test program, but could not be assigned a particular estimated frequency. These tasks, which were usually performed on an "as necessary basis," included items such as the manufacture of additional mirror facets, the replacement of damaged or delaminated facets, the replacement of control display lights, and structural paint touchup.

Additional Maintenance Checks

Several other maintenance checks are recommended based on experience with and the failure of certain subsystem components during the module test period. These are presented in the above tables as recommended tasks along with an estimated frequency. Some items in this category are discussed below. Other specific incidents of failure are reported in a subsequent section.

Condensation inside the sun-sensor unit was a persistent problem in the early months of operation, causing oscillation and tracking problems. The condition was alleviated by venting the sensor to the atmosphere, but periodic checks should continue.

Dish structure vibration can also indicate sources of potential problems. Excessive vibration may weaken the structure, may shake mirror facets out of alignment, and may loosen bolts and nuts throughout the module no matter what the source of the vibration. Effort should be made to isolate and correct the source of abnormal vibration by periodic vibration measurements. Vibration measurements made on the Vanguard module before and after the replacement of degrading engine gears are shown in Table 4-8. There appeared to be a significant reduction in dish vibration following this overhaul. Vibration measurements were also taken during normal daily startup of the module. These results are presented in Table 4-9.

Carbon deposits due to overheating of electrical components caused several short-term outages of the module. A quick check of all gimbal relays and motor controller boards should prevent some of these failures. It is estimated that these checks should be made once each month.

Table 4-8

VIBRATION MEASUREMENTS ON VANGUARD MODULE

Location	Date	Vibration[a] (g)
Lower radial strut - outside edge	10/17/84	0.30
	07/25/85	0.08
Lower radial strut - middle	10/17/84	0.50
	07/25/85	0.12

[a] Average from several readings

Table 4-9

VIBRATION MEASUREMENTS DURING DAILY STARTUP OF MODULE

Module Status	Vibration[a] (g)
Stow	0.01
Shutter plates opening	0.05
Slewing	0.06
Slewing; pump on	0.16
Slewing; pump, engine on	0.18
Slewing; pump, engine, compressor on	0.30
Normal operation	0.27

[a] All measurements were made on 7/25/85 with the sensor located in the middle of the upper radial strut.

The looseness of several gears within the tracking and gravity slew systems caused short-term outages. Periodic bimonthly checks of all cable/gear systems should indicate whether there exists a potential problem so that corrective action can be taken.

The gimbal mechanism rotates daily as the dish tracks across the sky. It is advisable to keep this mechanism lubricated to provide a smooth tracking path and to

minimize the parasitic power requirements in the dual-motor tracking system. A yearly greasing of all moving parts in the gimbal is expected to be adequate for continuous daily operation.

When continuous operation of the module was achieved, a black powdery material appeared regularly on the receiver tubes. This was thought to be an oxide of the receiver tube material. Receiver lifetime could be affected if depositing continued. Therefore, the presence and amount of this substance should be measured and reported monthly to provide a data base for determining receiver life.

Air compressor system leaks can be accommodated since the system will compensate by running more often for longer periods of time. However, longer operation is an additional parasitic load that is unnecessary. Every 3 months, the air system should be checked for potential leaks (rusted connections, degraded hoses); large leaks will be indicated by the increased power consumption of the unit.

The increased noise level of the Stirling engine can indicate potential problems before they become serious. Guidelines should be set up such that if the noise level reaches some threshold value, the engine should be removed and dismantled for repair. Under continuous operation, the noise level need only be measured monthly. Typical noise measurements from the Vanguard module are given in Table 4-10.

Table 4-10

NOISE MEASUREMENTS FROM VANGUARD MODULE

Location	Noise Level[a] (dB)
Background; system off	52
Operating; from trailer	75
Operating; under dish	82

[a]Average from several readings on 10/17/84

Frequently, loose bolts or screws on the power conversion unit resulted in component failure and even in portions of the power conversion unit falling onto the mirrors. This can be reduced by examining all component connectors monthly, especially if the vibration level of the dish is excessive.

The consumption of hydrogen gas by the system can be a major cost item when compared with other operating expenses. Effort should be made to maintain as tight a system as possible to prevent external dumping or leaking of the gas to the environment. The hydrogen system should be checked for leaks bimonthly to reduce gas consumption.

Engine radiator leakage should be evident by a low fluid indication in the control room; however, periodic checks for potential leakage sites (rust, weak hoses) may prevent a catastrophic failure. The radiator system should be examined at 3-month intervals to head off potential problems.

The module water pump experienced seizure due to the buildup of rust. A simple check every 6 months of continuous operation should detect rust buildup.

Fluid levels in all components should be checked frequently, and additional fluid should be added when necessary. On the engine, this includes the radiator water/antifreeze level and the engine oil level. On the backup emergency generator, the oil, coolant, fuel, and battery fluid levels must be checked periodically.

Accurate data taking and adequate safety/warning indicators in the control room depend on properly operating and properly calibrated sensors. Twice a year, checks of sensors important to the operation and safety of the module should be undertaken.

As the construction and operation of modules similar to the Vanguard continue, additional data will be collected that will either substantiate, modify, or supplement the type of tasks, the estimated frequencies, and the manpower requirements quoted above. In addition, it is hoped these data will provide a basis for estimating component lifetimes, an item of particular importance in the evaluation of system life-cycle costs.

Section 5

SUBSYSTEM PERFORMANCE

This section describes the performance of the module subsystems in detail, including specific events that occurred and frequent observations that were made during the Vanguard test program. The major subsystems are the parabolic dish concentrator, the solar receiver, the Stirling engine, the induction generator, the electrical grid interface, instrumentation and control, and the data acquisition system.

PARABOLIC DISH CONCENTRATOR

The parabolic dish concentrator subsystem can be divided into three categories: (1) mechanical components related to the drive mechanism, which include all motors, cables, and gears as well as the gravity slew system; (2) electronic components related to the tracking control, including the motor controller circuit boards, all wiring within the dish, and the control logic; and (3) the mirror facets themselves, including the facet racks, and the attachment and alignment hardware. The specific performance of components within each category is discussed below.

Mechanical Components

Specific operating incidents related to the mechanical components of the concentrator are listed in Table 5-1, with the individual columns as described in the previous section. Most of these events deal directly with the gravity slew system; the more important of these are discussed in detail below.

Gravity Slew System. The gravity slew system experienced several initial operating problems:

- Excessive parasitic power (300 W) consumption by the solenoid that holds the gravity slew weight up in the ready position
- Excessive solenoid noise

Table 5-1

CONCENTRATOR OPERATING INCIDENTS--MECHANICAL

INCIDENT DESCRIPTION	DATE	IMPACT ON AVAILABILITY	LOGBOOK REFERENCE PAGE
WEIGHT FELL OFF SLEW CABLE	27-Feb-84	1	16
GORE BOX BROKEN FROM HOLDING TABS	02-Mar-84	1	19
MOTOR CONTROLLER FOR SKEW AXIS NOT ENGAGING	10-Mar-84	1	20
LARGE GEAR CAME LOOSE	20-Mar-84	1	25
INTERNAL GEAR SLIPPED ON GRAVITY SLEW	22-Mar-84	1	27
TWISTED MICRO SWITCH ON SKEW	08-Aug-84	1	130
GRAVITY SLEW GEAR LOOSE, FELL OFF SHAFT	19-Sep-84	1	159
UPS UNIT FAILURE	19-Oct-84	1	176
INSOLATION TRACKER MOTOR FAILURE	29-Nov-84	1	186
FAILURE OF LOCKING PAWL DEVICE- NO DISENGAGEMENT	22-Dec-84	1	193
UPPER PAWL TIE CABLE BROKEN	03-May-85	1	260
MOTOR BURNOUT ON LOCKING PAWL	01-Jun-85	1	267
LOOSE CLAMP ON SYNCHRO AND ATTACHMENT SHAFT	10-Feb-84	2	11
SOLENOID OF SLEW SYSTEM MODIFIED- STIFF SHAFT	28-Feb-84	2	17
STIFFNESS AND SLIDING OF CABLE/WIRING IN POWER TRACK	12-Mar-84	2	22
GRAVITY SLEW DIDNT WORK DURING POWER FAILURE	26-Apr-84	2	40
GRAVITY SLEW TRIP	27-Apr-84	2	41
GIMBAL AXIS REACHED FULL TRAVEL	09-May-84	2	45
BANGING SOUND IN GIMBAL EVERY 10 SECONDS	21-May-84	2	54
OBSTRUCTION IN PATH OF GRAVITY SLEW WEIGHT	02-Jul-84	2	94
CLUTCH FOR PAWL CLICKED	16-Sep-84	2	157
BEARING GOING OUT ON MOTOR SYSTEM	17-Sep-84	2	158
EMERGENCY GENERATOR SYSTEM FAILED	19-Sep-84	2	160
GRAVITY SLEW PROBLEMS-SET SCREW,WEIGHT CATCHING	24-Sep-84	2	161
NEW GIMBAL STOW LOCK- OPEN LEAD TO PAWL	18-Feb-85	2	231
GRAVITY SLEW NOT OPERATIONAL	19-Feb-85	2	232
HYDROGEN HOSE TRACK BENT	27-Mar-85	2	251
GRAVITY SLEW CABLE BROKEN	15-Apr-85	2	255
BROKEN UPPER LOCK PAWL MOTOR	15-Apr-85	2	255

KEY:

1 = PREVENTED FURTHER OPERATION OF THE MODULE
2 = SIGNIFICANT IMPACT BUT OPERATION COULD CONTINUE
3 = INSIGNIFICANT EFFECT ON CONTINUED OPERATION

- Frequent readjustment of solenoid linkage due to loosening caused by solenoid vibration
- Excessive drum shaft [1.3-cm-diameter (1/2-in.)] deflection due to the gravity slew weight
- Slow gravity slewing speed caused by motor back-emf limits
- Inadequate slew axis travel.

During normal operation of the module, the gravity slew system shaft is in the ready position with the shaft retracted and locked, holding the weight up. On loss of power to the solenoid coil, the shaft moves down and to the right, engaging the pinion gear at the end of the motor and releasing the shaft to be turned by the weight, cable, and pulley. The present configuration of the gravity slew system is shown in Figure 5-1.

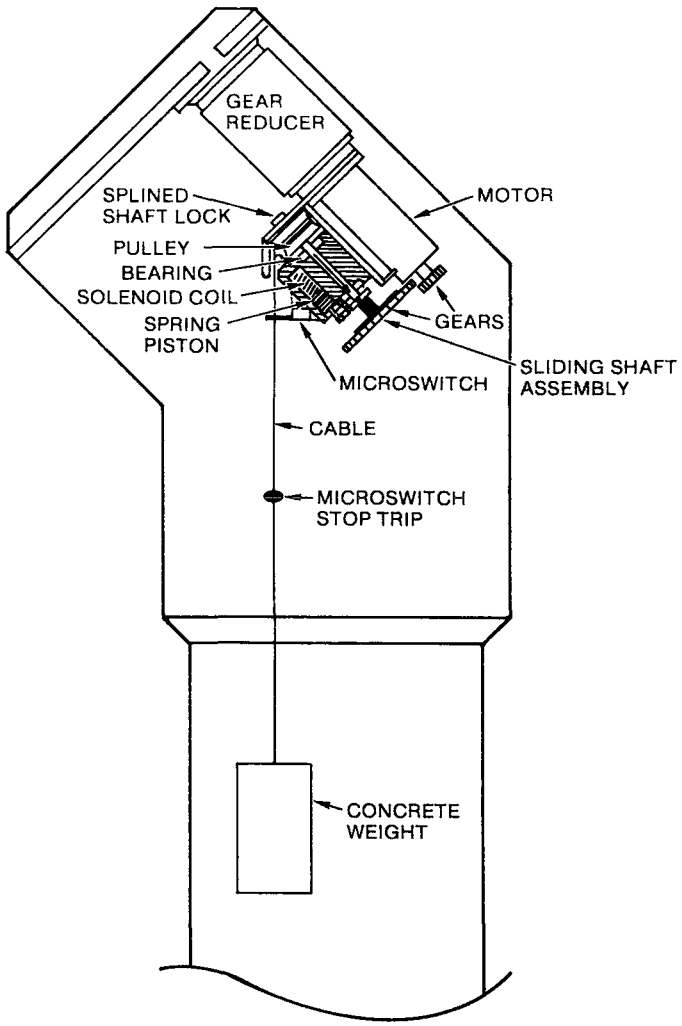

Figure 5-1. Existing Emergency Gravity Slew Mechanism

Site personnel indicated that the gravity slew system as presently designed was occasionally unreliable. They mentioned that the concentrator/tracker/slew mechanisms were not integrated as a whole system but were independently designed, and this contributed to the sporadic failure of the system.

To eliminate the problems associated with the solenoid and shaft deflection, an alternative configuration has been suggested by Advanco. This proposed configuration (Figure 5-2) uses a shaft brake that releases on power loss and a clutch that engages on power loss. Parasitic power would be reduced by more than one-half, the shaft diameter would be increased, and more shaft bearings would be installed.

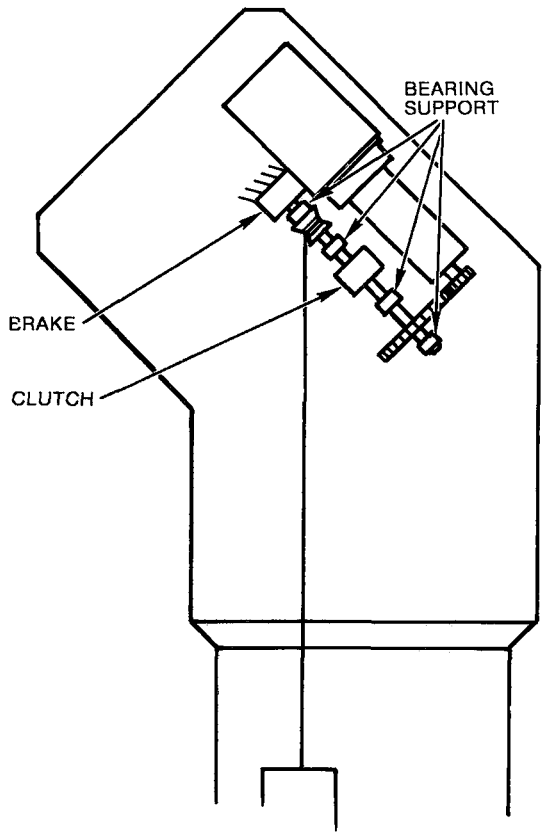

Figure 5-2. Advanco-Proposed Alternative Configuration for the Gravity Slew Mechanism

The weight on the gravity slew mechanism was initially insufficient to drive the concentrator off sun at extremely high elevations due to a slight imbalance in the concentrator's ballast. The movement of the concentrator during gravity slew was sluggish, especially at high dish elevations. As long as the emergency diesel generator provided power to enable a site operator to command the dish off sun, this presented no immediate problem. However, if a fault occurred in either the emergency generator, the tracking motors, or the motor controllers, the result could be disastrous. To ensure a quick slew-off at any dish position, the first recommendation was to increase the weight on the gravity slew system. This turned out to be unfeasible because the tracking drive motors remained connected to the motor controllers.

If the drive motor back-drives too fast, the motor back electromagnetic force (emf) will overload the motor controller with too high a current flow. Advanco suggested to Electrospace Systems, Inc. (ESI), that a "Delay-On-Operate" relay timer be installed on the skewed axis motor leads with the SCCU power source as an activator. ESI concurred with Advanco's suggestion and prepared such a relay, which was set at 20 seconds. On power loss, the relay disconnects the motor from the motor controller. The gravity slew system then engages and back drives the skew axis motor for 17 seconds at a high slew rate. When the power returns either by the backup generator or grid, the relay will not reconnect the motor controller for 20 seconds, thus ensuring adequate time for operation of the gravity slew system. Subsequently, with the motor isolated from the controller during gravity slew, the amount of weight was increased to provide quicker response.

The additional discovery of inadequate slew axis travel during emergency gravity slew was also cause for concern. To ensure clearance of off-axis rays on the PCU area, the travel of the emergency slew was increased from 10 to 20°. This was done by attaching a pulley to the weight and doubling the cable length. This increased movement ensured that the PCU would be completely clear of the concentrator off-axis image.

Pedestal Cable Support. Module power and instrumentation cables are routed underground to the pedestal, then up through the pedestal and inside the exocentric gimbal mechanism. A cable wrap is provided for the upper (skewed) and lower (azimuth) axis to accommodate the exocentric gimbal mechanism motion. The initial required movement was 180° in the skewed axis and 320° in the azimuth axis in an enclosed cylindrical area, 41 in. in diameter. An extensive but unsuccessful product search

was conducted by Advanco to find multiconductor power cables constructed in a flat configuration that could meet a minimum bend radius requirement of 6 in. Two rectangular metal tubes per axis, flexible in one plane, were ultimately selected to enclose the power and instrumentation cables. Two different suppliers were selected, and the two types of tubes were installed. The flexible tubes in both axes failed by breaking apart. The flexible tubes in the azimuth axis had started cutting the insulation of the cables inside. An open, heavy-duty cable track was installed as a replacement on that axis and has subsequently operated without problems or failures.

Movement in the gimbal (lower) axis reached its maximum travel position during May 1984, which resulted in early shutdowns in the afternoon. The limit was caused by the power (cable) track support tube hitting the pedestal tongue synchro shaft support. This interference occurred at a gimbal position of 322.7°. A computer analysis was performed by Advanco to determine the maximum gimbal movement for the site's longitude and latitude. This analysis is not straightforward as the skewed (elevation) axis contributes to the azimuth position, and the peak gimbal axis movement does not necessarily take place on the summer solstice. The maximum movement was determined to be 336°. During the period 10-17 May 1984, the pedestal tongue was notched, the power track was slightly relocated for the additional rotation, and the limit switch was relocated. The new gimbal limit was 337.4°. In April 1985, the locking pawl on the skewed axis became stuck in the engaged position. To free it, the upper axis was driven with the drive motor. This allowed the pawl to break free, but the bolt holding the jackscrew was bent and had to be replaced. Several days elapsed before a new bolt was fabricated and reinstalled. The cherry-picker was tied to the dish for overnight stowing during this period.

Electronic Components

Several problems with the electronic/electrical components of the concentrator were observed during the 18-month period of module operation. These are listed in Table 5-2. Most of these items are electronic short circuits. Some of these electronic failures are described below.

Electronics. On 2 July 1984, the azimuth motor controller board on the dish failed following a period of partly cloudy skies when the dish was cycling between the sun-sensor track conditions and memory track conditions. All emergency conditional responses were activated, but the gravity slew mechanism failed to completely drive

Table 5-2

CONCENTRATOR OPERATING INCIDENTS--ELECTRONIC

INCIDENT DESCRIPTION	DATE	IMPACT ON AVAILABILITY	LOGBOOK REFERENCE PAGE
BURNT CABLES AT FOCAL POINT	12-Jan-84	1	6
OPEN WIRE ON SUN SENSOR CABLE	11-Feb-84	1	12
CORROSION OF SUN SENSOR CIRCUIT BOARDS	02-Mar-84	1	19
OPEN RELAY- DIRTY CONTACTS ON JACK SCREW MOTOR	11-Mar-84	1	21
SEVERE BLACKENING OF QUADROPOD/BURNT CABLES	28-May-84	1	58
ENGINE MONITOR CIRCUIT BOARD DAMAGED/BURNED,CRACKED	18-Jun-84	1	72
MASTER CONTROLLER BOARD BAD- BLOWN FUSES	02-Jul-84	1	95
SOLONOIDS HAVE OVERHEATED DUE TO FIRE	19-Sep-84	1	159
RELAY CONTACT FAILURE DUE TO OVERHEATING	15-Jan-85	1	206
CONTROL BOARD BLOWN FUSE	28-Mar-85	1	252
MOTOR CONTROLLER BOARD FAILURE	04-Apr-85	1	254
SKEW AXIS BOARD REPLACED	19-Apr-85	1	256
DISH WILL NOT GO TO POSITION A	24-Apr-85	1	257
REPLACE FAULTY CONTROL CIRCUIT BOARD	27-Apr-85	1	258
MOTOR CONTROL CIRCUIT BOARD FAILURE	11-May-85	1	263
WATER IN SUN SENSOR	09-Feb-84	2	11
BENT PIN ON SOLAR SENSOR/ TRACKING OSCILLATION	13-Mar-84	2	22
MOTOR CONTROLLER BOARD GOING BAD	12-Jun-84	2	65
NEW ELECTROSPACE TRACKING PROMS DONT WORK	22-Dec-84	2	193
CONTROL BOX PROBLEMS	12-Mar-85	2	244
ELECTROSPACE PROMS DONT WORK	27-Mar-85	2	251
OSCILLATION OF DISH- MEMTRACK/SUNTRACK	18-Jan-84	3	8
DISH VIBRATION	09-Feb-84	3	11
CAMERA MELTED FROM OFF-AXIS RAYS	03-Sep-84	3	148
OSCILLATION BETWEEN SUN AND MEM TRACK	05-Mar-85	3	240

KEY:

1 = PREVENTED FURTHER OPERATION OF THE MODULE
2 = SIGNIFICANT IMPACT BUT OPERATION COULD CONTINUE
3 = INSIGNIFICANT EFFECT ON CONTINUED OPERATION

the dish 10° off sun due to an obstruction in the falling weight's path. The site operators drove the dish to stow and later found that two of the four silicon rectifiers on the azimuth controller board had failed. The board was shipped to the manufacturer and reinstalled by 11 July. Subsequently, a spare board was kept onsite.

On 19 September 1984, a power outage occurred, activating the gravity slew system, which took the dish off sun safely. However, during the rewind command, the gravity slew solenoids burned out, and the large gravity slew gear fell off its shaft.

The gear apparently had become loose on its shaft and prevented the solenoids from reaching full travel. The solenoids were repaired at the manufacturers within 2 days.

On 28 March 1985, the skewed axis motor controller board failed. The spare board (which previously had demonstrated an intermittent problem) was installed. On 5 April, the board with intermittent problems failed. Both boards were mailed back to Electrospace for repair. The original board was returned and installed on 15 April. The board, however, experienced a current resonance, which caused a physical "knocking" noise and vibration on the board, although it appeared to be operating properly. On 19 April, the board with the intermittent problem was returned. It was installed on 19 April, and the board with the "knocking" was removed. On 24 April, the board with the intermittent problems failed and a partial walk-off occurred, damaging a section of the aperture cavity.

Control Wiring. The module was inadvertently stowed in the zenith ("B") position over the 26-27 May 1984 weekend because the operator erroneously believed that the MCC was malfunctioning and might not move the dish from position A to position B in the event of high winds. Actually, the MCC CRT needed only to be reset/cleared, and the MCC would have operated correctly with or without the CRT. However, the Vanguard module experienced excessive heating of one of the tetrapod struts caused by off-axis rays from the sun during zenith stow of the dish. This melted the insulation of the power conversion unit control cables inside the heated strut.

Failure of the power conversion unit control cables as a result of the off-axis rays occurred at approximately 12:40 p.m. on Saturday, 26 May. This was evident from the IBM/DAS data logger recording, which was left on over the weekend. An additional amount of tetrapod heating must also have occurred on Sunday, 27 May, since the module was stowed in position B on this day as well, and it also was a sunny day with no site personnel in attendance. As a secondary consequence, the failure of the PCU cables resulted in an erroneous pressure transducer signal being sent to the group hydrogen compressor, which caused it to remain in the "ON" state for a 48-hour period. The group hydrogen compressor operated continuously the entire time, resulting in the failure of a flexible coupling between the shafts of the motor and compressor. Inspection of the coupling revealed a flaw that would have failed within 1 year, but the continuous operation caused it to fail prematurely. The coupling failure was determined to be due to incorrect assembly rather

than a design fault. In addition to the flexible coupling failure, there was an open diode and minor circuit board damage in the power conversion unit controller. All repairs were completed within 2 weeks.

This event indicates that, at least in the summer months, the zenith stow position is not advisable for daytime periods.

Mirror Facets

Specific incidents related to the mirror facets on the concentrator are listed in Table 5-3. In general, delamination and breakage were the major concerns. The following section discusses both the mirror delamination problem and the procedure devised by Advanco to align the facets on the dish.

Table 5-3

CONCENTRATOR OPERATING INCIDENTS--MIRROR FACETS

INCIDENT DESCRIPTION	DATE	IMPACT ON AVAILABILITY	LOGBOOK REFERENCE PAGE
SHATTERED MIRROR FACET WHEN WRAPPED IN BLACK PLASTIC	26-Mar-84	2	30
TOOLS DROPPED FROM RECEIVER BROKE TWO MIRRORS	04-Apr-84	2	32
DELAMINATION OF 10 FACETS	02-May-84	2	43
THREE INCH PIPE FROM ENGINE BROKE MIRROR	02-May-84	2	43
SIX DELAMINATED MIRRORS	26-May-84	2	56
FOUR DELAMINATED MIRRORS	29-May-84	2	58
TWO DELAMINATED MIRRORS	07-Jun-84	2	63
THREE DELAMINATED MIRRORS	19-Jun-84	2	73
FIVE DELAMINATED FACETS	21-Jun-84	2	77
DAMAGED MIRROR DUE TO VANDALISM	23-Jun-84	2	81
TWO DELAMINATED MIRRORS	05-Jul-84	2	96
MIRROR DAMAGED BY FALLEN OBJECTS	24-Apr-85	2	257
LIGHT SOURCE BURNED OUT DURING MIRROR ALIGNMENT	07-Jun-84	3	63

KEY:

1 = PREVENTED FURTHER OPERATION OF THE MODULE
2 = SIGNIFICANT IMPACT BUT OPERATION COULD CONTINUE
3 = INSIGNIFICANT EFFECT ON CONTINUED OPERATION

Mirror Delamination. Mirror delamination (glass separation from the foamglass substrate) was experienced in 19 of the original 328 facets (5.8%) installed on the Vanguard module. Delamination increases facet spillage by defocusing the facet image, thus decreasing the intercept factor and eventually requiring replacement of

the facet. Advanco extensively examined the 19 delaminated facets and combinations and investigated permutations of possible causes . Although the investigation was not conclusive, it appeared that the delaminations were largely caused by poor quality control in the manufacture of early facets. The delaminations were activated by a combination of dish vibration and high ambient temperature causing an eventual failure of the EPI-Bond adhesive between the mirror and foamglass. These conclusions are based on statistical patterns that developed during the investigation.

The quality control on the manufacturing of initial facets was conducted during a period of technology transfer from JPL to Advanco, and 68% of the delaminated mirrors had serial numbers of 0085 or less. This implies that during the initial 2 weeks of training of new Advanco personnel, lapses in quality control occurred and were possibly repeated, infrequently, during the balance of the manufacturing effort. Table 5-4 presents 10 potential areas of the manufacturing process that could have been the source of poor facet lamination. It was not possible for Advanco to determine the exact cause, but Advanco undertook efforts to eliminate future failures when manufacturing additional facets.

Table 5-4

POSSIBLE MANUFACTURING CAUSES OF MIRROR FACET DELAMINATION

Insufficient coating of EPI-Bond 1534 A/B applied to mirror surface that contacts foamglass material
Poor mixing of EPI-Bond 1534 A/B
Partial curing of bonding material prior to application
Bad weather condition and poor temperature environment in workshop area
Excessive residual foamglass particles or dust subsequent to foamglass grinding process
Poor foamglass material quality
Excessive leakage in vacuum process or removal of facet from vacuum process before full curing time elapsed
Large holes in foamglass material
Foamglass was not fully ground to the curvature of the grinding fixture master surface
Backside of mirror surface not sufficiently clean

Records of quality assurance testing of the delaminated facets indicated that prior to shipping, all facets met the specification of less than 1-mrad slope error. Delamination was not evident until the facets were installed and operating on the dish.

It was speculated that dish vibration and high ambient temperatures promoted the mirror delamination. The dish is subject to two sources of vibration that affect the racks and facets. The first source of vibration is the air compressor for the water-cooled aperture plate located at the center of the dish on the truss box structure. This 0.75-kWe (1-hp) air compressor typically cycles once every 60 minutes for a 10-second duration. The second source of vibration is the power conversion unit, which provides a constant vibration during on-sun operations. ETEC conducted accelerometer tests to measure the amount of vibration at various locations. Reasonably consistent readings of approximately 0.4 g were recorded in all directions on the lower dish support members and facet racks. This vibration is visible to the naked eye, and it was suspected that the truss structure attachment points to the tetrapod struts and the truss center node are the areas most significantly affected. Of the delaminated facets, 53% were located in proximity to the tetrapods, and another 16% were located near the center node. Thus, 69% of the delaminated facets were located in proximity to the two largest areas of vibration on the dish.

When the delamination problem was first discovered (seven delaminated facets were found on 8 May 1984), Advanco sought to reduce the source of vibration from the air compressor by placing it on snubbers. No immediate solution to the power conversion unit vibration was proposed.

Ambient temperature, although considered less of an initiator of delamination than vibration, was still considered to be a major factor. Exceptionally high ambient temperatures will cause delamination. Temperature-induced delamination could also be caused by gases produced from the Buty-lite 711 facet encapsulation material, the foamglass, or cool moist air could have been trapped inside the foamglass when assemblers sealed the facet with Buty-lite on a rainy day. It was uncertain whether delamination was induced by temperature, but delaminations commenced during a period when ambient temperatures were regularly reaching 48°C (118°F). An additional temperature-related statistic is that 89% of the delaminated facets were located on the dish area above the centerline when the dish elevation is zero. This elevation with azimuth position to the north is the frequent stowage position on

weekends and nonoperating weekdays. Therefore, the upper area of the dish's backside is frequently exposed to direct insolation, while the lower area is shaded by the upper area. This mode of insolation exposure, coupled with the high concentration of delamination occurring in the upper portion of the dish, further implies a correlation of delamination to high ambient temperature and high backside direct insolation exposure.

There are other possible causes and mechanisms suggested by Advanco that have not been substantiated or discounted. These include high facet stress induced by the mounting bracket of the rack-to-facet attachment and the high-pressure cleaning sprayer causing small breakage of foamglass cell structure by placing the sprayer too close to the mirror surface. The former mechanism is not statistically supported by the location of delamination on the mirror facets; 95% of the delaminations start at the corners of the facets, while only 39% are in the bottom left-hand corner and 26% in the bottom right-hand corner. These two corners are where two of the three attachment tabs are located on a facet. The third attachment point is in the middle of the facet opposite edge. Thus, the correspondence of facet delamination location and attachment point location is not significant. High-pressure spraying and/or mechanical rubbing during facet cleaning may explain the existence of delamination in some of the areas that are not near the high-vibration zones. This practice was subsequently discontinued.

The rate at which delaminated mirrors were discovered substantially decreased throughout the summer months of 1984, even though the vibration persisted and the ambient temperatures increased. All subsequent facet replacements were with recently manufactured facets. In mid-May 1985, several of the concentrator mirrors were showing signs of slight speckling due to mirror de-silvering. A total of 53 mirrors were replaced from the existing inventory of spare parts. The placement of the new mirrors on the concentrator required night time alignment of the new facets.

Facet Alignment. The major activity on the concentrator during November 1984 was related to "spot mapping" of the reflective surface facets and realigning the dish where necessary. The technique developed by Advanco in the absence of any other conventional and economical means was that of "spot mapping." Spot mapping is the process whereby facets on the dish are painted with a water-soluble paint except for a 3-in.-diameter circle at the center of each facet. An adhesive patch is then placed over the unpainted circle and selectively removed and reapplied while spot

mapping. The dish is placed on sun, each facet is uncovered, and the facet's image on the receiver is then video taped and simultaneously video printed for a hard copy record. The adhesive patch is reapplied and the process is repeated for each facet on the concentrator.

The net result of this process is a hard copy file of precisely where each facet reflection is striking the receiver. When these data are aggregated, it is possible to identify the number of facets that are striking the center plug of the Stirling receiver, the evenness of the flux distribution along a radial axis, and the number of facets that are striking beyond the outer receiver tubes on the receiver walls. It was discovered that the original recommendation by the Georgia Institute of Technology to use a single focal plane for the alignment process provided an unacceptable amount of flux on the center plug and to a lesser extent an unacceptable amount of flux on the outer walls. It was therefore necessary to reestablish the proper focal plane for the innermost facets and the outermost facets on the concentrator. This was accomplished while the dish was on sun and the majority of the reflective surface was opaque and by realigning a select number of facets until the desired flux patterns were achieved again. Using a sample number of realigned facets permitted the measuring of a new focal plane. This process was conducted for both the inner and outer facets in question.

The process resulted in variable focal planes being established for the Vanguard concentrator. The facets at the center of the dish had a focal plane 8.5 in. in front of the original position. The facets at the outer edge of the dish had a focal plane 1 in. behind the original focal plane. All other facets had focal planes distributed linearly over this 9.5-in. range, depending on the facet's distance from the center of the dish. This information was then put into the Advanco optical programs and loaded into the computer to generate a new set of alignment targets. The Advanco-developed target pattern was installed on one 6-ft-diameter target 0.616 m in front of the principal focus (which is 370 mm in front of the mounting plate) in front of the engine. Thus, all 336 mirrors could be aligned without removing the engine. Approximately 30 facets were realigned with the new target, and the above-mentioned spot mapping technique was used to determine if the process had reduced the flux striking the inner cone and outer wall while maintaining an even flux distribution along the receiver surfaces. The video prints indicated that all three objectives had been accomplished. The balance of the dish was then realigned using the revised alignment targets. The realignment produced a greater utilization of the delivered flux through the aperture and thus a higher efficiency factor for both the concentrator and the power conversion unit.

SOLAR RECEIVER

The United Stirling 4-95 engine is a four-cylinder Stirling-cycle heat engine that utilizes a high-temperature heat exchanger (the receiver) divided into four separate sections as shown in Figure 5-3. The receiver serves as the heat input end of the Stirling engine. The hot end of the Stirling cycle operates at temperatures of 700 to 820°C and at pressures up to 20 MPa (2900 lb/in.^{2}). During most of the testing to date on solar and automotive applications, high-cobalt superalloys have been used for the heater tubes and the casting of the heater head. In the Vanguard receiver, the high-cobalt superalloy was Multimet (also known as N-155) for the receiver tubes and HS-31 for the cast housing. It is generally agreed that a production version of this receiver will require less-expensive alloys that do not contain large amounts of strategic materials (e.g., cobalt, chromium, columbium, tantalum) and that are relatively easy to fabricate.

The nominal compositions and typical mechanical properties of Multimet and HS-31, as well as those for some of the more promising replacement alloys for heater tubes and housing, are shown in Table 5-5. Today's leading candidates for production quantities of heater tubes are Inconel Alloy 625 and CG-27. Both alloys can be cold drawn into thin-wall heater tubes (0.75-mm wall thickness) and bent into the required configurations. Similarly, XF-818 is a promising candidate for cast housings and has been successfully used as both an investment and shell casting.

In the solar application, receiver tubes are heated by concentrated sunlight at flux levels up to 700 kW/m^2, and expected design life is 16,000 hours at a nominal temperature of 720°C. This design life remains to be demonstrated, although the Vanguard-I receiver has accumulated the longest operating time of any receiver in actual solar testing (about 2000 hours through July 1985).

A potentially serious problem that could affect the life of the receiver tubes arose when test site personnel observed that a black powdery substance had formed on the exterior of the tubing. This topic is discussed below.

The solar receiver subsystem is composed of the insulated cavity, the aperture cone, the water-cooled shutter plate system, and the receiver tubes. Specific incidents involving the solar receiver are listed in Table 5-6, and the more significant of these are discussed below.

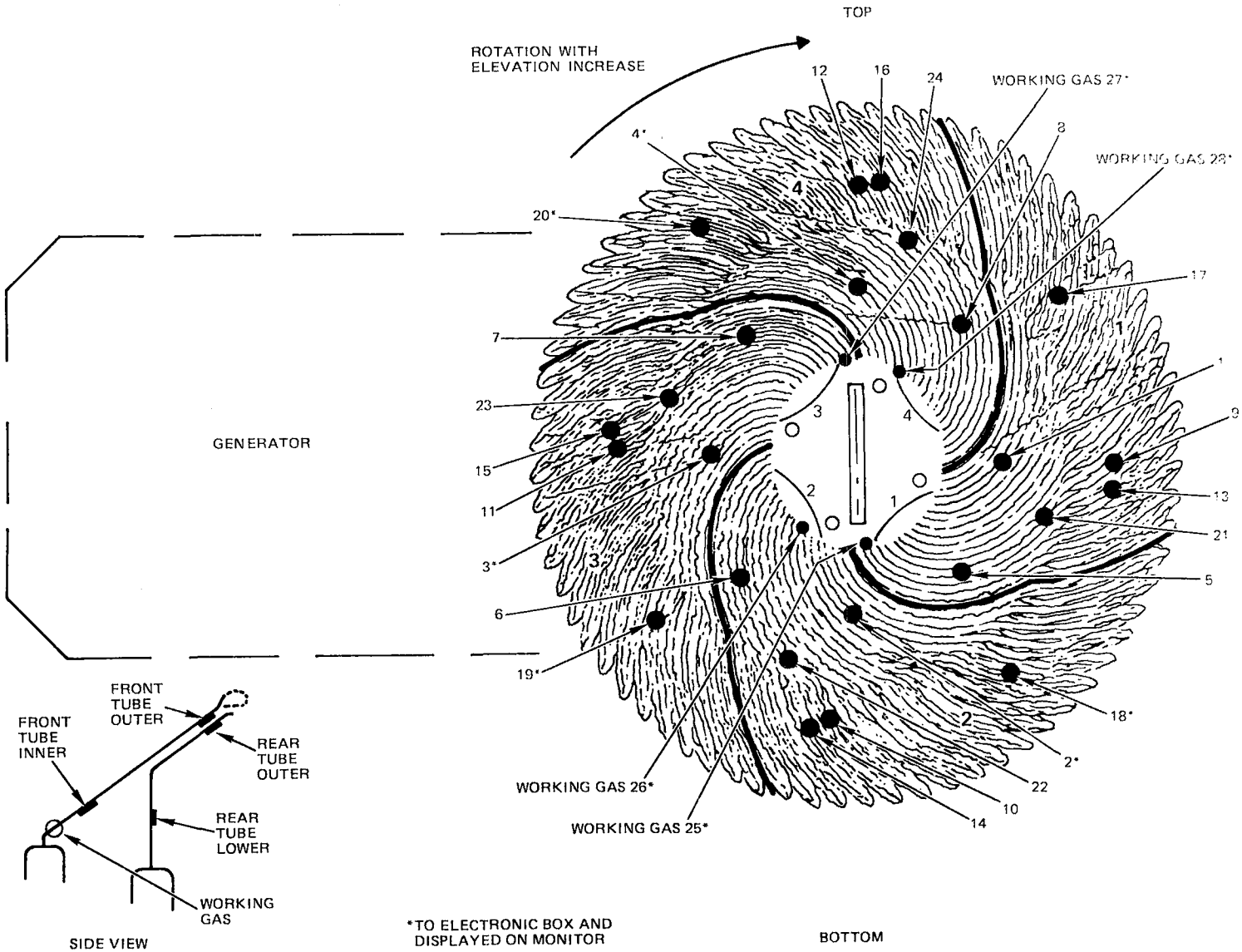

Figure 5-3. Vanguard Solar Receiver Showing Thermocouple Locations

Table 5-5

NOMINAL COMPOSITION AND TYPICAL MECHANICAL PROPERTIES FOR HEATER TUBES AND CAST HOUSING

	Heater Tubes			Cast Housing	
	Multimet	Inconel 625	CG-27	HS-31	XF-818
Composition (%)					
Cobalt	20	-	-	55	-
Nickel	20	58	38	10.5	18
Chromium	21	21	13	25.5	18
Iron	30	5[a]	28	2[a]	54
Molybdenum	3	9	5.75		7.5
Aluminum	-	0.4[a]	1.6		-
Titanium	-	0.4[a]	2.5		-
Niobium/tantalum	1	3.65	0.7		0.4
Boron	-	-	0.01	7.5	0.7
Tungsten	-	-	-	7.5	
Nitrogen	0.15	-	-	-	0.12
Carbon	0.15	0.1	0.05	0.05	0.2
Yield strength (MPa)					
25°C	340	427	931	775	400
700°C	177	325	895	395	300
800°C	156	300	620	315	270
Tensile strength (MPa)					
25°C	690	930	1413	885	650
700°C	414	725	1158	545	500
800°C	290	360	760	430	427
Elongation (%)					
25°C	40	56	20	2	1.6
700°C	-	40	11	5	5
800°C	-	80	14	9	6

[a]Maximum

Table 5-6

SOLAR RECEIVER OPERATING INCIDENTS

INCIDENT DESCRIPTION	DATE	IMPACT ON AVAILABILITY	LOGBOOK REFERENCE PAGE
REPAIR PLATE HARDWARE	08-Mar-85	1	242
REPAIR LEAKY AIR REGULATOR	08-Mar-85	1	242
APERTURE PLATE FELL OFF OF RECEIVER	20-Mar-84	1	26
CHARRED AIR HOSE TO PLATES	02-May-84	1	43
WATER COOLED PLATES WOULD NOT STAY OPEN	17-Jun-84	1	71
CENTER PLUG FELL FROM RECEIVER, HIT FACET	11-Aug-84	1	133
TILE BROKE LOOSE FROM APERTURE	14-Dec-84	1	188
FROST ON COMPRESSOR/FROZEN PLATES WOULDNT MOVE	15-Dec-84	1	189
PLATE PROBLEMS	23-Dec-84	1	194
FAILURE OF LIMIT SWITCH FOR PLATES	25-Feb-85	1	236
NEW RECEIVER TUBES EXPLODED	20-Jun-85	1	275
STICKING PLATES DUE TO DIRTY TRACKS	02-Apr-84	2	31
BOLTS ON COOLING PLATES LOOSE FROM VIBRATION	11-May-84	2	45
BOLT CAME LOOSE AT SHUTTER PLATE	11-Jul-84	2	98
SCREWS LOOSE ON PLATE TRACK SYSTEM	31-Jul-84	2	124
REPAIRED WATER COOLED APERTURE PLATES	12-Aug-84	2	134
CONTINUED PLATE PROBLEMS	25-Jan-85	2	209
FALLING INSULATION AROUND RECEIVER TUBES	25-Feb-85	2	236
BURNT FIBERGLASS DUE TO POWER LOSS	24-Apr-85	2	257
CONDUCTED REPAIRS ON RECEIVER	26-Apr-85	2	258
FIBERFAX MATERIAL COMING LOOSE	06-May-85	2	261
THERMOCOUPLE FAILURES	11-Jun-85	2	271
SLIDE PLATE OPENS TOO SOON	08-Feb-84	3	13
PCU APERTURE CONE SLIGHTLY DAMAGED	26-May-84	3	56
MAGNETIC DEPOSIT ON RECEIVER TUBES	08-Aug-84	3	130
MORE MATERIAL ON RECEIVER	05-Sep-84	3	150
BLACK POWDER IN RECEIVER AREA	19-Oct-84	3	172
APERTURE PLATE IS MELTED ON LOWER LEFT	23-Dec-84	3	194
TEMPERATURE DIFFERENTIAL DISCREPANCIES	18-Jun-85	3	273

KEY:

1 = PREVENTED FURTHER OPERATION OF THE MODULE
2 = SIGNIFICANT IMPACT BUT OPERATION COULD CONTINUE
3 = INSIGNIFICANT EFFECT ON CONTINUED OPERATION

Aperture Cone

The aperture cone of the PCU was another point of interest in terms of observations of material degradation on the solar receiver assembly. The PCU initially delivered to the Rancho Mirage test site included an aperture cone constructed of a conventional low-density insulation board. After about 1 month of operation from sunrise to sunset, the original board material was damaged beyond repair. Several of the Fiberfrax board cone segments fell out of their mounts and broke. Apparently,

the melting of the center section in combination with vibration from the engine had weakened cone supports. The current aperture cone is composed of high-purity silica material of a generally dense, brick-like consistency with very high strength and excellent reflectivity. The aperture cone consists of 12 segments mounted on a stainless steel conical shell with stainless steel brackets.

With the new silica ceramic aperture cone installed, the output of the module was lower at a given insolation than prior to its installation. It was theorized by Advanco that the probable reason for this lower performance was that either the cone was not mounted at the correct position and thus was intercepting more incoming light from the dish or that the cone was conducting more heat away from the power conversion unit either due to radiation or convection. A remote radiometer verified that in fact the light spillage from the power conditioning unit was higher, but not high enough to explain the drop measured. In early April 1984, insulation added around the aperture cone increased the output to levels near those measured before installation of the silica cone.

The appearance of the aperture cone after 1 year of operation was generally good with the exception of a degraded area on the lower left portion of the cone. The dark area appeared on only one of the segments of the aperture cone. Closer inspection of the cone revealed that the darker segment was due to melting on the surface. When melted, the silica material transforms from an opaque white color to a more transparent glassy appearance, with small bubbles trapped in the glassy structure. The material had generally remained in place, however, and the flow of the glassy material had been minimal. This is because of the extremely high viscosity of silica, even in its molten state.

The single segment of silica was damaged during a special test when the sun track threshold was elevated to a very high level while the insolation was high. The sun track threshold is the level of insolation at which the tracking system switches from memory (or ephemeris preprogrammed tracking) to tracking using the sun sensor, which is more accurate. When the sun track threshold was set to a very high level, the dish went to a position that put the focus of the dish significantly further off-center then would be observed during normal operation, since tracking was with the less accurate memory track system. This resulted in the focal point shifting toward the silica segment at the lower left and consequential melting.

The general conclusion by Advanco on the viability of the high-purity silica material for the aperture cone is that it will work well in most routine operations of the dish. This routine operation includes the slew-off and slew-on with no shutter plates or with open shutter plates. However, for cases when the tracking of the dish is impaired and when the focal point is directed to the aperture cone, the material is not sufficient to survive more than 1 minute. For example, if the sun sensor were to develop an offset (resulting, for example, from condensation or from the deposit of a nonsymmetrical dirt deposit), the cone could be severely damaged by this occurrence, possibly without the knowledge of operating personnel until a routine inspection at a much later time.

One possible way in which damage to the cone could be avoided is by detecting an out-of-bounds tracking position of the dish by the software logic of the tracker system. However, this fail-safe system could only work in conjunction with significant improvements in the accuracy of the memory track system, as discussed above.

In general, the silica aperture cone has proved to be an effective choice of material. Because the material is a dense ceramic, its insulation properties are not as good as the lower density materials such as the original Fiberfrax insulation board, and it is believed that some performance penalty was incurred with the silica. Also, mounting silica on the metallic PCU frame was somewhat of a challenge, requiring special mounting components.

Special tests conducted by Advanco at the test site in August 1984 indicated that low-density Fiberfrax insulation board, surface-treated with a silica cement material, was an effective solution to the problem of finding an aperture cone material that was lightweight, a good thermal insulator, and resistant to flux levels routinely experienced by the aperture cone. During one limited test, this material was mounted as a plate-type aperture for the PCU. The dish was placed in the memory track mode at 850-W/m^2 insolation for approximately 20 seconds, and the material survived quite well. However, further investigation is recommended by Advanco before such combined materials are adopted for future aperture cones.

Because of a continuing problem with the calculation of the ephemeral table in the Electrospace tracking controls, a walk-off of the concentrator occurred on 24 April 1985. No alarms were given, and before the shutter plates could be closed and the dish manually detracked, a large hole was burned through the aperture and insulation. No damage to the engine or receiver was observed. Since the cavity material

had started to degrade significantly even before the walk-off incident (due to the high temperatures and ambient conditions of normal operation), the entire cavity area was replaced with similar material. In late May 1985, the cavity and aperture cones were replaced with a new design utilizing new materials developed by USAB in Sweden. The new aperture was slightly damaged due to improper tracking during initial testing, but continued to perform its desired function for the remainder of the test program.

Shutter Plates

The most frequently occurring problem in the solar receiver subsystem was in the operation of the two water-cooled shutter plates. The ball bearing slides appeared to accumulate dirt and required routine cleaning. The brackets that trip the limit switches were not long enough and occasionally slipped. The flexible water hoses interfered with the pneumatic cylinders. Sometimes many attempts were required to open the plates before going on sun. The lower plate usually opened quickly, being aided by gravity; however, the upper plate had to work against gravity and was much slower in response. Frequently, a plate fault error occurred, indicating that the plates had not opened in the preset, allocated time. Site personnel indicated that the design of the aperture plate system should be improved in future models.

Receiver Tubes

Some of the incidents involving the receiver tubes dealt with uneven quadrant temperatures, receiver tube overheating, and receiver tube replacement. These are discussed below.

Uneven Quadrant Temperatures. Ideally, an even flux of insolation across the receiver surface should heat all four of the quadrants to the same temperature. Even temperature distribution in all quadrants maximizes the life of the receiver, since when one quadrant reaches the end of its life, it is likely that all four will be replaced. In addition to improving the life of the receiver as a whole, uniform temperature in all four quadrants results in the highest efficiency of the engine. This is because the average gas temperature is a maximum when each of the four quadrants is operating at the same temperature, which results in high engine efficiency. If, on the other hand, one quadrant runs hotter than the others, the overall effect is lower efficiency because the engine control system regulates the pressure in the engine based on the highest quadrant temperature. If one quadrant is hotter than the rest, the result will be a lower average working gas temperature and hence lower efficiency.

Even quadrant temperatures have not been demonstrated, as shown in Figure 5-4. This figure displays the difference between each quadrant working-gas temperature and the average of the quadrant temperatures throughout the day. The temperatures of the quadrants vary symmetrically about solar noon, suggesting that the quadrant temperature variations are either elevation or orientation dependent.

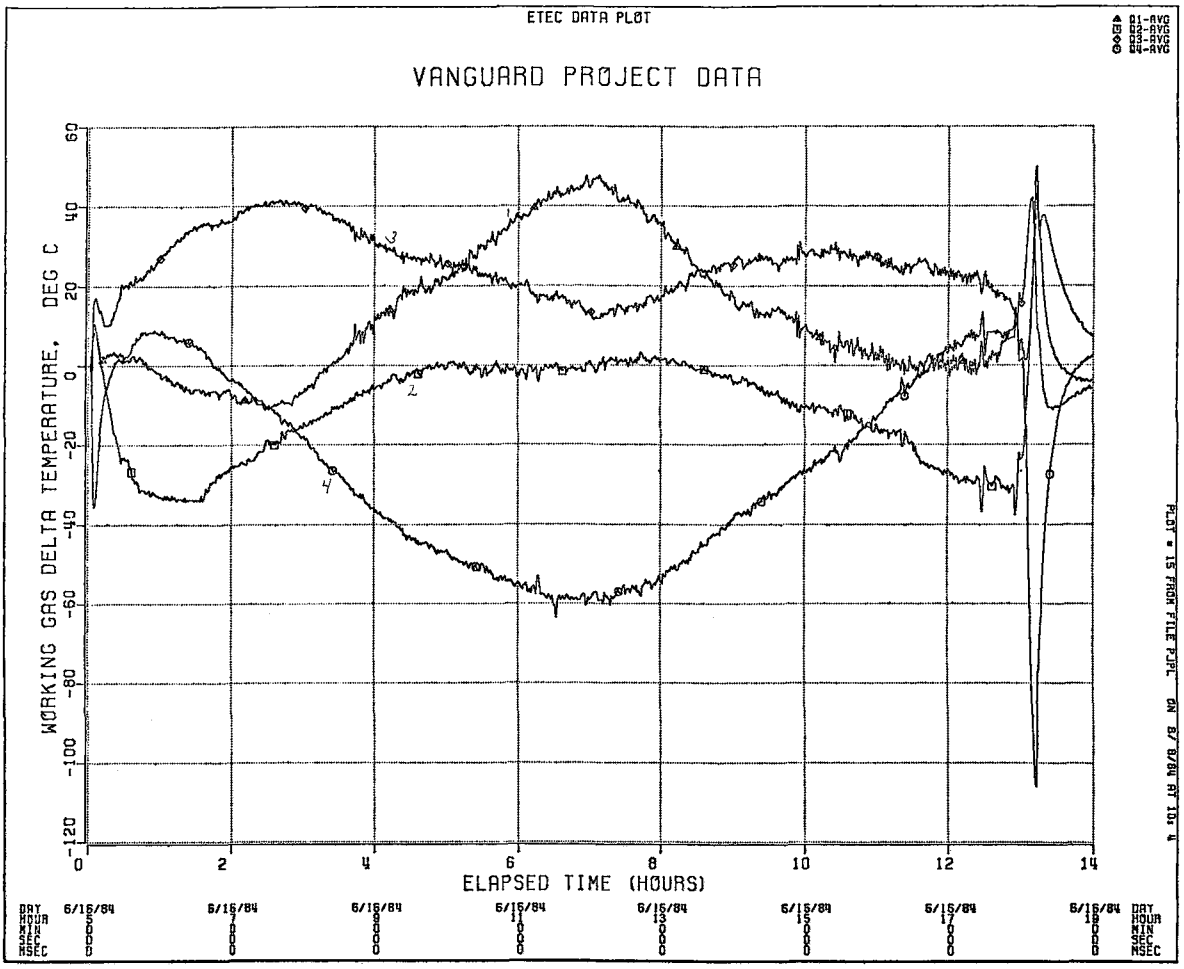

Figure 5-4. Variation Between Quadrant Working Gas Temperatures and Average Throughout the Day

The primary cause of the temperature variation shown in Figure 5-4 appears to be orientation-dependent convection heating of the receiver. The Stirling cavity receiver is similar to larger cavity-type central receivers. Numerous central receiver studies have noted that the lower portion of a typical solar cavity receiver generally runs at a lower temperature than the upper region for a cavity receiver oriented at a downward angle. The same effect would probably be expected

for the Stirling receiver and may help to explain the additional temperature difference observed. Apparently, the receiver quadrant in the upper position is heated by convection currents of rising air.

Also of importance is the deflection of the tetrapods. Advanco performed tests to determine the extent of power conversion unit deflection with elevation. Results of these tests showed that the total deflection for the worst-case (the axis along quadrants 2 and 4) was approximately 1 cm for dish movement from 10 to 75° elevation. The concentrator specification for beam accuracy is $\pm$1.25 cm. Therefore, though deflection of the tetrapods may be contributory, it is not the sole reason for the uneven quadrant temperature profile.

High differential temperatures between quadrants in excess of 380°C were noted on 22 July 1985. After several warnings and detracks, the dish was manually taken off sun. A broken check valve was discovered in quadrant 2, causing both the temperature and pressure to be excessive. This check valve was replaced, the engine was started, and subsequent differential temperature measurements were on the order of 60°C--a more reasonable operating value.

Overheating. Analysis of temperature and pressure data for transient conditions such as startups and partly cloudy days verified that the pressure regulation in the engine shows a delay due to the thermal inertia of the engine. Because the mass flow in the engine is dependent on pressure, and because heat transfer is also dependent on mass transfer rate, it was hypothesized that during transient conditions, the mass flow in the engine was not being regulated fast enough to respond to actual transient conditions present during midday startups and on partly cloudy days. This caused an overheating of the tubes during partly cloudy days that had many power-up and power-down cycles.

Receiver Tube Replacement. In concert with the cavity and aperture cone replacement in May 1985, a new receiver fabricated of Inconel by USAB in Sweden was installed on the power conversion unit. The new receiver design allowed replacing thermocouples on the receiver without requiring disassembly of the cavity. During initial testing of the system in early June, lowered performance and unbalanced quadrant temperatures were observed. These symptoms were believed to be due to the lower absorptance of the receiver tubes (since the tubes had not yet oxidized), which were reflecting a larger fraction of the incoming radiation. The new routing of the thermocouples on the receiver exposed some thermocouples to direct solar radiation. Because they were not adequately protected, several thermocouples

failed. The thermocouples and sleeves were subsequently protected with Kaowool insulation.

On 20 June 1985, the module was shut down to prepare the receiver for full performance testing the following day. The receiver tubes were painted with a high temperature flat black paint to increase their absorptance. When the module was put on sun at a high insolation level, the receiver failed within seconds. A 1/2-in. chip from a receiver tube in quadrant 3 was missing. It was proposed that the black paint insulated the thermocouples and caused a false lower temperature reading to be sent to the engine controller. The controller then allowed the pressure (and hence temperature) in the receiver tubes to rise, which eventually blew out the chunk of tube material. The new receiver was subsequently replaced with the old receiver, which was in place for the remainder of the test program.

Material Degradation

The Stirling cavity receiver operates at high temperature and contains both ceramic materials and metals. The receiver tubes are composed of N-155 (or "Multimet") and initially appeared dark due to a combination of oxides and carbides produced as a result of high-temperature oxidizing combustor flames impinging on them during testing in Sweden.

Ceramic Insulation. Shortly after a 2-week endurance test in June 1984, the tubes were inspected and a white, loosely bound powder material was observed on the tubes. This material was believed to be a volatilized component of some ceramic insulating material that had condensed on the relatively cooler tubes. This white material was speculated to be either from the loosely packed backup ceramic wool insulation used to insulate behind the receiver or from the ceramic insulation making up the walls. The white material appears to be deposited primarily on the outside walls of the receiver rather than elsewhere, and this outer region is an area of the receiver where the ceramic insulation is exposed to the highest flux levels of rays reflected by the concentrator.

Receiver Tubes. Following the 2-week endurance test, evidence of another type of material degradation was noticed within the receiver. A discoloration of the center ceramic plug was observed, which suggested that some sort of deposit had fallen on the plug and had then become heated and merged with the material of the center plug. The discoloration was of a bluish cast. The same material appeared also to have fallen on the cavity walls and caused discoloration.

It was deemed important to determine the source of the material since it was possible that the material had come from the receiver tubes, which would indicate possible overheating problems. However, the receiver tubes, which are made of N-155, a highly oxidation-resistant material, had not shown any previous tendency to flake off surface oxide.

In attempting to accumulate a sufficient sample for analysis, it was noticed that the black material was attracted by residual magnetism in the scalpel used to collect the samples. It was later found that a strong magnet could be used to collect the material from the inside cavity walls. When as much material was collected as was found practical, the total collected material was weighed. The total weight of the collected material amounted to about 1 g. It is estimated that the total amount of material produced was between 2 and 3 g.

A small amount of the material was placed in aerated water to determine if the substance was simple iron oxide, which would have transformed into the red ferric oxide. No color change occurred.

A sample of the material was analyzed with a mass spectrometer. Nickel, iron, and cobalt were all present, indicating that the material could be either the tube material or perhaps the casting material for the cylinders or regenerator housings, which are possible sources for these elements. Since the cylinder and regenerator housings are physically isolated from the receiver by the ceramic insulation packed behind the receiver tubes, it is unlikely that the material is from either of these sources. The evidence suggests that the receiver tubes are the source of the material. Through FY 1985, the deposition of this material gradually decreased, and no additional problems were noted.

STIRLING ENGINE

The Stirling engine subsystem consists of all major components associated with the mechanical operation of the engine, including items such as the hydrogen system and the water and vacuum pumps. The engine control circuitry and the United Stirling display monitor are also included in this subsystem. Important events from the test program related to this subsystem are listed in Table 5-7.

Table 5-7

STIRLING ENGINE OPERATING INCIDENTS

INCIDENT DESCRIPTION	DATE	IMPACT ON AVAILABILITY	LOGBOOK REFERENCE PAGE
BURNT RPM CABLES	17-Feb-84	1	13
BROKEN RETAINER BRUSH SPRING IN VACUUM PUMP MOTOR	26-Mar-84	1	28
REPLACED PISTON ROD & RINGS IN ENGINE	04-May-84	1	43
REPLACED AIR COMPRESSOR IN PCU	04-May-84	1	43
SHAFT COUPLING DISINTEGRATED IN H2 COMPRESSOR	05-Jun-84	1	62
DAMAGE TO PCU ANALOG OUTPUT	23-Jul-84	1	113
REPAIR OIL SENSOR UNIT	26-Jul-84	1	118
BURN MARK ON PINS 11,12 OF A/D CONVERTER	31-Jul-84	1	124
RPM SENSOR SHAFT BROKEN TWICE	29-Oct-84	1	177
BROKEN RPM SENSORS	08-Nov-84	1	183
RAIN ON PCU CAUSES USI MONITOR FAILURE	10-Dec-84	1	187
WATER PUMP STUCK AND/OR RUSTED	12-Dec-84	1	187
RPM SHAFT BROKE AGAIN	13-Dec-84	1	187
OIL PUMP SHAFT WORN OUT	16-Dec-84	1	190
INTERCONNECTING PUMP SHAFT WORN AWAY AGAIN	09-Jan-85	1	202
H2 COMPRESSOR OIL LEAK	19-Mar-85	1	248
OIL PUMP FAILURE - WORN SHAFT AGAIN	01-Apr-85	1	253
ONE BROKEN CHECK VALVE IN ENGINE	22-Jul-85	1	281
HYDROGEN DUMPING- BAD PLUMBING JOB	03-Feb-84	2	8
PROBLEM WITH H2 COMPRESSOR AND RELIEF VALVE	07-Feb-84	2	11
RADIATOR LEAK	04-May-84	2	43
OIL COOLER SYSTEM WONT SHUT DOWN AUTOMATICALLY	14-Jun-84	2	67
WATER PUMP WOULDNT SHUT DOWN	19-Jun-84	2	73
RELIEF VALVE PROBLEM IN H2 COMPRESSOR	10-Jul-84	2	98
USI ENGINE MONITOR NOT WORKING	20-Sep-84	2	160
LARGE HYDROGEN LEAK- VENT VALVE HAD LEAK	08-Oct-84	2	166
ALLEN SET SCREW LOOSE FROM PLAY IN ENGINE	29-Oct-84	2	178
ENGINE RPM OSCILLATION	18-Mar-85	2	247
HYDROGEN HOSES STIFF - REPLACED	29-Apr-85	2	258
ENGINE CONTROL BOX / US DISPLAY MONITOR	14-May-85	2	264
REPLACE SHOCK ABSORBERS ON AIR COMPRESSOR/ VIBRATION	11-May-84	3	46
POSSIBLE LEAKS IN AIR COMPRESSOR	11-May-84	3	50
INSTALL AIR COMPRESSOR MOTOR MOUNT	17-May-84	3	52
H2 COMPRESSOR ON FOR 48 HOURS	28-May-84	3	58
BURNED OUT LAMPS- U.S. CONTROL BOX	24-Sep-84	3	161
EXCESSIVE ENGINE NOISE	05-Oct-84	3	165
ENGINE OIL LEAK	16-Oct-84	3	170
NOISE LEVEL IN ENGINE INCREASING	07-Nov-84	3	182
PROBLEM REMOVING RADIATOR FROM ENGINE MODULE	14-Jan-85	3	205
AIR COMPRESSOR LEAK	25-Feb-85	3	236

KEY:

1 = PREVENTED FURTHER OPERATION OF THE MODULE
2 = SIGNIFICANT IMPACT BUT OPERATION COULD CONTINUE
3 = INSIGNIFICANT EFFECT ON CONTINUED OPERATION

First Overhaul/Check Valve Failure

Significant differences in working gas temperatures between quadrants can indicate problems from a variety of sources. On 27 April 1984, one such incident occurred where it was noticed that the temperature in quadrant 4 was running high by over 150°C. This symptom, coupled with a "RPM Hi/Lo" alarm, indicated that there was a problem in the engine.

The first components inspected were the check valves. Theoretically, it was possible that the excessive quadrant temperature was due to either a damaged piston ring or check valve. However, because experience on engine operation generally showed that piston ring problems lead to a different sympton (one high and one low quadrant temperature), a check valve fault was suspected. As expected, none of the check valves leading to cylinders 1, 2, and 3 showed any damage. However, when one of the check valves leading to quadrant 4 was opened for inspection, it showed signs of having oil present. On finding oil in the first check valve leading to quadrant 4, a decision was made to disassemble the engine to replace the old-style PL seals with newer seals, but the eighth check valve was not inspected until the engine had been fully disassembled. When this inspection finally did occur, it was found that the spring of the check valve leading from cylinder 4 was stuck in the open position due to the presence of a piece of spring material. This check valve connected cylinder 4 to the minimum pressure line, which kept the cylinder operation at a low pressure and thus caused the high-temperature reading. The source of the spring material lodged in the cylinder 4 check valve appeared not to be the cylinder 4 check valve, but the check valve located in the power control block.

Second Overhaul/Oil Pump Shaft Failure

Two identical problems with the oil pump shaft were observed in December 1984 and January 1985. On receipt of a loss-of-oil-pressure alarm, the power conversion unit was examined by Advanco personnel, and a worn-out drive peg for the oil pump was found to have failed. The drive peg is a hexagonal-shaped shaft that fits into a female hex notch connected to the pump. Apparently, the shaft had worn down and was spinning inside the notch.

United Stirling said that the first failure was probably due to the gears in the power conversion unit causing a nonuniform torque on the crank shafts, which broke the drive peg to the oil pump. They suspected that the second failure 3 weeks later was because of a poor quality shaft that may have been machined incorrectly.

New oil pump shaft parts from Sweden were installed, and the gears in the engine were replaced during an engine overhaul in early January.

A third failure of the oil pump drive peg occurred on 1 April 1985. Once again, the hexagonal peg was worn smooth. The oil pump was repaired within a few days without removing the engine from the dish. On 15 June 1985, another failure of the oil pump drive peg occurred. The most probable explanation for these recurring problems is that the tolerances between the drive peg and the front cover of the oil pump are not within specifications. A new design of drive peg and a new oil pump and front cover were installed on 17 June 1985. No failures occurred during the remainder of the test program.

Engine Noise and Vibration

In the latter months of 1984, power conversion unit noise and vibration levels were increasing and were cause for concern by Advanco personnel, even though no decrease in engine performance was observed.

Based on the experience from laboratory testing in Sweden, where gears causing higher noise/vibration levels have never caused any problems, United Stirling decided not to change gears because they were convinced that no severe problems were present. They believed the source of the noise was the wear on unhardened gears between the engine and alternator, but stated that an engine failure would not occur due to gear wear. Discussions between United Stirling and Advanco indicated, however, that the failure of the oil pump shaft and the rpm sensor shaft might be attributed to the unhardened gears. When the engine was removed for repair of the oil pump shaft, engine inspection indicated significant wear on the gear teeth, which verified the original assumption.

The second time the engine was removed to replace the oil pump shaft, the engine was overhauled and the generator/crankshaft gears were replaced with hardened gears. The replacement of these three main gears eliminated the excessive engine noise problem.

Radiator Replacement

A new radiator design by USAB in Sweden featured a sealed-off Stirling engine to protect the engine parts against ambient conditions, and a low-power-consumption fan to reduce the auxiliary power requirement. This radiator was delivered to the

site in June 1985 and was installed when the power conversion unit was down for receiver replacement. Preliminary checkout of the radiator in mid-July shortly before the test program was completed gave good indications of performance.

Engine Instrumentation

Several related items dealing with Stirling engine instrumentation are grouped into this category, including the rpm sensor, the controller circuit boards, and the display monitor. These are discussed below.

Engine RPM Sensor. On 26 October 1984, the shaft that drives the Onan rpm sensor broke. This shaft is located on the end of the induction generator. It is a 3/8-in.-diameter shaft that tapers down to a 1/4 in. diameter. The 1/4-in. end is pressed into the generator shaft. The 3/8-in. end is attached to a flexible coupling which, in turn, is attached to the rpm sensor 3/8-in. shaft. The flexible coupling is large and heavy (2 lb) and is believed to be the cause of the shaft breakage. On 30 October, a new shaft of similar design was installed, which broke the following day. The decision was made to replace the flexible coupling with a new lightweight design.

On 8 November, the system was on sun with the new flexible shaft coupling installed; however, the rpm sensor broke after a few hours of operation. The spare sensor was installed, and it also broke after a few hours of operation. The rpm sensors were not repaired until the beginning of December. It is believed that these failures were related to the increased vibration in the engine. United Stirling believes that initial installation error was the cause of the rpm sensor breakage.

The power conversion unit was not in operation during the remainder of November. The problems with the broken shaft for the rpm transducer were analyzed, and it was decided to continue with the original design. Preparations for installation were made by United Stirling personnel, and a new shaft was fabricated by Advanco. The new shaft was installed 6 December.

The power conversion unit was restarted on 13 December, and the new shaft broke almost immediately. A new design with a lighter coupling was fabricated by Advanco as a backup alternative, and this was installed 14 December. In addition, two

lightweight flexible couplings made out of neoprene were installed, which reduced the vibration to the sensor and the eccentricity loading on the shaft. No subsequent problems with either the rpm sensors or the shaft were experienced.

Stirling Engine Control Boards. The Stirling controller, in addition to its control function, also provides eight analog output channels of information to the data acquisition system, including engine pressure, set temperature, rpm, and other data. On 23 July 1984, which was a Monday following a weekend of thunderstorms, the output voltage from each of the eight channels was found to be reading low by about 30%. The problem persisted even after replacing both the A/D converter integrated circuit and a LM347 reference voltage integrated circuit. The circuit board was then carefully examined, and small gray spots were discovered on the underside. These were suspected of being short-circuit paths to the A/D converter chip reference circuitry. These spots were removed by scraping, and the unit then functioned properly. United Stirling control boards are not coated with a sealant, which perhaps would be helpful in preventing this effect in the future.

USI Display Monitor. On 20 September, the USI display monitor was discovered to be nonoperational. This monitor remained down until 4 October when United Stirling was able to repair it. The problem was a faulty component (zener diode), which fluctuated in value. This type of failure apparently was not caused by the power outage of the previous day. The USI engine could have operated without the monitor, but the decision was made to wait and fix the monitor before running the engine.

On 25 December, testing was again interrupted due to a similar problem of loss of communication to the power conditioning unit monitor. With support from United Stirling personnel, certain electronic components were exchanged on the USI monitor circuit board and the system made operational again. Burned out electronic components were the reason for the failure. The same two chip locations on the circuit board in the USI monitor were the source of the repeated failure. The chips turned brown in color and felt hot to the touch, indicating they were being overloaded. No long-term solution was proposed.

Hydrogen System

Early in 1984, it was noted during operation that the hydrogen supply valves and dump valves were being activated too frequently, causing the hydrogen compressor to

run excessively. This problem was resolved by changing the control parameters in the Stirling control unit to effectively increase the deadband in the hydrogen supply/control servo loop.

A persistent slow hydrogen leakage rate was observed, which was traced to an irreparable leak in one of the low-pressure manometers on the group hydrogen system. A pressure relief valve also gave indications of hydrogen leakage. No repairs of these problems were undertaken, since they had no direct effect on module operation other than the increased consumption of hydrogen.

Engine Performance

The main control variable for the Stirling engine is engine gas pressure. Power output from the engine is determined by the working gas pressure, which is varied to maintain a constant working gas temperature. When the insolation level on the receiver increases to a point where the working gas set temperature would be exceeded, the pressure is increased, thereby maintaining the temperature at the set point. This effect is shown in Figure 5-5. In this example, the working gas temperature rises with insolation to approximately 650°C, the gas temperature set point, where it remains constant even though insolation continues to climb. Variations in insolation above about 500 W/m^2 have no discernible effect on working gas temperature. In this region, the working gas pressure is being varied to maintain the temperature, as shown in Figure 5-6. The relationship between gas pressure and gas temperature is shown more clearly in Figure 5-7, where these two parameters are plotted against each other over the same time period.

Incident power, generated power, gas pressure, and gas temperature are plotted in Figure 5-8 on a relative scale to show the interactions between these parameters. As the incident power from the sun begins to drop due to cloud passage, the generated power also decreases. The gas pressure is dropped to maintain the gas temperature at the set point. When the insolation drops to a point where the gas pressure can decrease no further to maintain the gas temperature (i.e., it reaches the lower H_2 gas-reservoir pressure), the temperature is then forced to decline as well. The thermal lag in the system is evident when the insolation sharply peaks again. The gas temperature begins to respond, but cannot reach the operating temperature before the incident energy decreases. During this period, the gas pressure does not increase. These data indicate that the response time of gas temperature to a step change in insolation is on the order of 1 minute. This is

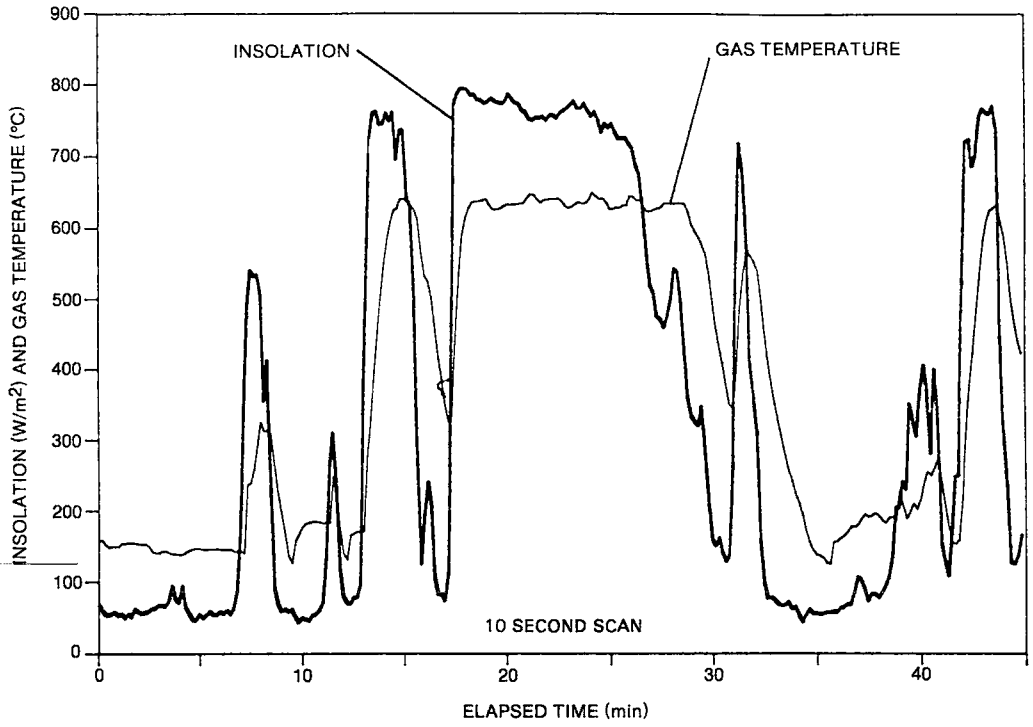

Figure 5-5. Response of Average Working Gas Temperature to Variations in Incident Insolation - 26 July 1984

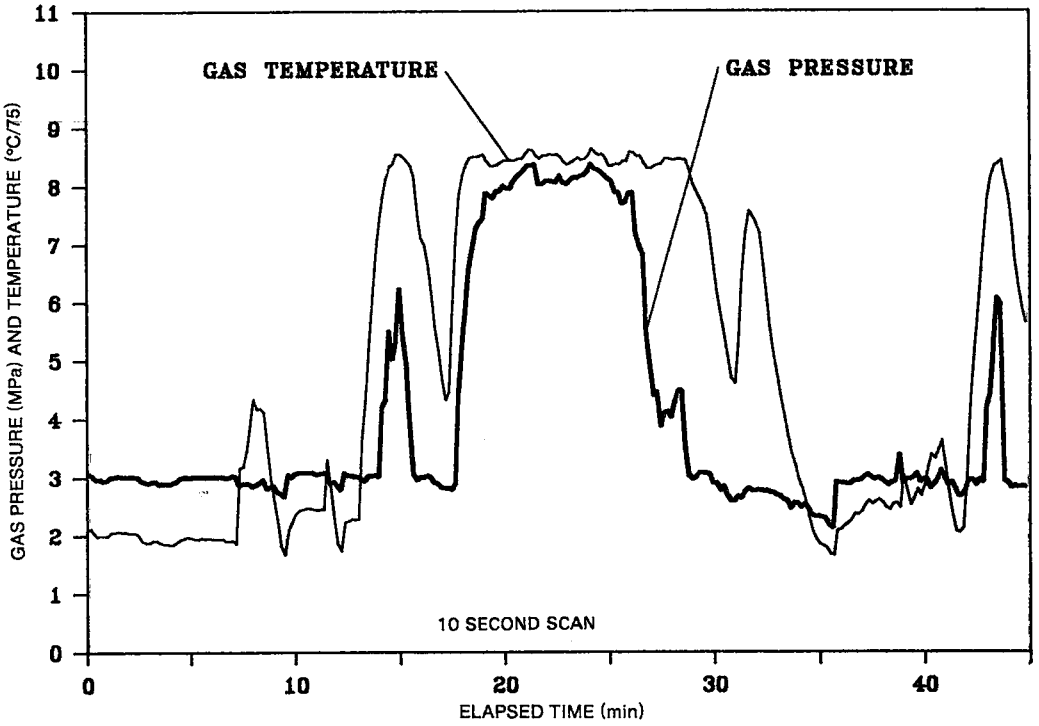

Figure 5-6. Average Working Gas Temperature and Pressure Over a Period of Variable Insolation - 26 July 1984

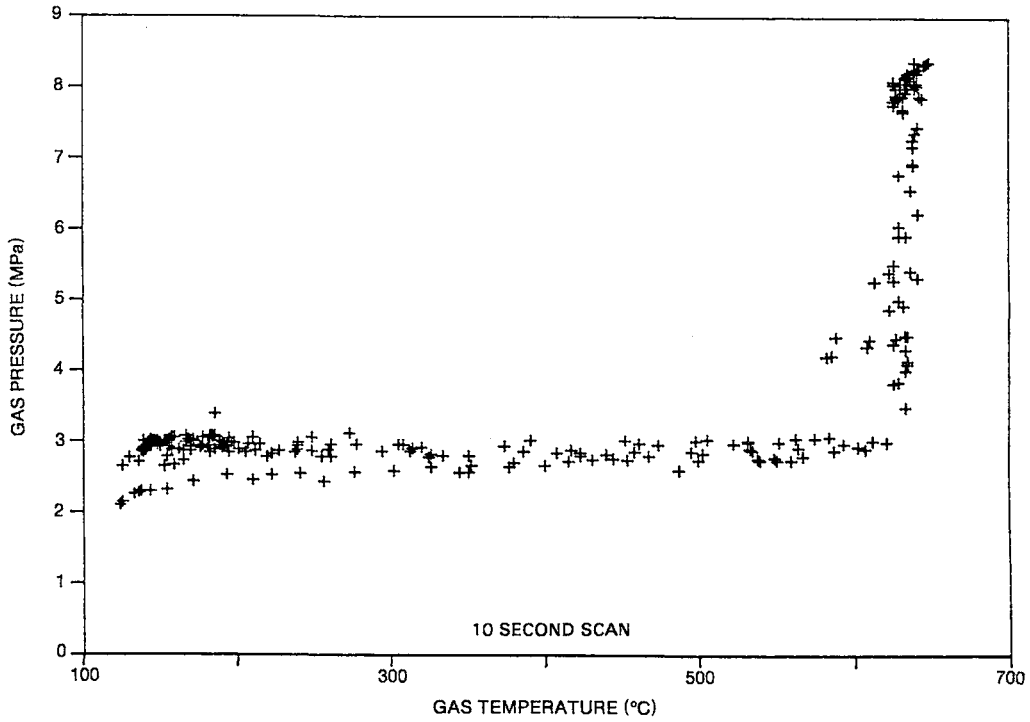

Figure 5-7. Relationship Between Working Gas Temperature and Pressure Over a Variable Insolation Period - 26 July 1984

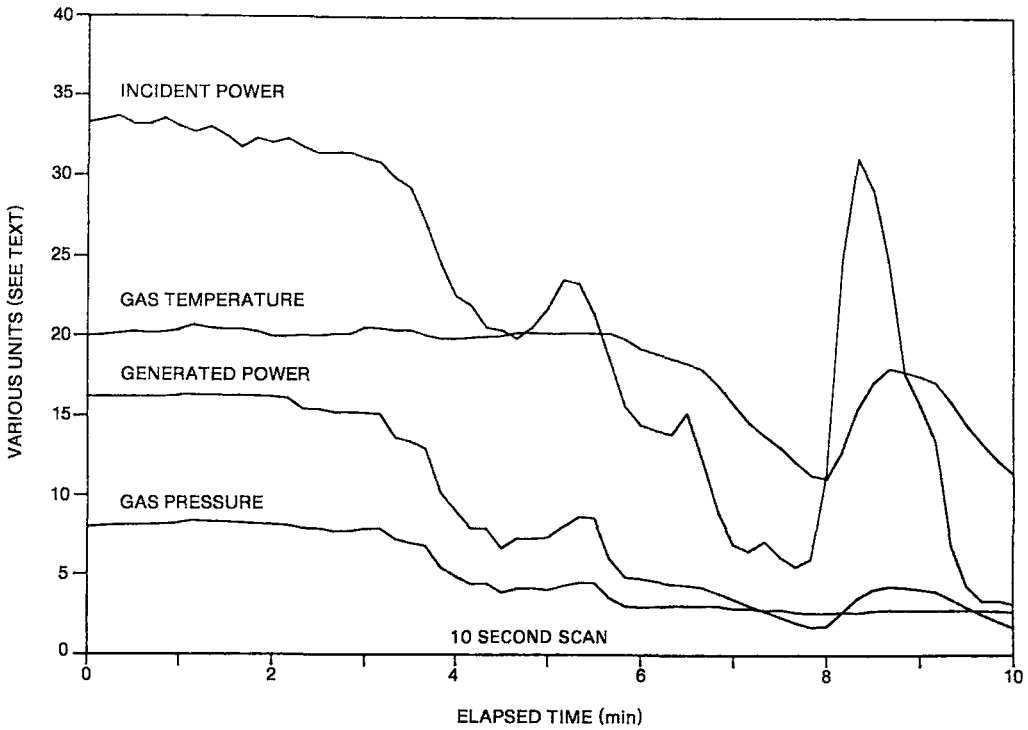

Figure 5-8. Incident Power, Generated Power, Gas Temperature, and Gas Pressure Over a 10-Minute Span - 26 July 1984

considered the thermal lag of the system, and it is actually quite short when compared with other solar thermal technologies.

Power output tracks either the gas pressure or the gas temperature, depending on within which regime the engine is currently operating (high insolation--constant temperature, varying pressure; low insolation--constant pressure, varying temperature). The lag time between power output and either pressure or temperature is on the order of less than 10 seconds, indicating excellent control between the engine and induction generator. Figure 5-9 shows the linearity between power and engine pressure above an engine pressure of 4 MPa. This again indicates good control.

The Stirling engine comes up to operating speed (1800 rpm) very quickly when energized. This is shown in Figure 5-10, which graphs engine speed and power output as a function of time. It is clear that the Stirling engine begins producing power almost immediately after being placed into operation. In this example, the engine speed appears to be fluctuating around 1700 rpm, but this is due to an offset in the sensor reading. Figure 5-11 shows the relationship between engine speed, insolation, and average working gas temperature. Fluctuations in working gas temperature are not as dominant as in engine speed; this consistency maintains higher engine efficiency. As expected, the engine reaches operating speed before the hydrogen gas reaches operating temperature, simply due to a small thermal lag in the receiver/engine.

The effect of a change in the working gas set point temperature is shown in Figure 5-12. A higher gas temperature set point allows the engine to produce more power at the same gas pressure, but the consequences include reduced lifetimes for the engine and receiver components. A lower gas temperature set point would maximize component life spans but might not produce enough power to be cost effective. Therefore, a balance between these factors must be struck; based on their experience, United Stirling recommended a gas temperature set point of 720°C.

The effect of ambient temperature on engine performance is also of interest. Two separate days were chosen, one in the summer and one in the winter, so the average at-power ambient temperature difference was very large (in this case 30°C). When both sets of data were normalized to eliminate reflectivity effects, gas pressure was plotted versus generated power; the result is shown in Figure 5-13. There is an obvious, albeit slight, difference between the two sets of data. On the day with the lower average temperature, the same power is produced at a gas pressure approximately 1 MPa lower than that on the warmer day. This effect is manifested

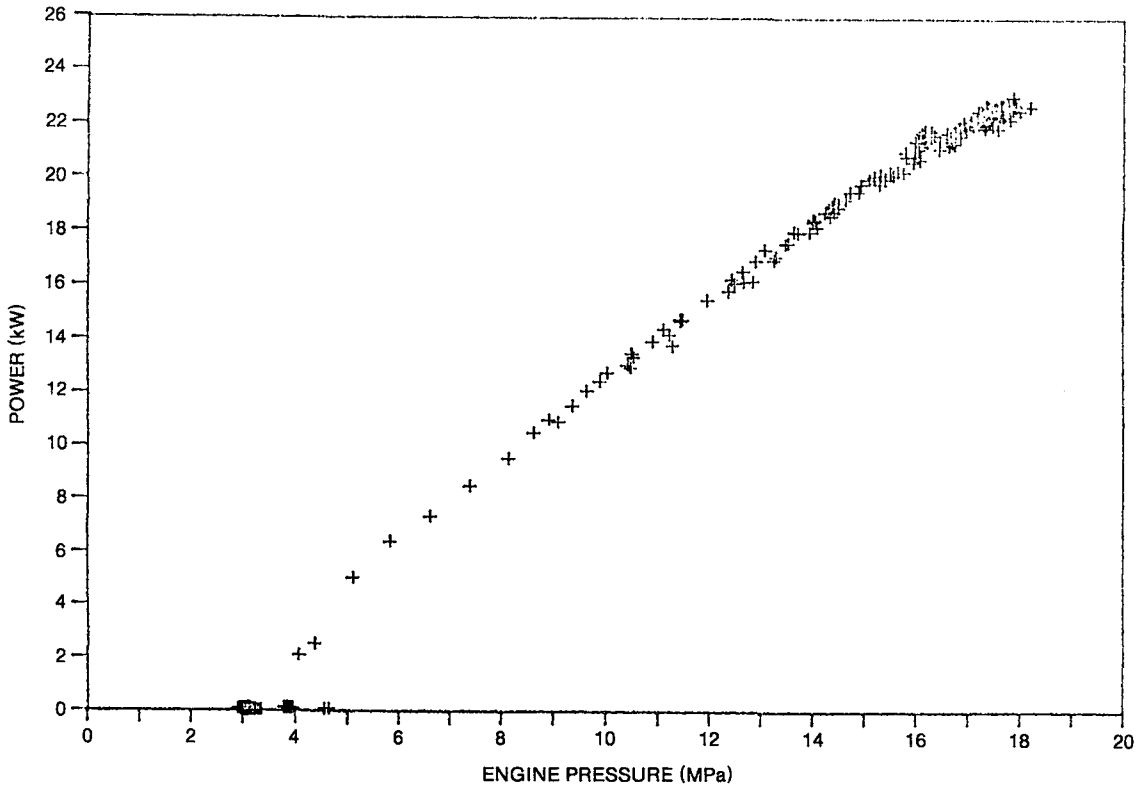

Figure 5-9. Gross Generated Power as a Function of Working Gas Pressure for 23 October 1984

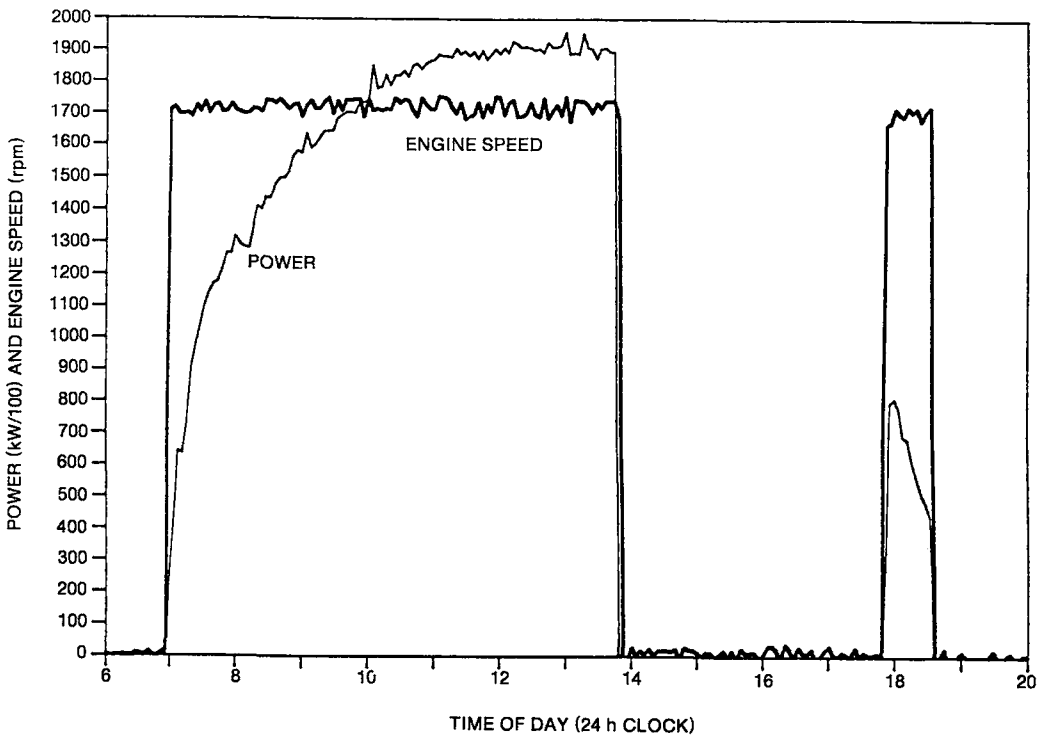

Figure 5-10. Gross Generated Power and Engine Speed versus Time for 7 August 1984

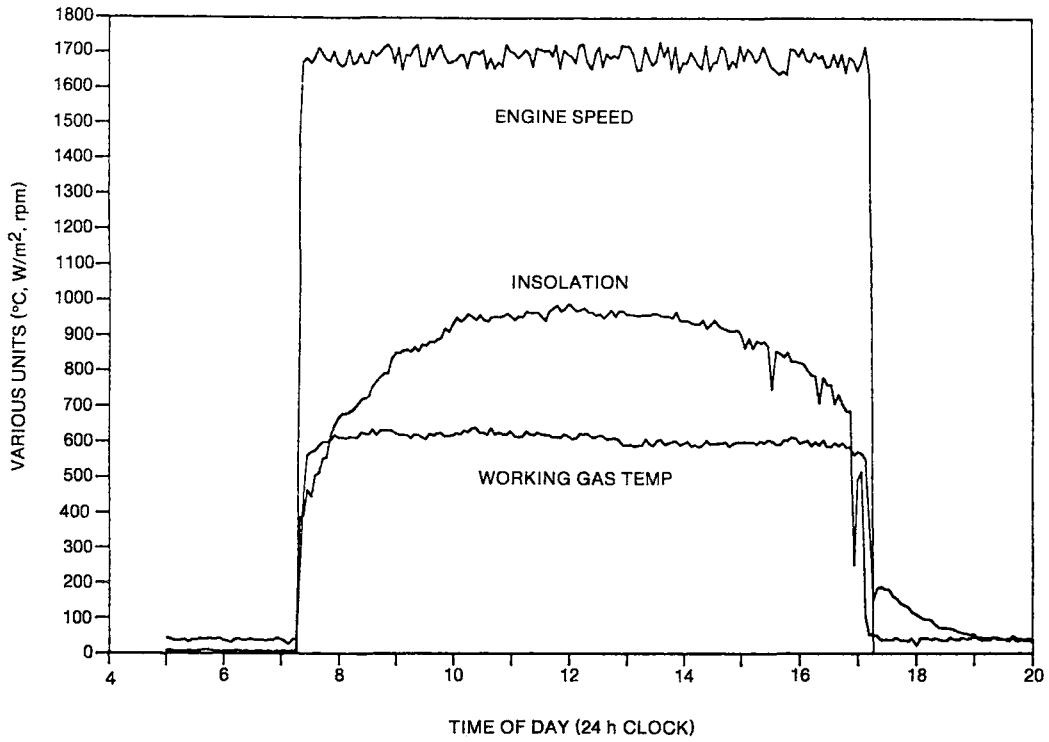

Figure 5-11. Engine Speed, Incident Insolation, and Average Working Gas Temperature Throughout the Day for 12 October 1984

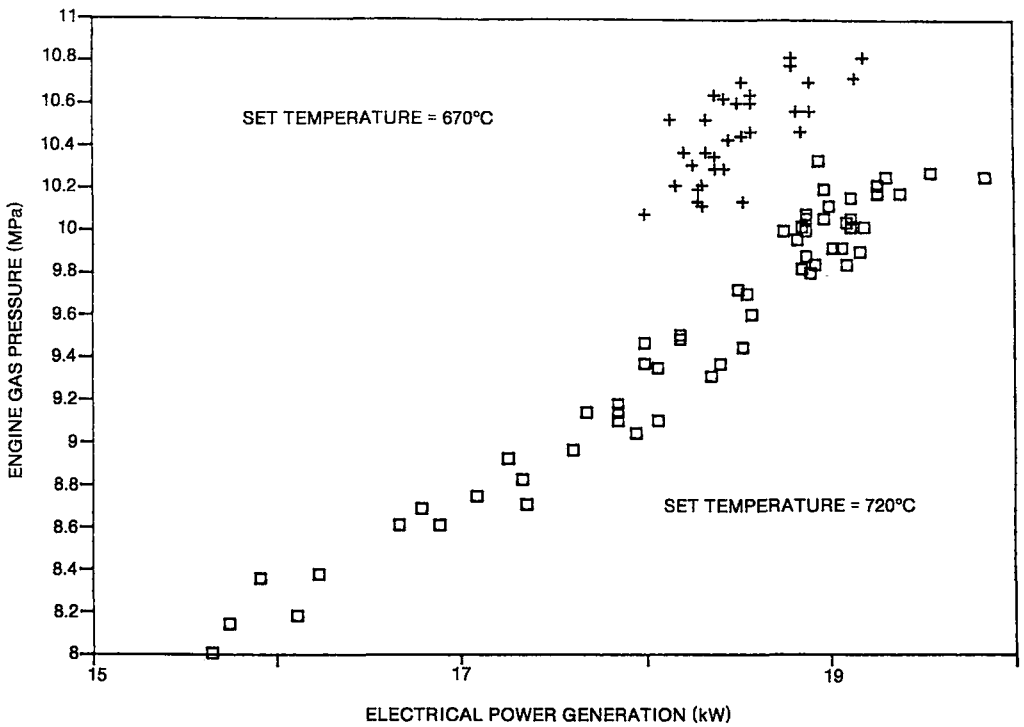

Figure 5-12. Effect of Working Gas Temperature Set Point On Engine Pressure versus Generated Power Curve

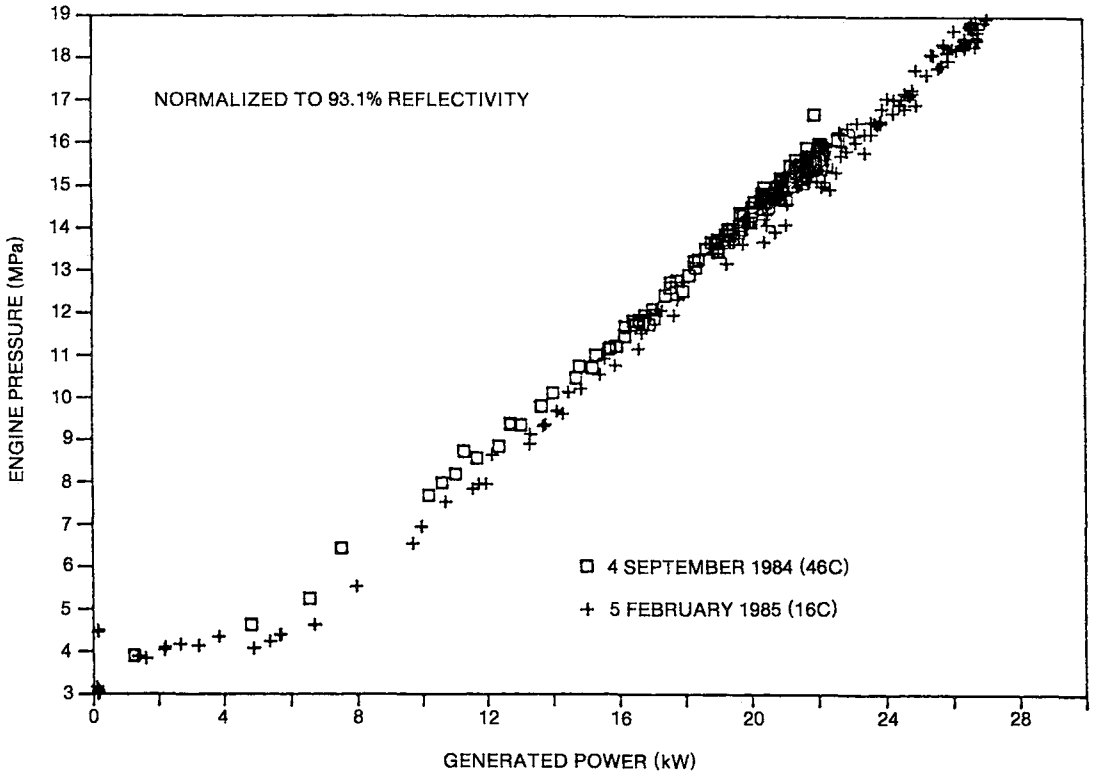

Figure 5-13. Effect of Ambient Temperature on Engine Pressure versus Generated Power Curve for a Summer Day and a Winter Day

over the entire pressure span of the engine and indicates that cooler days are more beneficial to operation (either in terms of increased component lifetimes or increased electrical energy output).

The effect of ambient temperature on fan power is shown in Figure 5-14. On the warm day, the fan operates on low power for approximately 2 hours. When the increasing air temperature requires additional cooling of the engine, the fan switches to high power, where it remains throughout most of the afternoon. The fan drops back to low power as the ambient temperature also decreases, about 1 hour before the system is shut down. The cold day shows a different phenomenon. The ambient temperature on this day is low enough that the fan is not required to operate continuously to maintain the engine coolant temperature; hence, it cycles on and off throughout the day on low power.

The actual coolant temperatures for these days are shown in Figure 5-15. The light lines represent the temperature of the coolant coming from the engine; the dark

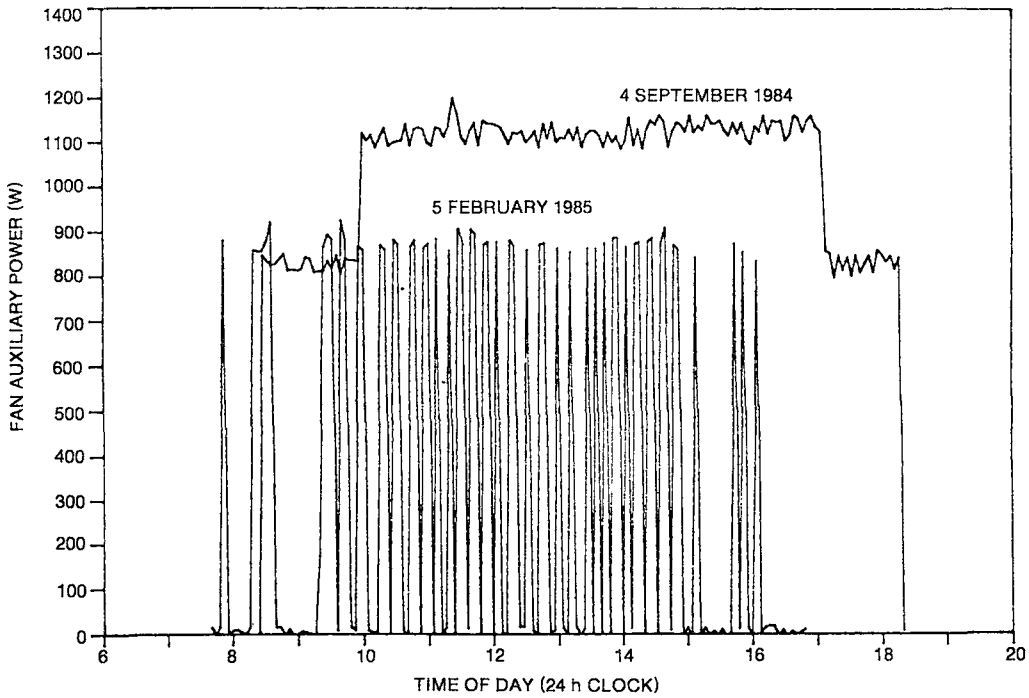

Figure 5-14. Effect of Ambient Temperature on Fan Power Throughout the Day for a Summer Day and a Winter Day

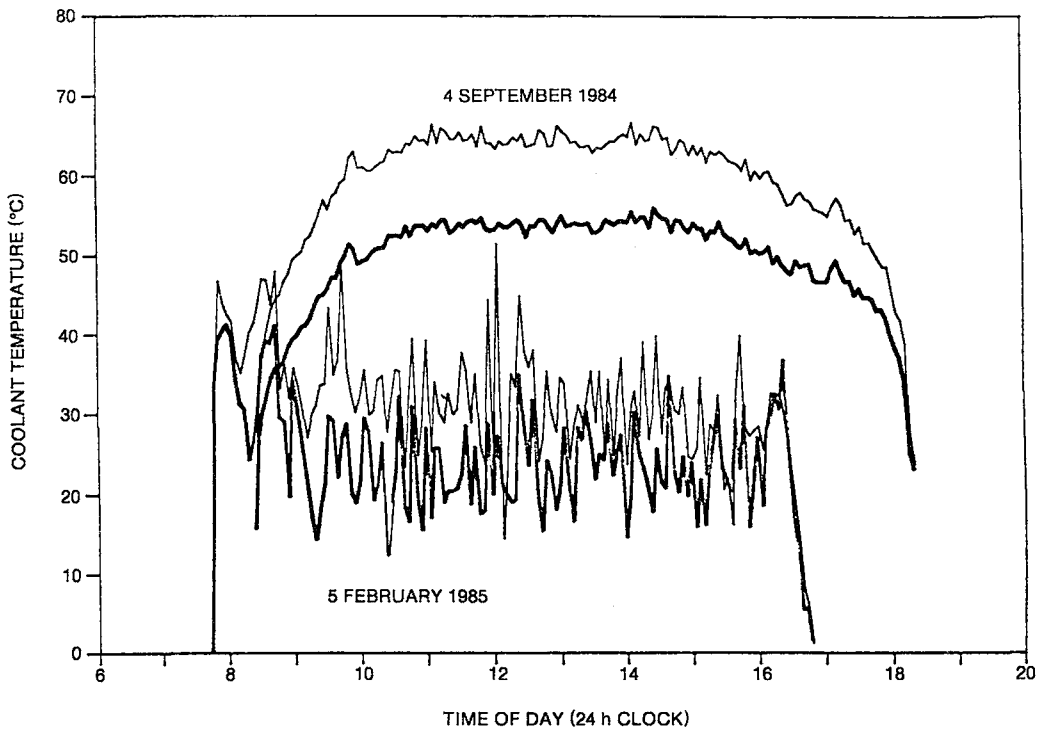

Figure 5-15. Engine Coolant Inlet and Outlet Temperatures Throughout the Day for a Summer Day and a Winter Day

lines represent the temperature of the coolant returning to the engine from the radiator. As expected, the coolant temperature on the warm day exceeds that of the cold day. The "jaggedness" of the February temperature is the result of the fan on/off cycling; much more stable temperatures are observed when the fan operates continuously. On both days, the average temperature difference across the radiator is approximately 8 to 10°C and is fairly constant throughout the day.

INDUCTION GENERATOR

After evaluating four generic types of electrical generation technologies (induction, synchronous, alternator inverter, and wound-rotor induction inverter) for the Vanguard module, an induction generator was the choice of Onan Corporation. This selection was based on the potential need for a starter motor to accelerate the Stirling engine to "running" speed, on the relative simplicity of induction machine controls for motoring and generator-parallel operation with the utility, and on lower capital costs than for synchronous generators. Induction generators are readily available as a purchased component from several sources. A Reliance Model XE 286T induction generator was selected with the following modifications: (1) wound for 480 Vac, (2) shaft directly coupled to the Stirling engine, (3) optical tachometer to measure generator speed, and (4) a 2-hp induction motor with chain drive and an overrunning clutch for starting the engine/generator. The induction generator characteristics make a good match with the Stirling engine, especially in torque and rpm range. The Vanguard module generator full-load continuous ratings at 60 Hz are 480 Vac, 22.5 kWe, 0.90 pF, and 1830 rpm. The generator is capable of long-term operation output levels up to 30 kWe without damage; however, operation at these levels will result in slightly lower efficiencies. Generator speed and efficiency as a function of power produced are shown in Figures 5-16 and 5-17, respectively, where generator speed varies between 1800 and 1840 rpm. Between 0 and 1800 rpm, the induction generator acts as a motor (Figure 5-18) and, if connected to the grid, would actually draw current.

The induction generator is located in the power conversion unit, which is positioned near the focal plane of the parabolic dish. As the dish tracks the sun, the dish moves through several azimuthal and elevational positions depending on date and time of day. In so doing, the long axis of the generator shaft also is subjected to complementary changes in orientation, which deviate from the stable horizontal position for which most commercial generators are designed. As the long axis of the generator shaft is tilted away from the horizontal plane, larger axial

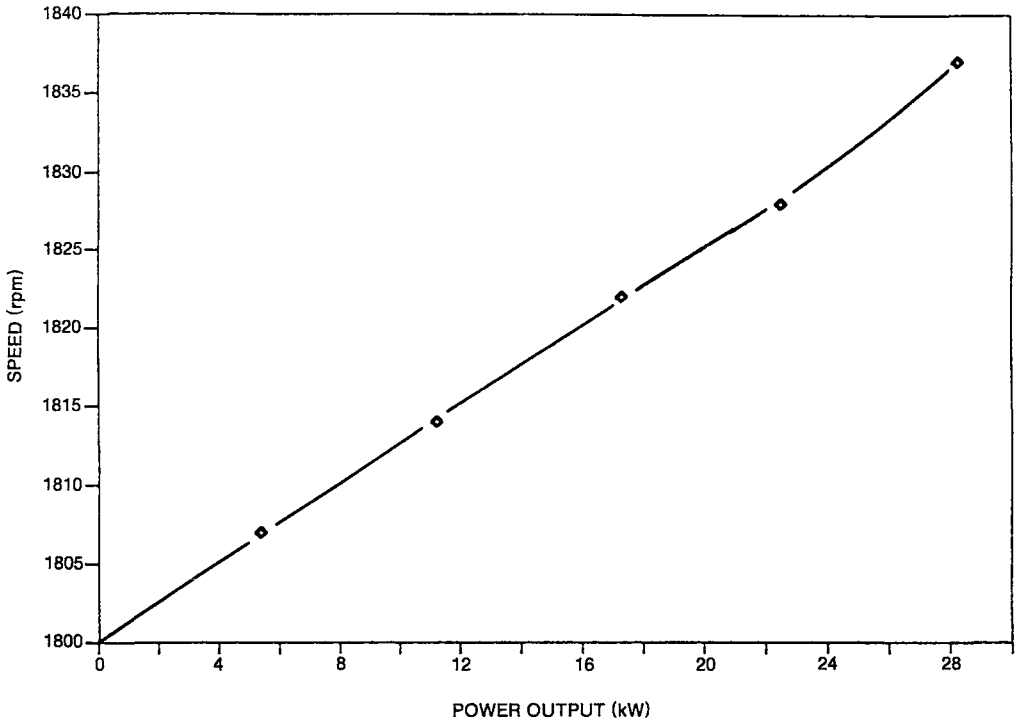

Figure 5-16. Induction Generator Speed as a Function of Gross Power Output

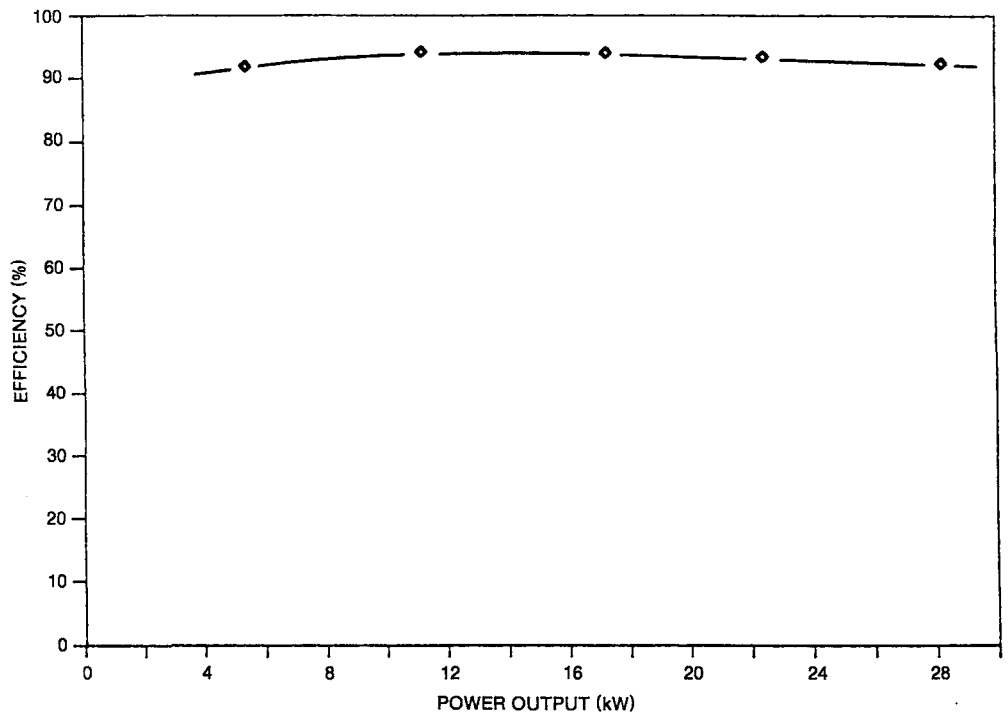

Figure 5-17. Induction Generator Efficiency as a Function of Gross Power Output

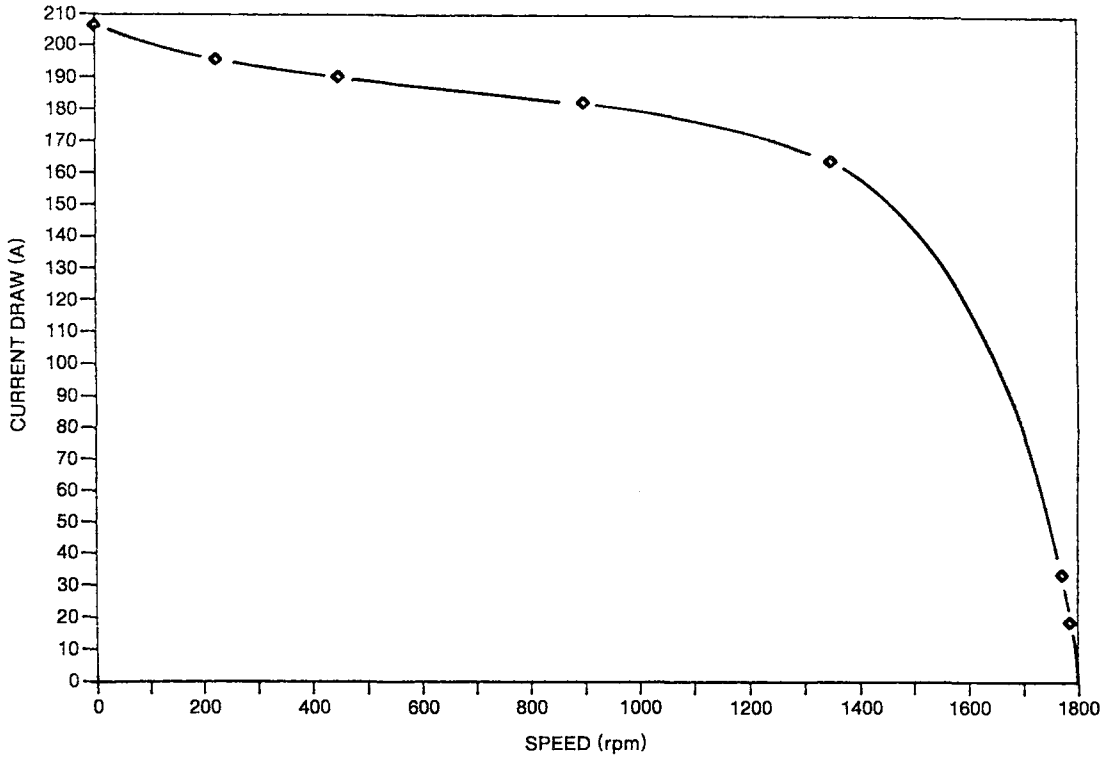

Figure 5-18. Induction Generator Current Draw at Speeds Below 1800 rpm

thrusts and loads are imposed on some of the bearings. During the test period, however, no problems were encountered with the induction generator bearings.

Unlike a synchronous generator, which can produce power at a power factor of 1.0, the induction generator produces power that requires reactive volt-amperes (V•Ar) at lagging power factor from the utility for excitation. When the power produced by the dish/Stirling module is small relative to the kV•A rating of the interconnected utility line, the effect of lagging power is also small. Operation at peak power generating levels, however, requires power factor correction. Power factor correction capacitors have been installed in the Vanguard test module to correct the power factor to approximately 0.95 at full-power output. The capacitors switch in unison with the generator to protect against any possibility of generator self-excitation or overvoltage condition after generator disconnect. The induction generator characteristics with and without power factor corrections are shown in Figures 5-19 and 5-20.

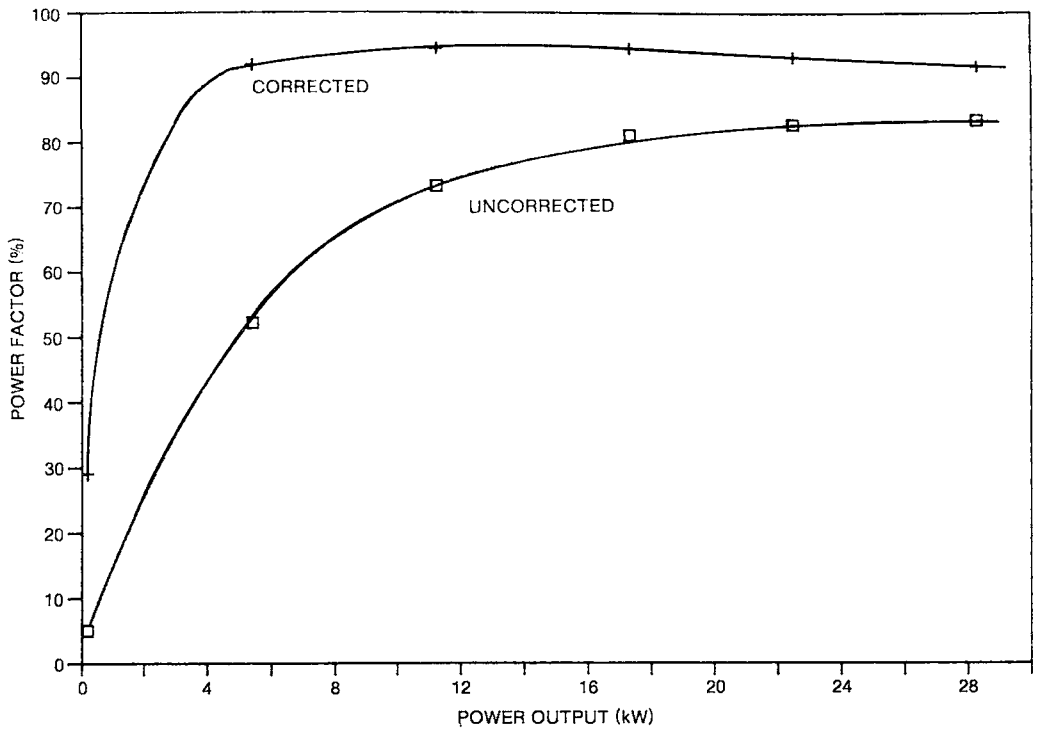

Figure 5-19. Induction Generator Power Factor as a Function of Power Output with and without Power Factor Correction

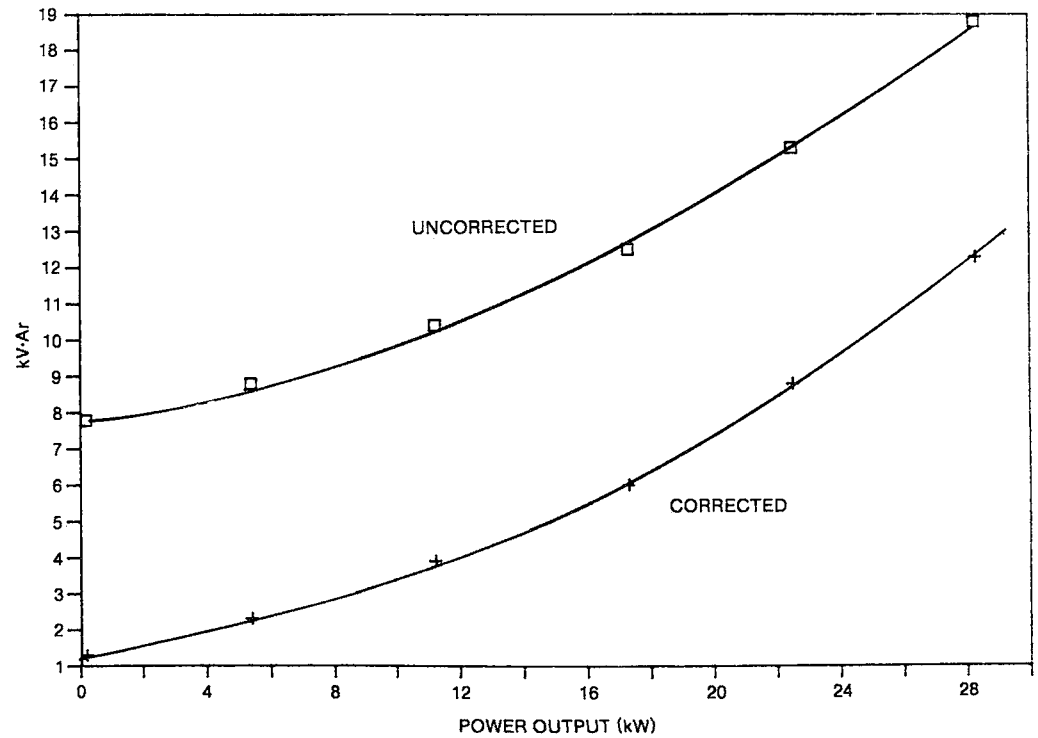

Figure 5-20. Induction Generator Kilovars as a Function of Power Output with and without Power Factor Correction

The rated synchronous speed of the Vanguard induction generator is 1800 rpm. An induction motor/generator will behave like a motor and provide shaft power at any rpm below synchronous speed and will behave like a generator and utilize shaft power at any rpm above synchronous speed. To avoid the possibility of wasting power when the generator is operating below synchronous speed, the utility connect/disconnect controls are set to open below 1800 rpm and to close at or above 1800 rpm. The rpm sensor and controls have been designed with very little lag times between sensing and initiating contactor operation. This will ensure that large variations or reversals of torque and current will not occur.

A reconnect time delay of 1 to 1.5 seconds has been incorporated to protect the generator and Stirling engine against damaging torques that accompany a nearly instantaneous reconnection of the generator to the utility subsequent to a control-directed contactor opening or a momentary utility interruption.

The generator controls incorporate fail-safe features to assure that either the loss of the utility connection or rpm sensor will automatically open the contactor. By powering the contactor coil with utility power, the generator disconnect occurs automatically on loss of power. Since the induction generator will not, except for special cases, self-excite, the loss of utility power will drop out the contactor. This system appears to have worked satisfactorily throughout the test period, and no serious problems with the induction generator have been noted.

ELECTRICAL GRID INTERFACE

The interface between the utility grid and the Vanguard module is made through group electrical power systems and module electrical power systems. The group electric power system can accommodate up to 32 modules by supplying electrical power to, or accepting electrical power from, each module through its module electrical power system. At the SCE Santa Rosa substation, adjacent to the Vanguard test site in Rancho Mirage, there is one intermediate transformer. This intermediate transformer is sized to handle eight group electrical power systems but had only one during testing. Features of the group electrical power system and module electrical power system are shown in Figure 5-21.

The group electrical power system provides the interface between SCE's power grid and various components of the Vanguard module. These components include the backup power generator set and its battery charger, the module electrical power system, the hydrogen compressor, the subconcentrator control unit, the master concentrator

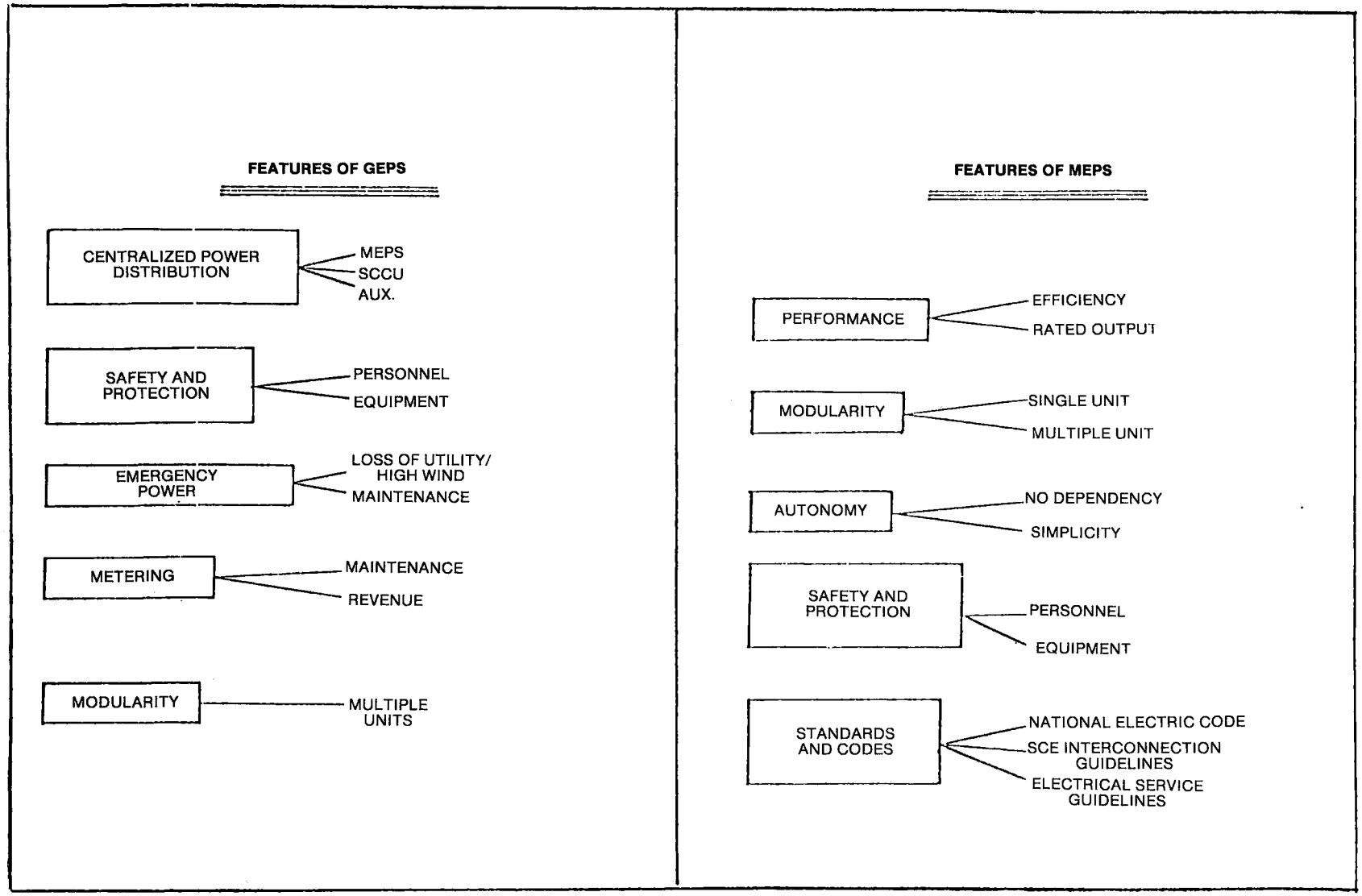

Figure 5-21. Features of the Group and Module Electrical Power Systems

control unit, the data collection unit, weather station, and emergency light. Each circuit contains wattmeters to measure the power consumed. Schematics of the group electrical power systems and module electrical power system are shown in Figure 5-22.

Loss of grid power is considered a probable occasional occurrence at the Santa Rosa site. The backup functions to detrack the parabolic dish concentrator should operate at this time, and the standby diesel generator should start. On proper functioning of the emergency controls, the GEPS will be reconnected to the power grid and the module placed back in normal operation.

The module electrical power system interfaces with the group electrical power systems, and this provides for power to the module and in turn supplies power to the generator windings, the engine starter motor, the engine coolant pump, and heat rejection system fan. Connection is also made to the generator, connected through a wattmeter, to monitor gross power delivered to the grid. Wattmeters are also installed in each of the above power-consuming circuits.

The major significant events directly involving the electrical grid interface subsystem were power outages. These occurred sporadically throughout the test period, numbering fewer than 10, and most often lasting for less than 1 minute.

The response of the Vanguard system to a power outage while operating was noted during a grid failure in April 1984. The sequence of events that occurred and the necessary steps taken following the grid outage are described below.

At 11:26 a.m. on 26 April 1984, the SCE grid went down for approximately 3 minutes, and all power to the test site was lost during this period. Design features to protect the module from damage in this event, known as a grid loss, were incorporated into the module's hardware and software. At the moment of grid loss, the following planned events occurred:

- The induction alternator disconnected from the grid, and the engine rpm promptly decreased to zero.
- The solenoid controlling the water-cooled aperture plates was activated and the plates closed.
- The emergency diesel generator started and provided auxiliary power to the drive motors and controllers. This required about 10 seconds.
- The gravity slew mechanism tripped.

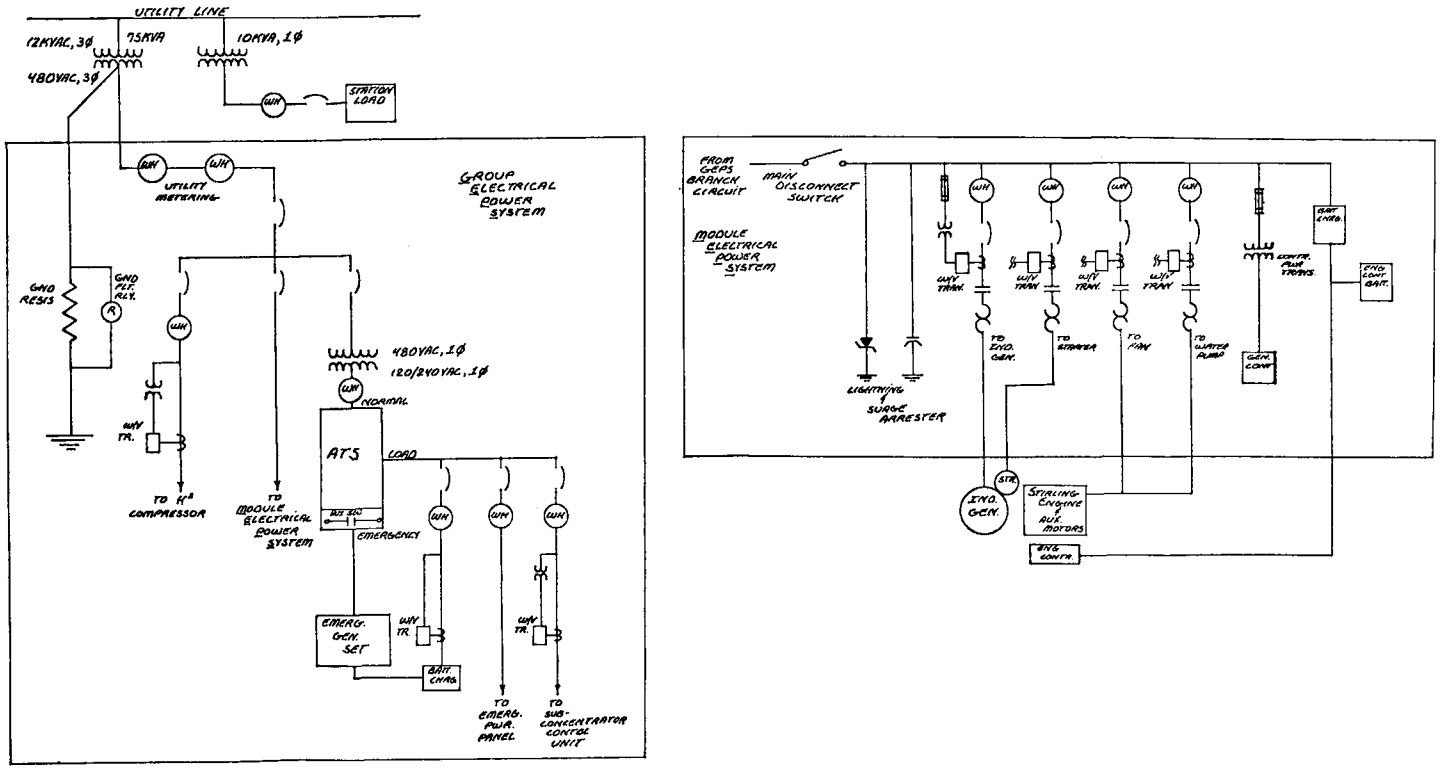

Figure 5-22. Schematic of the Group and Module Electrical Power Systems

The weight of the gravity slew mechanism was insufficient to drive the concentrator off sun due to the extremely high elevation at the time of occurrence and a slight imbalance in the concentrator center of mass (see previous discussion under Parabolic Dish Concentrator). This event was of no consequence since the water-cooled aperture plates had closed immediately, and the emergency diesel generator provided the power to enable a site operator to command the dish off sun using the tracking drive motors.

The control system for the Stirling engine, which remained fully operational due to its battery backup system, brought the engine to a controlled stop as programmed. The control logic was set up to bring the engine to a complete stop as soon as possible once the loss of the grid was detected.

The loss of the grid resulted first in the rapid acceleration of the engine, since the grid no longer acted as load. The Stirling controller detected this alarm condition and activated the solenoid valves on the pneumatically powered water-cooled shutter plates. The controller then opened the "short-circuit valve," a valve used to brake the engine. The engine was brought to a stop and remained stopped with no water pump or fan power during the remainder of the outage. It is not known exactly how rapidly this stop occurred, but based on tests on other engines, the time to halt the engine is estimated to be about 1 second. Because it was not known whether any damage to any seals or piston rings or other components had occurred, module operation was terminated for the remainder of the day, and a careful check was made for possible signs of leakage. After these checks proved the system to be operational, the engine was run the next day to check for further problems. One quadrant had a high-temperature condition, indicating that an engine problem might be present.

It was decided to dismount the engine for inspection and minor repair. The failure was due to a stuck check valve (see previous discussion under Stirling Engine), which was not thought to be brought about by an overheating condition. No major or costly damage occurred, and no personnel were jeopardized during the accident. It appears that the check valve failure was due to the extreme high gas-surge transients caused by short circuiting the engine, rather than by any effects of overheating due to pump power loss. Corrective actions were taken to increase the gravity slew mechanism's weight for slewing at higher elevations, and the engine's control logic during grid loss was reexamined.

Other incidents involved the repeated failure of the uninterruptible power supply and the weather station power supply. The uninterruptible power supply went out on 19 October 1984. This was the third failure of this system. It is a 1-kW system and provides power to the master concentrator control units, IBM-DAS, and Autodata Nine data logger. The unit is designed to switch back to grid power automatically on failure; however, it did not do this, resulting in loss of data and detrack of the dish. The unit was shipped back to the manufacturer for repair. The power supply for the weather station failed during the latter part of January and was repaired in February. Wind speed, ambient temperature, and wind direction data were not recorded during the days it was down.

INSTRUMENTATION AND CONTROL

The Vanguard I module was designed to demonstrate a proof-of-principle test of a parabolic dish concentrator/Stirling engine/generator system and to gain experience in its operation and maintenance. For this reason, the module is extensively instrumented with devices used to either indicate, control, alarm, or serve as interfaces among system components. The following section describes the instrumentation and control of the Vanguard module and presents operating incidents related to this category.

Instrumentation

In general, the outputs from the various instruments are analog signals. The outputs from the various transducers are fed into an Acurex Autodata Nine computer and/or a Keithly DAS 520 Data Acquisition System (coupled to an IBM-XT computer). Summaries of the channel designations and measurement parameters for both the Autodata Nine and IBM-XT systems are given in Tables 5-8 and 5-9, respectively. By far the largest number of sensors consists of thermocouples in the receiver cavity and in the Stirling engine.

In general, the instrumentation installed at the site performed satisfactorily, with only minor exceptions. Insolation meter tracking problems, sun-sensor condensation, and confusion over conversion factors for some of the instrumentation readings were the most significant.

Table 5-8

DATA CHANNELS FOR AUTODATA NINE SYSTEM
(Sheet 1 of 3)

Channel	Parameter	Units	Conversion Factor
150	Ambient temperature	°C	V (8.5) - 30
151	Wind speed, A	mph	10
152	Wind speed, B	mph	10
153	Wind direction	deg	54
154	Total insolation - dish	W/m^2	94.16
155	Total insolation - ground	W/m^2	109.5
156	Current, dc azimuth motor	A	0.1
157	Voltage, azimuth motor	V	100
158	Current, dc skew motor	A	0.1
159	Voltage, skew motor	V	100
160	-	-	-
161	-	-	-
162	-	-	-
163	-	-	-
164	Front tube inner T5Q1	°C	Type K t.c. conversion
165	Front tube inner T5Q2	°C	Type K t.c. conversion
166	Front tube inner T5Q3	°C	Type K t.c. conversion
167	Front tube inner T5Q4	°C	Type K t.c. conversion
168	Front tube inner T14Q1	°C	Type K t.c. conversion
169	Front tube inner T14Q2	°C	Type K t.c. conversion
170	Front tube inner T14Q3	°C	Type K t.c. conversion
171	Front tube inner T14Q4	°C	Type K t.c. conversion
172	Front tube outer T14Q1	°C	Type K t.c. conversion
173	Front tube outer T14Q2	°C	Type K t.c. conversion
174	Front tube outer T14Q3	°C	Type K t.c. conversion
175	Front tube outer T14Q4	°C	Type K t.c. conversion
176	Rear tube outer T14Q1	°C	Type K t.c. conversion
177	Rear tube outer T14Q2	°C	Type K t.c. conversion
178	Rear tube outer T14Q3	°C	Type K t.c. conversion
179	Rear tube outer T14Q4	°C	Type K t.c. conversion
180	Rear tube outer T5Q1	°C	Type K t.c. conversion
181	Rear tube outer T5Q2	°C	Type K t.c. conversion
182	Rear tube outer T5Q3	°C	Type K t.c. conversion
183	Rear tube outer T5Q4	°C	Type K t.c. conversion

Table 5-8

DATA CHANNELS FOR AUTODATA NINE SYSTEM
(Sheet 2 of 3)

Channel	Parameter	Units	Conversion Factor
184	Rear tube lower T14Q1	°C	Type K t.c. conversion
185	Rear tube lower T14Q2	°C	Type K t.c. conversion
186	Rear tube lower T14Q3	°C	Type K t.c. conversion
187	Rear tube lower T14Q4	°C	Type K t.c. conversion
188	Working gas temperature - Q1	°C	Type K t.c. conversion
189	Working gas temperature - Q2	°C	Type K t.c. conversion
190	Working gas temperature - Q3	°C	Type K t.c. conversion
191	Working gas temperature - Q4	°C	Type K t.c. conversion
192	Cavity temp. circ. 1 top	°C	Type K t.c. conversion
193	Cavity temp. circ. 2 front	°C	Type K t.c. conversion
194	Cavity temp. circ. 3 bottom	°C	Type K t.c. conversion
195	Cavity temp. circ. 4 gen	°C	Type K t.c. conversion
196	Cavity temperature inner	°C	Type K t.c. conversion
197	Cavity temperature outer	°C	Type K t.c. conversion
198	Engine water in temperature	°C	Type K t.c. conversion
199	Engine water out temperature	°C	Type K t.c. conversion
200	Power, gen net USI	kW	(V - 2) 10
201	Engine pressure USI	MPa	4
202	H_2 pressure hi tank	MPa	4
203	H_2 pressure lo tank	MPa	4
204	Control temperature	°C	200
205	Engine speed	rpm	1000
206	Working gas mean temperature	°C	200
207	Working gas diff temperature	°C	200
208	Shutter status	On/off	1
209	Water pump status	On/off	1
210	Fan high status	On/off	1
211	Fan low status	On/off	1
212	Generator status	On/off	1
213	Voltage, gen/starter, pump/fan	V	60
214	Power, gen	kW	(V - 3) 5
215	Power, starter	kW	0.8
216	Power, pump	kW	0.8
217	Power, fan	kW	0.8

Table 5-8

DATA CHANNELS FOR AUTODATA NINE SYSTEM
(Sheet 3 of 3)

Channel	Parameter	Units	Conversion Factor
218	Current, generator	A	5
219	Current, starter	A	1
220	Power, tracking drive and motor	kW	0.8
221	Power, batt emer generator	W	25
222	VARS, tracking motor	kV·Ar	0.8
223	VARS, H_2 compressor	kV·Ar	1.2
224	Power, H_2 compressor	kW	1.2
225	Utility status	On/off	1
226	Spare	-	-
227	X alarm status	On/off	1
228	Y alarm status	On/off	1
229	Sun track status	On/off	1
230	Position A status	On/off	1
231	Position B status	On/off	1
232	Memtrack status	On/off	1
233	Insolation (ground mounted)	W/m^2	117.1
234	VARS, generator	kV·Ar	4
235	VARS, starter	kV·Ar	0.8
236	VARS, pump	kV·Ar	0.8
237	VARS, fan	kV·Ar	0.8
238	100 mV reference	mV	1
239	-	-	-

Table 5-9

DATA CHANNELS FOR IBM SYSTEM

Channel	Parameter	Units
C1	Reference temperature - DAS	
C2	Generator power - gross	kW
C3	Generator power - USI	kW
C4	Pump power	kW
C5	Fan power	kW
C6	Sun sensor photocell No. 1	mV
C7	Sun sensor photocell No. 2	mV
C8	Tracking power	kW
C9	Reference junction for slot 3	
C10	Ground-mounted insolation (Eppley)	W/m^2
C11	100-mV reference	mV
C12[a]	Dish-mounted insolation (Spectran)	W/m^2
	Dish-mounted insolation (Eppley)	W/m^2
C13	Engine pressure	MPa
C14	Working gas mean temperature	°C
C15	Working gas differential temperature	°C
C16	Ambient temperature	°C
C17	Wind speed A	mph
C18	Not connected	-
C19	Working gas temperature - quadrant 1	°C
C20	Working gas temperature - quadrant 2	°C
C21	Working gas temperature - quadrant 3	°C
C22	Working gas temperature - quadrant 4	°C
C23	Engine water temperature - in	°C
C24	Engine water temperature - out	°C
C25	Sun sensor photocell No. 3	mV
C26	Sun sensor photocell No. 4	mV
C27	Engine speed	rpm

[a]The Spectran pyrheliometer was connected until 10 January 1985. On that date, it was replaced with an Eppley pyrheliometer to permit better comparison with the ground-mounted Eppley pyrheliometer.

On a few occasions, it was obvious that the insolation meter mounted on the ground was not tracking the sun adequately, giving lower values for direct insolation than were actually present. This was due to one of two reasons. Either the initial alignment of the meter based on site latitude was done incorrectly or the meter was moved from one location to another without realignment. When operators at the site were made aware of the problem, they corrected the alignment.

While running a sunrise-to-sundown test on 23 March 1984, water beads were discovered on the inside of the sun sensor which caused tracking oscillation. An experiment was tried where the sun sensor housing was vented to the atmosphere to allow condensation removal. The experiment appeared to have been quite successful during the summer months, as no internal window condensation problems were observed.

Although venting the sun sensor resolved the initial condensate problem at the Rancho Mirage site for the summer months, water entering the sensor was a problem during rainy periods. Occasionally, the sun sensor filled up with water due to rainy weather and atmospheric moisture and had to be drained out by opening up the back of the sensor periodically. Long-term solutions suggested by Advanco include evacuation of the sensor after assembly and additional internal sensor volume space to contain a desiccant.

There was some uncertainty in the exact conversion factor to calculate dish tracker power. Some anomalies resulted from the fact that an electrical receptacle for field use permitted power drains attributable to tracking. Rewiring of the receptacle was needed to avoid the resulting uncertainty; however, this was not accomplished.

Several of the sensors hooked to the IBM/XT had questionable conversion factors, namely, the working-gas quadrant temperatures and the engine coolant temperatures. No resolution on this aspect was achieved. However, since the same information was available on the Autodata Nine system, this posed no major problem.

Electric power consumption by auxiliaries, such as coolant pump and fan power, tracking drives, and other support equipment, could also be monitored manually to determine these power requirements. Table 5-10 shows a listing of the electrical meters and other manual readings at the Vanguard I test site.

The calibration of the instrument sensors generally followed normal plant practices with the manufacturer's data providing the basic calibration. Review of the

Table 5-10

VANGUARD MANUAL DATA READINGS

Parameter	Units
H_2 tank valve pressure	lb
Reflectometer measurements on facets	%
Watt-hour meter, generator	W•h
Watt-hour meter, fan	W•h
Watt-hour meter, water pump	W•h
Watt-hour meter, starter	W•h
Watt-hour meter, support equipment	W•h
Watt-hour meter, tracking drives and motor	W•h
Watt-hour meter, batteries for emergency generator	W•h
Watt-hour meter, net Vanguard equipment usage	W•h
Watt-hour meter, net Vanguard equipment output	W•h
Watt-hour meter, trailer and operational usage	W•h
Watt-hour meter, H_2 compressor	W•h
Watt-hour meter, total station load	W•h

sensors being recorded by the data acquisition system indicated that performance parameters that required good measurement accuracy included gross electrical power output; all parasitic power requirements (tracker, pump, fan, starter, and hydrogen compressor); receiver temperatures; and direct insolation. End-to-end calibration (from sensor to data acquisition system) of the power and temperature parameters was performed by ETEC on two separate occasions. The first occurred during September 1984, and the final check was performed on the last day of operation before dish dismantling began in late July 1985. Calibration of selected input channels to the data acquisition system was performed by inputting a known millivolt signal and noting the corresponding temperature indication. Since the calibration equipment was on hand and the measurements could be performed with little additional effort, all volt-ampere-reactive (V•Ar) sensors also were calibrated for gross power output and parasitic power measurement. The V•Ar measurements are used in conjunction with the power measurements to calculate power factor. The resulting percent error in measuring power factor is usually only one-half or one-third as great as that of the V•Ar measurement. For example, at a power factor near 0.9, a 2% error in the V•Ar measurement results in only a 1% error in power factor. At a power factor near 0.8, a 2% error in the V•Ar measurement results in only a 0.7% error in power factor.

Calibration curves were prepared using data recorded on the Autodata Nine computer and, where applicable, on the IBM-XT. Figure 5-23 shows the relationship between a known power input and the power indicated on the data acquisition system for the generator power sensor on both calibration dates. Indicated power was obtained by using conversion factors supplied by the sensor manufacturers. There appeared to be no significant difference in the calibration over the 10-month interval between calibration checks. Figure 5-24 shows the relative error between the input power and the indicated power for the same sensor on both calibration dates. Less than 2% error is observed over the entire range, and the sensor appeared to be in better calibration on the later date.

Another typical parameter whose calibration was checked was pump auxiliary power. In this case, data from both the IBM and the Autodata Nine systems were available. Again, as shown in Figure 5-25, no significant difference between calibration dates or data acquisition systems is evident. Relative error between input power and indicated power is plotted in Figure 5-26, and although some variation is seen, all errors are again within 2%. Inputs on selected receiver thermocouple channels in the 100 to 800°C range showed agreement within less than 1°. Since the receiver thermocouples are in place and cannot be removed, the manufacturer's calibration was accepted for millivolt output as a function of temperature.

All power and V•Ar sensors showed excellent linearity over the measurement range and, with one exception, yielded very low percent error measurements. The single exception was the gross power measurement recorded by the IBM-XT, and the error was primarily due to the use of an offset value that was slightly in error. When a more appropriate offset value was substituted, the error was reduced to less than 1%.

A positive V•Ar value indicates a leading power factor, while a negative value indicates a lagging power factor. This can lead to some confusion in assigning plus or minus signs to the V•Ar error values for lagging power factors. For the V•Ar error curves, a plus sign was used if the indicated V•Ar value is larger in absolute value than the known V•Ar input, regardless of whether the V•Ar input was positive or negative (Figure 5-27); a minus sign was used if the indicated V•Ar value is smaller.

Control

Although there was only one dish/Stirling module at the test site, the control system that was installed was capable of handling a cluster of 32 dish/Stirling modules. As the 32-module cluster is the basic Vanguard building block for larger arrays, this permitted testing of all the basic hardware items in the control system.

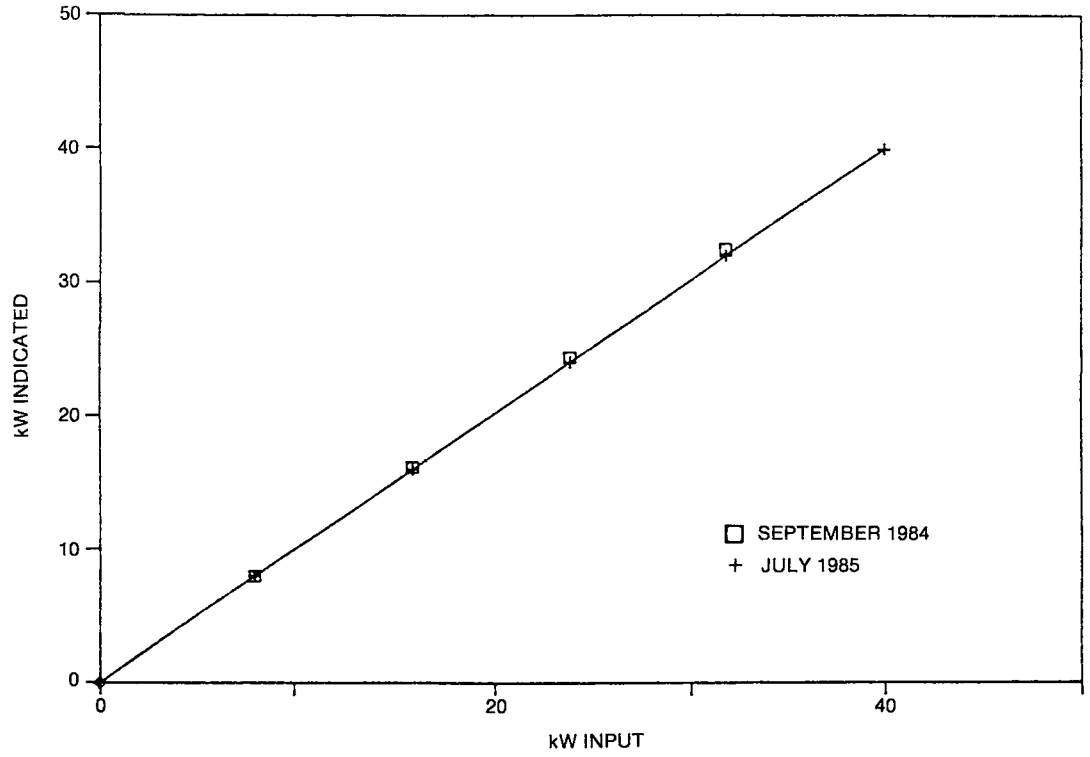

Figure 5-23. Calibration Curve for Generated Power on the Autodata Nine System

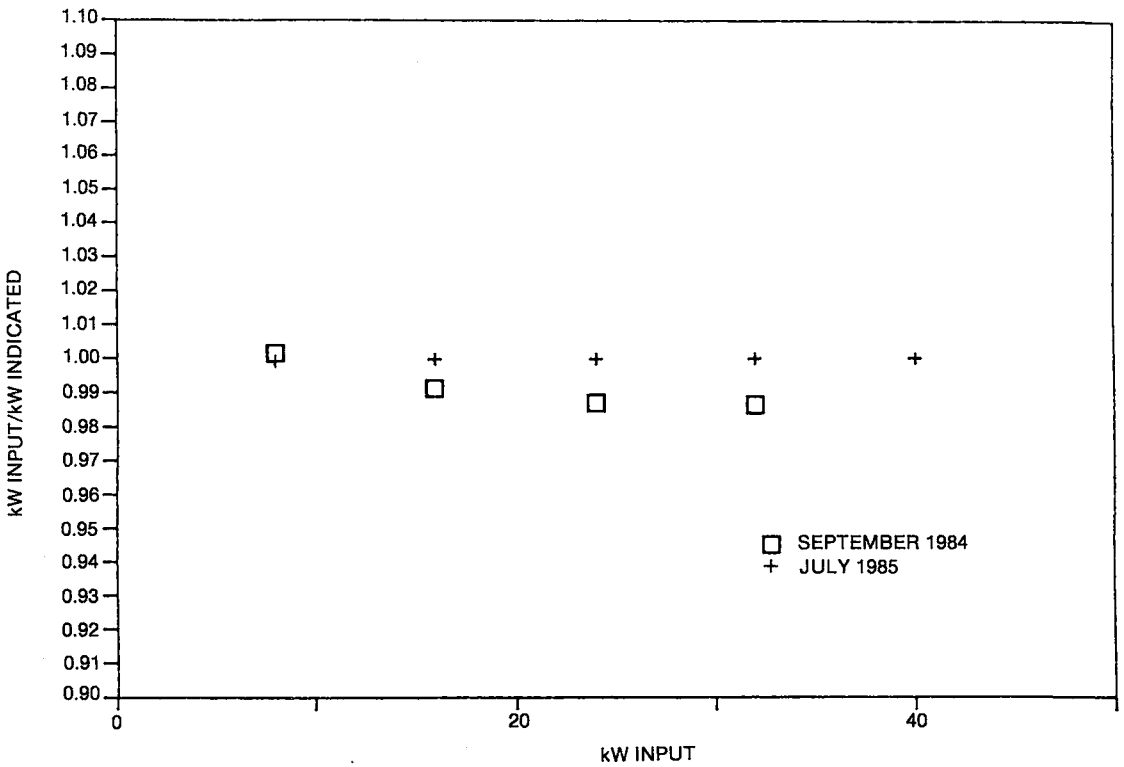

Figure 5-24. Accuracy of Calibration for Generated Power on the Autodata Nine System

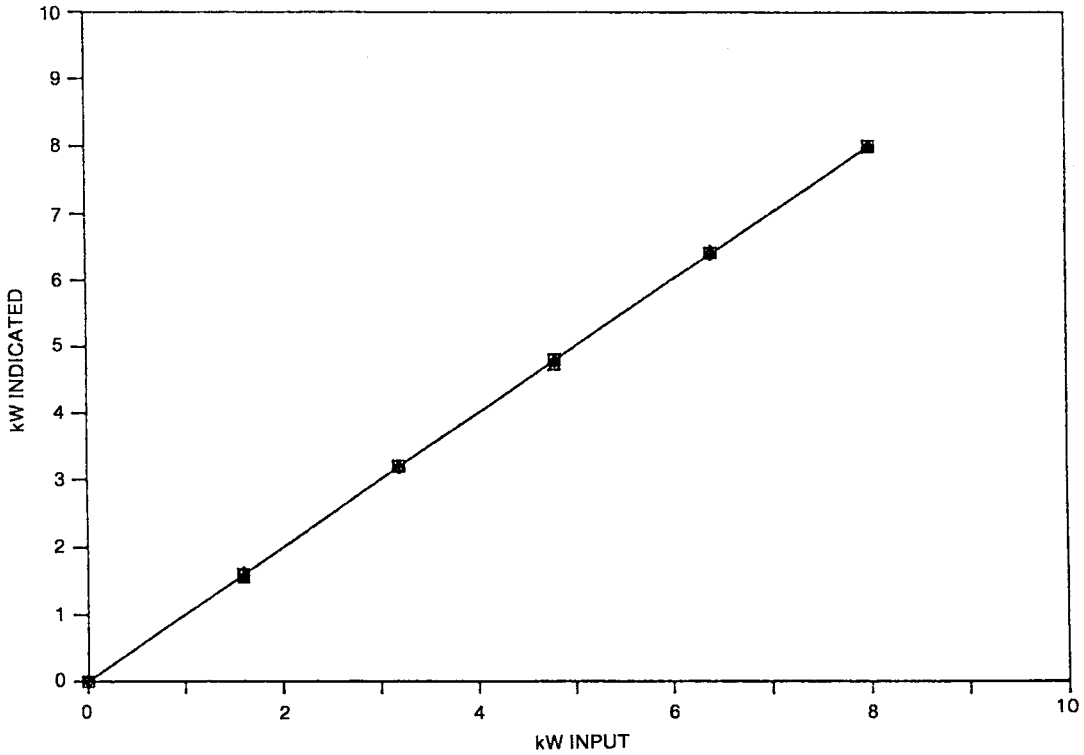

Figure 5-25. Calibration Curve for Pump Auxiliary Power on the IBM and Autodata Nine Systems

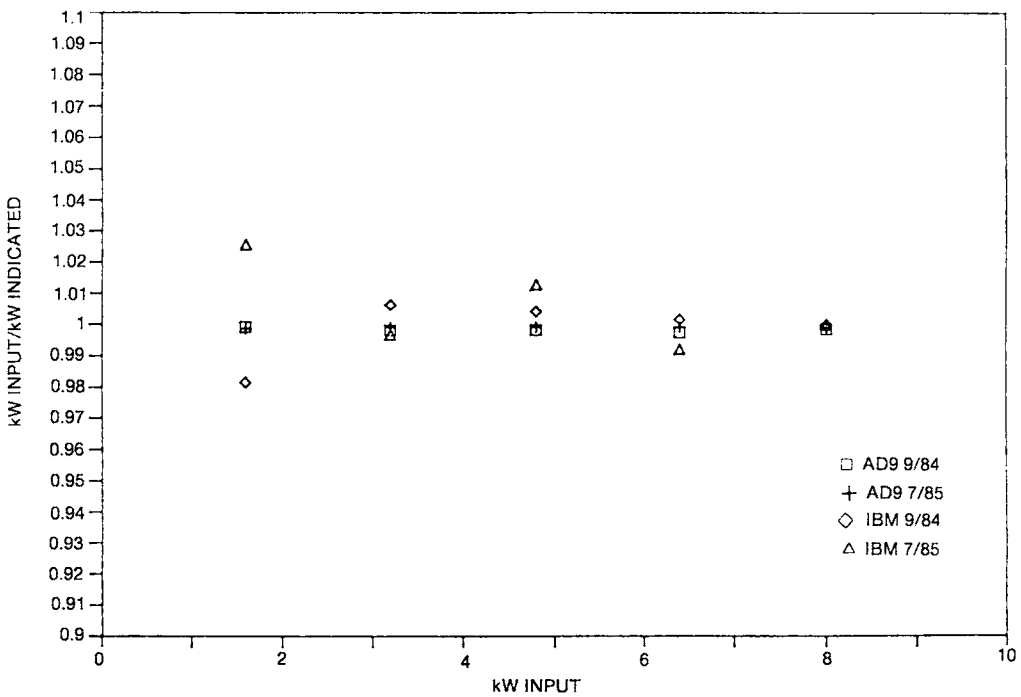

Figure 5-26. Accuracy of Calibration for Pump Auxiliary Power on the IBM and Autodata Nine Systems

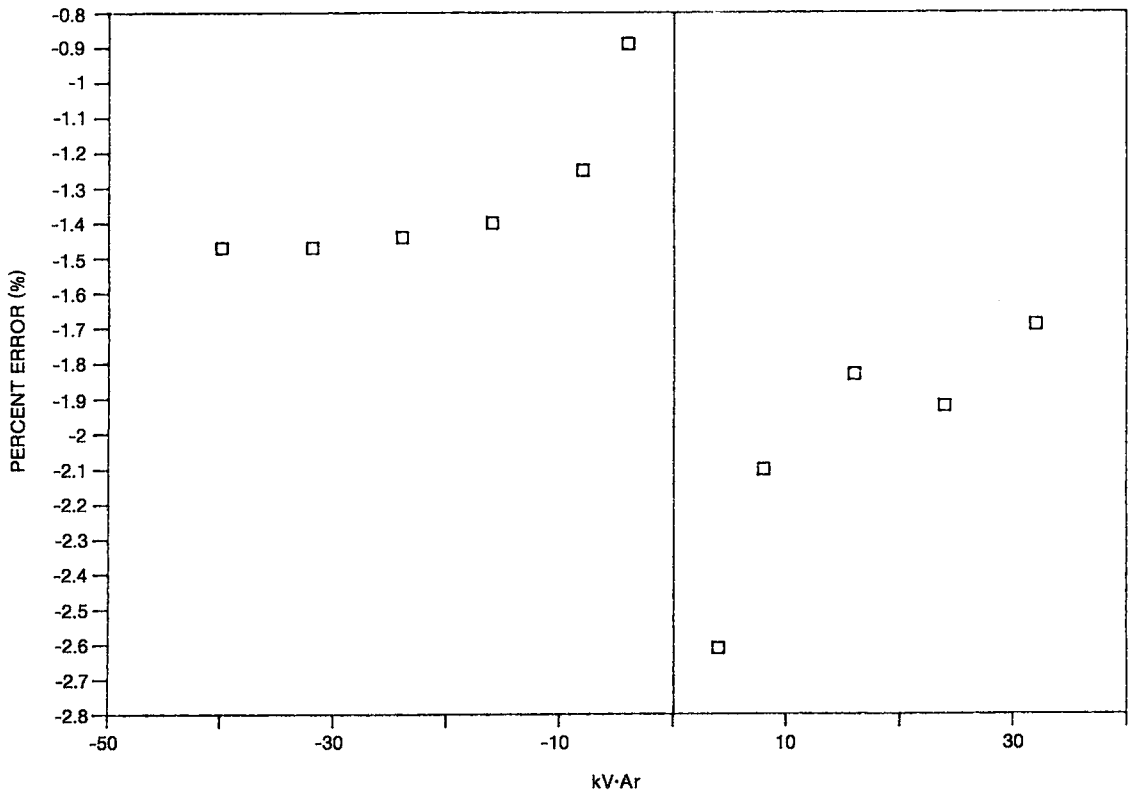

Figure 5-27. Percent Error of Calibration for Reactive Power on Autodata Nine System

Figure 5-28 shows a block diagram of the supervisory controls. The master concentrator control unit can control up to 32 individual modules. Each individual module contains its own subconcentrator control unit, which interfaces with the MCCU, the concentrator drive system, the Stirling engine control unit, and Advanco monitoring and metering. The Electrospace concentrator drive system controls the positioning of the dish so that it is aimed at the sun while tracking. The Stirling digital control unit controls the Stirling engine and interfaces with the subconcentrator control unit and the Onan system. The Onan system includes controls for the induction generator and the utility interface. The utility interface is between the dish/Stirling module and the utility grid.

The master concentrator control unit exercises supervisory control over each subconcentrator control unit, with a maximum interfacing capability of 32 subconcentrator control units. As there was only one subconcentrator control unit and dish/Stirling

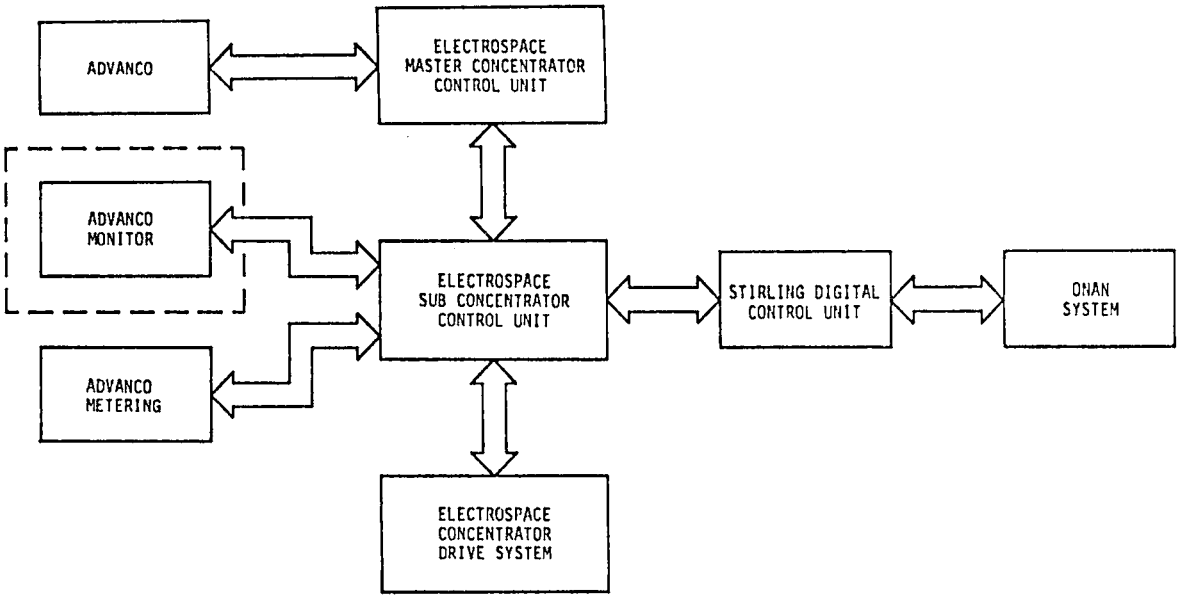

Figure 5-28. Supervisory Controls Block Diagram

module at the Santa Rosa test site, the master concentrator control unit actually interfaced with only one subconcentrator control unit.

The master concentrator control unit interfaces with each subconcentrator control unit over a separate RS 422 serial link. The balanced line characteristics allow this type of line to traverse long distances without detriment to data flow. This is essential for a 32-unit collector array due to its physical size.

Master Concentrator Control Unit. A diagram of the master concentrator control unit is shown in Figure 5-29. The master concentrator control unit consists of two main units: the CRT terminal/keyboard and the card cage unit. Each card for RS 422 input/output (I/O) can accommodate four modules, and thus eight cards would be required for 32 modules. The prototype master concentrator control unit utilizes only two cards for RS 422 I/O and hence had the capability of controlling eight subconcentrator control recorders.

Subconcentrator Control Unit. As shown in Figure 5-30, the subconcentrator control unit is capable of monitoring several points for limit and status purposes. The subconcentrator control unit is a Motorola 6809 microprocessor-based unit, which has extensive I/O capability. A keyboard permits the operator to enter, recall, and alter various parameters, select modes, and monitor status points. The 20-character

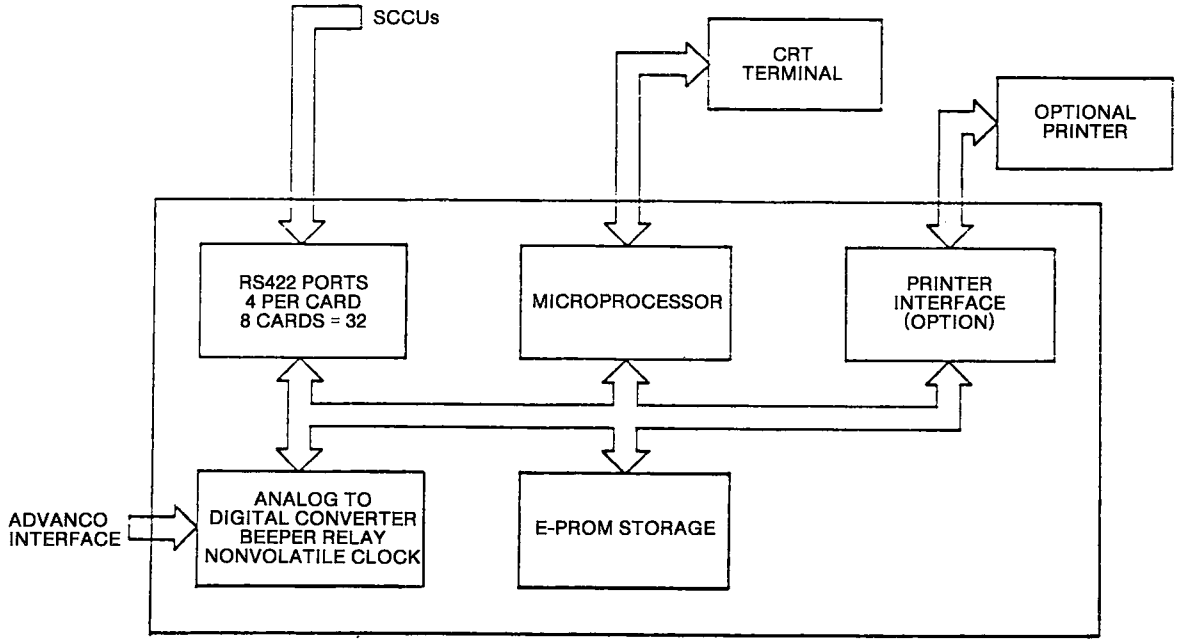

Figure 5-29. Master Concentrator Control Unit Diagram

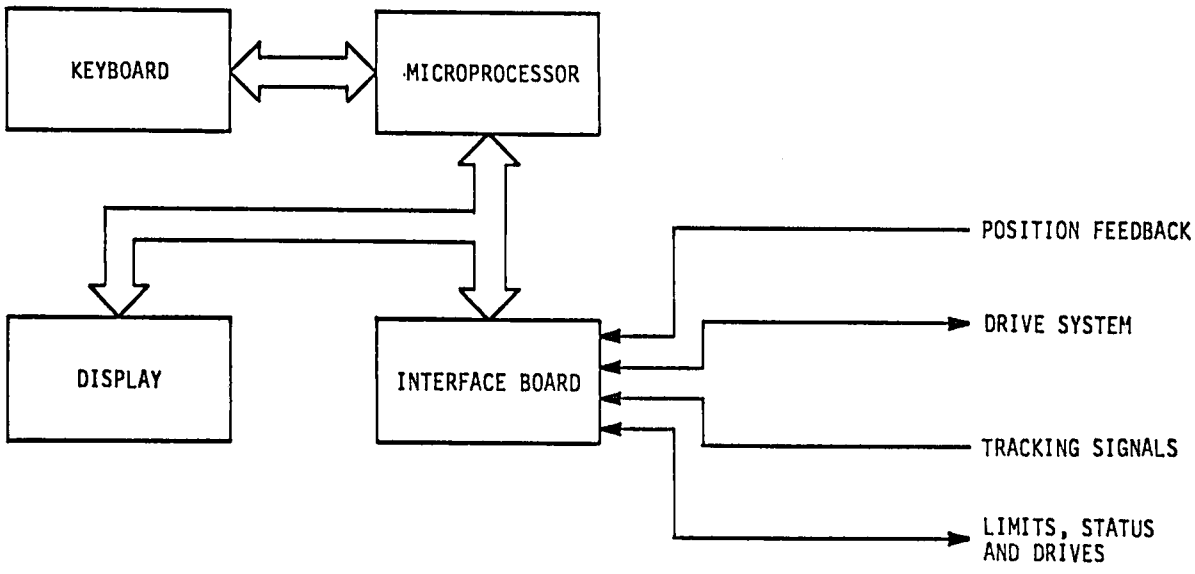

Figure 5-30. Subconcentrator Control Unit Diagram

display encompasses dual-axis position readout to 0.1° (azimuth and elevation) and present operation mode and may display alarms on operator request. The interface board is a versatile design that serves as a medium between the controller and all of its intersystem connections.

The subconcentrator control unit/Advanco interface is shown in Figure 5-31. The subconcentrator control unit monitors analog signals from an insolation meter and a power level meter. This information is gathered in the control room via the master concentrator control unit. In the event it becomes necessary to detrack the parabolic dish concentrator, the subconcentrator control unit provides a contact closure for drive system disengagement.

Software-controlled relays in the subconcentrator control unit provide contact closures to indicate status of the system on the Advanco monitor. However, that presence of the Advanco monitor is not necessary for normal operation of the subconcentrator control unit.

The subconcentrator control unit interfaces with the parabolic dish concentrator to sense the position of the concentrator and provide command signals to the dual-axis drive motor to maintain alignment with the sun. A block diagram of the subconcentrator control unit drive system is shown in Figure 5-32.

A dual-axis photovoltaic sun sensor located on the concentrator can continuously report the error voltage levels that are representative of how well the concentrator is aligned with the sun. These voltage levels are processed by software to arrive at a position command to compensate for concentrator misalignment with the sun.

Precision synchros are located on each of the two axes of rotation to provide dual-axis position feedback to the subconcentrator control unit. This feedback is summed with the position command to derive the rate command that is issued to the drive system. The drive system utilizes the emf to determine the rate feedback. This feedback is summed with the rate demand to arrive at a current demand. Motor current feedback is summed with the current command to derive a firing command for the silicon-controlled rectifier bridge. The silicon-controller rectifier bridge then delivers current to the azimuth and/or skewed axis dc motors. The subconcentrator control unit can also monitor limit positions and status of the concentrator.

The Stirling engine is monitored by the Stirling digital control box. The subconcentrator control unit interfaces with the Stirling digital control box are shown in

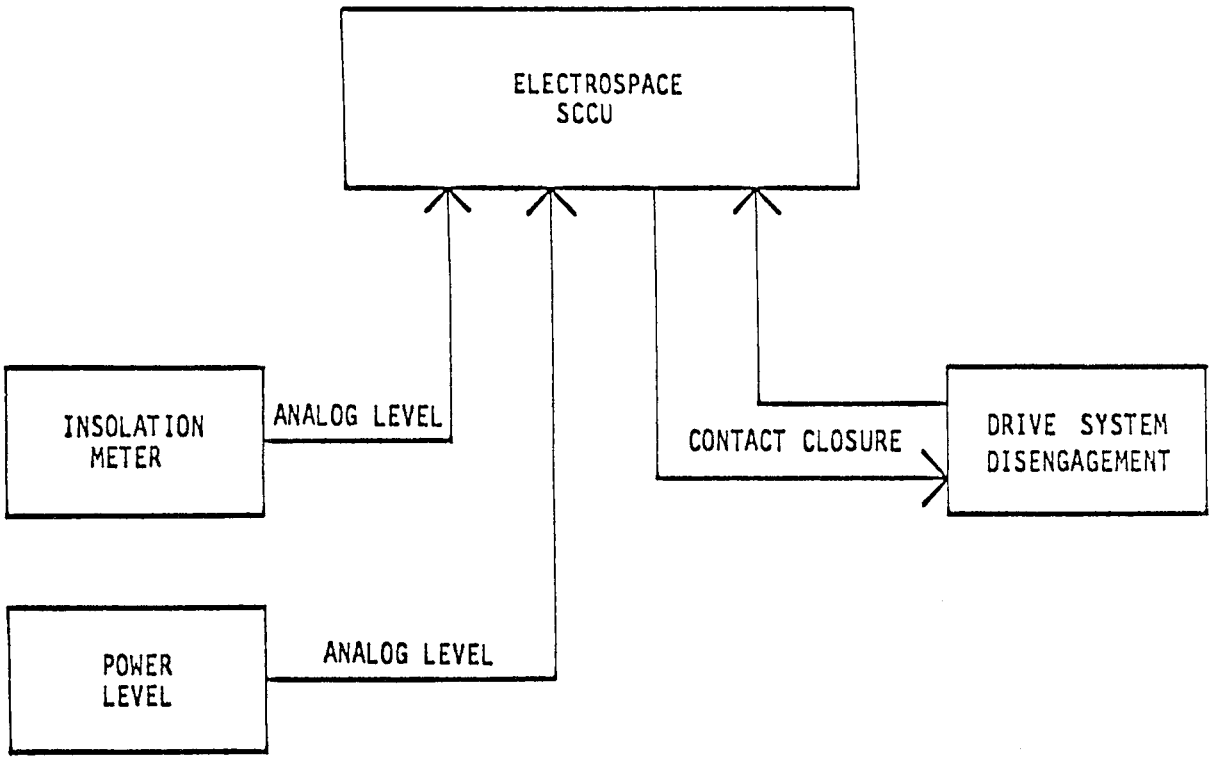

Figure 5-31. Advanco/Subconcentrator Control Unit Interface

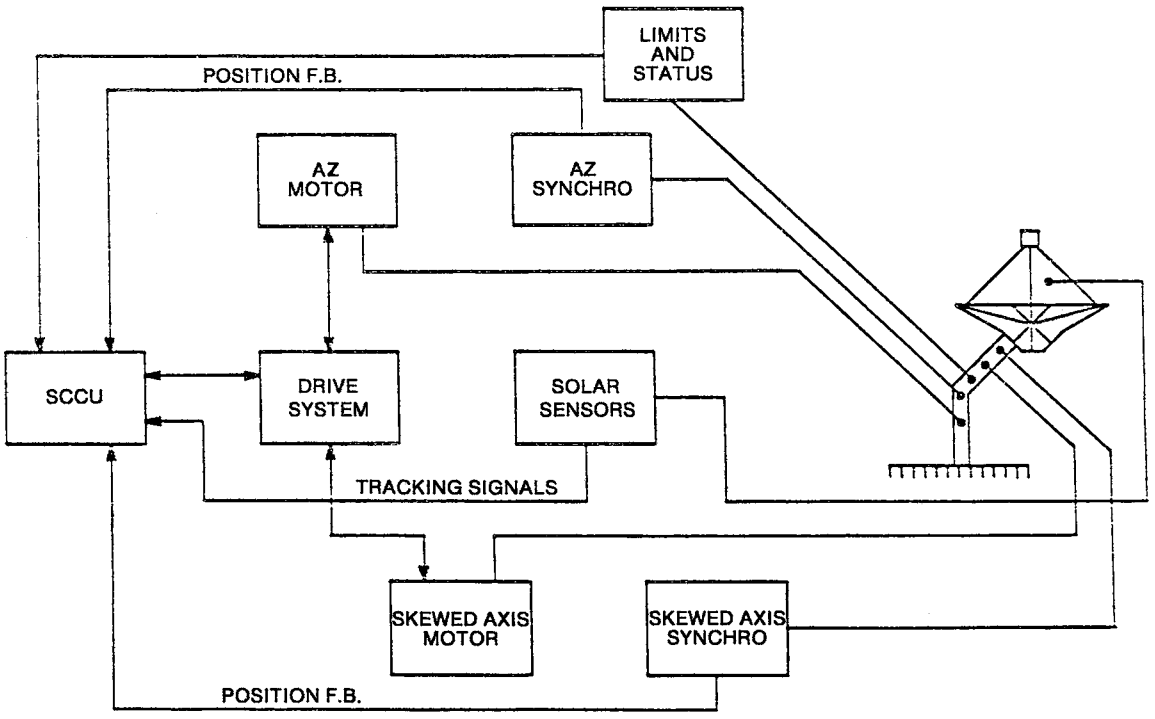

Figure 5-32. Subconcentrator Control Unit Drive System Diagram

Figure 5-33. This interface has two "handshake" routines. One is an enable (the WAKE-UP line) signal sent from the subconcentrator control unit to the Stirling digital control box to determine if any condition exists in the Stirling engine system or the generator system that would cause a detrack of the concentrator. Replies on the detrack status are sent from the Stirling digital control box to the subconcentrator control unit via the TRACK line. Therefore, if a condition should occur in the Stirling engine system or generator system that necessitated a detrack, the "handshake" would be broken, and the subconcentrator control unit would signal a command to detrack the concentrator. The other "handshake" concerns the possible grid-voltage-dip problem if 32 engines are started simultaneously. The engine start handshake was not required at the Santa Rosa test site because only one module was employed.

Several minor subconcentrator control problems occurred during the 18-month period of operation of the tracking control system. These items are discussed below. Recommendations by site personnel of hardware and software improvements are also included.

During the sun track mode, when the dish is on sun with adequate insolation to activate the sun sensor, an ephemeral offset table is developed. The values for this table are calculated at every degree of elevation by comparing synchro positions with calculated ephemeral data (based on longitude, latitude, and time of day). The differences are recorded in the table. Values generated in this table have on occasion been of sufficient magnitude with opposing signs to make the dish go into an oscillation mode driven by the drive motors. New tracking programmable read-only memories were requested from Electrospace Systems, Inc., to correct the problem; however, when tested, the new programmable read-only memories were also faulty, causing the subconcentrator control unit display to go blank. This problem was subsequently corrected, but the programmable read-only memories were a repeat source of problems throughout the test period.

There were three or four random occurrences when the dish would not drive up in the skewed axis out of the preferred stowage position facing north. These "lockups" have been random, with no apparent cause. The only way to get the dish out of this lockup mode has been to activate the gravity slew system. Once the dish has been driven up a few degrees by the gravity slew system, it operates well in all positions.

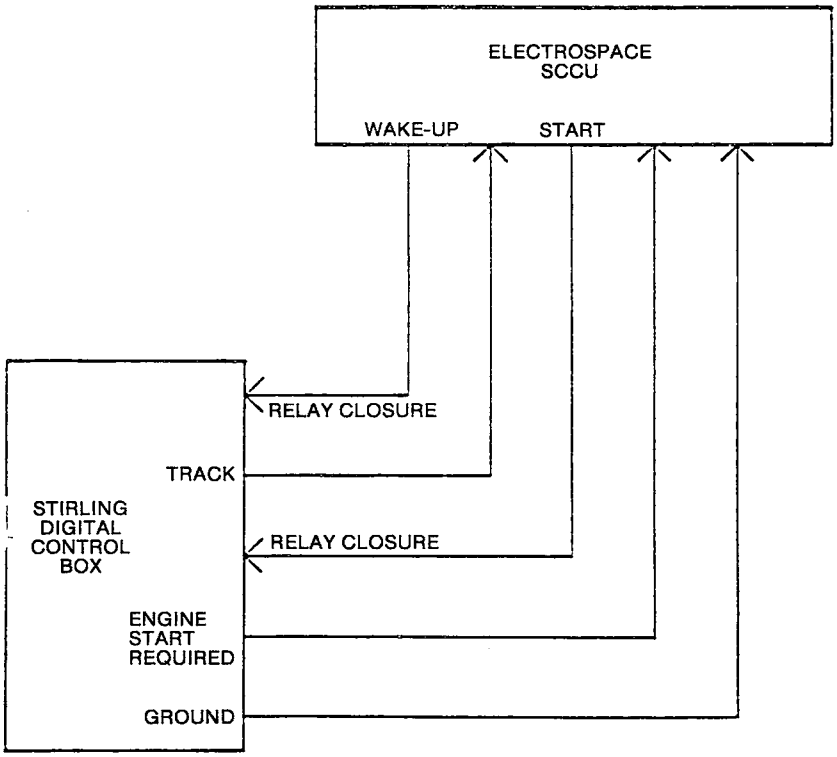

Figure 5-33. Stirling Engine/Subconcentrator Control Unit Interface

When operating the dish at small angles above the horizon at sunrise, the dish was on various occasions driven out of stow counterclockwise in the azimuth axis only, across the sun, with the off-axis rays passing across the power conversion unit and tetrapods. The dish then stopped in the azimuth axis when it was lined up on the "gangplank" and driven up in the skewed axis onto the sun. There was no proximity alert when this occurred. The solution to this problem was to come on sun from above.

At low-elevation sun angles (i.e., 15° elevation or less), the sun's apparent image position and the sun's ephemeral calculated position differ due to refraction through the earth's atmosphere. Also, the insolation level is lower at these elevation angles as compared with midday elevations. A typical value at which the sun track threshold (the minimum insolation level required to sun track) is set during midday elevations is 20. At lower sun track threshold values, the dish will track bright clouds, which results in an alarm based on the ephemeric/track error (limit value data comparison limit between ephemeral and tracking data). Low-elevation sun

angles can result in image offsets. The solution is a software improvement allowing programmable sun track threshold settings.

The characteristics of the exocentric gimbal mechanism make the dish susceptible to motor-induced oscillations. The drive motors driving back and forth could shake the dish and pedestal out of manufacturing and installation tolerances. Software needs to be developed that will measure and limit the rate of motor-driven direction changes.

Ephemeral data are calculated in 1/2-hour increments for sun elevations above 0°. Often the first value that is calculated greater than zero is as high as 5°. The dish will not track but waits in position A until the time has reached the first 1/2-hour value greater than zero.

The test site has an unobstructed view to the east and a field of palm trees to the west. The elevation minimum threshold parameter is used to restrict tracking that would result in the dish being partially shaded. One elevation minimum threshold was designed into the control system, but at least two would have been needed to completely compensate for the different sunrise and sunset elevations.

When the subconcentrator control was reset (turned off and back on), it sometimes changed various parameters. Advanco personnel recommend the use of a small, nonvolatile memory to eliminate the need for reentering these values.

Due to design changes in the locking pawl that were made after the final design of the subconcentrator control, additional logic relays were incorporated into a separate weatherproof box inside the gimbal. The additional expense of the relays and box should be eliminated by incorporating this logic in the subconcentrator control software. Light-emitting diodes on the subconcentrator control that indicate when the locking pawls are engaged or retracted would be useful displays.

Stirling Engine Control System. The control system for the Stirling engine was designed by United Stirling AB of Sweden. It features a digital control system with a USAB-designed microcomputer based on a Texas Instrument 9995 microprocessor (Figure 5-34). Fully automatic operation is based on control of receiver tube temperature by adjusting the hydrogen gas pressure in the engine (Figure 5-35). Control is provided for start/stop, cloud passages, and routine operation. Several safeguard sensors serve as interlocks to permit the parabolic dish to track; if preset operating limits are exceeded, the guard sensors will direct the parabolic dish to detrack.

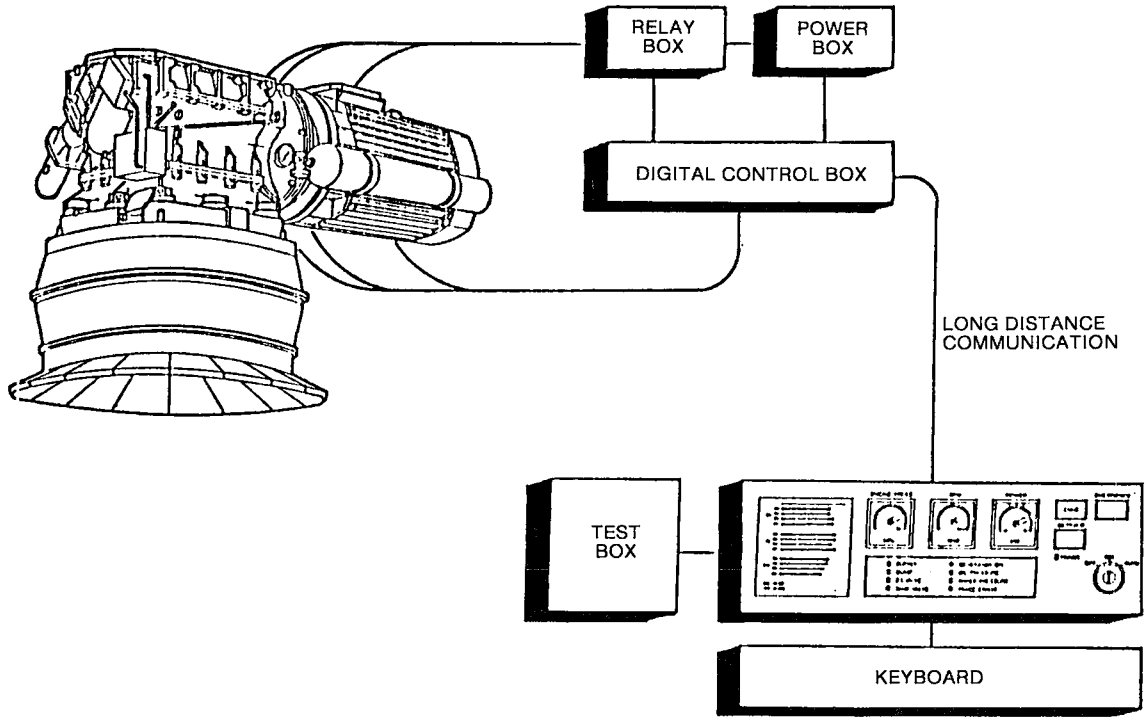

Figure 5-34. United Stirling (USAB) Digital Control System Layout

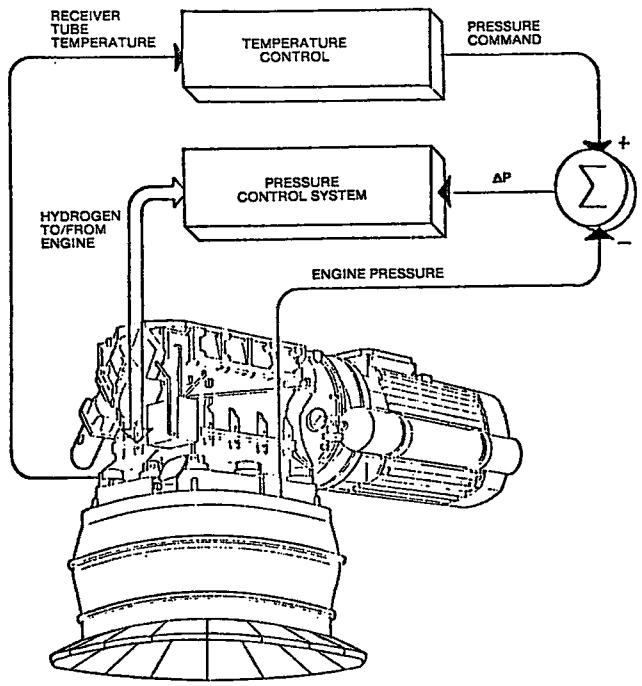

Figure 5-35. Block Diagram for United Stirling (USAB) Control System for Grid Connection

The Stirling engine in the Vanguard module operates at a control point setting of approximately 720°C. Thermocouple sensors located within the solar receiver sense the receiver tube temperature. A rise or fall in temperature about the control point signals the engine control systems to increase or decrease, respectively, the pressure of the hydrogen working fluid.

On startup, a command is sent to start the engine when the receiver temperature reaches 400°C. Temperatures in excess of the limit set for operation of the receiver result in a signal to detrack the dish. Likewise, hydrogen pressures in excess of the set operating conditions cause a signal that detracks the dish. Engine control logics for operation of the module are summarized in Figure 5-36. An rpm sensor on the generator shaft generates signals to control a contactor that connects the generator to the power grid. At less than 1800 rpm, this contactor remains open; it then closes when the rpm is equal to or greater than 1800 rpm. There is also overspeed protection; if the rpm exceeds 1840, it must go below 1830 rpm to reclose the contactor. The engine water-coolant temperature sensor generates signals that control the speed of the heat rejection unit fan; in case of temperatures in excess of prescribed operating limits, a command is sent to detrack the dish. Similarly, too high an oil temperature will execute a dish detrack signal. The module is also provided with undervoltage protection that opens a line contactor if the line voltage drops below 70% of nominal. The control system is provided with an operator discretionary emergency or "panic" switch; this switch operates a short-circuiting valve and also sends a signal for the dish to detrack.

Several problems occurred in the integration of the various control schemes for the concentrator and the Stirling engine. One problem noticed early in the operational test period was an apparent contradiction in when the shutter plates were to be closed.

The Electrospace control system was set up to open the plates whenever the insolation was above a threshold insolation value. Thus, when the sun went behind a cloud and the subconcentrator control unit went into ephemeris tracking mode, it issued a command to close the shutter plates. However, the Stirling controller was programmed to assume that the plates are supposed to be open at all times during daylight hours, and it interpreted a close shutter command as an indication of a system fault. It then responded by going into the "Detrack" state, causing the module to shut down. Thus, to achieve full automatic operation, a change was necessary in either the Electrospace or the Stirling controllers, since the existing

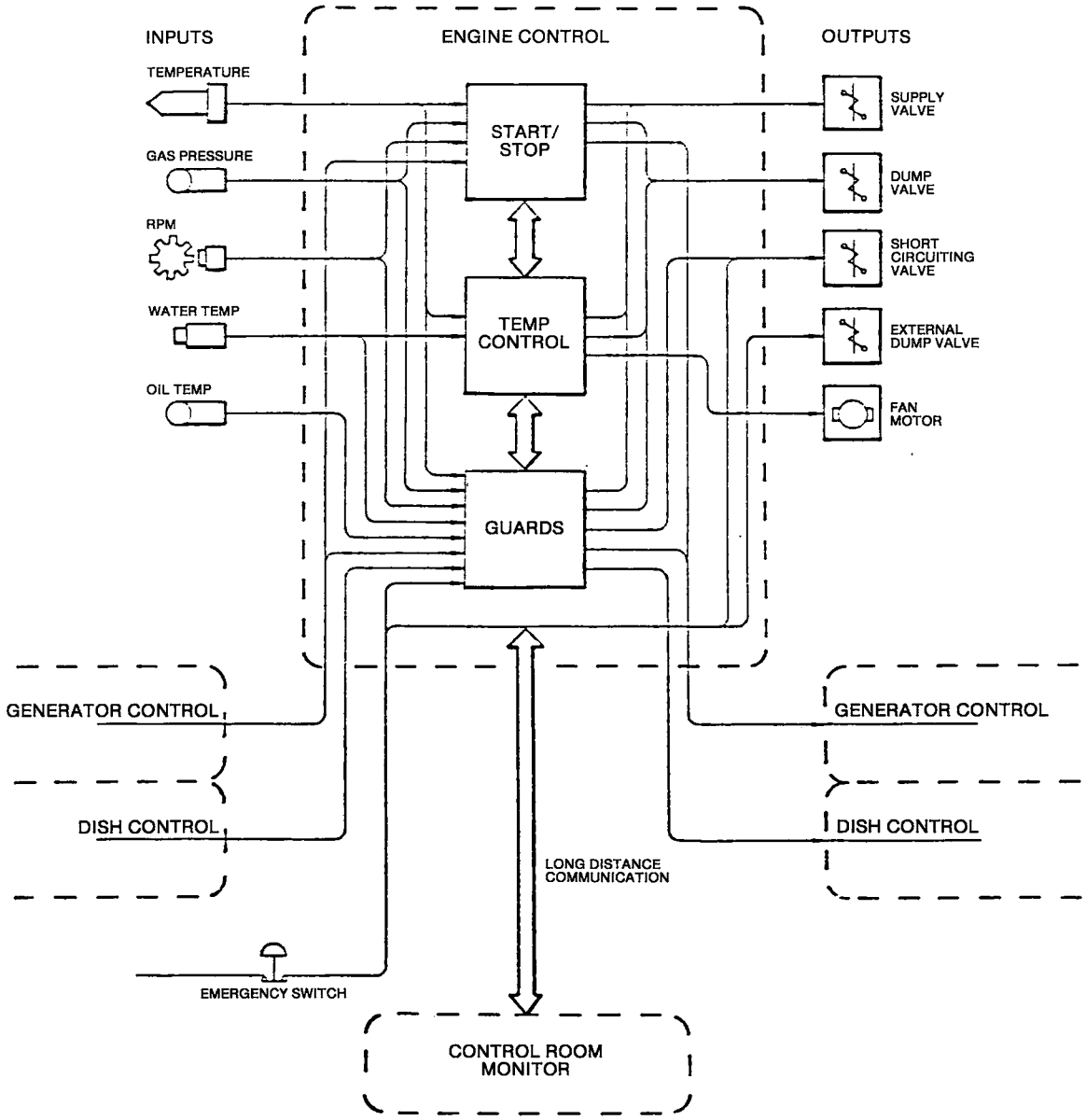

Figure 5-36. Vanguard Engine Control Logic

configuration caused the system to shut down whenever a cloud passed. Electrospace indicated that their system could not be programmed from the current configuration without extensive modification. Temporary operation of the module on the fully automatic mode was achieved by installation of a jumper wire from the Stirling controller "TRACK" relay to the "OPEN PLATES" relay. Later, however, United Stirling provided a new controller program IC with the necessary changes.

The electronic control system was overhauled, spare boards for the electronics were set up, and new programmable read-only memories for the electronics were installed, having new logic that would avoid the earlier problems with detracks from the water-cooled plate signals.

DATA ACQUISITION SYSTEM

In the Vanguard project, a unique opportunity arose for gathering data both by a more traditional computer-type data acquisition system and by a separate IBM personal computer-based subsystem. The experience gained from this subsystem and the problems and features on the subsystem will be discussed in this section.

The first DAS installed and operated onsite was the Acurex Corporation Autodata Nine DAS. The Autodata Nine was coupled to a Kennedy Model 1629 serial communications interface, which interfaced with a Kennedy Model 9800 reel-to-reel tape system. The Autodata Nine had been used at the Jet Propulsion Laboratory (JPL) during previous tests by United Stirling, so JPL personnel, who installed the unit at the Vanguard test site, were very familiar with the requirements of the Stirling unit. Eighty-two channels of data were monitored at 1-minute intervals and stored on the tape. One tape, which is 21.6 cm (8-1/2 in.) in diameter and uses 1.3-cm-wide (1/2-in.) magnetic tape, is capable of storing about 3 days of data.

The only onsite data immediately available from the Autodata Nine was a paper tape printout of all 82 channels. To determine performance, the raw voltage printouts on the tape had to be multiplied by conversion factors using a hand calculator. No integrated power or insolation calculations were practical, as this would have required the paper tape printer to operate continuously, resulting in a daily tape over 300 m (1000 ft) long.

Once the magnetic tapes were filled, they were initially sent to a mainframe computer system at JPL for reduction. As had been done in previous interpretations of

United Stirling solar engine test data, only plots of parameter values versus time were made. After May 1984, JPL was no longer able to provide this data reduction service.

The Energy Technology Engineering Center (ETEC), operating under subcontract to EPRI, offered to perform special analysis on the tape data, such as integration of parameters and special plots (e.g., power versus insolation). ETEC received all prior tapes from JPL. However, the time delay in accumulating data on a reel of tape, sending it to be analyzed, and then returning the resulting plot to the test site remained a distinct disadvantage. Furthermore, the raw data on tape are useful only to large institutions having reel-to-reel data tape systems and associated computer interface.

In addition to these disadvantages, the Autodata Nine data acquisition system was not automatically activated. Onsite personnel were required to turn the data unit on manually in the morning and then turn it off in the evening to conserve tape. Although the system could have been run continuously for 24 hours, the capacity of the reel would have been halved, requiring twice as many tapes per month. Also, collection of insolation data over the weekend was not desirable with the Autodata Nine tape system, since this would have required either leaving the unit on continuously or having personnel work weekends. On several occasions, the reel of tape in the tape recorder system ran out during testing. Operating personnel were not aware of this, since no alarm was connected to the end of tape marker, and test data were lost during such times.

The advantages of the Autodata Nine system were that (1) all thermocouples from the engine and receiver were connected; (2) the sampling rate was short enough to allow good transient analysis; and (3) once the software was developed to process the data, all plots, integration, and analysis of the data could be completed in a matter of minutes.

In June 1984, a Keithley DAS, a small, low-cost data acquisition component designed by Data Acquisition Systems, Inc., was put into operation onsite. The Keithley DAS was designed to work with a similar number of data channels as the Autodata Nine; however, only 27 data channels were connected. Instead of interfacing with a tape recorder system such as the Kennedy system, it interfaced with an IBM-XT personal computer.

The advantages of the Keithley DAS coupled with an IBM-XT included the capability of storing the data on a more convenient medium (floppy diskettes) and the ability to reduce data and display it onsite with a low-cost personal computer system using widely available software. Further advantages were the operator-free startup and operation of the DAS and the enhanced possibility of disseminating data to other locations (e.g., utilities, other solar energy companies, private individuals), as the only requirement was that the recipient have a compatible personal computer with modem. Problems have occurred with this system also, and some days' data have been accidentally erased during power failures.

Though many of the Autodata Nine tapes had format errors or were otherwise difficult to read due to operating errors onsite, eventually, all 70 of the tapes received, comprising the entire 18-month test program, were reduced. All of these data were available in evaluating the performance of the module, and where data were lacking, information was available from the IBM-XT disks for the period after June 1984.

To provide quick onsite analysis of the IBM-XT discs, EPRI provided Advanco with an IBM-PC, a Hewlett-Packard six-pen color plotter, and an Epson printer. This additional equipment permitted Advanco to acquire data with the Keithly DAS and IBM-XT combination during the day and simultaneously reduce previously acquired data with the IBM-PC and the printer or plotter. Before acquiring the EPRI-loaned equipment, it was necessary for Advanco personnel to stay at the test site after the end of the working day to reduce data.

Section 6

ASSESSMENT OF STATUS AND FUTURE POTENTIAL

In this section, the authors present an assessment of the current status and future potential of the parabolic dish/Stirling engine system for utilizing solar energy to generate electricity. The assessment is based upon insights gained from monitoring performance of the Vanguard module during operational testing, and from numerous discussions with participants and other interested parties.

PRESENT STATUS

A thumb-nail description of the present status of the Vanguard dish/Stirling module is that the module has been very successful from a technical viewpoint in the conversion of solar energy into electricity, but is not economically viable based upon the present low cost of oil and related fossil energy sources. Many impressive performance characteristics were demonstrated during the 18-month period of operational testing, however, both the operating and maintenance costs and the capital costs were high. Also, considerably more operating data must be acquired before reliable estimates can be made of such important economic factors as receiver life, time between engine overhauls, and mirror life.

The remainder of this assessment section will be devoted to topics related to the future economic potential of the dish/Stirling module.

McDONNELL-DOUGLAS/USAB DISH/STIRLING SYSTEM

McDonnell-Douglas Corporation and United Stirling AB of Sweden are engaged in a cooperative endeavor to jointly develop, manufacture, and market the dish/Stirling solar-powered electric generating plant. The concentrators are designed and manufactured by McDonnell-Douglas Corporation, and each has a mirror area of 91 square meters, which is approximately the same as that for Vanguard (86.7 square meters). The solar power conversion unit is designed and manufactured by United Stirling AB of Malmo, Sweden, and the Stirling engine is a derivative of their Mark 4-95 engine. The module has a nominal rating of 25 kilowatts electrical.

McDonnell-Douglas/USAB planned activities include the fabrication and assembly of eight modules that will be tested at selected sites, including the Huntington Beach facility of McDonnell-Douglas. Testing of these modules should generate additional data and insights on mirror reflectivity and life, receiver absorptivity and life, and maintenance and overhaul requirements of the United Stirling 4-95 engine and its derivatives.

MIRROR REFLECTIVITY AND LIFE

The mirrors in a parabolic dish are arranged to collect and concentrate the low-level solar radiation to thermal power levels which are practical and efficient for electrical power generation. The amount of energy concentrated for a specific mirror area is proportional to the reflectivity, which for Solar One mirrors at Barstow and also for the Vanguard mirrors has been about 93% in the clean, as-received condition. Outdoor exposure subjects the mirrors to environmental conditions which can quickly degrade the reflectance. Losses as great as 25% have been observed in some cases for mirrors after only a few weeks of exposure. Because of the decrease in efficiency of the dish/Stirling system as power level is decreased, more than a 25% reduction in electrical power output can result.

The optics of a parabolic dish can affect the ability to concentrate the radiant energy within the receiver aperture and also the uniformity of energy distribution on the receiver tubes. Nonuniform distribution between the four quadrants of the receiver affects the distribution of power to the four corresponding cylinders and this can affect performance and life of the Stirling engine. Should mirror delamination occur, this drastically affects the focusing of reflected energy.

The rate and amount of degradation of reflectivity will vary with site location and with time of day and year. Moreover, the amount of degradation is affected by mirror orientation with respect to horizontal and by height above ground level. The preferred stow orientation to have the least change in reflectivity is downward, with mirrors facing the ground. The least preferred orientation is with the mirrors inverted to face the sky, a difference of 180°. Generally, the drop in reflectivity decreases as the stowage altitude angle decreases, so that stowage in the vertical north-facing position has an intermediate effect on reflectivity between the down-facing and zenith-facing positions. Due to its design, the Vanguard concentrator could not be stored in a down-facing position. However, a number of other concentrators, including the McDonnell-Douglas concentrator, can be stored in this position.

The thrust of these comments on reflectivity has been that the operators of a dish/Stirling system must be concerned not only by the amount of degradation of reflectivity, but also by the uniformity of degradation. This influences the frequency of washing or rinsing of mirrors, which in turn can have a significant impact on operating and maintenance costs.

STIRLING ENGINE LIFE AND MAINTENANCE REQUIREMENTS

United Stirling AB has estimated the life and maintenance requirements for their solar Stirling engine and receiver. The following four applicable paragraphs are quoted from a United Stirling AB letter on this subject, addressed to the Jet Propulsion Laboratory, dated December 19, 1984, from S. Holgersson, United Stirling AB to J. Stearns, Jet Propulsion Laboratory. This letter is Appendix A of a report entitled "Stirling Engine Alternatives for the Terrestrial Solar Application" by J. Stearns, DOE/JPL-1060-91, dated October 1985.

> "The basic parameters to be used for the O & M evaluation are life for the complete engine, heater life, piston ring and piston rod seal life.
>
> The design life for the mature complete engine is 20 years with a yearly operation of 2500-3000 hours per year. The 20 year life includes two major overhauls, where most of the moving parts are exchanged, however, the basic structural components can be used over the whole life period.
>
> The design life for the mature receiver is 16000 hours, which will mean an exchange of heater two times over the system life.
>
> The life for piston rings and piston rod seals is 3000-4000 hours, which will result in a periodic service once a year for exchange of these components."

In the following analysis, when using United Stirling quotes on ranges for design life, the most optimistic estimate will be selected (i.e., the longest design life). Thus, engine life will be assumed as 20 years at 3,000 hours per year or 60,000 operating hours, rather than 2,500 hours per year or only 50,000 operating hours. To match this, this design life of the receiver will be assumed as 20,000 hours, to give an exchange of heater two times over the 20-year system life. Life

for piston rings and seals will be assumed as 4,000 hours, to give a total of 15 sets of piston rings and seals during 60,000 hours of operation.

While net power generation of the Vanguard module occasionally reached 23 kilowatts during operational testing, the average net generation of electricity was only about 15 kilowatt-hours per operating hour. Thus, during a 20-year system life, the module would generate (60,000 hours) (15 kilowatt-hours/hour) or 900,000 kilowatt-hours.

Assuming a revenue of 10 cents per kilowatt-hour, during a 20-year period, the gross revenues would be (900,000 kilowatt-hours) ($0.10 per kilowatt-hour) or $90,000. The $90,000 would have to pay for all capital costs and operating and maintenance expenses, and the remainder would need to return a reasonable profit to the investor. Capital costs would include those for the parabolic dish concentrator, Stirling engine, power conversion unit, instrumentation and control, and land. Operating and maintenance costs would include the material and labor costs involved in overhauling the engine twice, replacing the receiver twice, and replacing piston rings and seals 14 times, as well as other miscellaneous costs such as periodic washing of mirrors, and periodic addition of gaseous hydrogen. This presents a real challenge to the development of a cost-effective dish/Stirling module competitive with other conventional, electrical energy-producing systems.

TIME-OF-DAY POWER GENERATION

As in any solar-based technology, input of solar energy from a dish/Stirling module will commence after sunrise on a clear day and will increase to a peak value at solar noon, and then will decrease during the afternoon and end at sunset. Since the output of electrical energy is proportional to the input of solar energy, electrical output will tend to follow the same pattern, as long as the insolation level remains above a minimum threshold; below this threshold, no electrical output is produced. This variation pattern makes it impossible for a solar-only power plant to operate around the clock as a base-loaded power plant. Instead, the role of a solar-only plant appears to be that of a peaking plant to supply electricity during the daylight hours.

It then becomes instructive to examine the rate structure for a plant operating in this mode. The Power Purchase Agreement of the Southern California Edison Company for cogenerators and small power producers offers a concrete example (Table 6-1).

Table 6-1

SUMMARY OF TIME-DIFFERENTIATED PAYMENTS
(cents per kilowatt-hour)

Summer Payments (Late April to Late October)

	On-Peak (1 p.m.-7 p.m.)	Mid-Peak (9 a.m.-1 p.m. and 7 p.m.-11.p.m.)	Off-Peak (All Other Hours)
Avoided Energy Payment	6.27	4.85	4.16
Avoided Capacity	10.33	0.12	0.05
Total Payment in Summer	16.60	4.97	4.21

Winter Payments (Late October to Late April)

	On-Peak (5 p.m.-10 p.m.)	Mid-Peak (8 a.m.-5 p.m.)	Off-Peak (All Other Hours)
Avoided Energy Payment	5.92	4.82	4.16
Avoided Capacity Payment	2.47	0.55	0.07
Total Payment in Winter	8.39	5.37	4.23

The payment schedule in this table shows that electricity produced during the six-month "summer" period in the afternoon hours (from 1:00 to 7:00 p.m.) would earn 3.4 times the revenue produced in the mid-peak morning hours (from 9:00 a.m. to 1:00 p.m.). Thus, in the summer, there is a very strong incentive to maximize the generation of electricity throughout the period from 1:00 p.m. to 7:00 p.m., but unfortunately in a solar-only plant, the kilowatt-hours produced decline during the afternoon hours. Also, a solar system cannot produce power during winter on-peak hours, when the revenue earned would be 1.6 times that during mid-peak hours.

HYBRID PLANTS

A hybrid plant consists of a solar plant with a fossil-fired heat source to supplement and, if necessary, to replace the solar heat source. Such a plant offers three very powerful advantages over a solar-only plant:

- The plant could be operated continuously at maximum output throughout the on-peak hours
- Whenever the solar input is below 1 kW/m^2, for example, the fossil assist could be used to boost the power so that the module could be operated at rated power level and maximum efficiency throughout the day, thus enhancing the benefits of the solar input

- Having the option to completely substitute a fossil-fired energy input for the solar energy input would also permit the module(s) to be operated at rated power if desired, on a cloudy day or during the night. The SCE pricing schedule gives a qualifying facility a bonus capacity cost if performance consistently exceeds specified threshold levels. This enhances the revenues from on-peak generation of power even further.

A hybrid receiver was tested at the JPL Edwards Test Station in late 1981. Testing spanned a 1-month period and was prematurely terminated by a braze-joint failure. A number of other problems were encountered but the feasibility of a hybrid solar Stirling engine receiver fired by natural gas was demonstrated.

In late 1985, Advanco Corporation initiated Phase I of a hybrid receiver program under the joint sponsorship of the Gas Research Institute and the Department of Energy. This will be primarily a study phase.

SCALE-UP IN SIZE

Future dish/Stirling module development should be aimed at larger dishes and larger Stirling engines. Advantages accruing from this approach may be illustrated for the case where the electrical output of the dish/Stirling module is doubled in capacity due to increased dish size:

- Assuming the mean time between failures of a given component depends primarily on hours of operation, then O&M costs in mils per kilowatt-hour would be halved, since the number of kilowatt-hours output is doubled.
- Additional savings would arise from the economics of scale-up in size. Assuming a scale-up cost factor ranging from the 0.5 power to the 0.8 power, capital costs in mils per kilowatt-hour would be decreased by about 13% to 30%.
- The efficiency of the Stirling engine increases marginally with size. An increased efficiency yields a larger kilowatt-hour output, resulting in lower costs in mils per kilowatt-hour.

INNOVATIVE CONCENTRATOR PROJECT

The Department of Energy is sponsoring an innovative concentrator project that is being managed by Sandia National Laboratories-Albuquerque. Project objectives are to design a point-focus concentrator system that will (1) meet prescribed performance and survivability criteria; (2) be modular and mass producible; (3) be easy to manufacture, operate, and maintain; and (4) have low life-cycle costs.

Contractors selected in August 1984 were (1) Acurex Corporation, Mountain View, California; (2) Entech Incorporated, Dallas, Texas; and (3) LaJet Energy Company, Abilene, Texas. Key features of the concentrator from each contractor were delineated at the Semi-Annual Review of Distributed Receiver Development at Williamsburg, Virginia, on 1 October 1985 and are shown in Table 6-2.

Table 6-2

INNOVATIVE CONCENTRATORS - KEY DESIGN FEATURES

Acurex	Entech	LaJet
• Integrated panel and panel support structure -- light weight	• Refractive optical system -- slope error tolerant	• Faceted reflective optics -- adjustment
• PCA directly coupled to the drive unit -- no loads on the optical part of the dish	• PCA location -- Near the ground for easy access	• Stretched film membrane facets -- inexpensive ECP-91, ECP-94
• Stamped sheetmetal "petals" -- low cost, mass production	• Low profile -- reduced wind loads	• Polar axis mount -- simplified tracking
• Tilted azimuth bearing -- eliminates the "keyhole" effect	• 14 tools required for fabricating lenses -- mass production	• Tracking system "learns" and adjusts for structural alignment
• Redundant, low parasitic hydraulic drive	• Small base carousel tracking system	• Light weight structure -- easy field assembly

In Table 6-3, the design features of the Vanguard concentrator are compared with those of the three innovative concepts now under development. A very interesting feature is that the thermal output from the innovative concept designs range from 60 to 127% greater than that for Vanguard. This is in the desirable direction to take advantage of the economics of scale-up discussed previously.

SITE REQUIREMENTS

In most tests to date of solar-thermal power systems, the host utility has provided the land and the site. Because of the relatively diffuse nature of solar energy as a heat source, it is illuminating to examine the land and site requirements. Early Vanguard studies showed that a typical layout for a 10-MWe plant would involve about 400 modules occupying close to 78 acres, or approximately five modules per acre. McDonnell-Douglas estimates that one acre for each six or seven modules

Table 6-3

COMPARISON OF VANGUARD CONCENTRATOR WITH INNOVATIVE CONCENTRATOR DESIGNS* NOW UNDER DEVELOPMENT

	Vanguard	Acurex	Entec	LaJet
Aperture area (square meters)	87.6	177.5	154.0	163.9
Concentrator diameter (meters)	10.7	15.0	14.0	19.3
Focal length (meters)	6.2	7.5	11.1	11.6
Receiver aperture diameter (meters)	0.2	0.3	0.36	0.51
Concentrator weight (kilonewtons)	101.8	137.9	114.3	91.6
(pounds)	22,900	31,000	25,700	20,600
Optical efficiency (percent)	82.0	92.0	82.0	75.0
Thermal output at 1-kW/m^2 solar input (kilowatts-thermal)	71.8	163.1	116.0	123.0

*Data on Innovative Concentrator Designs presented by J. A. Leonard and T. R. Mancini at U.S. Department of Energy, Division of Solar Thermal Technology, Semi-Annual Review, Williamsburg, Virginia (October 1 1985).

would be acceptable. A typical plant might involve 400 to 1000 modules. At today's prices, undeveloped desert land is estimated to cost from $500 to $1,000 per acre, depending on access to water and power.

The purchased land might require grading and the field would have to be covered with rock, asphalt, or treated to retard dust formation and weed growth. Service and access roads would be needed. A multi-module plant would require a control room, office space, restrooms, a structure and yard for maintenance and engine overhaul, and an electrical substation. In a typical layout of 400 modules, there might be 16 pad-mounted transformers with a capacity of 750 kVA each. A large amount of copper wire would be required for all electrical cable. Some arrangement of piping or hose would be necessary for periodically washing the mirrors; if this approach is not used, then the plant layout must allow for unimpeded access of a water tank-truck to each dish; cost accounting must allow for purchase or lease of a suitable truck, water tank, and spray equipment. Cost and availability of water must be considered also.

The preceding discussion on the plant site was presented to point out that costs other than the capital costs of the dish and power conversion unit should be considered in the economics calculations.

ASSESSMENT WRAP-UP

A feeling for the challenge involved in making a dish/Stirling module competitive may be obtained by estimating the daily revenues. A liberal estimate of the net kilowatt-hours of electricity delivered to the grid annually for a module similar to Vanguard at a desert site (i.e., a favorable solar location) is 50,000 kilowatt-hours. At 10 cents per kilowatt-hour, this would earn annual revenues of $5,000. Assuming it operated 90% of the days during the year, the daily revenue would be $15. This daily revenue must be sufficient to cover capital costs, operating and maintenance costs, and a reasonable profit for the investor.

To achieve an economically viable power-generating system, the following general directions are indicated. Reduce projected capital costs primarily by design innovations and secondarily by scale-up in size. Reduce operating and maintenance costs primarily by scale-up in size and by simplifying design. Increase revenues by taking advantage of time-differentiated payments by delivering power during on-peak and mid-peak hours. Accomplish this by adding a fossil-assist (oil- or gas-fired heating capability). Also, increase conversion efficiency by operating at rated output in a hybrid plant, utilizing the fossil assist.

Developmental effort along the lines indicated is now in place in work sponsored by the Department of Energy and managed by Sandia National Laboratories-Albuquerque. In the case of hybrid plants, this work is under joint sponsorship of the Department of Energy and the Gas Research Institute. In addition, a continuing effort is under way on developing Stirling engines for automotive applications. The automotive work also is being performed under Department of Energy sponsorship and is being managed by NASA Lewis Research Center. Some of the improvements in engine performance obtained by this program should be applicable to the solar version of the Stirling engine. The McDonnell-Douglas and United Stirling joint effort should provide utilities with operating experience yielding valuable data.

Section 7

REFERENCES

1. B. J. Washom, "Vanguard I, Solar Parabolic Dish - Stirling Engine Module, Final Report," (28 May 1982-30 September 1984), DOE-AL-16333-2 (84-ADV-5) (30 September 1984)

2. Advanco Corporation Monthly Progress Reports from February 1984 through June 1985

3. F. R. Livingston, "Activity and Accomplishments in Dish/Stirling Electric Power System Development," DOE/JPL-1060-82 (15 February 1985)

4. J. Stearns, "Stirling Engine Alternatives for the Terrestrial Solar Application," DOE/JPL-1060-91 (October 1985)

5. E. P. Roth and R. B. Pettit, "The Effect of Soiling on Solar Mirrors and Techniques Used to Maintain High Reflectivity," SAND 79-2422 (June 1980)

6. Department of Energy, Division of Solar Thermal Technology, Semi-Annual Review, Williamsburg, Virginia (1 October 1985), papers presented by J. A. Leonard and T. R. Mancini, Sandia National Laboratories, Albuquerque, New Mexico

7. B. J. Washom, "Vanguard I, Solar Parabolic Dish - Stirling Engine Module, FY 1985 Test Plan," DOE-AL-16333-3 (84-ADV-6) (December 1984)

Appendix A

OPERATING PRINCIPLES OF THE STIRLING ENGINE*

A Stirling engine operates as an externally heated piston-driven prime mover. It uses either helium or hydrogen for internal heat transport; hydrogen is the preferred working gas because it has the best heat transfer properties and thereby results in the highest engine efficiencies.

The engine was first developed in 1816 by a Scottish clergyman, Robert Stirling. Since then, a number of prototype engines have been either designed or constructed by small and large organizations including General Motors, Ford Motor Company, General Electric, Mechanical Technology Incorporated, Philips Laboratories of Holland, and United Stirling of Sweden. Construction and operation of the Stirling cycle engine is by far the most complicated of any practical engine in use today, and there is essentially no commonality between any conventional engine and the relatively sophisticated engine type discussed here.

The simplest way to explain how a Stirling engine operates is to take some technical liberties and separate the key components in a simplified operation diagram as shown in Figure A-1. A Stirling engine has three key components--a power piston, a "displacer," and a heat conserving and storage component called a "regenerator." Movement of the displacer is precisely coordinated with the lower piston in order to maximize utilization of heat which is cyclically stored in, and removed from, the regenerator.

Operation of the power piston is the main part of the Stirling process, and it delivers power to the engine crankshaft on each stroke in the downward direction (similar to a 2-cycle internal combustion engine). The displacer function is only to move hydrogen gas back and forth from the heated to the cooled regions of the engine, acting like a valve which operates in advance of the power piston to move the hydrogen at optimally timed intervals. The regenerator captures and stores heat as hydrogen passes from the hot power piston to the cool displacer. This stored heat is efficiently delivered back to the hydrogen as it passes from the cool displacer to the heated power piston.

*Prepared by Southern California Edison Company.

Thus, the key to understanding the overall effect of this cyclic heating and movement of hydrogen is to recognize that power is produced on the downward stroke of a Stirling engine by the combined effect of heat released from the regenerator and steady heat input from the fuel source which causes the hydrogen working gas to expand and force the power piston downward. The power piston and displacer are returned to the beginning of the process by inertia of the engine flywheel.

United Stirling has developed a four-cylinder engine which eliminates the displacer. This is accomplished by coordinating the bottom end of a power piston with the top end of an adjacent power piston. Such an arrangement is called a double-acting Stirling engine, because a single-piston performs both functions of delivering power to the crankshaft as well as displacing the working gas back and forth from the hot to the cold regions of the engine in a precisely timed manner. United Stirling of Sweden has perfected such an engine configuration to a degree that by heating and cooling the hydrogen more than 60 times per second, the engine can operate at high efficiency in excess of 4000 rpm.

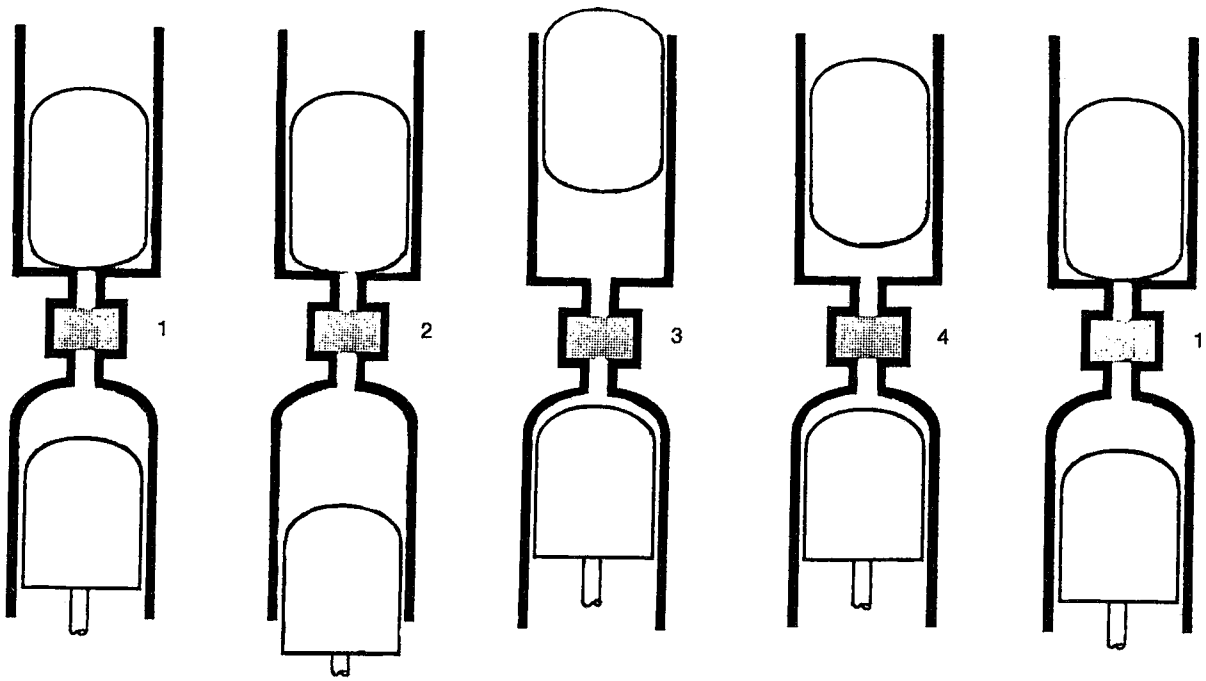

1-2 EXPANSION
WORK IS PERFORMED WHEN THE WORKING GAS EXPANDS ON THE HOT SIDE WHILE IT IS HEATED AT HIGH PRESSURE.

3-4 COMPRESSION
WORK IS SUPPLIED BY COMPRESSING THE WORKING GAS ON THE COLD SIDE; THE GAS IS COOLED AT LOW PRESSURE.

2-3 DISPLACEMENT
THE GAS MOVES FROM THE HOT TO THE COLD SIDE AT CONSTANT VOLUME. HEAT IS STORED IN THE REGENERATOR, PRESSURE DECLINES.

4-1 DISPLACEMENT
THE GAS IS MOVED FROM THE COLD TO THE HOT SIDE AT CONSTANT VOLUME. THE REGENERATOR GIVES OFF STORED HEAT. PRESSURE INCREASES.

Figure A-1. Double-Acting Stirling Engine

Appendix B

STIRLING CYCLE THERMODYNAMICS*

The Stirling engine is a reciprocating, external combustion, closed-cycle heat engine. It is gaining popularity because of its potential for high efficiency and its ability to use any source of heat.

Both a temperature-entropy and a pressure-volume diagram for the ideal Stirling cycle are shown in Figures B-1 and B-2. Heat is supplied to the working fluid during the constant-volume process (4-1) and during the isothermal expansion process (1-2). Heat is rejected during the constant-volume process (2-3) and during the isothermal compression process (3-4). During the constant-volume cooling process (2-3), heat is removed from the working fluid and stored in a regenerator. This heat is returned to the working fluid during the constant-volume heat process (4-1). In the ideal process, all the heat rejected during the cooling process (2-3) is returned during the heating process (4-1).

The thermodynamic efficiency of the Stirling cycle is defined the same as for the Rankine and Brayton cycle; that is,

$$S = \frac{W_N}{Q_{in}} = \frac{W_{ex} - W_{comp}}{Q_{in}}$$

The expansion work (1-2) is given by

$$W_{ex} = \int_{V_1}^{V_2} P \, dV$$

for an isothermal expansion

$$PV = \text{Constant} = mRT_1$$

---

*Extracted from Handbook of Data on Selected Engine Components for Solar Thermal Applications, U.S. DOE, DOE/NASA/1060-78/1, June 1979

or

$$P = \frac{RT_1}{V}$$

Therefore,

$$W_{ex} = \int_{V_1}^{V_2} mRT_1 \frac{dV}{V} = mRT_1 \ln\left(\frac{V_2}{V_1}\right)$$

In the ideal cycle this quantity W_{ex} is also the heat input to the cycle Q_{in}. The compression work (3-4) is obtained in the same manner as the expansion work

$$W_{comp} = \int_{V_4}^{V_3} mRT_3 \frac{dV}{V} = mRT_3 \ln\left(\frac{V_3}{V_4}\right)$$

Therefore,

$$\eta_S = \frac{mRT_1 \ln\left(\frac{V_2}{V_1}\right) - mRT_3 \ln\left(\frac{V_3}{V_4}\right)}{mRT_1 \ln\left(\frac{V_2}{V_1}\right)}$$

since $V_3 = V_2$ and $V_4 = V_1$

$$\eta_S = 1 - \frac{T_3}{T_1}$$

So the ideal efficiency of the Stirling cycle is equal to the Carnot efficiency operating over the same temperature range. However, the ideal efficiency cannot be realized in practice because of the inefficiencies associated with the various processes.

One of the chief engine inefficiencies is that of the regenerator. With this inefficiency, only a portion (4-5) of the heat rejected during the cooling process is returned during the heating process (4-1). This means that external heat must

be added during the remaining portion of the constant-volume heat-addition process (5-1). The additional external heat that must be added is given by

$$Q' = mC_v (T_1 - T_5)$$

Therefore,

$$\eta_S = \frac{W_{ex} - W_{comp}}{Q_{in} + Q'} = \frac{mRT_1 \ln\left(\frac{V_2}{V_1}\right) - mRT_3 \ln\left(\frac{V_2}{V_1}\right)}{mRT_1 \ln\left(\frac{V_2}{V_1}\right) + mC_v (T_1 - T_5)}$$

If regenerator effectiveness is defined as

$$E_r = \frac{T_5 - T_3}{T_1 - T_3}$$

then

$$\eta_S = \frac{T_1 - T_3}{T_1 + \frac{C_v}{R} \frac{(T_1 - T_3)(1 - E_r)}{\ln \frac{V_2}{V_1}}}$$

The real Stirling engine processes differ significantly from the ideal cycle so that the basic performance equations just presented are useful for only the grossest approximations. The actual and ideal cycles are shown on a pressure-volume diagram in Figure B-3. Other factors, besides regenerator inefficiency, that lead to deviations from the ideal cycle are piston motion, dead air spaces, leakage, and external heat transfer. These factors are intimately related to one another and make strict analytical formulation difficult.

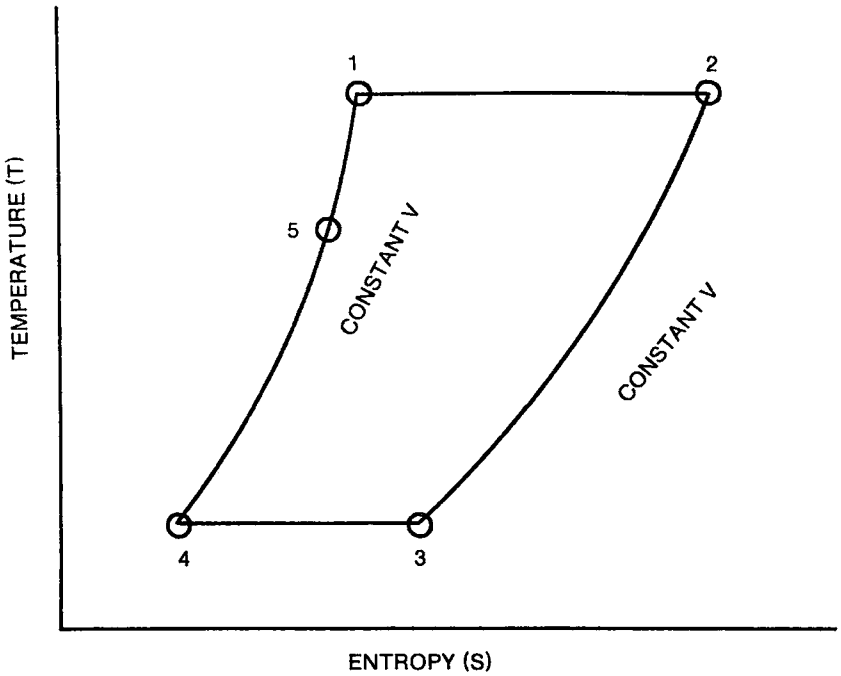

Figure B-1. Temperature-Entropy for the Ideal Stirling Cycle

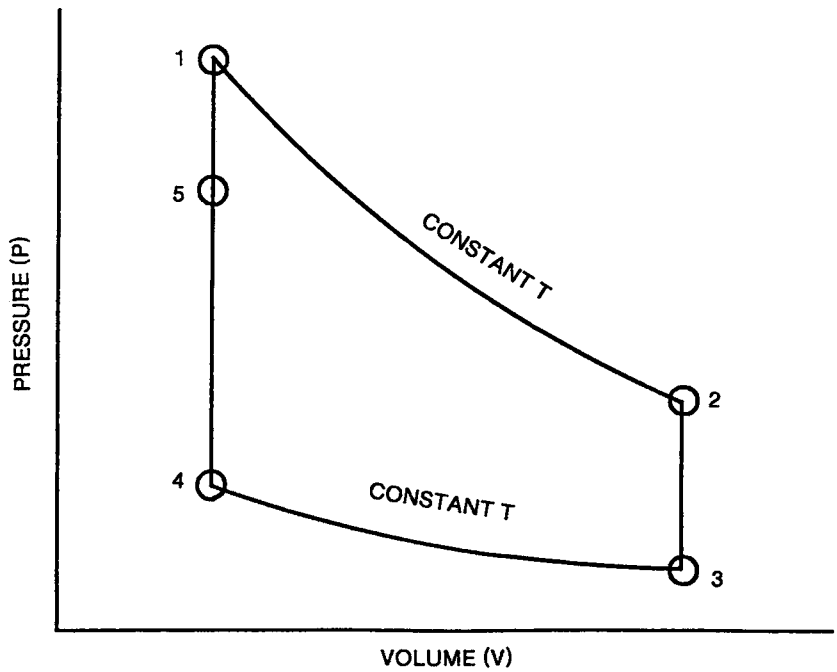

Figure B-2. Pressure-Volume for the Ideal Stirling Cycle

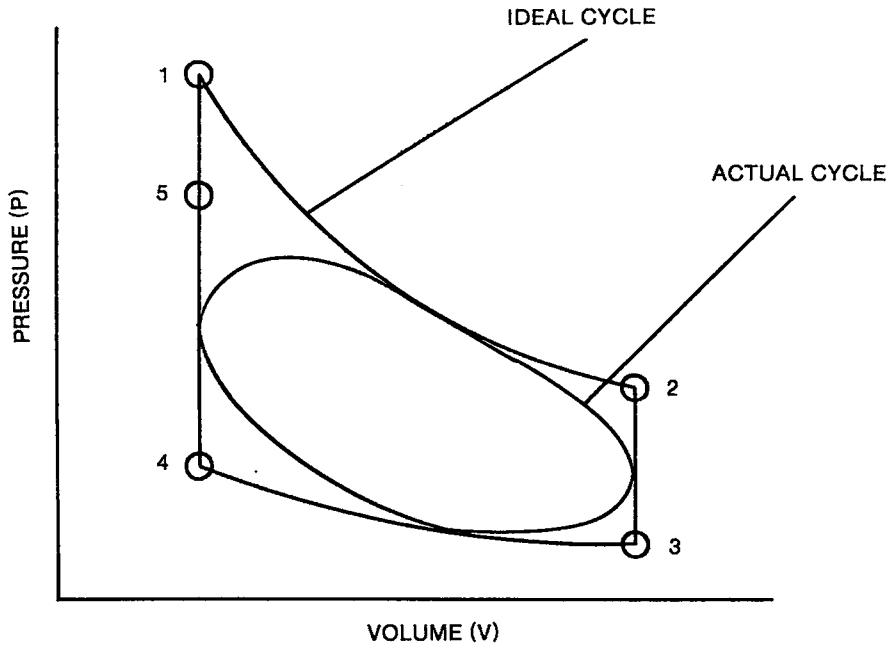

Figure B-3. Actual and Ideal Cycles

Appendix C

TEST PLAN SUMMARY

Under EPRI auspices, a draft copy of a test plan for the Vanguard module was prepared by ETEC and distributed to program participants in April of 1984. This test plan draft served as a "straw man" to elicit comments on and suggestions for additions and deletions. As such, it provided early input to Advanco on utility needs and concerns for the Vanguard test program. Using these inputs and results from the initial test phase, Advanco revised the test plan to reflect activities they intended to perform during the remainder of the test program. Advanco issued the test plan as DOE-AL-16333-3 (84-ADV-6), "Vanguard 1, Solar Parabolic Dish - Stirling Engine Module, FY 1985 Test Plan." The following pages summarize the items in the revised and updated test plan.

Table C-1

SYSTEM RELIABILITY TEST ACTIVITIES

Test Activity	Description	Purpose	Test Frequency
1	Measure direct normal insolation using sensors mounted on ground and on dish	- Determine max solar energy available - Data for system efficiency	Constant Daytime
2	Measure gross electrical power production	- Quantity electricity generated daily - Data for system efficiency - Variation with other factors	Constant Daytime
3	Measure parasitic electrical power requirements	- Determine parasitic energy requirements for module and site - Obtain net power output - Identify areas for improvements	Constant Daytime
4	Plot gross electrical power vs direct insolation	- Determine day-to-day variations in performance - Measure certain energy losses - Monitor mirror reflectivity	Daily
5	Obtain O&M data	- Basis for O&M costs	Daily
6	Measure hydrogen consumption	- Determine hydrogen requirements - Detect any excessive leaks	As Required
7	Record availability of module to generate power and record malfunctions	- Determine normal and solar availability - Determine reliability	Daily
8	Measure kilowatt-hours electricity actually produced	- Determine capacity factor	Daily

Table C-2

SPECIAL EXPERIMENTAL TEST ACTIVITIES
(Sheet 1 of 5)

Test Activity	Description	Purpose	Test Frequency
1	Measure reflectivity of mirror facets on the dish	- Determine variation of reflectivity vs time	Weekly
2	Measure dish heat loss at extremes of ambient temperature experienced at site	- Determine effect of ambient temperature on receiver heat losses	4X
3	Measure variation in electrical power production as function of wind speed and direction	- Determine effects of wind on dish aiming errors due to dish deflection	6X
4	Measure thermal flux distribution of the receiver by various means (TBD)	- Determine uniformity of flux on receiver tubing	Quarterly
5	Record any changes in receiver tube behavior	- Determine factors influencing receiver lifetime	As occurs Examine on Weekly Basis
6	Visually inspect aperture cone	- Determine condition of cone - Obtain data on cone life - Decision on when to replace	Weekly
7	Evaluate shutter operation	- Note failures and repair time	As they occur
8	Monitor temperature of receiver tubes	- Variation of temperature with solar energy input, hydrogen pressure, and absorptivity of tubing	Monthly
9	Monitor temperature and pressure of working gas in each receiver quadrant and each piston of engine	- Determine uniformity of working gas temperature	Monthly
10	Measure leakage rate of hydrogen by consumption and by pressure decay tests	- Determine integrity of the working-gas system - Establish basis for engine overhaul	Quarterly

Table C-2

SPECIAL EXPERIMENTAL TEST ACTIVITIES
(Sheet 2 of 5)

Test Activity	Description	Purpose	Test Frequency
11	Measure coolant flow rate and inlet and exit temperatures of heat rejection system at extremes of ambient temperature	- Obtain semi-quantitative data on heat losses - Evaluate performance of heat rejection system - Effect of ambient temperature on engine coolant temperature	One time
12	Check coolant level, consumption, and condition of pump, seals, hoses, and fan	- Determine coolant losses and makeup requirements - Determine inspection intervals	Monthly
13	Monitor starting currents of starter motor during startup of module at extremes of ambient air temperatures	- Determine starting motor power requirements as function of ambient temperature	Once at High and Low Ambient Temperature
14	Measure engine efficiency as a function of direct normal insolation at two widely different ambient air temperatures (no wind and same mirror reflectivity)	- Determine effect of ambient air temperature on engine efficiency	Once During Program
15	Perform tests with approximately same direct normal insolation at wind speeds of near zero mph and approximately 25-30 mph	- Determine effect of wind speed and angle of attack on module efficiency	Once During Program
16	Make reference measurements of generator shaft end play and torque	- Monitor wear of generator shaft/ bearing	During Engine Teardown
17	Obtain vars and kilowatt reading of generator output at various loads and without the power-factor-correction capacitors	- Determine effectiveness of the power-factor-correction capacitors - Measure change in power factor as function of generator power output	Once During Program

Table C-2

SPECIAL EXPERIMENTAL TEST ACTIVITIES
(Sheet 3 of 5)

Test Activity	Description	Purpose	Test Frequency
18	Obtain data with rapid passage of small clouds so utility disconnect switch opens and closes rapidly	- Obtain data on time to open and close the utility disconnect switch	Once During Program
19	Using signals to simulate wind speeds 30 mph, monitor response of alarm/stow system	- Obtain time constants of the alarm/stow system - Determine time duration of sustained excess wind speed required to initiate a stow command	Once During Program
20	Perform tests using simulated signals to check beeper alert and operator acknowledge system	- Verify that system works - Determine range of the system - Effect of battery conditions	Once During FY 1985
21	Perform calibration check of kilowatt and vars meters	- Calibration check	Near Beginning and End of FY 1985
22	Compare values obtained from readings of kilowatt-hours with those from integrated readings of power in kilowatts	- Effectiveness of data sampling rate	Near Begin- meter ning and End of FY 1985
23	Perform calibration checks of pyrheliometers used to measure direct normal insolation	- Calibration check	Near Beginning and End of FY 1985
24	Conduct tests to attempt to start module operation when (simulated) alarm conditions exist	- Verify ability of alarm sensors to prevent unauthorized startup	Once During Program
25	Simulate various alarm signals and observe response time for appropriate actions	- Determine response times and verify control logic system	Once During Program

Table C-2

SPECIAL EXPERIMENTAL TEST ACTIVITIES
(Sheet 4 of 5)

Test Activity	Description	Purpose	Test Frequency
26	Obtain data during startup at ten different insolation levels of time: (1) working-gas pressure, (2) working-gas temperature, (3) gross power, and (4) generator rpm	- Characterize module behavior during startup	Once During Program
27	Conduct tests during passage of small clouds to evaluate conditions which do and do not result in engine stoppage	- Determine engine behavior during cloud passage	Once During Program
28	Obtain data on module performance for periods of one week preceding and following summer and winter solstices, and spring and fall equinoxes	- Characterize seasonal effects	Each Solstice and Equinox
29	Obtain data on module performance during fully-automatic operation on clear days and on cloudy days	- Checkout of fully-automatic mode of operation	Until System Works Correctly
30	Measure control of the hydrogen working fluid pressure as a function of receiver temperature; verify the engine start command when the receiver reaches 500°C; determine response time and amount of undershoot or overshoot of the temperature to initiate the start command, verify module detrack command with simulated signal of excessive receiver temperature	- Determine control characteristics of receiver temperature input to control system and verify guard functions	Once During Program
31	Measure Stirling engine output as a function of hydrogen gas pressure; verify module detrack command with application of hydrogen pressure in excess of normal range	- Determine correlation between hydrogen gas pressure, receiver temperature, and power output - Verify guard functions of excessive or inadequate gas pressure	Once During Program

Table C-2

SPECIAL EXPERIMENTAL TEST ACTIVITIES
(Sheet 5 of 5)

Test Activity	Description	Purpose	Test Frequency
32	Verify closure of contractor beween generator and utility grid when generator shaft speed increases to 1800 rpm; verify contactor opening when rpm increases to 1840, and then contactor reclosing when rpm decreases to 1830	- Verify guard functions of engine speed being too high or too low	Once During Program
33	Check control of radiator fan as a function of coolant water temperature; verify detrack commands with simulated input corresponding to excessive coolant temperature	- Determine correlation between coolant water temperature, power level, and ambient temperature - Verify guard functions	Once During Program
34	Use simulated input for oil temperature above permissible range - Observe detrack response	- Verify detrack command in case of excessive oil temperature	Once During Program
35	Check operation of the emergency switch with the module at normal power; repeat near minimum and maximum power		
36	Simulate loss of power from the utility grid by opening main GEPS grid connection switch - Monitor behavior of diesel generator, detrack, and engine - Upon proper functioning, reconnect GEPS to power grid and resume operation	- Check out module shutdown functions for loss of grid power	Once During Program
37	Simulate loss of generator load while module is producing net power to grid by opening switch in MEPS	- Observe response to module to loss of generator load while module is producing net power to grid	Once During Program

Appendix D

DAILY SUMMARIES OF OPERATING HOURS, AVAILABLE SOLAR ENERGY, AND ELECTRICAL OUTPUT BY MONTH

This appendix contains daily summaries organized by month of key factors needed to evaluate performance of the Vanguard module. Solar energy columns are in units of kilowatt-hours of direct insolation incident on the dish. Electrical output columns are in units of kilowatt-hours. Further breakdowns are given for data acquired on magnetic tape by the Autodata Nine computer and reduced by ETEC and for data acquired on diskettes by the IBM computer and reduced independently by ETEC and Advanco. The IBM data acquisition system was started on 11 June 1984. The source of daily data reported by Advanco was the Advanco monthly progress reports; for days where daily summaries were not available in the Advanco progress report, the corresponding spaces have been left blank.

DATE	ENGINE OPERATING HOURS		AVAILABLE SOLAR ENERGY	AT-POWER SOLAR ENERGY		GROSS ELECTRICAL OUTPUT			NET ON-SUN ELECTRICAL OUTPUT		NET 24-HOUR ELECTRICAL OUTPUT		
FEB 1984	ETEC-IBM*	ETEC-AD9	ETEC-IBM*	ETEC-IBM*	ETEC-AD9	ADVANCO	ETEC-IBM*	ETEC-AD9	ETEC-IBM*	ETEC-AD9	ADVANCO	ETEC-IBM*	ETEC-AD9
1													
2													
3													
4													
5													
6													
7		1.5			124.1			16.4		14.9			3.0
8													
9													
10													
11													
12													
13													
14													
15													
16		2.1			152.4			26.4		24.4			12.8
17													
18													
19													
20													
21													
22													
23		3.6			282.6			83.4		77.9			67.1
24		0.9			35.4			11.0		10.0			-2.2
25													
26													
27													
28													
29		4.4			250.4			74.8		67.9			57.5
TOTAL	0.0	12.4	0.0	0.0	844.9	0.0	0.0	212.0	0.0	195.1	0.0	0.0	138.1

* IBM Data Acquisition System unavailable in February of 1984

DATE	ENGINE OPERATING HOURS		AVAILABLE SOLAR ENERGY	AT-POWER SOLAR ENERGY		GROSS ELECTRICAL OUTPUT			NET ON-SUN ELECTRICAL OUTPUT		NET 24-HOUR ELECTRICAL OUTPUT		
MAR 84	ETEC-IBM*	ETEC-AD9	ETEC-IBM*	ETEC-IBM*	ETEC-AD9	ADVANCO	ETEC-IBM*	ETEC-AD9	ETEC-IBM*	ETEC-AD9	ADVANCO	ETEC-IBM*	ETEC-AD9
1		8.9			459.2			127.3		115.2			107.2
2													
3													
4													
5													
6													
7													
8													
9													
10													
11													
12													
13													
14		2.4			92.2			18.9		16.3			4.8
15		1.5			79.6			18.1		16.5			4.6
16		6.6			419.7			96.3		88.2			79.0
17													
18													
19		9.8			719.6			199.0		187.0			179.5
20		7.0			543.2			146.4		138.2			129.2
21		1.4			57.4			10.8		9.4			-2.6
22		10.4			740.5			165.3		153.0			145.8
23		6.8			474.9			129.0		120.6			111.5
24													
25													
26													
27													
28													
29													
30		8.2			543.3			145.3		135.5			127.1
31													
TOTAL	0.0	63.0	0.0	0.0	4129.5	0.0	0.0	1056.4	0.0	979.8	0.0	0.0	886.0

* IBM Data Acquisition System unavailable in March of 1984

DATE	ENGINE OPERATING HOURS		AVAILABLE SOLAR ENERGY	AT-POWER SOLAR ENERGY		GROSS ELECTRICAL OUTPUT			NET ON-SUN ELECTRICAL OUTPUT		NET 24-HOUR ELECTRICAL OUTPUT		
APR 84	ETEC-IBM*	ETEC-AD9	ETEC-IBM*	ETEC-IBM*	ETEC-AD9	ADVANCO	ETEC-IBM*	ETEC-AD9	ETEC-IBM*	ETEC-AD9	ADVANCO	ETEC-IBM*	ETEC-AD9
1													
2		9.6			673.2			196.8		185.3			177.6
3		10.3			729.4			214.0		201.6			194.3
4		10.4			669.1			187.9		176.1			168.9
5		10.4			684.6			190.2		178.2			171.0
6		6.0			244.3			80.7		75.3			65.8
7													
8													
9		10.4			524.3			138.8		127.9			120.7
10		5.6			271.1			68.3		62.4			52.6
11		8.7			604.6			162.4		150.9			142.8
12		4.1			314.4			92.3		86.4			75.9
13		6.6			461.3			130.4		121.3			112.0
14													
15													
16		9.1			595.5			159.1		145.7			137.8
17													
18		5.0			300.1			78.5		72.8			62.7
19		8.5			577.6			153.2		143.4			135.2
20		11.1			802.6			216.7		203.4			196.6
21													
22													
23		12.1			833.6			215.0		198.2			191.9
24		5.3			319.8			92.2		84.3			74.4
25		7.7			376.9			88.5		80.2			71.6
26		5.0			314.3			84.3		78.5			68.5
27		0.2			5.7			0.1		0.1			-12.6
28													
29													
30													
TOTAL	0.0	146.0	0.0	0.0	9302.1	0.0	0.0	2549.3	0.0	2371.9	0.0	0.0	2207.7

* IBM Data Acquisition System unavailable in April of 1984

DATE	ENGINE OPERATING HOURS		AVAILABLE SOLAR ENERGY	AT-POWER SOLAR ENERGY		GROSS ELECTRICAL OUTPUT			NET ON-SUN ELECTRICAL OUTPUT		NET 24-HOUR ELECTRICAL OUTPUT		
MAY 84	ETEC-IBM*	ETEC-AD9	ETEC-IBM*	ETEC-IBM*	ETEC-AD9	ADVANCO	ETEC-IBM*	ETEC-AD9	ETEC-IBM*	ETEC-AD9	ADVANCO	ETEC-IBM*	ETEC-AD9
1													
2		0.1			3.1			0.3		0.3			-12.4
3													
4													
5													
6													
7													
8													
9													
10													
11		11.1			698.4			53.1		41.6			34.7
12		0.4			28.7			1.6		1.3			-11.2
13													
14		7.2			460.7			106.5		96.5			87.6
15		7.3			466.3			119.7		109.9			101.1
16		6.0			437.2			105.6		98.5			88.9
17													
18		0.8			54.1			11.1		10.2			-2.1
19		1.2			86.5			18.5		17.1			5.0
20													
21		7.0			473.3			102.5		94.9			85.9
22		9.3			584.6			113.9		103.3			95.5
23													
24		3.1			173.7			45.9		41.7			30.6
25													
26													
27													
28													
29													
30													
31													
TOTAL	0.0	53.4	0.0	0.0	3466.6	0.0	0.0	678.7	0.0	615.3	0.0	0.0	503.6

* IBM Data Acquisition System unavailable in May of 1984

DATE	ENGINE OPERATING HOURS		AVAILABLE SOLAR ENERGY	AT-POWER SOLAR ENERGY		GROSS ELECTRICAL OUTPUT			NET ON-SUN ELECTRICAL OUTPUT		NET 24-HOUR ELECTRICAL OUTPUT		
JUN 84	ETEC-IBM*	ETEC-AD9	ETEC-IBM*	ETEC-IBM*	ETEC-AD9	ADVANCO	ETEC-IBM*	ETEC-AD9	ETEC-IBM*	ETEC-AD9	ADVANCO	ETEC-IBM*	ETEC-AD9
1													
2													
3													
4													
5													
6													
7		0.2			39.8			2.2		2.0			-10.6
8													
9													
10													
11		2.4			155.5			39.3		36.3			24.9
12	0.1		16.2	8.3			1.1		1.0				
13	2.9	3.5	574.9	185.0	200.6		46.4	49.3	43.1	45.4		33.5	34.5
14		12.6	864.4		824.5	220.0		221.1		203.2	200.0		197.2
15	12.9	12.4	854.5	889.5	824.2	227.0	227.5	222.9	210.6	205.3	207.0	205.5	199.2
16	3.9	12.9	829.7	256.6	816.0	213.0	63.6	213.9	58.6	195.8	193.0		189.9
17	12.9	12.9	826.6	846.8	817.2	210.0	211.1	210.3	192.6	191.7	189.0	187.8	185.8
18	12.9	13.0	806.2	822.2	792.7	204.0	203.9	203.1	185.9	184.4	184.0	181.1	178.6
19	13.1	13.2	876.6	894.3	869.3	221.0	226.0	226.5	207.1	207.5	199.0	201.0	201.7
20	13.2	13.2	911.5	930.9	900.8	236.0	236.1	235.3	218.2	216.0	216.0	213.5	210.3
21		13.1	943.3		908.4	258.0		256.6		237.6	238.0		231.8
22	13.0	12.9	924.1	936.9	902.1	249.0	249.9	247.1	230.6	227.5	227.0		221.7
23	11.9	11.8	851.8	862.4	831.8	228.0	228.5	226.3	211.0	208.0	208.0	205.1	201.5
24	0.0	0.1	99.4	0.0	2.7	0.0	0.0	0.1	0.0	.0	-8.0	-11.7	-12.7
25	3.9	4.1	330.2	194.8	197.8	39.0	40.7	41.0	35.1	34.7	24.0	23.5	24.1
26	12.8	10.3	771.3	774.6	655.0	202.0	205.5	179.5	187.1	164.0	181.0	181.7	156.7
27	12.5		776.7	777.6		205.0	206.5		187.8		184.0	182.6	
28	8.5	8.5	443.3	423.0	407.4	96.0	96.7	97.8	84.7	85.5	77.0	75.2	77.3
29	2.7	2.7	162.8	116.3	110.9		21.3	22.1	17.8	18.2		4.7	6.9
30													
TOTAL	137.1	159.6	11863.5	8919.2	10256.6	2808.0	2264.8	2694.2	2071.2	2463.0	2519.0	1683.5	2318.8

* IBM Data Acquisition System unavailable from June 1 through June 11

DATE	ENGINE OPERATING HOURS		AVAILABLE SOLAR ENERGY	AT-POWER SOLAR ENERGY		GROSS ELECTRICAL OUTPUT			NET ON-SUN ELECTRICAL OUTPUT		NET 24-HOUR ELECTRICAL OUTPUT		
JUL 84	ETEC-IBM	ETEC-AD9	ETEC-IBM*	ETEC-IBM*	ETEC-AD9	ADVANCO	ETEC-IBM	ETEC-AD9	ETEC-IBM	ETEC-AD9	ADVANCO	ETEC-IBM	ETEC-AD9
1													
2	5.3		424.3	357.2			90.4		82.8			79.2	
3	0.0		350.7	0.0			0.0		0.0			0.0	
4													
5													
6	0.0		281.7	0.0			0.0		0.0			0.0	
7													
8													
9													
10	0.0		0.0	0.0			0.0		0.0			0.0	
11		5.2			293.1			64.8		56.7			46.7
12	5.8	5.8	489.4	397.6	384.3		95.2	94.7	86.6	85.6		76.2	76.0
13	4.8	2.7	360.8	251.5	153.0		51.5	35.0	44.7	30.7		33.7	19.4
14													
15	3.7		306.4	256.2			60.6		55.5			46.2	
16													
17	1.2		139.4	58.6			10.8		9.2			-1.2	
18	2.3		114.3	100.1			15.3		12.7			2.3	
19	9.2	9.2	544.8	539.6	517.6		119.9	118.7	107.1	105.1		100.5	97.3
20	6.0	6.0	348.2	307.1	286.2		59.0	58.0	51.3	49.9		42.4	40.3
21													
22													
23	8.3	5.5	625.8	608.5	380.0		147.6	93.5	136.1	85.3		129.3	75.5
24	8.3	8.4	696.0	590.8	593.8		158.1	158.7	145.4	145.2		138.0	136.9
25	12.3	12.3	819.3	809.4	803.2		213.4	213.8	194.3	193.8		189.0	187.6
26		0.5			25.1			5.4		4.7			1.1
27		1.1			47.7			8.9		7.5			4.2
28													
29													
30	6.3	6.4	489.7	468.7	463.3		116.1	115.6	107.1	106.2		98.6	96.9
31		8.2			542.9			125.9		113.6			105.2
TOTAL	73.5	71.3	5990.8	4745.3	4490.1	0.0	1137.9	1092.9	1032.8	984.2	0.0	934.2	887.1

* Supplemented by Advanco data when ETEC-IBM data unavailable

DATE	ENGINE OPERATING HOURS		AVAILABLE SOLAR ENERGY	AT-POWER SOLAR ENERGY		GROSS ELECTRICAL OUTPUT			NET ON-SUN ELECTRICAL OUTPUT		NET 24-HOUR ELECTRICAL OUTPUT		
AUG 84	ETEC-IBM	ETEC-AD9	ETEC-IBM*	ETEC-IBM*	ETEC-AD9	ADVANCO	ETEC-IBM	ETEC-AD9	ETEC-IBM	ETEC-AD9	ADVANCO	ETEC-IBM	ETEC-AD9
1	5.3	5.3	404.7	402.8	307.2	67.9	69.1	68.4	60.9	60.2	58.3	52.4	50.2
2		4.8		749.6	324.5	172.0		75.6		68.7	150.7		58.5
3	9.5	12.1	630.6	775.8	760.7	178.1	149.6	179.0	136.0	161.5	156.3	129.1	155.2
4	0.0		956.7	0.0		0.0	0.0		0.0		0.0	-10.1	
5	0.0		0.0	0.0		0.0	0.0		0.0		0.0	-9.8	
6	0.0	9.4	0.0	698.5	643.4	151.4	0.0	152.3	0.0	138.2	135.8	-10.3	130.5
7	7.5	7.6	804.9	510.0	501.1	115.5	116.0	115.0	105.3	103.9	99.0	96.7	95.2
8	1.6		642.0	188.2		18.0	17.7		15.1		4.4	1.4	
9	3.0	3.1	503.3	180.1	181.0	38.3	39.5	38.9	34.6	33.9	23.0	22.0	22.8
10	1.5	1.6	566.9	109.5	111.2	25.1	25.5	25.5	23.2	22.9	11.7	9.3	11.1
11	0.9	0.9	769.8	52.2	64.1	13.0	12.8	13.7	11.4	12.3	2.1	-1.1	0.1
12	1.0		762.2	68.2		16.2	16.3		14.5		5.6	2.2	
13	7.5	7.6	584.3	450.7	432.3	105.9	106.5	105.4	94.9	93.6	87.1	84.1	84.9
14	3.7	3.7	162.0	164.2	150.0	30.2	30.3	29.6	25.2	24.5	15.6	13.5	13.7
15	4.5	2.5	294.5	252.7	123.8	55.3	58.3	29.5	52.7	26.1	40.7	41.9	14.7
16	6.7	6.8	489.4	444.5	444.3	119.0	119.8	119.7	110.5	110.0	102.3	100.7	100.9
17	6.8	7.0	353.2	326.3	333.5	77.0	78.1	78.4	68.9	68.8	61.3	60.0	59.8
18	3.2	3.1	231.7	184.1	188.2	49.3	48.5	49.4	44.5	45.2	38.5	35.7	34.1
19	0.0		113.5	38.3		0.6	0.0		0.0		-7.0	-10.4	
20	0.0		42.3	20.9		0.4	0.0		0.0		-7.5	-11.2	
21	10.2	10.2	699.6	632.2	657.5	176.6	176.2	174.6	162.1	160.0	157.4	155.9	152.7
22	8.6	8.6	451.8	378.0	397.8	88.3	89.8	88.6	77.8	76.4	69.7	69.0	68.2
23	10.5	10.5	699.8	601.2	655.6	167.3	167.6	166.1	152.7	150.3	147.1	146.0	143.1
24	10.5	10.5	774.6	661.7	720.4	184.7	184.9	183.5	169.3	166.9	164.6	163.2	159.7
24	2.9	2.9	445.4	170.6	180.9	45.5	45.6	44.8	41.8	40.8	34.7	32.6	29.6
26	0.0		671.1	67.0		0.0	0.0		0.0		-7.2	-9.4	
27	5.4	5.6	562.1	374.8	410.4	104.6	104.4	105.2	96.6	96.6	88.6	86.4	86.9
28	10.8	10.8	724.8	624.0	682.9	169.8	170.5	168.8	154.5	152.4	148.8	147.7	145.4
29	11.1	11.2	777.9	672.3	755.2	188.1	188.4	188.2	171.2	169.9	164.9	164.2	163.0
30	9.4	9.1	662.3	510.4	556.4	129.7	128.5	130.0	113.9	115.3	107.3	104.7	107.4
31	11.0	3.9	778.1	752.2	277.4	184.9	185.0	70.2	168.6	64.5	162.5	161.4	53.8
TOTAL	153.1	158.3	15559.5	11061.0	9859.8	2672.7	2328.9	2400.4	2106.2	2162.6	2216.3	1817.8	1941.2

* Supplemented by Advanco data when ETEC-IBM data unavailable

DATE	ENGINE OPERATING HOURS		AVAILABLE SOLAR ENERGY	AT-POWER SOLAR ENERGY		GROSS ELECTRICAL OUTPUT			NET ON-SUN ELECTRICAL OUTPUT		NET 24-HOUR ELECTRICAL OUTPUT		
SEP 84	ETEC-IBM	ETEC-AD9	ETEC-IBM*	ETEC-IBM*	ETEC-AD9	ADVANCO	ETEC-IBM	ETEC-AD9	ETEC-IBM	ETEC-AD9	ADVANCO	ETEC-IBM	ETEC-AD9
1	5.9		755.0	416.5		97.8	98.2		90.2		81.8	80.4	
2	7.5		541.2	491.5		110.4	110.6		100.0		92.9	91.3	
3	9.4		782.2	665.3		163.6	164.2		149.6		143.9	142.9	
4	9.9		745.7	668.3		185.2	185.2		169.3		164.7	162.6	
5	10.9		771.6	754.5		203.9	204.3		187.3		182.1	180.9	
6	11.1	1.7	773.5	751.4	77.6	199.9	200.0	20.7	183.7	18.1	179.4	177.9	6.3
7	8.9	5.7	693.4	594.5	413.8	153.6	153.4	112.1	141.4	103.6	138.1	136.4	93.9
8	7.9	8.1	508.7	415.1	414.0	97.8	98.5	98.7	87.8	87.1	81.6	80.0	78.7
9	1.3		157.3	60.7		11.1	11.6		10.1		2.1	0.3	
10													
11	6.1		340.1	347.9		83.0	81.7		73.2		67.8	64.7	
12	9.7		618.5	617.4		146.8	145.6		132.6		129.1	126.3	
13	11.1		724.0	721.1		195.1	195.5		179.2		174.7	172.3	
14	10.1	9.7	690.9	678.8	660.3	181.6	181.8	178.7	166.4	162.5	161.2	159.5	154.9
15	7.9	8.0	452.9	437.7	420.4	99.9	100.8	100.2	90.0	88.9	82.3	81.4	80.4
16	8.1	8.1	476.7	460.9	459.6	117.9	117.8	117.4	106.7	105.7	102.4	101.5	97.2
17		7.5	520.3	518.2	390.5	124.0		118.7		107.4	111.9		98.6
18	10.6	10.4	634.3	636.0	612.6	153.1	153.4	151.6	138.7	136.4	133.9	132.8	129.2
19	6.3	6.3	383.8	362.9	359.8	85.0	84.8	84.6	76.4	75.7	71.5	69.5	66.3
20	0.0		703.0	0.0			0.0		0.0			-4.4	
21	0.0		745.4	0.0			0.0		0.0			-4.6	
22	0.0		586.7	0.0			0.0		0.0			-3.3	
23	0.0		610.0	0.0			0.0		0.0			-3.2	
24	0.0		522.1	0.0			0.0		0.0			-5.5	
25	0.0		213.3	0.0			0.0		0.0			-9.7	
26	0.0		552.9	0.0			0.0		0.0			-11.0	
27	0.0		685.2	0.0			0.0		0.0			-10.1	
28	0.0		717.5	0.0			0.0		0.0			-9.6	
29	0.0		630.1	0.0			0.0		0.0			-9.5	
30	0.0		310.3	0.0			0.0		0.0			-10.4	
TOTAL	142.5	65.6	16846.6	9598.7	3808.6	2409.7	2287.4	982.7	2082.6	885.3	2101.4	1879.4	805.5

* Supplemented by Advanco data when ETEC-IBM data unavailable

DATE	ENGINE OPERATING HOURS		AVAILABLE SOLAR ENERGY	AT-POWER SOLAR ENERGY		GROSS ELECTRICAL OUTPUT			NET ON-SUN ELECTRICAL OUTPUT		NET 24-HOUR ELECTRICAL OUTPUT		
OCT 84	ETEC-IBM	ETEC-AD9	ETEC-IBM*	ETEC-IBM*	ETEC-AD9	ADVANCO	ETEC-IBM	ETEC-AD9	ETEC-IBM	ETEC-AD9	ADVANCO	ETEC-IBM	ETEC-AD9
1	0.0		688.6	0.0			0.0		0.0			-9.5	
2	0.0		655.2	0.0			0.0		0.0			-9.2	
3	0.0		660.4	0.0			0.0		0.0			-9.5	
4	0.0		525.5	0.0			0.0		0.0			-7.4	
5	0.5		466.4	39.4		9.0	8.2		7.5		-1.3	-4.0	
6	0.0		610.5	0.0		0.0	0.0		0.0		-11.5	-12.9	
7	0.0		690.9	0.0		0.0	0.0		0.0		-8.3	-10.8	
8	4.9		824.8	337.8		20.0	84.2		77.1		11.6	68.9	
9	5.1		641.2	345.7		93.4	92.5		85.3		80.4	77.6	
10	9.4		562.6	574.1		142.5	143.6		131.3		125.8	125.2	
11	0.8		78.6	28.2		3.1	2.8		2.0		-5.7	-8.5	
12	9.9	9.9	692.1	722.8	679.0	188.7	188.4	187.8	175.3	174.0	171.1	169.1	166.5
13	0.0		712.5	0.0		0.0	0.0		0.0		-7.2	-9.6	
14	0.0		452.1	0.0		0.0	0.0		0.0		-7.6	-10.2	
15	8.1	8.2	461.8	487.9	434.9	94.3	94.0	93.0	85.7	83.7	80.9	77.8	75.4
16	8.9	9.0	605.6	638.4	574.3	132.6	131.4	130.6	122.0	120.9	118.3	115.3	112.9
17	8.9	8.9	643.7	668.3	616.0	146.3	145.1	144.4	134.8	133.0	131.8	128.5	125.0
18	9.7	9.7	568.1	686.0	556.9	155.2	155.1	152.9	144.9	141.8	140.3	138.7	134.2
19			508.7	157.8		28.7					25.4		
20	0.0		244.1	0.0		0.0	0.0		0.0		-8.1	-10.5	
21	0.0		422.2	0.0		0.0	0.0		0.0		-7.8	-10.0	
22	8.3		631.2	668.6		160.3	159.4		148.7		144.4	141.3	
23	9.2		568.3	721.2		185.1	184.0		172.5		168.7	166.1	
24	9.5		620.9	668.4		167.9	166.6		154.2		151.7	148.0	
25	9.3		531.9	707.3		180.9	179.5		168.1		164.9	161.9	
26	3.1		592.6	221.1		53.8	53.0		50.0		42.7	39.6	
27	0.0		619.0	0.0		0.0	0.0		0.0		-7.7	-10.5	
28	0.0		615.3	0.0		0.0	0.0		0.0		-8.6	-10.8	
29	0.0		406.4	0.0		0.0	0.0		0.0		-7.6	-9.8	
30	3.8		481.0	202.1		49.9	49.3		44.8		39.0	35.4	
31	3.3		529.8	195.7		44.8	43.3		40.3		34.9	29.9	
TOTAL	112.8	45.6	17312.0	8070.8	2861.0	1856.5	1880.4	708.7	1744.5	653.4	1550.5	1480.1	614.0

* Supplemented by Advanco data when ETEC-IBM data unavailable

DATE	ENGINE OPERATING HOURS		AVAILABLE SOLAR ENERGY	AT-POWER SOLAR ENERGY		GROSS ELECTRICAL OUTPUT			NET ON-SUN ELECTRICAL OUTPUT		NET 24-HOUR ELECTRICAL OUTPUT		
NOV 84	ETEC-IBM	ETEC-AD9	ETEC-IBM*	ETEC-IBM*	ETEC-AD9	ADVANCO	ETEC-IBM	ETEC-AD9	ETEC-IBM	ETEC-AD9	ADVANCO	ETEC-IBM	ETEC-AD9
1	0.0		670.0	0.0			0.0		0.0			-10.5	
2	0.0		626.4	0.0			0.0		0.0			-10.0	
3	0.0		641.4	0.0			0.0		0.0			-9.8	
4	0.0		612.5	0.0			0.0		0.0			-9.8	
5	0.0		604.4	0.0			0.0		0.0			-10.0	
6	0.0		369.4	0.0			0.0		0.0			-10.2	
7	0.1		589.6	0.0			0.2		0.1			-10.1	
8	4.2		571.8	286.6			72.8		67.9			58.0	
9	0.0		635.0	0.0			0.0		0.0			-10.2	
10	0.0		665.7	0.0			0.0		0.0			-10.5	
11	0.0		447.2	0.0			0.0		0.0			-9.7	
12	0.0		360.2	0.0			0.0		0.0			-9.7	
13	0.0		61.5	0.0			0.0		0.0			-11.7	
14	0.0		164.4	0.0			0.0		0.0			-12.3	
15	0.0		412.0	0.0			0.0		0.0			-11.6	
16	0.0		481.9	0.0			0.0		0.0			-13.1	
17	0.0		612.2	0.0			0.0		0.0			-10.0	
18	0.0		0.0	0.0			0.0		0.0			-10.2	
19	0.0		496.1	0.0			0.0		0.0				
20	0.0		631.5	0.0			0.0		0.0				
21	0.0		83.6	0.0			0.0		0.0			-11.2	
22	0.0		331.7	0.0			0.0		0.0			-10.3	
23	0.0		195.8	0.0			0.0		0.0			-9.8	
24	0.0		47.2	0.0			0.0		0.0			-10.0	
25	0.0		325.6	0.0			0.0		0.0			-10.3	
26	0.0		646.3	0.0			0.0		0.0			-11.4	
27	0.0		512.4	0.0			0.0		0.0			-10.5	
28	0.0		0.0	0.0			0.0		0.0			-12.2	
29	0.0		0.0	0.0			0.0		0.0			-11.5	
30	0.0		0.0	0.0			0.0		0.0			-9.7	
TOTAL	4.3	0.0	11795.8	286.6	0.0	0.0	73.0	0.0	68.0	0.0	0.0	-228.3	0.0

* Supplemented by Advanco data when ETEC-IBM data unavailable

DATE	ENGINE OPERATING HOURS		AVAILABLE SOLAR ENERGY	AT-POWER SOLAR ENERGY		GROSS ELECTRICAL OUTPUT			NET ON-SUN ELECTRICAL OUTPUT		NET 24-HOUR ELECTRICAL OUTPUT		
DEC 84	ETEC-IBM	ETEC-AD9	ETEC-IBM*	ETEC-IBM*	ETEC-AD9	ADVANCO	ETEC-IBM	ETEC-AD9	ETEC-IBM	ETEC-AD9	ADVANCO	ETEC-IBM	ETEC-AD9
1	0.0		0.0	0.0		0.0	0.0		0.0		0.0	-10.3	
2	0.0		0.0	0.0		0.0	0.0		0.0		0.0	-10.2	
3	0.0		0.0	0.0		0.0	0.0		0.0		0.0	-11.1	
4	0.0		0.0	0.0		0.0	0.0		0.0		0.0	-10.3	
5			0.0			0.0					0.0		
6	0.0		0.0	0.0		0.0	0.0		0.0		0.0	-11.5	
7	0.0		0.0	0.0		0.0	0.0		0.0		0.0	-9.4	
8	0.0		0.0	0.0		0.0	0.0		0.0		0.0	-9.8	
9	0.0		0.0	0.0		0.0	0.0		0.0		0.0	-9.3	
10			0.0			0.0					0.0		
11	0.0		83.8	0.0		0.0	0.0		0.0		0.0	-9.7	
12	0.0		171.3	0.0		0.0	0.0		0.0		0.0		
13	1.3	1.4	342.2	76.6	65.4	17.8	14.0	13.1	13.1	11.9	9.1	3.1	-0.1
14	0.5	0.4	364.1	20.8	9.2	7.6	4.0	3.2	3.6	2.9	-0.3	-6.6	-9.6
15	2.1	1.9	259.2	130.6	107.7	13.6	26.0	21.5	24.2	19.8	8.0	13.6	8.1
16	0.0		350.2	0.0		0.0	0.0		0.0		0.0		
17	0.0		405.0	0.0		0.0	0.0		0.0		0.0	-2.5	
18	0.0		9.7	0.0		0.0	0.0		0.0		0.0	-6.9	
19	0.5		264.1	39.5		0.0	6.3		5.9		0.0	-5.0	
20	6.9	3.2	576.5	534.9	197.7	142.9	141.9	59.2	134.4	55.3	126.6	122.0	44.3
21	8.0	7.9	543.0	582.2	516.3	149.3	147.5	145.7	139.3	136.9	129.9	122.9	120.4
22	2.6	2.6	222.8	171.5	160.9	44.6	43.2	42.1	40.4	39.3	28.4	21.3	20.0
23	6.1	6.2	516.9	432.5	390.5	107.4	104.0	103.8	98.2	97.0	89.4	81.9	87.9
24	7.5	7.6	570.9	574.6	517.5	148.6	146.7	146.2	137.2	135.1	128.5	121.2	126.4
25	0.3	0.3	588.3	16.8	18.8	4.1	3.7	3.4	3.4	2.9	-6.3	-10.4	-9.6
26	0.0		10.7	0.0		0.0	0.0		0.0		0.0	-9.5	
27	0.0		0.0	0.0		0.0	0.0		0.0		0.0		
28	5.7		384.9	415.6		103.3	101.1		95.4		92.1	87.8	
29	0.0		169.1	0.0		0.0	0.0		0.0		0.0	-9.3	
30	0.0		531.2	0.0		0.0	0.0		0.0		0.0	-8.9	
31	0.0		568.4	0.0		0.0	0.0		0.0		0.0	-14.3	
TOTAL	41.7	31.4	6932.3	2995.6	1983.8	739.2	738.4	538.2	695.1	501.1	605.4	408.8	403.6

* Supplemented by Advanco data when ETEC-IBM data unavailable

DATE	ENGINE OPERATING HOURS		AVAILABLE SOLAR ENERGY	AT-POWER SOLAR ENERGY		GROSS ELECTRICAL OUTPUT			NET ON-SUN ELECTRICAL OUTPUT		NET 24-HOUR ELECTRICAL OUTPUT		
JAN 85	ETEC-IBM	ETEC-AD9	ETEC-IBM*	ETEC-IBM*	ETEC-AD9	ADVANCO	ETEC-IBM	ETEC-AD9	ETEC-IBM	ETEC-AD9	ADVANCO	ETEC-IBM	ETEC-AD9
1	0.0		0.0	0.0		0.0	0.0		0.0		-13.5	-18.3	
2	5.8	5.8	595.1	458.8	419.9	122.6	123.4	123.2	117.4	116.9	110.0	109.5	107.2
3		7.9	597.9	521.3	574.3	149.7		168.0		160.4	143.1		151.9
4	7.3	7.7	525.5	557.2	542.6	141.8	148.6	153.7	141.6	146.0	134.9		137.4
5	7.7		555.2	548.6		143.6	141.6		135.0		133.5	131.9	
6	0.0		12.2	30.3		2.7	0.0		0.0		0.6	-2.6	
7	0.0		0.0	13.3		2.8	0.0		0.0		-1.6	-3.4	
8	4.6		536.8	319.3		87.3	84.8		81.3		78.7	77.9	
9			556.1			0.0					-8.3		
10	0.0		541.0	0.0		0.0	0.0		0.0		-4.4	-4.6	
11	0.0		631.4	0.0		0.0	0.0		0.0		-2.1	-2.7	
12	0.0		567.1	0.0		0.0	0.0		0.0		-2.1	-3.4	
13	0.0		637.1	0.0		0.0	0.0		0.0		-2.4	-2.9	
14	0.0		633.1	0.0		0.0	0.0		0.0		-2.1	-2.9	
15	0.0		633.6	0.0		0.0	0.0		0.0		-4.8	-5.5	
16	0.0		665.7	0.0		0.0	0.0		0.0		-2.6	-3.7	
17	0.0		647.1	0.0		0.0	0.0		0.0		-2.6	-3.1	
18	0.0		588.9	0.0		0.0	0.0		0.0		-2.8	-4.3	
19	3.6	3.7	458.8	187.4	183.6	44.3	42.2	42.0	39.0	38.3	37.4	34.9	27.5
20	0.0		519.6	23.3		2.4	0.0		0.0		-0.5	-3.7	
21	5.3	5.5	279.2	250.2	238.9	53.8	51.6	52.1	47.9	48.2	46.1	43.4	38.4
22	0.3		40.8	12.9		4.2	1.3		1.2		0.1	-3.6	
23	0.1		20.5	4.8		2.8	0.2		0.2		-2.0	-5.2	
24	7.6		588.8	543.8		145.3	142.1		135.2		135.9	131.7	
25	2.6	2.6	139.9	98.7	93.2	15.6	14.0	13.8	12.6	12.4	8.0	5.1	1.0
26	6.7	6.5	487.7	463.7	441.9	120.6	119.0	118.2	111.2	110.5	107.7	104.4	101.2
27	7.7		613.9	569.4		153.2	151.6		143.7		139.6	136.7	
28	4.1	3.7	295.8	267.4	246.1	66.9	63.7	60.7	59.5	56.7	55.6	49.5	46.0
29	3.9	4.0	244.9	162.8	159.4	29.8	28.0	28.5	25.3	25.2	19.4	14.9	14.6
30	0.1	0.2	29.9	1.7	5.8	2.5	0.4	0.4	0.3	0.3	-6.6	-11.7	-12.3
31	3.1	3.1	238.4	174.9	162.5	41.2	40.3	39.9	37.4	36.6	31.8	25.6	25.5
TOTAL	70.5	50.7	12882.0	5209.8	3068.1	1333.1	1152.8	800.5	1088.8	751.4	1124.0	783.9	638.3

* Supplemented by Advanco data when ETEC-IBM data unavailable

DATE	ENGINE OPERATING HOURS		AVAILABLE SOLAR ENERGY	AT-POWER SOLAR ENERGY		GROSS ELECTRICAL OUTPUT			NET ON-SUN ELECTRICAL OUTPUT		NET 24-HOUR ELECTRICAL OUTPUT		
FEB 85	ETEC-IBM	ETEC-AD9	ETEC-IBM*	ETEC-IBM*	ETEC-AD9	ADVANCO	ETEC-IBM	ETEC-AD9	ETEC-IBM	ETEC-AD9	ADVANCO	ETEC-IBM	ETEC-AD9
1	7.8	7.8	661.0	603.5	576.7	170.5	168.6	167.6	160.9	159.2	157.8	154.1	150.6
2	0.0		0.0	0.0		0.0	0.0		0.0		-3.6	-4.2	
3	0.0		66.9	0.0		0.0	0.0		0.0		-3.7	-4.2	
4	0.0		9.2	0.0		0.0	0.0		0.0		-9.2	-12.1	
5	8.5	8.6	643.4	621.3	602.6	173.0	171.1	170.6	162.4	161.5	159.2	155.5	153.3
6	7.3	7.3	474.6	419.6	397.8	105.5	104.2	102.2	97.6	95.3	94.7	90.6	86.4
7	8.3		482.0	463.0		115.5	114.2		106.3		93.1	100.7	
8	2.2		99.3	89.3		18.4	15.9		14.0		-3.2	4.3	
9	4.2	4.2	191.6	195.3	188.8	36.3	36.0	37.9	32.7	33.6	15.3	23.3	23.1
10	8.2		700.2	631.7		177.8	176.7		166.3		150.5	157.5	
11	8.5		666.6	618.3		169.2	168.4		156.5		150.8	146.9	
12	8.8		703.5	653.5		180.4	183.0		170.7		162.8	163.4	
13	9.1		720.7	689.0		192.7	191.4		178.6		173.1	170.0	
14	9.2		758.0	731.2		204.6	203.8		190.5		185.8	184.1	
15	9.4	9.5	772.0	757.0	741.8	205.6	204.5	203.9	193.5	192.0	190.4	187.7	184.3
16	9.2	9.2	715.0	688.3	678.1	187.3	186.3	185.6	175.4	174.3	173.1	170.2	166.4
17	5.9		297.9	261.6		52.3	51.4		46.9		42.8	39.0	
18	0.5	0.6	100.6	21.5	22.2	1.7	3.3	3.2	3.0	3.0	-5.1	-3.0	-9.5
19	4.9	5.1	292.1	283.0	275.3	66.9	65.2	63.8	60.2	58.2	55.6	52.6	48.1
20	5.3	5.3	350.7	326.8	323.8	83.0	81.5	80.3	76.7	75.2	73.1	69.4	65.3
21	2.7	2.9	174.1	159.3	149.6	35.4	33.9	33.6	31.4	31.1	26.7	23.9	19.9
22	6.8		394.3	329.2		95.3	92.5		84.3		83.3	77.6	
23	0.0		0.0	0.0		0.0	0.0		0.0		-3.6	-5.1	
24	0.0		0.0	0.0		0.0	0.0		0.0		-4.7	-6.2	
25	9.4		618.5	599.6		177.8	178.2		167.6		163.2	161.1	
26	9.5	9.5	682.0	691.6	674.1	193.0	192.2	191.7	180.8	180.1	178.0	175.3	172.5
27	9.3	9.4	667.0	644.4	619.3	162.2	161.8	160.5	152.0	149.9	147.0	146.9	142.1
28	9.7		367.6	684.6		179.3	178.3		166.4		163.3	161.1	
TOTAL	164.9	79.3	11608.8	11162.6	5250.2	2983.7	2962.4	1400.7	2774.7	1313.2	2606.5	2580.4	1202.6

* Supplemented by Advanco data when ETEC-IBM data unavailable

DATE	ENGINE OPERATING HOURS		AVAILABLE SOLAR ENERGY	AT-POWER SOLAR ENERGY		GROSS ELECTRICAL OUTPUT			NET ON-SUN ELECTRICAL OUTPUT		NET 24-HOUR ELECTRICAL OUTPUT		
MAR 85	ETEC-IBM	ETEC-AD9	ETEC-IBM*	ETEC-IBM*	ETEC-AD9	ADVANCO	ETEC-IBM	ETEC-AD9	ETEC-IBM	ETEC-AD9	ADVANCO	ETEC-IBM	ETEC-AD9
1	5.5		344.6	303.4		68.7	68.6		63.8		56.6	55.9	
2	6.7		441.2	434.0		104.5	102.9		97.5		93.5	89.0	
3	9.2	1.9	689.7	668.0	116.2	183.2	182.2	32.8	171.7	30.6	169.0	163.3	18.9
4	9.7	9.7	645.5	633.9	621.1	167.0	166.2	165.5	157.5	155.3	151.9	148.4	147.7
5	2.6	2.8	235.6	124.4	123.8	27.7	26.7	26.0	24.6	23.8	17.4	13.3	12.5
6	8.1	8.1	571.4	560.1	541.7	140.2	140.1	140.1	132.4	131.4	126.6	123.9	123.0
7	9.5	8.8	619.9	606.3	549.2	146.7	146.1	138.9	137.4	129.5	132.3	127.9	121.4
8	0.7	0.9	140.2	24.1	25.4	2.5	1.9	1.8	1.5	1.1	-6.2	-7.1	-11.2
9	1.9	2.0	117.8	72.7	76.5	9.8	9.4	9.3	8.4	7.9	3.1	1.4	-3.7
10	7.1	7.1	451.4	446.0	421.7	100.0	101.4	98.1	94.4	90.5	89.9	90.6	81.6
11	4.2	4.2	255.8	240.9	230.6	50.3	51.0	49.7	47.5	46.2	42.3	42.7	35.7
12	10.1	10.2	783.1	775.1	754.9	196.8	196.2	195.3	186.6	184.6	184.6	183.6	177.2
13	10.3	6.3	755.6	753.3	448.3	210.1	209.6	129.5	199.1	121.8	196.6	195.7	112.4
14	9.3	8.8	663.1	646.5	614.3	174.4	174.7	170.5	165.7	160.9	162.7	162.2	152.9
15	9.4	9.5	546.2	536.6	521.1	134.4	133.2	132.3	125.8	124.5	124.4	122.6	116.8
16	5.9	6.0	300.1	268.8	259.8	53.9	53.8	52.9	50.2	48.6	46.5	45.5	39.1
17	9.8	9.8	574.7	564.3	545.7	137.4	136.5	135.7	128.1	126.6	125.8	124.6	119.1
18	8.8	8.8	650.5	614.7	608.4	155.3	153.7	152.1	145.7	143.8	144.6	142.3	135.7
19	10.3	10.3	746.0	731.6	717.1	183.0	182.7	181.8	172.9	171.1	171.1	170.3	163.8
20	10.1	10.2	729.9	706.5	703.1	171.4	170.8	169.9	160.4	158.3	157.8	156.8	151.0
21	10.1	10.2	630.3	625.9	610.8	166.7	166.1	165.3	156.4	154.5	154.2	153.2	147.2
22	10.2		683.2	682.9		182.0	181.3		171.0		167.6	167.6	
23	10.1	10.1	773.9	751.6	729.0	202.8	202.1	201.0	191.3	189.1	189.2	188.9	181.8
24	10.0	1.9	653.2	632.9	90.5	169.3	168.3	22.7	157.6	20.5	156.0	154.6	8.8
25	8.7	8.6	510.5	483.4	464.9	114.0	113.3	110.6	106.5	103.1	104.3	103.0	94.9
26	9.1	4.0	546.8	525.6	187.2	122.0	121.7	39.4	114.6	36.6	112.8	111.7	25.9
27	2.1	2.1	234.6	138.0	129.5	32.6	31.7	31.0	29.4	29.0	25.4	23.3	17.4
28	6.9	7.0	526.0	447.7	441.7	102.3	102.8	104.0	97.8	97.9	94.4	94.4	88.9
29	9.5	9.6	726.1	695.3	661.4	172.1	172.2	164.0	164.5	155.6	161.5	161.6	147.9
30	10.1	10.0	850.3	807.7	789.8	208.0	207.3	204.7	196.7	193.1	194.7	194.2	185.7
31	8.9	8.8	781.7	672.5	656.8	168.8	168.2	166.0	158.7	156.1	157.2	156.2	148.1
TOTAL	245.0	197.7	17178.9	16174.7	12640.6	4038.1	4042.7	3190.9	3815.7	2991.9	3707.8	3661.6	2740.6

* Supplemented by Advanco data when ETEC-IBM data unavailable

DATE	ENGINE OPERATING HOURS		AVAILABLE SOLAR ENERGY	AT-POWER SOLAR ENERGY		GROSS ELECTRICAL OUTPUT			NET ON-SUN ELECTRICAL OUTPUT		NET 24-HOUR ELECTRICAL OUTPUT		
APR 85	ETEC-IBM	ETEC-AD9	ETEC-IBM*	ETEC-IBM*	ETEC-AD9	ADVANCO	ETEC-IBM	ETEC-AD9	ETEC-IBM	ETEC-AD9	ADVANCO	ETEC-IBM	ETEC-AD9
1	8.6	7.2	820.1	681.2	561.6	191.2	190.5	157.6	181.1	148.8	179.0	178.0	127.2
2	0.0		820.9	0.0		0.0	0.0		0.0		-3.0	-4.4	
3	0.0		501.1	0.0		0.0	0.0		0.0		-3.0	-4.3	
4	0.0		765.5	0.0		0.0	0.0		0.0		-2.1	-4.1	
5	0.0		657.1	0.0		0.0	0.0		0.0		-1.5	-2.1	
6			606.4	0.0		0.0					-2.6		
7	0.0		796.0	0.0		0.0	0.0		0.0		-5.1	-3.4	
8	0.0		735.0	0.0		0.0	0.0		0.0		-5.5	-3.7	
9	0.0		805.4	0.0		0.0	0.0		0.0		-6.1	-4.2	
10	0.0		861.8	0.0		0.0	0.0		0.0		-9.2	-8.1	
11	0.0		805.1	0.0		0.0	0.0		0.0		-8.8	-11.9	
12	0.0		817.1	0.0		0.0	0.0		0.0		-10.6	-13.3	
13	0.0		853.6	0.0		0.0	0.0		0.0		-10.9	-15.0	
14	0.0		826.6	0.0		0.0	0.0		0.0		-11.4	-16.1	
15	2.4	2.4	657.9	132.0	123.9	27.2	27.7	27.0	24.3	23.5	15.5	13.5	12.0
16	7.3	5.2	457.0	403.2	288.6	88.9	89.3	63.9	79.2	57.0	72.4	71.0	47.0
17	3.5		255.8	179.0		36.2	35.8		32.2		24.6	21.7	
18	10.3		678.7	672.6		166.4	165.7		153.7		149.3	146.9	
19	10.0		732.0	659.8		161.4	160.8		149.1		145.1	142.6	
20	1.6		133.6	69.6		11.9	10.8		9.5		2.8	-0.5	
21	7.8		794.4	584.3		140.7	139.7		130.9		127.1	124.5	
22	11.1		839.7	827.0		202.6	201.9		187.4		184.3	182.1	
23	10.7		813.7	797.3		191.3	190.9		176.5		173.2	170.9	
24	7.7	3.4	659.8	467.8	201.9	114.8	114.2	48.3	104.5	43.5	100.0	97.0	32.5
25	0.0		407.4	0.0		0.0	0.0		0.0		-4.6	-7.1	
26	0.0		785.6	0.0		0.0	0.0		0.0		-0.6	-13.0	
27	2.7	2.8	356.1	181.7	172.0	44.8	44.0	43.3	40.4	39.5	36.5	33.5	28.3
28	0.0		774.2	0.0		0.0	0.0		0.0		-7.3	-9.5	
29	10.3	10.2	640.6	623.6	603.7	142.1	142.2	140.4	128.5	126.6	123.3	121.6	119.3
30	10.9	11.0	750.4	733.6	720.9	188.4	188.4	186.1	173.3	170.1	168.9	166.9	163.2
TOTAL	104.9	42.1	20408.6	7012.7	2672.6	1707.9	1701.9	666.6	1570.6	608.9	1409.7	1349.5	529.9

* Supplemented by Advanco data when ETEC-IBM data unavailable

DATE	ENGINE OPERATING HOURS		AVAILABLE SOLAR ENERGY	AT-POWER SOLAR ENERGY		GROSS ELECTRICAL OUTPUT			NET ON-SUN ELECTRICAL OUTPUT		NET 24-HOUR ELECTRICAL OUTPUT		
MAY 85	ETEC-IBM	ETEC-AD9	ETEC-IBM*	ETEC-IBM*	ETEC-AD9	ADVANCO	ETEC-IBM	ETEC-AD9	ETEC-IBM	ETEC-AD9	ADVANCO	ETEC-IBM	ETEC-AD9
1	11.5	11.5	846.5	830.6	810.5	220.5	220.6	217.8	204.1	200.2	200.5	198.3	193.6
2	11.9	11.9	812.8	801.1	788.2	205.3	205.1	202.6	188.2	184.8	184.7	182.9	178.4
3	9.7	9.7	711.1	635.1	636.2	160.5	160.4	159.3	146.6	144.5	141.3	139.3	136.9
4	7.3	7.3	757.5	478.3	479.2	116.9	116.6	115.9	105.9	104.7	100.9	98.5	95.8
5	2.1	2.1	205.9	88.5	84.9	15.6	15.1	15.0	13.0	12.6	3.9	0.5	1.0
6	4.9	4.7	759.3	304.5	301.7	68.7	68.8	67.7	63.1	61.7	56.9	54.7	51.5
7	11.5	11.5	802.3	771.6	766.2	191.6	191.5	188.9	176.1	172.6	160.1	169.5	165.9
8	7.8	7.9	488.4	458.4	463.5	98.5	98.7	98.9	88.4	87.9	62.3	80.5	79.4
9	11.1	11.2	747.6	718.0	721.5	163.3	162.9	161.3	147.6	145.1	127.5	141.9	138.4
10	11.0	11.0	852.9	797.4	78.3	181.1	180.7	177.9	167.7	163.4	139.7	154.5	156.5
11	3.5		868.2	276.2		65.8	64.2		59.8		51.5	45.7	
12	7.7		829.2	587.3		137.4	136.4		126.7		120.3	115.7	
13	12.2	12.2	893.7	889.5	870.2	203.1	202.8	201.4	186.9	184.3	182.6	180.6	178.0
14	8.9		809.8	546.7		116.5	116.7		105.4		97.7	94.7	
15	10.3		651.4	637.4		131.6	131.6		118.5		113.0	110.6	
16	10.1		836.9	738.4		193.9	193.4		179.8		175.5	173.9	
17	10.5	10.5	916.0	805.9	791.3	209.6	209.0	208.3	194.5	193.0	190.7	187.2	185.8
18	7.5	7.5	861.2	590.7	582.3	157.0	156.2	155.2	145.9	144.4	139.6	137.0	135.6
19	7.7	7.7	756.5	544.0	539.1	139.4	139.2	138.2	128.5	127.3	122.3	118.0	118.7
20			0.0	0.0		0.0					0.0		
21			0.0	0.0		0.0					0.0		
22			0.0	0.0		0.0					0.0		
23	0.0		398.2	0.0		0.0	0.0		0.0		0.0	0.0	
24	0.0		738.1	0.0		0.0	0.0		0.0		0.0	-0.2	
25			0.0	0.0		0.0					0.0		
26			0.0	0.0		0.0					0.0		
27			0.0	0.0		0.0					0.0		
28			0.0	0.0		0.0					0.0		
29	0.0		165.2	0.0		0.0	0.0		0.0		0.0	-1.8	
30	3.5		264.2	209.1		49.1	48.8		44.9		40.8	39.3	
31	12.7	4.8	842.5	832.3	266.8	206.7	206.4	65.1	193.5	59.7	190.1	189.1	49.5
TOTAL	183.3	131.3	17015.4	12541.0	8179.8	3032.1	3025.1	2173.8	2785.1	1986.1	2601.9	2610.4	1864.8

* Supplemented by Advanco data when ETEC-IBM data unavailable

DATE	ENGINE OPERATING HOURS		AVAILABLE SOLAR ENERGY	AT-POWER SOLAR ENERGY		GROSS ELECTRICAL OUTPUT			NET ON-SUN ELECTRICAL OUTPUT		NET 24-HOUR ELECTRICAL OUTPUT		
JUN 85	ETEC-IBM	ETEC-AD9	ETEC-IBM*	ETEC-IBM*	ETEC-AD9	ADVANCO	ETEC-IBM	ETEC-AD9	ETEC-IBM	ETEC-AD9	ADVANCO	ETEC-IBM	ETEC-AD9
1	0.0	0.5	869.9	28.5	27.7	0.9	0.0	6.2	0.0	5.8	-2.2	-4.7	-6.7
2	2.3	3.3	593.9	120.4	180.7	25.7	25.2	39.6	23.5	36.8	21.1	19.0	25.8
3	6.0	5.8	561.5	360.8	346.5	78.8	78.2	77.6	73.5	72.2	71.4	69.9	62.6
4	10.0	10.1	846.9	743.9	716.4	182.5	182.3	181.3	171.8	169.6	168.7	168.2	162.2
5	10.6	9.2	823.8	771.3	642.1	188.6	188.5	167.0	176.9	155.8	175.0	174.9	148.0
6	8.7	10.0	874.1	658.9	731.7	158.0	158.0	176.5	147.3	163.6	145.3	144.8	156.2
7	10.6	10.9	886.8	753.2	761.6	189.7	189.8	194.6	176.0	179.4	160.2	172.9	172.5
8	5.3	3.8	930.6	412.5	309.1	106.2	106.8	81.4	100.1	76.0	80.1	96.7	65.3
9	0.0	0.3	946.9	0.0	20.2	0.0	0.0	2.3	0.0	2.0	-11.3	-2.4	-10.6
10	6.0	3.0	894.4	429.0	233.0	106.0	106.0	61.0	98.0	56.6	94.2	95.4	45.5
11	4.1		441.0	254.2		58.5	58.4		53.7		51.7	50.9	
12	11.1	0.8	786.0	743.3	48.6	176.6	176.6	10.4	164.2	9.4	162.5	162.3	-2.8
13	8.5	10.1	787.3	583.1	636.9	139.4	139.2	151.9	129.2	139.8	126.7	126.2	132.5
14	12.7	8.0	802.8	809.6	554.7	197.3	197.1	143.8	182.6	133.6	180.7	180.8	125.2
15	10.9		815.3	730.6		173.1	173.2		161.6		158.7	158.8	
16	0.0		770.7	652.6		149.6	0.0		0.0		148.1	-2.4	
17	3.7	1.4	596.0	206.1	78.1	45.3	45.5	16.7	40.6	15.2	38.8	37.9	3.2
18	11.7	12.5	815.8	779.3	784.2	177.0	176.7	177.6	161.9	161.0	160.4	160.2	154.9
19	12.8	13.0	818.0	823.7	839.0	184.8	184.7	194.8	170.3	179.2	168.5	168.6	173.4
20	6.6	4.3	937.1	491.9	344.2	113.8	113.5	82.0	106.5	76.8	104.2	103.6	66.3
21	0.0		257.8	0.0		0.0	0.0		0.0		0.0	-2.1	
22			0.0	0.0		0.0					0.0		
23			0.0	0.0		0.0					0.0		
24			0.0	0.0		0.0					0.0		
25			0.0	0.0		0.0					0.0		
26			0.0	0.0		0.0					0.0		
27			0.0	0.0		0.0					0.0		
28			0.0	0.0		0.0					0.0		
29			0.0	0.0		0.0					0.0		
30			0.0	0.0		0.0					0.0		
TOTAL	141.7	107.0	16056.6	10352.9	7254.6	2451.8	2299.7	1764.7	2137.7	1632.8	2202.8	2079.5	1473.2

* Supplemented by Advanco data when ETEC-IBM data unavailable

DATE	ENGINE OPERATING HOURS		AVAILABLE SOLAR ENERGY	AT-POWER SOLAR ENERGY		GROSS ELECTRICAL OUTPUT			NET ON-SUN ELECTRICAL OUTPUT			NET 24-HOUR ELECTRICAL OUTPUT		
JUL 85	ETEC-IBM	ETEC-AD9	ETEC-IBM*	ETEC-IBM*	ETEC-AD9	ADVANCO	ETEC-IBM	ETEC-AD9	ETEC-IBM	ETEC-AD9	ADVANCO	ETEC-IBM	ETEC-AD9
1													
2													
3													
4													
5													
6													
7													
8													
9													
10		5.2			275.9			64.4		58.2			57.1
11		5.3			347.7			85.0		77.9			77.0
12		0.3			20.8			4.5		4.1			0.5
13													
14													
15													
16	10.7		596.7	570.5			130.6		116.8			103.6	
17	3.1	4.3	174.2	109.5	158.8		18.7	26.1	17.1	20.8		0.6	10.3
18	2.9	3.0	192.6	129.6	121.5		23.5	23.1	21.8	21.4		17.2	10.2
19	6.1	6.2	409.3	349.7	352.4		82.0	82.1	78.2	78.1		74.2	68.6
20	0.0		16.0	0.0			0.0		0.0			-2.7	
21	0.0		22.9	0.0			0.0		0.0			-2.4	
22	4.3		679.6	214.0			45.9		43.0			37.7	
23	8.9		774.5	586.9			153.1		147.4			145.1	
24	10.2		817.1	684.6			175.4		169.3			166.9	
25													
26													
27													
28													
29													
30													
31													
TOTAL	46.1	24.3	3682.9	2644.8	1277.1	0.0	629.2	285.2	393.6	260.4	0.0	540.2	223.7

* Supplemented by Advanco data when ETEC-IBM data unavailable

RESEARCH REPORTS CENTER

P.O. BOX 50490 • PALO ALTO • CA 94303
(415) 965-4081 • FID #94-2396182

INVOICE NO. 058482

PLEASE REFER TO THIS NO. ON ALL CORRESPONDENCE

BILL TO:

HUGH REILLY/DIV 6227
SANDIA NATIONAL LABS
POB 5800
ALBUQUERQUE NM 87185

SHIP TO:

HUGH REILLY/DIV 6227
SANDIA NATIONAL LABS
POB 5800
ALBUQUERQUE NM 87185

PLEASE USE CUSTOMER NO. WHEN ORDERING

PO#

INVOICE DATE	CUSTOMER NO.	PURCHASE ORDER NO.	TERMS	SHIP VIA
09/17/86	000507		NO CHARGE	SPEC 4TH CL/BOOKS

BIN NO.	QUANTITY ORDERED	QUANTITY BACK ORDERED	TITLE NO.	DESCRIPTION	LIST PRICE		AMOUNT
1134	1		AP4608	RP 2003.5 P. 248	0.00		0.00

COMMENTS: SITE: 1 NO. BKS: 1 TOT WGHT: 1.8
THE ABOVE REPORTS ARE SENT TO YOU GRATIS

SUBTOTAL	0.00
SALES TAX	0.00
SHIPPING & HANDLING	0.00
CK. NO.	
AMOUNT DUE	0.00

057391

ORIGINAL